

**Structural and Functional Analysis of the Caspase –dependent and –independent**

**Domains of the X-linked Inhibitor of Apoptosis Protein in Inflammatory Breast**

**Cancer Tumor Biology**

by

Myron K. Evans II

Department of Pathology  
Duke University

Date: February 9<sup>th</sup>, 2016

Approved:

---

Gayathri R. Devi, Co-Supervisor

---

Soman N. Abraham, Co-Supervisor

---

Jen-Tsan Chi

---

Sally Kornbluth

---

Jeffrey R. Marks

Dissertation submitted in partial fulfillment of  
the requirements for the degree of Doctor  
of Philosophy in the Department of  
Pathology in the Graduate School  
of Duke University

2016

ABSTRACT

**Structural and Functional Analysis of the Caspase –dependent and –independent**

**Domains of the X-linked Inhibitor of Apoptosis Protein in Inflammatory Breast**

**Cancer Tumor Biology**

by

Myron K. Evans II

Department of Pathology  
Duke University

Date: \_\_\_\_\_

Approved:

\_\_\_\_\_  
Gayathri R. Devi, Co-Supervisor

\_\_\_\_\_  
Soman N. Abraham, Co-Supervisor

\_\_\_\_\_  
Jen-Tsan Chi

\_\_\_\_\_  
Sally Kornbluth

\_\_\_\_\_  
Jeffrey R. Marks

An abstract of a dissertation submitted in partial fulfillment of the requirements for the degree of Doctor of Philosophy in the Department of Pathology in the Graduate School of Duke University

2016

Copyright by  
Myron K. Evans II  
2016

## **Abstract**

Inflammatory breast cancer (IBC) is an extremely rare but highly aggressive form of breast cancer characterized by the rapid development of therapeutic resistance leading to particularly poor survival. Our previous work focused on the elucidation of factors that mediate therapeutic resistance in IBC and identified increased expression of the anti-apoptotic protein, X-linked inhibitor of apoptosis protein (XIAP), to correlate with the development of resistance to chemotherapeutics. Although XIAP is classically thought of as an inhibitor of caspase activation, multiple studies have revealed that XIAP can also function as a signaling intermediate in numerous pathways. Based on preliminary evidence revealing high expression of XIAP in pre-treatment IBC cells rather than only subsequent to the development of resistance, we hypothesized that XIAP could play an important signaling role in IBC pathobiology outside of its heavily published apoptotic inhibition function. Further, based on our discovery of inhibition of chemotherapeutic efficacy, we postulated that XIAP overexpression might also play a role in resistance to other forms of therapy, such as immunotherapy. Finally, we posited that targeting of specific redox adaptive mechanisms, which are observed to be a significant barrier to successful treatment of IBC, could overcome therapeutic resistance and enhance the efficacy of chemo-, radio-, and immuno- therapies. To address these hypotheses our objectives were: 1. to determine a role for XIAP in IBC pathobiology and

to elucidate the upstream regulators and downstream effectors of XIAP; 2. to evaluate and describe a role for XIAP in the inhibition of immunotherapy; and 3. to develop and characterize novel redox modulatory strategies that target identified mechanisms to prevent or reverse therapeutic resistance.

Using various genomic and proteomic approaches, combined with analysis of cellular viability, proliferation, and growth parameters both *in vitro* and *in vivo*, we demonstrate that XIAP plays a central role in both IBC pathobiology in a manner mostly independent of its role as a caspase-binding protein. Modulation of XIAP expression in cells derived from patients prior to any therapeutic intervention significantly altered key aspects IBC biology including, but not limited to: IBC-specific gene signatures; the tumorigenic capacity of tumor cells; and the metastatic phenotype of IBC, all of which are revealed to functionally hinge on XIAP-mediated NF $\kappa$ B activation, a robust molecular determinant of IBC. Identification of the mechanism of XIAP-mediated NF $\kappa$ B activation led to the characterization of novel peptide-based antagonist which was further used to identify that increased NF $\kappa$ B activation was responsible for redox adaptation previously observed in therapy-resistant IBC cells. Lastly, we describe the targeting of this XIAP-NF $\kappa$ B-ROS axis using a novel redox modulatory strategy. Together, the data presented here characterize a novel and crucial role for XIAP both in therapeutic resistance and the pathobiology of IBC; these results

confirm our previous work in acquired therapeutic resistance and establish the feasibility of targeting XIAP-NF $\kappa$ B and the redox adaptive phenotype of IBC as a means to enhance survival of patients.

## **Dedication**

For my parents, who have supported me and always believed in me.

# Contents

Abstract.....	iv
List of Figures .....	xvii
1. Introduction.....	1
1.1 Introduction to Inflammatory Breast Cancer.....	1
1.1.1 Clinical, pathological, and epidemiological features of IBC and patients.....	2
1.1.2 Molecular features of IBC.....	4
1.1.2.1 Incidence of molecular subtypes by genomic sequencing in IBC and non-IBC.....	4
1.1.2.2 Immunohistochemical findings.....	5
1.1.2.3 EGFR/HER2 oncogenic signaling.....	6
1.1.2.4 Hormone receptor status.....	6
1.1.2.5 Overexpression of eIF4G1.....	7
1.1.2.5.1 Tumor emboli formation.....	7
1.1.2.5.2 Protection from hypoxia.....	8
1.1.2.6 Lymphangiogenesis and vasculogenesis.....	9
1.1.2.7 Hyperactivation of the NF $\kappa$ B pathway .....	9
1.1.2.8 Hyperactivation of the MAPK pathway.....	11
1.1.2.8.1 RhoC GTPase.....	11
1.1.2.8.2 NF $\kappa$ B activation and ER negativity.....	12
1.1.2.9 Apoptotic dysregulation.....	13

1.1.3	Current treatment options for IBC.....	13
1.1.3.1	Standard of care: multimodal therapy.....	13
1.1.3.2	Targeted therapies.....	15
1.1.3.3	Immunotherapy.....	19
1.1.3.3.1	Immunotherapy in IBC.....	19
1.1.3.3.2	Antibody-dependent cellular cytotoxicity.....	20
1.1.4	Unmet needs for the disease.....	22
1.1.4.1	Increased awareness.....	22
1.1.4.2	Use of molecular targets for diagnosis and treatment.....	23
1.1.4.3	Elucidation of therapeutic resistance mechanisms.....	24
1.2	Apoptotic dysregulation and therapeutic resistance in cancer.....	26
1.2.1	Overview of apoptosis.....	26
1.2.1.1	The extrinsic pathway.....	27
1.2.1.2	The intrinsic pathway.....	28
1.2.1.3	Anti-apoptotic proteins.....	29
1.2.1.3.1	Bcl-2 family.....	29
1.2.1.3.2	IAP family.....	29
1.2.2	Dysregulation of the components of the apoptotic machinery.....	30
1.2.2.1	Extrinsic components.....	30
1.2.2.1	Intrinsic components.....	31
1.2.2.1	Caspases.....	32

1.2.2.1	Anti-apoptotic proteins.....	32
1.2.2.1.1	Bcl-2 and Bcl-xL.....	32
1.2.2.1.2	IAPs .....	33
1.2.2.1	Apoptotic dysregulation in inflammatory breast cancer .....	34
1.2.3	X-linked inhibitor of apoptosis protein (XIAP).....	35
1.2.3.1	Regulation of expression level.....	36
1.2.3.1.1	Transcriptional.....	36
1.2.3.1.2	Translational.....	37
1.2.3.1.3	Post-translational.....	40
1.2.3.2	Caspase-independent signaling.....	41
1.2.3.2.1	NFκB activation.....	41
1.2.3.2.2	Akt activation.....	42
1.2.3.2.3	ROS modulation.....	43
1.2.3.2	XIAP as a prognostic factor .....	44
1.3	Redox adaptation and therapeutic resistance in cancer.....	45
1.3.1	Redox homeostasis: ROS production and elimination.....	45
1.3.1.1	Reactive species .....	45
1.3.1.2	Sources of ROS.....	46
1.3.1.3	Antioxidants .....	47
1.3.1.4	Oxidative stress.....	48

1.3.2	Redox control mechanisms: Nrf2 and NFκB.....	49
1.3.3	Oxidative stress response and adaptive mechanisms in breast cancer.....	50
1.3.4	Targeting redox imbalances in cancer.....	53
1.3.4.1	Promoting ROS production.....	53
1.3.4.2	Altering ROS breakdown and clearance.....	54
1.3.4.3	Targeting control mechanisms.....	55
1.4	Inflammatory breast cancer cell lines.....	57
1.4.1	Patient-derived cell lines.....	57
1.4.2	Acquired resistance models: rSUM149 and rSUM190.....	59
1.4.3	Resistance reversal model: rrSUM149.....	61
1.5	Research objectives outlined in this dissertation.....	62
1.5.1	Objective 1.....	62
1.5.2	Objective 2.....	62
1.5.3	Objective 3.....	63
2.	Materials and Methods.....	65
2.1	Cell Culture.....	65
2.1.1	Cell lines and reagents.....	65
2.1.2	Generation of XIAP mutant cell line models.....	69
2.1.3	shRNA-mediated knockdown of XIAP.....	70
2.1.4	shRNA-mediated knockdown of eIF4G1.....	70
2.1.5	Transient transfection of mutant XIAP constructs.....	70

2.2 NRAGE peptide manufacture and use for treatment.....	71
2.3 Determination of cell viability, apoptosis, and proliferation.....	71
2.3.1 Trypan blue exclusion assay.....	71
2.3.2 MTT assay.....	72
2.3.3 Clonogenic growth assay .....	72
2.3.4 Caspase activity assay .....	73
2.3.5 TUNEL staining.....	73
2.3.6 Wound healing assay .....	74
2.4 Assessment of SOD mimetics.....	74
2.4.1 MnP-based SOD mimics.....	74
2.4.2 Spectrophotometrical study of the reaction of MnPs with ascorbate .....	77
2.5 Western immunoblotting.....	77
2.6 Immunoprecipitation of TAB1 and associated proteins.....	80
2.7 Preparation of nuclear and cytosolic extracts.....	80
2.8 Flow cytometric analyses .....	81
2.8.1 Annexin V.....	81
2.8.2 Measurement of intracellular reactive oxygen species .....	81
2.8.3 Measurement of surface EGFR and Her2 levels.....	82
2.9 Measurement of reduced glutathione content.....	82
2.10 Immunofluorescence analysis.....	83
2.11 Immune assays .....	83

2.11.1 Chromium based ADCC assay.....	83
2.11.2 CytoTox-One non-radioactive ADCC assay .....	84
2.11.3 Granzyme B loading.....	85
2.12 Assessment of anchorage-independent growth potential .....	85
2.13 Assessment of intracellular ALDH activity .....	86
2.14 RNA analysis.....	87
2.14.1 RNA isolation .....	87
2.14.2 Quantitative polymerase chain reaction analysis.....	87
2.14.3 Affymetrix GeneChip analysis .....	89
2.14.3.1 Expressions2Kinases analysis .....	89
2.14.3.2 Gene set enrichment analysis .....	90
2.15 Immunohistochemistry of human tumor microarrays.....	91
2.16 Human breast tumor xenograft studies.....	92
2.17 Statistical analysis.....	93
3. Investigation of the role of XIAP and identification of functional partners in IBC pathogenesis .....	94
3.1 Introduction.....	94
3.2 Results.....	97
3.2.1 XIAP translation is regulated by MAPK signaling in IBC cells .....	97
3.2.2 High XIAP expression correlates with increased expression of a proliferative cluster of genes .....	103
3.2.3 XIAP drives constitutive NFκB activity in IBC cells .....	106

3.2.4 High XIAP expression correlates with increased expression of a proliferative cluster of genes .....	112
3.2.5 Expression of XIAP correlates with an IBC-specific gene signature and is essential for in vivo tumorigenesis.....	114
3.2.6 XIAP expression alters the transcriptomic landscape of primary tumors, correlating with high NFκB activation.....	123
3.2.7 XIAP activates NFκB through a TAB1:IKKβ-dependent mechanism.....	127
3.2.8 Targeting the XIAP:TAB1 interaction with NRAGE decreases AIG and reverses resistance to an EGFR kinase inhibitor.....	133
3.3 Discussion.....	141
4. Elucidation of the mechanism of XIAP-mediated tumor cell evasion/inhibition of immunotherapy.....	146
4.1 Introduction.....	146
4.2 Results.....	150
4.2.1 IBC cells with apoptotic dysregulation are resistant to ADCC.....	150
4.2.2 Caspase dependent apoptosis is inhibited in ADCC-resistant cells.....	154
4.2.3 The caspase-binding function of XIAP contributes to ADCC resistance.....	156
4.2.4 Reactive oxygen species generation is required for granzyme-mediated ADCC response .....	159
4.2.5 XIAP overexpression inhibits granzyme B-mediated ROS generation.....	162
4.2.6 XIAP suppresses ROS accumulation in a caspase-independent manner by increasing the antioxidant pool.....	164
4.2.7 XIAP-mediated suppression of ROS is dependent on NFκB signaling.....	166
4.2.8 RNAi-mediated targeting of XIAP enhances sensitivity to ADCC-mediated apoptosis.....	170

4.3 Discussion.....	172
5. Development and characterization of a novel combination therapy to antagonize redox imbalance in IBC.....	179
5.1 Introduction.....	179
5.2 Results.....	182
5.2.1 Combination of MnP+asc decreases cell viability and proliferation in therapy – sensitive and –resistant IBC cells.....	182
5.2.2 E2+asc induces significant ROS accumulation in IBC cells.....	186
5.2.3 Peroxide is essential for MnP+asc cytotoxicity, consuming the reduced glutathione pool.....	188
5.2.4 MnP+asc antagonizes pro-survival NFκB and ERK signals .....	190
5.2.5 Apoptosis induced by this combination is caspase independent.....	192
5.2.6 MnP+asc leads to translocation of apoptosis-inducing factor (AIF) to the nucleus.....	194
5.2.7 Ascorbate oxidation/consumption is catalyzed by E2 at faster rate .....	196
5.3 Discussion.....	200
6. Conclusions and Implications.....	206
References.....	218
Biography.....	278

## List of Tables

Table 1.1 Prevalence of molecular phenotypes by genome sequencing .....	4
Table 1.2 Prevalence of immunohistochemical findings in IBC and non-IBC.....	5
Table 1.3 Classification of previously described NF $\kappa$ B inhibitors .....	56
Table 2.1 Antibodies used in this dissertation.....	79
Table 2.2 Information for NF $\kappa$ B target gene qPCR primers used in Chapter 3 .....	88
Table 3.1 Results of XIAP staining of tumor tissue from 3 cohorts.....	105
Table 3.2 Statistics of mice used in XIAP modulation <i>in vivo</i> studies .....	116
Table 5.1 Approximate EC <sub>50</sub> values for each MnP+asc in cell lines tested.....	182

## List of Figures

Figure 1.1 Cell lines used in this dissertation.....	64
Figure 2.1 Chemical structures of compounds used in this dissertation .....	68
Figure 2.2 Chemical structures and physical characteristics of MnPs used.....	76
Figure 3.1 Targeting the MAPK pathway decreases eIF4G1 and XIAP expression in parental IBC cells .....	98
Figure 3.2 Targeting the MAPK pathway decreases XIAP expression and sensitizes to TRAIL treatment.....	100
Figure 3.3 <i>eIF4G1</i> silencing decreases XIAP expression in parental SUM149 cells and enhances sensitivity to TRAIL in resistant rSUM149 .....	102
Figure 3.4 XIAP expression in normal tissue, advanced breast cancer (non-IBC), and IBC .....	104
Figure 3.5 Validation of XIAP expression and function in XIAP modulated cell lines .	107
Figure 3.6 Modulation of XIAP expression alters NFκB localization and transcriptional activity.....	109
Figure 3.7 XIAP expression is necessary for expression of and IBC-specific NFκB signature in parental SUM149 cells .....	111
Figure 3.8 XIAP expression correlates with proliferative gene expression.....	113
Figure 3.9 XIAP expression is necessary for <i>in vivo</i> tumor growth of IBC cells.....	115
Figure 3.10 Modulating XIAP expression alters number of ALDH+ cells and is dependent on NFκB signaling.....	118
Figure 3.11 XIAP expression strongly correlates with migratory capacity in IBC cells.	120
Figure 3.12 XIAP expression correlates with an IBC patient gene signature.....	122
Figure 3.13 XIAP overexpressing tumors exhibit extensive activation of NFκB signaling .....	124

Figure 3.14 XIAP overexpressing primary tumors have high expression of NFκB target genes and proteins.....	126
Figure 3.15 Silencing <i>XIAP</i> reduces binding of TAB1 and IKKβ in IBC cells decreasing IκBα phosphorylation.....	128
Figure 3.16 Mutation of the oligomerization domain of XIAP inhibits NFκB nuclear translocation.....	130
Figure 3.17 Administration of NRAGE peptide can decrease NFκB phosphorylation and downstream signaling in IBC cells.....	132
Figure 3.18 NRAGE treatment decreases anchorage-independent growth in a dose-dependent manner.....	134
Figure 3.19 XIAP overexpression blocks the NFκB inhibitory effects of EGFR TKI, lapatinib .....	136
Figure 3.20 NRAGE treatment sensitizes resistant wtXIAP and rSUM149 cells to lapatinib .....	138
Figure 3.21 Lapatinib resistance correlates with increased expression of genes related to NFκB and MAPK.....	140
Figure 3.22 Schematic of MAPK pathway-mediated <i>XIAP</i> translation induction and subsequent NFκB activation.....	142
Figure 4.1 Apoptotic dysregulation inhibits antibody-dependent cell cytotoxicity (ADCC) in breast cancer cells.....	151
Figure 4.2 Antibody administration alone does not have differential effects on receptor internalization or inhibition of proliferation.....	153
Figure 4.3 Apoptosis caused by ADCC is caspase-dependent and inhibited in rSUM149 cells.....	155
Figure 4.4 XIAP overexpression inhibits ADCC response in SUM149 cells through caspase inhibition.....	158
Figure 4.5 Inhibition of granzyme accumulation prevents ROS- and caspase- dependent ADCC.....	161

Figure 4.6 Granzyme B-mediated ROS accumulation is inhibited in XIAP overexpressing cells.....	163
Figure 4.7 XIAP overexpression inhibits ROS accumulation through upregulation of antioxidant capacity.....	165
Figure 4.8 Inhibition of NFκB nuclear translocation reverses resistance to ROS accumulation.....	167
Figure 4.9 Administration of NRAGE inhibits NFκB phosphorylation in IBC cells and reverses resistance to ADCC .....	169
Figure 4.10 Targeted inhibition of XIAP by RNAi sensitizes ADCC-resistant cells to apoptosis .....	171
Figure 4.11 Schematic of XIAP effect on immune effector cell-mediated antibody-dependent cellular cytotoxicity .....	174
Figure 5.1 Combining MnP and ascorbate induces significant cell death in IBC cells ..	183
Figure 5.2 MnP+asc treatment reduces cellular proliferation of IBC cells.....	185
Figure 5.3 Combination of MnP and ascorbate induces ROS accumulation and overcomes redox adaptation in rSUM149 cells .....	187
Figure 5.4 MnP+asc induced cytotoxicity is reversible by administration of catalase ...	189
Figure 5.5 Peroxide generated by MnP+asc treatment reduces pro-survival signaling	191
Figure 5.6 Cell death induced by MnP+asc is caspase-independent.....	193
Figure 5.7 MnP+asc treatment induces translocation of mitochondrial protein, AIF, to the nucleus.....	195
Figure 5.8 H <sub>2</sub> O <sub>2</sub> -driven degradation of MnPs in the presence of ascorbate, and consumption of ascorbate.....	199
Figure 5.9 Schematic of the interaction between MnP and ascorbate and the cellular effects .....	202

## Acknowledgements

First, I would like to thank my advisor, Gay, for all of help and guidance over the years of graduate school. She has been there and watched me grow from a fresh out-of-college student with some lab experience to the scientist I am today. She has taught me the importance of collaboration and asking for help when it's needed and I truly appreciate all of the time and effort she has put into this process. I also need to thank the members of my committee, Sally Kornbluth, Jeff Marks, Ashley Chi, Mark Dewhirst, Duane Mitchell, and Soman Abraham, for their support, advice, and scientific guidance. To Michael Morse, Ines Batinic-Haberle, Joseph Geradts, and Steven van Laere, I owe a great debt to you all for allowing me to work closely with you, learn from you, and publish with you. Special thanks must be made to my DGS Soman Abraham for his advice about matters both scientific and professional. I would like to thank both the Developmental and Stem Cell Biology Program, for believing in me from Day 1, and the Pathology Program, for their training throughout the years, for being a home the past several years. All of you have helped in some way to make this a success for me, and for that I am truly grateful.

I would be absolutely remiss to not thank my friends and co-workers from the 4<sup>th</sup> floor of MSRB1. So many of you have contributed in ways you may not even know to help me finish this journey. I would like to especially thank Zack Hartman, for all of his

insights and being an awesome sounding board for ideas, and Mike Brown, for always lending reagents whenever I needed and answering any questions I had far outside my area of expertise.

The members of the Devi Lab deserve so much more thanks than I can offer in this section. Scott, Amy, and Jennifer have been there with me since the day I walked into the Devi Lab. Amy, thank you for being the greatest lab manager and friend that a graduate student could have asked for. Your dedication to science and joy for the job were such a delight to see day in and day out. Jennifer, if it wasn't for you I may never have found my place in this lab. You have been such an amazing mentor and inspiration to me, and seeing your success after you've left the lab, has pushed me to finish so I could get out and excel in the world. Scott, there is no way I could have possibly survived the last few years without you. Your mentorship and friendship have been invaluable to me and are things that I'll take with me for the rest of my life, even though I know I'll never find another lab mate like you. The three of you have taught me so much about science and friendship and continually made working a fun experience. I'd also like to thank the numerous undergraduates (John, Kim, Adrian, Arianna, Courtney, Johnny, Akshay, Jess) that we've had in the lab for giving me an opportunity to get a taste of what it's like to be a mentor and train students. I'm so proud of all of you and know you'll all be amazing at whatever you decide to do in the future.

I would also like to thank my amazing group of friends from outside the lab; meeting people isn't always the easiest thing to do, but I'm lucky I've met each and every one of you. Laura, if it wasn't for meeting you all those years ago in San Francisco I might never have even considered Duke for graduate school so a lot of thanks to you. You've been an amazing friend and I honestly don't know what I would do without you. I was lucky to have the support and love of some amazing friends from back home in Florida who have been there for me every step of the way since my days as an undergraduate pretending to do research; Ashley, Karissa, and Ty your friendship means the world to me and I'm thankful to have you all in my life. Emily, Roketa, and Anthony, you've been there since that fateful trip to Beaufort when I knew the three of you would be people I would want to keep in my life through thick and thin. Scott, Brian, and Brad, we've had our fair share of wild times and now I'm finally going to join you guys with my Ph.D.; hopefully I'm half as successful as all of you are. Nick, Eve, Kelly, Beth, and Jenn, I don't know that you guys know exactly how much "Tuesday Dinner Club" has meant to me since we started it. You guys have been the perfect distraction from science and grad school and I cherish every moment we've spent together. Megan, Ellie, Steve, Amber, and Lin you guys have been awesome roommates and great friends to come home to at night after long days of doing science. Raquel, there is nothing remotely close to all of the thanks you deserve for putting up with my

complaining and questions and everything else since we've been friends. I'm so proud of all you've accomplished since we met and hope that our friendship continues to grow even when we don't live in the same state. Sherilynn, even though I know it's part of your job, I'd like to think that we've grown together and as much help as you've been to me I hope that I've been something other than a nuisance to you. I know I've missed a few names in here, but I'm just so grateful to have had such amazing people in my life to help me get through grad school.

Finally, I of course have to thank my family. My parents have prepared and pushed me for this my entire life and even though I didn't always appreciate it, I know that without your love and encouragement I could never have completed this journey. Thank you both so much for everything. Thanks also to the rest of my extended family, for being supportive and encouraging and being great examples of what to strive for in life.

Without each and every person that I have crossed paths with over the past years in school, I would never have grown into the person that I am today, both personally and professionally. For that, I am truly grateful.

# **1. Introduction**

## ***1.1 Introduction to Inflammatory Breast Cancer***

Inflammatory breast cancer (IBC) is a highly aggressive and, arguably the most lethal subtype, of breast cancer that was first described in 1924 by Lee and Tannenbaum (1). IBC has been shown to be distinct from other forms of locally advanced breast cancer (LABC) (2) and is relatively rare, accounting for only 1 to 5 percent of all cases diagnosed in the United States (3,4). Unlike other subtypes of breast cancer, the incidence of IBC in the United States seems to be increasing; however, this may be due to greater awareness in both patients and oncologists (4,5). IBC progresses extremely rapidly, with most patients being at Stage IIIb (chest wall/lymph node involvement) or Stage IV (distant metastasis) at the time of diagnosis (6,7). This initial high staging combined with late therapeutic intervention due to timing of diagnosis more often than not leads to poorer survival for patients with IBC. At the time of its description and the years following, IBC had a 5-year overall survival rate of less than 5% (median survival of 15 months), with local recurrence occurring in about half of patients (8,9). Due to the advent of multidisciplinary therapy modalities in the last 30 years, survival has increased with 5-yr rates being reported as high as 30% (10). Despite these progresses, the majority of patients experience recurrence and eventually succumb to the disease.

### **1.1.1 Clinical, pathological, and epidemiological features of IBC and patients**

One important distinction between IBC and other forms of LABC is that diagnosis is completely clinical and not based on any specific pathologic findings (6). IBC often presents as redness or erythema of the breast, which although diffuse early on, can extend to cover the entire breast (11,12). This can be accompanied by swelling or edema, which mimics an inflammatory response and as such, IBC is often mistaken for relatively harmless conditions such as mastitis or dermatitis. Physicians should be aware, however, that the lack of fever and immune involvement normally associated with infection rule out these possibilities (13). Another problem with diagnosis is that unlike other forms of LABC, there is usually no large mass or tumor upon palpation, and only a small number of cases show a discrete mass upon mammography (14). One classic symptom that is distinctive to IBC is presentation with peau d'orange (orange peel) appearance to the skin. Dramatic changes in skin color from red to purple (similar to bruising), ulceration of nodules, and nipple retraction are other clinical symptoms that can arise (15). Every case of IBC, however, is different and with presentation unique to each patient, diagnosis of IBC is difficult.

IBC tumor cells tend to present as clusters of tumor cells, termed tumor emboli, which have been shown to preferentially invade the dermal lymphatics (11). Blockage of the lymphatic system by these emboli underlies the significant edema that is a common clinical finding (12,13). Skin punch biopsies are the best procedure for analysis as it not

only captures breast tissue, but also the overlying skin. A vast majority of patients (55-85%) show some lymph node involvement, however, confirmation of ductal involvement cannot always be done making pathological findings good tools, but not 100% confirmatory.

Epidemiological research into IBC has been poor compared to other forms of LABC. This is in part due to the rarity of the disease, which makes large prospective clinical trials near impossible, but also to no agreed upon case definition in clinical diagnostics. The majority of data, from retrospective studies however, has offered some information about diagnosis rates. The incidence of IBC in North African countries – Tunisia, Morocco, and Egypt specifically, is much higher than North America with reports between 10% and 15% (7,16). Within the United States there is also a significant disparity between ethnic groups. IBC has historically been diagnosed in African American women with a 50% higher incidence in this population, while Asian and Pacific Islander women have been observed to have the lowest risk (17). Median survival is lower in African American (AA) women (18), and although the age of diagnosis is significantly lower in all IBC patients (median 58 years vs median 68 years), AA women are diagnosed at even younger ages (17). Much like LABC, obesity has been shown to correlate with IBC incidence (19). One retrospective study at MD Anderson Cancer Center noted that over 50% of patients had a BMI over 30, while cohort analysis has shown that women with a BMI above 26 are at a greater risk (12).

## 1.1.2 Molecular features of IBC

### 1.1.2.1 Incidence of molecular subtypes by genomic sequencing in IBC and non-IBC

Similar to its distinct clinical and histopathological presentation, IBC has certain molecular features that distinguish it from non-IBC. Some of these features have been shown to be involved in disease pathobiology, and as such, represent potential therapeutic targets. A recent whole-genome study of 137 IBC and 252 non-IBC patients attempted to first determine if one of the molecular phenotypes associated with breast cancer [defined by the Perou laboratory at UNC-Chapel Hill (20)] were more prevalent as a means to define aggressiveness (21). Although the Luminal A subtype was revealed to be more prevalent in non-IBC, all others showed little to no variation in this study (Table 1.1).

**Table 1.1 Prevalence of molecular phenotypes by genome sequencing**

<b>Phenotype</b>	<b>IBC (%)</b>	<b>Non-IBC (%)</b>	<b>p-value</b>
<b>Luminal A</b>	26 (19%)	105 (42%)	<0.001
<b>Luminal B</b>	26 (19%)	49 (19%)	1.000
<b>Basal type</b>	24 (17%)	31 (12%)	0.172
<b>Claudin-low</b>	23 (17%)	32 (13%)	0.288
<b>Normal-like</b>	8 (6%)	12 (5%)	0.638

### 1.1.2.2 Immunohistochemical findings

Immunohistochemical (IHC) analysis of biopsy tissue has revealed more about clinically relevant genomic alterations than whole genome sequencing as shown in Table 1.2. A recent study published late in 2015 confirmed used newer genomic technologies to confirm these data (22). Increased prevalence of the oncogenic drivers, epidermal growth factor receptor (EGFR/ErbB1) (23,24) and the related family member Her2/ErbB2 (25,26) has been observed in IBC tissues. A large proportion of IBC tissues are also negative for expression of progesterone and estrogen receptors (PR and ER, respectively) (4,27,28) and show characteristics of high vascularization (29).

**Table 1.2 Prevalence of immunohistochemical findings in IBC and non-IBC**

<b>Phenotype</b>	<b>IBC (%)</b>	<b>Non-IBC (%)</b>	<b>Reference</b>
<b>EGFR positive</b>	30	18	(23,24)
<b>Her2 amplified</b>	36-42	17	(25,26)
<b>ER/PR positive</b>	59	69	(4,27)
<b>Triple negative</b>	29	10-20	(30-32)
<b>Highly vascular</b>	51	14	(29)

### **1.1.2.3 EGFR/HER2 oncogenic signaling**

EGFR/ErbB1 is a transmembrane receptor tyrosine kinase that is overexpressed in over 25% of IBC cases (33) and shows a strong prognostic significance correlating with increased recurrence and poor 5-year survival rate (24). EGFR stimulates multiple signaling networks including the mitogen-activated protein kinase (MAPK), phosphatidylinositol 3-kinase (PI3K/Akt), and phospholipase C  $\gamma$  (PLC- $\gamma$ ) pathways which all promote proliferation, progression, and invasion and metastasis (34,35). ErbB2, also known as Her2, is another member of the EGFR family that also mediates through the same signaling pathways and also protein kinase C (PKC) and signal transducer and activator of transcription (STAT) pathways (36). Her2 has been shown to be amplified in upwards of 30% of IBC tissues (25), but there is conflicting evidence on whether this indicates a poorer or better prognosis. Inappropriate activation of either family member, by both paracrine and autocrine signaling, results in uncontrolled cell growth and resistance to apoptosis by therapeutics, playing a role in both tumorigenesis and progression.

### **1.1.2.4 Hormone receptor status**

Multiple studies have shown low levels of ER and PR expression in IBC tissues. These tissues are largely of the basal subtype (37), and although genomic studies reveal no differences at the transcriptome level, one study found that basal-type comprises 34%

of IBC cases compared to only 16% non-IBC by IHC (38). These tumors are most commonly triple negative (TN), based on the absence of ER, PR, and Her2, and as such fewer therapies are available as no targeted agents can be used (39-41). TN status in tumors is associated with increased risk of recurrence (38.6% vs. 22.6% non-TN) and metastasis (56.7% vs. 28.8 non-TN), which leads to poor overall survival (42.7% vs. 54-74% non-TN) compared to patients positive for some combination of ER, PR, and Her2 (31).

#### **1.1.2.5 Overexpression of eIF4G1**

##### *1.1.2.5.1 Tumor emboli formation*

Eukaryotic translation initiation factor eIF4G1 is a component of the eIF4F complex, which is involved in recognition of capped messenger RNAs (mRNAs), unwinding of secondary structure, and recruitment of ribosomes to RNAs for translation (42). Further work showed that eIF4G1 actually preferentially promotes the cap-independent translation of internal ribosomal entry site (IRES)-containing mRNAs (43). These sites, contained in the 5' UTR of mRNAs, allow for translation initiation in the middle of RNAs and can increase the rate of protein production even under times of stress, when cap-dependent translation is abrogated (44,45). The study that first identified eIF4G1 overexpression also revealed its contributions to the pathogenic properties of IBC through demonstrating that knockdown of eIF4G1 significantly inhibits the formation of IBC-specific tumor emboli (46). This inhibition was shown to be due to a decrease in E-cadherin protein expression, which promotes tumor emboli

formation through tumor cell-to-cell interactions rather than tumor-stroma interactions (47). E-cadherin mRNA does not contain an IRES, however, p120 catenin does (48) and p120 translation is significantly inhibited in eIF4G1 knockdown cells. p120 is a protein responsible for anchoring E-cadherin at the plasma membrane and regulating its expression (49,50). These changes in E-cadherin and p120 caused a significant decrease in the ability of IBC cells to grow in two *in vivo* models: one mouse and one chicken allantoic membrane (CAM).

#### 1.1.2.5.2 *Protection from hypoxia*

Hypoxia, specifically as it pertains to cancer, is defined as the situation when cancer cells are deprived of molecular oxygen (51). IBC tumor emboli, because of their structure, are inherently in a state of constant hypoxia and must overcome this lack of oxygen in order to survive (52). One feature of hypoxia beyond the canonical activation of hypoxia-inducible factor 1 (HIF-1) and activator protein 1 (AP-1), both of which are high in IBC tissue (53), is the inhibition of cap-dependent translation (54). This inhibition elicits an eIF4G1 and eIF4E binding protein 1 (4E-BP1)-dependent switch to cap-independent, IRES-mediated translation. Along with increasing p120 translation, they note that eIF4G1 drives the translation of vascular endothelial growth factor (VEGF), another IRES containing mRNA (52). VEGF, as a key regulator of the process of angiogenesis, enhances tumor vascularity and is able to protect these emboli and cells from the effects of hypoxia (55). This correlates strongly with the observation that IBC patient tissues show increased vascular density compared to non-IBC (29) and multiple

studies, both at the RNA and protein levels, that show increased expression of angiogenic factors such as basic fibroblast growth factor (bFGF), VEGF receptors VEGFR2 and VEGFR3, and VEGF-A, -C, and -D (56).

#### **1.1.2.6 Lymphangiogenesis and vasculogenesis**

Expression of certain subunits of the VEGF family leads to another process known as lymphangiogenesis (57). This refers to the branching, remodeling, and growth of lymphatic vessels from pre-existing ones and has been observed in both human tumors and animal models of IBC (58). This is in contrast to previously hypothesized models where tumor emboli escaped into already formed lymph vessels, however, work revealing increased lymphangiogenesis genes and higher fractions of proliferating endothelial cells in IBC patient tissue (59), is consistent with this metastatic behavior.

Another process used to increase oxygen and nutrient flow is vascular mimicry, or vasculogenesis, which allows tumors to form vessel-like structures without endothelial cells (60). Although animal studies hint at this possibility for disease biology (61), this has not been studied in patient populations to determine translation to clinic.

#### **1.1.2.7 Hyperactivation of the NF $\kappa$ B pathway**

Although *in vitro* and *in vivo* studies have determined that certain genes, including *E-cadherin*, *MUC1* (Mucin 1), *RhoC* (discussed in detail in Section 1.1.2.8.1), and *LIBC* (lost in breast cancer), have a role to play in IBC pathogenesis, none of these alterations are specific to the IBC-specific phenotype. With the advent of DNA

microarray technology, whole genome approaches can be used to identify specific molecular signatures that underlie diseases. While this has been exhaustively undertaken in non-IBC, only a handful of studies have done this with IBC and strikingly, they all land on the same pathway: the transcription factor, NF $\kappa$ B.

NF $\kappa$ B, or nuclear factor kappa-light-chain-enhancer of B cells, is a complex comprised of multiple subunits that all lead to control of transcription of nuclear DNA, activating pathways that in normal cells drives cytokine production and cell survival. In many cancers, NF $\kappa$ B is deregulated and constitutively active, activating proliferative gene networks and expression of proteins that enhance survival. The first such study in IBC utilized 81 patients (37 IBC, 44 non-IBC) and identified a 109-gene set that discriminated IBC from non-IBC (62). This gene set had a prediction accuracy of 85%, lending evidence to its overall robustness. Some of these genes were NF $\kappa$ B-related, associated with signal transduction, motility, and angiogenesis. A second study the following year used a smaller number of patients (16 IBC, 18 stage-matched non-IBC) and identified a 50-gene set that had an 88% prediction accuracy in a validation set (63). These genes were largely characterized by NF $\kappa$ B target genes and a follow up study confirmed this by real-time RT-PCR of genes and immunohistochemistry of the transcription factors themselves in patient tissue (64). Lerebours et. al. continued this and again confirmed increased NF $\kappa$ B activation, after careful extraction of a set of only

60 major NFκB genes, but also used this gene signature to show its power to discriminate cases based on prognosis (65).

#### **1.1.2.8 Hyperactivation of the MAPK pathway**

As previously mentioned, IBC is characterized by activation and overexpression of the ErbB family members EGFR and HER2. Both of these membrane-bound receptors converge on the activation of the MAPK pathway (66), which has been shown to drive proliferation, migration, angiogenesis, chromatin remodeling and transcription, and cell survival. The MAPK pathway is deregulated in multiple types of cancer (67) and has been heavily studied with a multitude of inhibitors available in clinic (68). In IBC particularly, MAPK activation has been linked to two other molecular pathways shown to be specific to IBC and dubbed “molecular determinants”.

##### *1.1.2.8.1 RhoC GTPase*

The first study linked MAPK activation to RhoC induced motility, invasion, and angiogenesis (69). RhoC is a small signaling GTPase that is associated with metastasis and tumor malignancy (70,71). van Golen et. al. found that RhoC was overexpressed in 90% of IBC patient tissues compared to only 30% for non-IBC (72). Further work went on to show that not only does knockdown of RhoC limit IBC aggressiveness, but also that overexpression in human mammary epithelial cells (HMECs) could recapitulate the IBC phenotype including tumor formation in mice (73). In an effort to target this pathway farnesyl transferase inhibitors (FTIs), which had been shown to modulate growth and motility in Ras-driven cancers (74), were tested. The authors found that treatment of

SUM149 IBC cells and HMEC-RhoC transfectants with an FTI could significantly reduce cell growth, migration, and invasion (75). Mechanistically, they revealed that although RhoC levels were not decreased, FTI treatment increased RhoB levels suggesting that RhoB plays a role in FTI-mediated reversion of the RhoC-driven phenotype. This pointed to the possibility of using FTIs clinically, which is discussed later in Section 1.1.3.2.

#### 1.1.2.8.2 *NFκB activation and ER negativity*

The second study linked EGFR/Her2 overexpression, commonly associated with IBC, to NFκB and estrogen receptor status (26). They utilized a MAPK signature, which was derived in MCF7 breast cancer cells with overexpressed EGFR/Her2 and is composed of 223 genes (76), to test its correlation with the NFκB phenotype. They also tested its correlation to ER status, as it has previously been shown that IBC is particularly prone to ER negativity and studies have correlated NFκB to this as a possible crosstalk pathway (77,78). Expectedly, the genes in this set correlated with other previously identified MAPK genes, but they also showed strong significance to the Notch, Wnt, VEGF, and Toll-like receptor pathways. Next, they correlated this to ER status, and showed that the signature had great predictive power, performing at 88% in identifying ER status. Finally, using IHC they revealed that the majority of tumors with transcriptionally active NFκB dimers also had strong staining for EGFR/HER2 ( $p < 0.004$ ), which also correlated with ER negativity ( $p = 0.031$ ). This study was suggestive of an

interaction between MAPK and NF $\kappa$ B, however, no conclusive mechanistic relationship had been defined until new data presented in Chapter 3 of this dissertation.

#### **1.1.2.9 Apoptotic dysregulation**

Evasion of apoptosis, or programmed cell death, is a feature of every cancer cell that continually grows and as such was included as a hallmark of cancer by Hanahan and Weinberg (79). This commonly occurs through changes in the machinery that drives apoptosis, be they pro- or anti- apoptotic. Comparison of IBC and non-IBC cell samples have revealed that IBC has a greater ability to sustain insults that would normally cause apoptosis; this will be discussed in greater detail in Section 1.2.2.1.

### **1.1.3 Current treatment options for IBC**

#### **1.1.3.1 Standard of care: multimodal therapy**

Since the first complete description of IBC in 1924 (1), and with the help of knowledge derived from non-IBC and other cancers, there have been steady advances in improving patient prognosis. Survival has improved from a 5% 5-year overall survival to what is now considered top survival at 40% 3yr OS, which is abysmal compared to a greater than 85% 3yr OS in non-IBC (5). Trimodal therapy, as it's used today in clinic, consists of neoadjuvant chemotherapy, in IBC this includes taxanes and anthracyclines, and for patients where indicated targeted therapies, followed by surgery, and radiation (80,81). Additional chemotherapy, in the form of either systemic or targeted therapies, may be given after radiation.

Taxanes are a class of diterpene molecules originally isolated from the plants of the genus *Taxus* (82). Taxanes stabilizes GDP-bound tubulin during the formation of microtubules, which inhibits the catalytic lengthening of microtubules. This leads to a block in cell division, making taxanes mitotic inhibitors (83). Paclitaxel and docetaxel are the two commonly used members of the taxane family (84), while a third member, cabazitaxel, was FDA-approved in 2010 for prostate cancer (85). The anthracyclines have four mechanisms of action including: 1) inhibition of topoisomerase II activity (86), 2) inhibition of DNA/RNA synthesis by intercalating between base pairs (87), 3) inducing the production of cell-damaging free radicals (88), and 4) induction of histone eviction (89). Daunorubicin, doxorubicin, epirubicin, idarubicin, mitoxantrone, and valrubicin are all FDA-approved and used in the treatment of multiple forms of cancer, as they are touted as the most effective anticancer treatments ever developed (90). Common drug combinations include doxorubicin/cyclophosphamide (AC) followed by taxane, docetaxel/cyclophosphamide (TC), and docetaxel/doxorubicin/cyclophosphamide (TAC), however doctors may prescribe other combinations and include other approved drugs as they see fit (91).

Although surgery is commonly performed after neoadjuvant chemotherapy, mastectomy alone offers no prognostic benefit to IBC patients (92). This is most likely due to the fact that even prior to chemotherapy, in part due to the aggressive nature of IBC, cancer cells have most likely already begun to metastasize. In IBC, mastectomies are

commonly performed with axillary lymph node dissection (7); however, without complete resection prognosis does not change. Because of this, in some patients, surgery is skipped in order to move onto radiation therapy or clinical trials for alternative therapies that may actually enhance prognosis and survival (93).

Radiation therapy in IBC is usually targeted to the breast and internal mammary regions, the chest wall, and any undissected lymph nodes (axillary, infraclavicular, and supraclavicular) (12,13,94). This large coverage area is necessary to target any partially invaded or invaded tumor emboli in the surrounding area. Treatment regimens differ drastically between hospitals and centers and as such review of the literature as to the benefits of radiotherapy can be unclear. A recent review, however, cited 5 yr. locoregional control rates from anywhere between 73% to 92%, which is still lower than the 97% rate for non-IBC (95).

#### **1.1.3.2 Targeted therapies**

Targeted therapies are any class of compounds that are directed toward a particular molecular aspect that is either cancer cell-specific or increased in cancer cells. This is advantageous compared to the systemic chemotherapies described above as they usually result in lower toxicity and enhanced efficacy against the tumor. Multiple targeted therapies have been developed for clinical use and some have been incorporated into treatment regimens for IBC.

Trastuzumab (Herceptin <sup>TM</sup>) is a monoclonal antibody that as mentioned earlier is commonly given in combination with neoadjuvant systemic chemotherapy (96). As trastuzumab targets ErbB2/Her2, it is only prescribed to patients that are denoted as Her2 positive by immunohistochemistry which accounts for upwards of 30% of IBC patients (25). Trastuzumab binds to domain IV of the extracellular region of Her2 inhibiting downstream signaling through the PI3K/Akt and MAPK pathways (97,98). Trastuzumab treatment has been shown to induce G1 phase cell cycle arrest through induction of the cyclin-dependent kinase (CDK) inhibitor p27, inhibit angiogenesis, and induce apoptosis in cells (99,100). Trastuzumab also functions to mediate immune-mediated cell death in a process known as antibody-dependent cellular cytotoxicity (ADCC) (101), which will be discussed in further detail in Section 1.1.3.3.2. Addition of this Her2-targeting therapy can significantly enhance pathological complete response (pCR) in patients with one study showing an increased pCR of 55% compared to only 20% for standard-of-care (102). The true efficacy of trastuzumab is somewhat hard to determine, however, because in multiple studies patients not receiving trastuzumab are switched to this arm mid-study if their cancer progresses. Resistance to trastuzumab, even in patients who initially respond well, usually occurs within one year (103,104). Trastuzumab's efficacy in targeting is so great that a second-generation drug, called trastuzumab emtansine (T-DM1 or Kadcyra <sup>TM</sup>) was developed for patients who failed front-line antibody therapy. T-DM1 is an antibody-drug conjugate (ADC) linking

trastuzumab to DM1, a potent antineoplastic agent that disrupts microtubules (105). Much like the monoclonal antibody alone, T-DM1 has shown great clinical efficacy in breast cancer when compared to standard-care therapies, and even to other Her2-targeted agents (106).

EGFR is a related family member to Her2 that is also overexpressed in IBC and multiple other cancer types. Monoclonal antibodies that mimic the effects described above for trastuzumab have been developed and are in use for other forms of cancer but have not been approved for IBC. Lapatinib (Tykerb™) is a dual tyrosine kinase inhibitor that blocks signaling downstream of both EGFR and Her2, by binding to the ATP pocket of the intracellular domains of these receptors preventing phosphorylation and activation (107,108). Multiple other mechanisms of action for lapatinib have been discovered over the years: inhibition of NFκB activation (109), downregulation of the anti-apoptotic protein survivin (110), induction of oxidative stress (111), and inhibition of expression of drug transporters shown to drive drug resistance (112,113). In clinic, lapatinib showed little to no adverse effects in Phase I trials and was moved to Phase II for both non-IBC and IBC. Lapatinib monotherapy has shown significant responses in clinical trials, with one study reporting a clinical response of 50% in Her2-overexpressing patients (114). Initial data showed that patients were more likely to respond if they were ER and PR negative, and declines in serum Her2 extracellular domain levels correlated with response. Response was significantly low in EGFR+/Her2-

tumors even though lapatinib targets both receptors. Recent Phase III clinical studies have shown that combining lapatinib with chemotherapy (paclitaxel/capecitabine), hormonal therapy (letrozole), or trastuzumab can lead to significant increases in overall response rate compared to the drugs alone (115-118). Again, these patients revealed that Her2 expression was essential to lapatinib's effect. Similar to trastuzumab, patients respond initially to lapatinib, but development of resistance occurs frequently and usually within the first 12 months after the initiation of treatment (119).

As mentioned earlier, angiogenesis genes and proteins have been shown to be upregulated in IBC and therapies to target them have moved forward in clinical trials. Bevacizumab is a human monoclonal antibody targeting VEGF, which was evaluated in a trial in combination with docetaxel and doxorubicin (120). In 20 patients, this combination revealed an overall response rate of 67%, which follow-up studies correlated to a decrease in phosphorylation of VEGFR2 (121). This led to the hypothesis that bevacizumab may not only affect angiogenesis, but may also have a direct anti-tumor effect. Pazopanib is a multi-target tyrosine kinase inhibitor that along with targeting VEGFR has also been shown to PDGFR (platelet-derived growth factor receptor), FGFR (fibroblast growth factor receptor), and c-KIT (stem cell growth factor receptor) (122). It is a potent inhibitor of angiogenesis and has had significant efficacy in renal cell carcinoma (123), soft tissue carcinoma (124), and ovarian cancer (125). A study in Her2+ IBC revealed that although the combination of pazopanib with lapatinib

increased overall response rates compared to either drug alone, it did not increase progression-free survival. There were however significant adverse events that resulted in treatment delays, dosing changes, and modifications, which may have influenced the outcome of the trial (126). Semaxanib is another small molecule inhibitor of VEGFR2 that showed decreased tumor blood flow by dynamic contrast-enhanced MRI; however, due to cardiac toxicities the trial was discontinued (127).

### **1.1.3.3 Immunotherapy**

Cancer immunotherapy represents a novel means of systemic, but specific, targeting of tumor cells at their site of origin and at metastatic sites. Immunotherapy is focused on using the body's own immune system to eradicate cancer and can be done in two ways: 1) enhancing or stimulating the present immune system or 2) infusion of immune system components (i.e. – man-made proteins). In IBC, unlike LABC and other forms of cancer, very little work and few clinical trials have explored immunotherapy as a treatment; a few smaller studies, however, have indicated that this may be useful to increase survival.

#### *1.1.3.3.1 Immunotherapy in IBC*

Wiseman et. al. published the first study of immunotherapy for the treatment of IBC in 1982 (128). In this study, 13 patients with IBC were first treated with cyclic chemotherapy followed by radical mastectomy. At the time of mastectomy, viable tumor cells were isolated, irradiated, and admixed with Bacillus Calmette-Guérin (BCG) vaccine prior to reinjection into patients. BCG vaccine is a vaccine prepared from an

attenuated strain of bovine tuberculosis bacillus, *Mycobacterium bovis*, which cannot cause disease in humans (129,130). The BCG vaccine is commonly used for preventing tuberculosis (although never in the USA and the Netherlands), however, a number of cancer vaccines use BCG as an adjuvant including those for bladder and colorectal cancer (131). The addition of BCG significantly inhibited relapse at a 21-month follow up, where in previous trials chemo/radiotherapy and radiotherapy alone yielded relapse in all patients. A 10-year follow up of this first trial revealed that 31% of patients were still alive 10 years later, with an apparent plateau of the survival curve at 5 years (132). In 1988, a trial using intratumoral injections of *Prionibacterium granuloso* KP-45 followed by chemotherapy was performed in diagnosed IBC patients (133). After initial inflammatory response, and surgical intervention, all patients were in “complete remission” with no local recurrences at 32 months. Eibl et. al. reported the use of allogeneic bone marrow transplantation (BMT) to induce a graft-versus-tumor (GVT) effect in IBC in 1996 (134). In this report, a patient with IBC received BMT from an HLA-matched sibling and reductions of liver metastasis along with clinical symptoms of graft-versus-host disease were seen within a few weeks. T cells obtained from the patient were cytotoxic *in vitro* against several cell lines, suggesting the feasibility of this therapeutic modality to induce GVT.

#### 1.1.3.3.2 *Antibody-dependent cellular cytotoxicity*

Although the previous clinical trials showed some efficacy, larger follow-up studies have either not been completed or showed little to no increase in survival.

Another mechanism by which immunotherapy can occur in the context of IBC is through the induction of antibody-dependent cellular cytotoxicity (ADCC) (101). As mentioned earlier, trastuzumab, a monoclonal antibody targeting Her2, has shown great activity clinically in IBC patients. Our previous work revealed that IBC cells are inherently resistant to the signaling inhibitory effects of trastuzumab, but that in the presence of immune cells trastuzumab can elicit a potent ADCC response (135). Since the time of our findings, other monoclonal antibodies such as panitumumab (EGFR-targeting) and pertuzumab (Her2-targeting) have also been evaluated clinically, however, no studies have been specifically done towards understating ADCC. ADCC represents a cell-mediated response wherein immune effectors, most commonly NK cells or eosinophils, lyse target cells that are bound by antibody. Antibodies bind to their target antigen (Her2, for example) and NK cells recognize the Fc portion of the antibody, binding with their CD16 receptor, inducing degranulation of NK cells and subsequent tumor cell lysis (136). ADCC is a broad-ranging immune function which can be mediated by a multitude of clinically available monoclonal antibodies in various cell types. Similar to chemo- and radio- therapies, however, therapeutic resistance to monoclonal antibody therapy in IBC is extremely rapid (103,104). The mechanism for this observed resistance in inflammatory breast cancer cells was unknown, but has possibly been elucidated in data presented in Chapter 4.

### **1.1.4 Unmet needs for the disease**

Although advances in the treatment of IBC have been made and lead to improved survival, most patients still progress and succumb to the disease. IBC research must continue in order to understand the basic biology of the disease that may allow better and earlier diagnosis and also allow for the development of therapeutics.

#### **1.1.4.1 Increased awareness**

As a rare disease, patients with IBC suffer from both a lack of knowledge about the basic biology of the disease and the disease itself. While most people in the world have heard of breast cancer, they have never heard of IBC; most physicians and oncologists have never seen a case of it. Clinically, the diagnosis of IBC is completely subjective, as emphasis for identification of the disease is based on physical symptoms, which differ drastically patient-to-patient. Due to misdiagnosis of the disease, patients have usually progressed to Stage IIIB or Stage IV. In 2010, at the First International Conference on Inflammatory Breast Cancer, a panel of IBC experts reached a consensus on the minimal requirements for diagnosis of IBC (137). This panel also developed education materials for distribution to both patients and physicians to increase awareness. Literature review by the panel revealed that although multimodal therapy shows some effectiveness in treating IBC, that standard changes from center-to-center. There is also no standard treatment for metastatic disease, which most patients either present with or progress to very rapidly.

#### 1.1.4.2 Use of molecular targets for diagnosis and treatment

Several factors have been identified that can differentiate IBC from non-IBC in patient tissue and in cell samples, as discussed in Section 1.1.2. For the time being, although these factors have been recognized in tissue samples, not enough evidence is there to use them as diagnostic or prognostic tools. Further studies may allow for this, which may permit for earlier detection in both primary and secondary IBC. The use of some of these factors, however, has guided the development of clinical regimens for drugs targeting these molecular features, i.e. Her2 and trastuzumab/lapatinib. Other features such as E-cadherin overexpression, RhoC activity, and NF $\kappa$ B hyperactivation have been targeted in preclinical and clinical trials and have shown minor success.

One preclinical study showed that targeting of E-cadherin with calcium chelation, E-cadherin antibodies, or viral therapy could disrupt emboli formation and tumorigenesis in a preclinical IBC model (138). Farnesyl transferase inhibitors (FTIs), which antagonize the function of RhoC, showed significant preclinical success in mouse models of IBC and continued to clinical trials. Breast cancer patients treated with tipifarnib in combination with chemotherapy showed a slightly increased clinical complete response, with a 60% partial response, which yielded an overall clinical response of greater than 75% (139). Bortezomib, a proteasome inhibitor that shows potent activity against NF $\kappa$ B, showed a modest response rate in patients with metastatic breast cancer (140). The combination of these trials in non-IBC with the knowledge of

expression and activity in IBC suggests that some of these therapies may be efficacious in IBC; however, no clinical trials in IBC patients have been performed in this subset.

#### **1.1.4.3 Elucidation of therapeutic resistance mechanisms**

Although Her2-targeting therapies have shown the most success in IBC clinical trials, and have been added into treatment regimens where applicable, almost every patient rapidly develops resistance.

Multiple mechanisms for trastuzumab resistance in non-IBC have been described in detail. At the receptor level, a mutation leading to truncation of the Her2 receptor through proteolysis generates a p95 isoform, which has constitutive kinase activity but is insensitive to trastuzumab (141). Expression of Mucin-4, an *O*-glycosylated membrane protein, has been shown to “mask” the trastuzumab-binding site on Her2, effectively driving trastuzumab resistance in breast cancer cells (142). High expression of insulin-like growth factor 1 receptor (IGF-1R) was shown to induce trastuzumab resistance in Her2-expressing SKBR3 cells (143). Intracellularly, PTEN loss (144), downregulation of CDK inhibitor p27 (145), Src activation (146), and activating mutations in PIK3CA (147) all significantly contribute to inherent and acquired resistance to trastuzumab. Our lab was the first to identify the mechanism of resistance to trastuzumab in IBC, demonstrating that upregulation of the anti-apoptotic molecules X-linked inhibitor of apoptosis (XIAP) and survivin are associated with resistance (135).

Resistance to lapatinib occurs with differing mechanisms that are distinct from those applying to trastuzumab. Loss of PTEN (148), expression of p95 Her2 (141,149), IGF-1R expression (150), and mutations in PIK3CA (114) have all been demonstrated to have no effect on lapatinib sensitivity. Activation of the forkhead box transcription factor FOXO3A, which is normally repressed by PI3K/Akt activity, was shown to mediate resistance in two cell lines (BT474 and SKBR3) (150,151). This increases ER signaling in these cells and was confirmed in non-IBC patient biopsies by demonstrating FOXO3A activation and increased expression of ER. Activation of FOXO3A also increases HER3 expression (152). Due to the connection between ER and NFκB, it's not unsurprising that further work revealed that these same cells had increased NFκB activity mediated by increased RelA (153). Both targeting of RelA reversing sensitivity and examination of RelA activation in non-responding patients substantiated the claims made by *in vitro* analysis. Another study also revealed NFκB signaling as the cause of lapatinib resistance in breast cancer cells further validating NFκB as a central mediator (154). NFκB has been shown to increase expression of survivin and also Bcl-2 and Mcl-1, two other anti-apoptotic proteins identified in colorectal cancer cells to mediate lapatinib resistance (155).

Although these studies revealed mechanisms for the resistance to this powerful drug, no studies at the time had been performed in IBC. Using two different cell line models of IBC, our lab developed models of acquired therapeutic resistance

(156). Resistance in these two lines was determined to be dependent on upregulation of the anti-apoptotic protein, XIAP (further discussed in Section 1.2.3), again highlighting the importance of apoptotic dysregulation in resistance. Further work by our group delineated a novel mechanism of action for lapatinib in mediating oxidative stress, which was inhibited in these XIAP-overexpressing cells although the full mechanism was not elucidated (111). As Her2 amplification and EGFR activation drives the growth of most IBC tumor cells, defining the exact mechanisms of resistance and developing strategies that target these mechanisms could affect a large population of IBC patients.

## ***1.2 Apoptotic dysregulation and therapeutic resistance in cancer***

### **1.2.1 Overview of apoptosis**

In order to understand how dysregulation of the apoptotic machinery can contribute to the pathobiology of IBC and therapeutic resistance, one must first understand all of the components that regulate apoptosis. Apoptosis is a form of programmed cell death that is ATP-dependent and extremely regulated, for which the 2002 Nobel Prize was awarded. It plays a vital and integral role during development and in the maintenance of normal tissues. For apoptosis to occur correctly, a copious number of factors must cooperate in perfect sync, and when they do not a range of pathological conditions from autoimmune disorders to muscular atrophy to cancer can occur. Unlike necrosis, which transpires after cellular damage, apoptosis does not activate an immune response, but rather phagocytic cells engulf apoptotic bodies

preventing damage to nearby cells. Approximately 60 million cells undergo the process of apoptosis every day in the human body. No matter how apoptosis is activated (further explained below), the final execution is dependent on a group of enzymes known as caspases (157,158).

Caspases, or cysteine-dependent aspartate-directed proteases, are a family of enzymes that play an essential role in apoptosis. They are separated into two groups: 1) the initiator caspases (caspase -2, -8, -9, and -10) and 2) the effector caspases (caspase -3, -6, -7). Caspases are originally synthesized as pro-caspases, an inactive form, which contains a prodomain and two functional subunits. The initiator caspases contain specific domains, such as a CARD (caspase recruitment domain) or a DED (death effector domain) domain, that mediate clustering allowing them to undergo autocatalytic cleavage. These activated initiator caspases then go on to activate the effector caspases, which cleave specific cellular substrates and proteins inducing cell death (159). A caspase-independent apoptotic program mediated by a cellular component known as apoptosis-inducing factor (AIF) has also been identified (160).

#### **1.2.1.1 The extrinsic pathway**

The extrinsic signaling pathway of apoptosis involves the binding of ligands to transmembrane death receptors that are all of the tumor necrosis factor (TNF) receptor superfamily. TNF-TNFR1/2, Fas ligand-Fas/CD95, and TNF- $\alpha$ -related apoptosis-inducing ligand (TRAIL)-death receptor (DR) 4/5 constitute the ligand-receptor pairs

that are known to induce cell death (161,162). Ligand binding induces receptor oligomerization and recruitment of adaptor molecule Fas-associated death domain (FADD) (163,164). FADD then recruits initiator procaspases-8 to form the death inducing signaling complex (DISC), which allows cleavage to form the functional caspase-8 (165). Two cell types have been identified as they have two different reactions after activation here: Type I cells, in which caspase-8 activation is sufficient to cause cell death, and Type II cells, in which mitochondrial damage – and activation of the intrinsic pathway – is necessary to induce full activation of caspase-3 (166).

#### **1.2.1.2 The intrinsic pathway**

The intrinsic pathway of apoptosis, also known as the mitochondrial pathway, is non-receptor mediated. It can be activated by numerous stimuli including viral infections, toxin damage, free radicals/oxidative stress, DNA damage, as well as by radiotherapy and chemotherapeutics (167,168). These stimuli activate a set of proteins of the Bcl-2 family (explained in greater detail in Section 1.2.2.1.1) leading to the oligomerization of Bax and Bak proteins (168). These proteins induce mitochondrial outer membrane permeabilization (MOMP), which releases molecules such as cytochrome *c*, second mitochondrial activator of caspases (Smac/DIABLO), endonuclease G, AIF, and Omi/HtrA2 (169). After being translocated to the cytoplasm, cytochrome *c* binds to the C-terminal domain of Apaf-1, a cytosolic protein with a CARD domain (170). Following this dATP and procaspase-9 are recruited forming a complex

known as the apoptosome. The apoptosome then recruits and activates caspase-3 (171,172).

### **1.2.1.3 Anti-apoptotic proteins**

#### *1.2.1.3.1 Bcl-2 family*

The Bcl-2 family is an evolutionarily conserved set of proteins, composed of approximately 25 genes that have been identified to date. All members of the family share at least one of the Bcl-2 homology (BH) domains: BH1, BH2, BH3, and BH4. The members are grouped into the anti-apoptotic and pro-apoptotic groups; all anti-apoptotic members contain a BH1 or BH2 domain, while the pro-apoptotic proteins contain a BH3 domain (173). The anti-apoptotic members (Bcl-2, Bcl-xL, Bcl-w, and Mcl-1) maintain mitochondrial integrity, preventing apoptosis by binding and inhibiting the pro-apoptotic function of the BH3-containing proteins. The BH3 proteins (Bim, Bid, Bad, Noxa, and Puma) respond to death signals and activate two final proteins Bax and Bok, which induce MOMP (174).

#### *1.2.1.3.2 IAP family*

The inhibitor of apoptosis (IAP) family of proteins is also evolutionarily conserved, and the human IAP family is composed of 8 members. The IAPs are functionally and structurally related with each family member being composed of one to three baculoviral IAP repeat (BIR) domains (175,176). Some members contain a really interesting new gene (RING) domain that mediates E3 ligase activity, allowing some family members to ubiquitinate other proteins (177), driving them to degradation or

enhancing their function (178). The IAP family is unique compared to the Bcl-2 family in that they can block both the intrinsic and extrinsic pathways of apoptosis (179). The IAPs bind specific caspases through these BIR domains (179), while one specific member, XIAP, can inhibit caspases -3, -7, and -9 (180). Through ubiquitination, they target the caspases themselves (181,182), and other pro-apoptotic proteins such as Smac/DIABLO and AIF (183). They can also autoubiquitinate or target other proteins – TNF receptor-associated factors (TRAFs), receptor-interacting protein kinases (RIPKs), and NF $\kappa$ B-inducing kinase (NIK) – that can drive so-called IAP-mediated signaling (183).

## **1.2.2 Dysregulation of the components of the apoptotic machinery**

### **1.2.2.1 Extrinsic components**

Modifications to the death receptor-dependent signaling pathway have been found in multiple cancers. Transcriptional silencing of Fas and somatic mutations in the coding sequence can lead to the oncogenic formation of germinal center (GC)-derived B-cell lymphoma (184), while this same loss in other cancer subtypes can lead to evasion of apoptosis mediated by FasL expressing cytotoxic T cells (185,186). Tumor cells can also aberrantly express FasL, avoiding autocrine Fas/FasL binding, and target helper T cells in the microenvironment that may be capable of recognizing antigens (185,186). Deletion or mutation of the TRAIL receptors (DR4/5) has also been demonstrated in cancers (187,188). Deficiencies in downstream effectors such as FADD and c-FLIP have also been seen (189,190). Low FADD expression has been noted in acute myelogenous leukemia

(AML) and has been correlated with resistance to therapy and poor prognosis (191). High c-FLIP expression has been observed in colon cancer samples and cell lines where it can suppress caspase-8 activity and mediate resistance to TRAIL (192). Targeting of c-FLIP by metabolic inhibitors has shown promise in sensitizing various cancer cells to FasL/TRAIL mediated death (193).

#### **1.2.2.1 Intrinsic components**

Similar to the extrinsic pathway, alterations in the components of the intrinsic pathway have been demonstrated in cancer. Transcriptional silencing of *Apaf-1* has been seen in metastatic melanoma and reduced expression of the protein correlates with disease progression (194). Plasma-membrane sequestration of Apaf-1 in B-cell lymphoma has been shown to mediate chemoresistance (195). In addition to Apaf-1 loss, modulators of apoptosome formation have also been implicated in cancer pathogenesis (196). Reduced expression of the pro-apoptotic members of the Bcl-2 family can lead to the inhibition of mitochondrial outer membrane permeabilization (MOMP) (197). *BAX* inactivation due to frameshift mutations caused by single nucleotide substitutions is present in colon, stomach, and hematopoietic malignancies (198-200). Bak expression is significantly reduced in primary colorectal adenocarcinoma (201) and knockout experiments have revealed that Bax/Bak-double-deficient mouse embryonic fibroblasts undergo oncogenic transformation at rates similar to *p53*-null fibroblasts (202).

### 1.2.2.1 Caspases

Suppression of caspase activity can abrogate both the extrinsic and intrinsic pathways of apoptosis and allow survival of cells that should be removed. Hypermethylation of caspase-8 leading to decreased expression has been reported in neuroblastoma, medulloblastoma, and small cell lung cancer (203-205). Caspase-8 inhibition has been correlated with drug resistance whether mediated by methylation or c-FLIP overexpression (206,207). Interferon can drive transcriptional activation of caspase 8 (208), and combined with studies using demethylating agents or gene transfer (206), it is well established that restoration of caspase 8 expression can sensitize to therapeutic apoptosis. Caspase-3 mutations have been seen in the MCF-7 cell line, suggesting that mutation or deficiency may be found in tumor samples (209).

### 1.2.2.1 Anti-apoptotic proteins

#### 1.2.2.1.1 *Bcl-2 and Bcl-xL*

Bcl-2 and Bcl-xL function by binding the other pro-apoptotic members of the Bcl-2 family preventing their insertion into the mitochondrial membrane and induction of MOMP. Bcl-2 overexpression is common in many subtypes of cancer including mesothelioma, diffuse large B cell lymphomas (DLBCL), acute myelogenous leukemia (AML), glioblastoma, melanoma, and prostate cancer (210). In non-Hodgkin's lymphoma, a translocation between chromosomes 14 and 18 places the open reading frame of *BCL-2* within the immunoglobulin heavy chain (IgH) locus, dysregulating expression at the transcriptional level (211). Loss of microRNAs that control *BCL-2*

expression and gene hypomethylation are also contributing factors to lead to elevation of Bcl-2 protein expression (212,213). Due to its role in inhibition of apoptosis, Bcl-2 expression has been linked to resistance to apoptosis by a variety of stimuli, including growth factor loss, hypoxia, oxidative stress, and therapeutic intervention. Almost every chemotherapeutic used in the treatment of cancer, regardless of the primary mode of action, relies on Bcl-2/Bax-dependent mechanism for cytotoxicity. This most likely explains why Bcl-2 expression has been seen as an independent prognostic factor for both solid and liquid tumors treated with chemotherapy (214). Bcl-xL overexpression has been reported in fewer malignancies [multiple myeloma (MM), Kaposi's sarcoma, and colorectal adenocarcinoma] (201,215,216), and in prostate cancer where it is associated with disease progression and androgen resistance (217).

#### 1.2.2.1.2 IAPs

High expression of multiple members of the IAP family is found in numerous malignancies and is often associated with chemotherapeutic resistance, making expression a marker of poor prognosis in these cancers (218). Prognostic significance does, however, vary between the different IAPs. XIAP as a prognostic factor will be covered in Section 1.2.3.2, where overexpression does not always correlate with poor outcome. Survivin is another member of the IAP family whose expression is limited to embryonic tissues and is absent in almost all adult tissues; its expression, however, was noted in every tumor cell line in the NCI 60 cell line panel, but no untransformed cells

(219). *In vivo*, expression is frequent in pancreas, prostate, lung, and breast cancers, with little to no expression in corresponding non-neoplastic cells (220).

In renal cell carcinoma, esophageal squamous cell carcinoma, medulloblastoma, and other malignancies a chromosomal amplification event of the 11q21-q23 region leads to increased cIAP1 and cIAP2 expression (112,221). Comparisons of mouse tumors reveal similar amplification in the syntenic region at mouse 9qA1 (222). In 50% of extranodal marginal zone mucosa-associated lymphoid tissue (MALT) B-cell lymphomas, a translocation event between chromosomes 11 and 18 t(11;18)(q21;q21) results in a fusion between the *MALT1* and *cIAP2* genes (223). The resulting chimeric protein promotes a positive feedback loop by activating NFκB (224), which in turn transcriptionally activates the *cIAP2* promoter leading to increased expression of cIAP2, c-FLIP, and MnSOD. cIAP1 in combination with YAP (located at 9qA1) can transform murine ES cells, and in addition, exhibits a similar feature in combination with c-Myc overexpression in p53-null hepatoblasts (222).

#### **1.2.2.1 Apoptotic dysregulation in inflammatory breast cancer**

Molecular analysis of IBC and non-IBC has identified that dysregulation of apoptosis may be a unique feature that can distinguish IBC. In the first study to note this, Bertucci et. al. discovered high expression of the STE20-related kinase adaptor protein beta enzyme, ALS2CR2 (62), which is known to directly interact with XIAP and enhance the kinase activity of c-Jun terminal kinase (JNK) (225). A second study

revealed increased expression of BAX, which although pro-apoptotic, may reflect increased apoptosis resulting in high cell turnover (40). Gene set enrichment analysis performed by Iwamoto et. al. found that gene sets associated with apoptosis were enriched in IBC compared to non-IBC tumors of the same molecular phenotype, revealing IBC-specific and receptor-specific changes (226). As mentioned earlier (Section 1.1.2.7), NF $\kappa$ B hyperactivation is a highly relevant molecular determinant of IBC (63,65). Under the transcriptional control of NF $\kappa$ B are a number of anti-apoptotic genes including XIAP, Bcl-2, Bcl-xL, MnSOD, survivin, cIAP1/2, and TRAF1/2 (227). Members of the IAP family may also drive NF $\kappa$ B activation, resulting in the enhancement of a feedback loop (228). Our recent work in understanding the acquisition of therapeutic resistance in IBC demonstrates increased expression of a protein known as the X-linked inhibitor of apoptosis protein, XIAP, and its necessity for resistance to therapy in IBC cells (156); the regulation and functions of XIAP will be explained in Section 1.2.3, while the findings in our seminal papers in IBC will be further described in Section 1.4.2. This indicates that understanding the mechanisms and effectors that drive apoptosis inhibition in IBC may lead to the development of better therapeutics that could enhance the efficacy of chemo- or radio- therapy in patients.

### **1.2.3 X-linked inhibitor of apoptosis protein (XIAP)**

The X-linked inhibitor of apoptosis (XIAP) has been described as the most potent member of the IAP family because of its ability to impede the activity of effector

caspases -3 and -7 and also the initiator caspase-9 (180). Caspases -3 and -7 bind to the same portion of the protein in the BIR2 domain (229), while caspase-9 binding domain is via the BIR3 domain (230). The binding constant for caspases -3 and -7 are 100 times stronger for XIAP than any other IAP family member; this has been posited to be due to sequence and structure features that are not contained in the other members (231).

### **1.2.3.1 Regulation of expression level**

#### *1.2.3.1.1 Transcriptional*

XIAP is ubiquitously expressed in all cells throughout the body, however the level of expression can be highly heterogeneous (232,233). Expression is typically cytoplasmic, however, studies have noted both nuclear and mitochondrial expression of XIAP (234). XIAP is located on the X chromosome (position q25) (235) and can be transcriptionally controlled by a multitude of transcription factors: positively by NF $\kappa$ B (236), STAT5 (237), STAT1 (238), Sp1 (239); and negatively by p53 (240,241). Although the binding sites adjacent to the transcriptional start site have been identified, not much is known about the contexts in which these transcription factors regulate expression. NF $\kappa$ B is the most widely studied transcription factor that activates XIAP expression. After the initial discovery that NF $\kappa$ B could increase mRNA levels in 1998, multiple studies have confirmed this result and extended it to show that this increased XIAP can drive therapeutic resistance in a variety of cell types (242). As mentioned previously, IBC is characterized by hyperactivation of the NF $\kappa$ B signaling pathway (64,65) and this may play a role in the increased XIAP mRNA expression noted in IBC cell lines compared to

non-IBC cells (135). This in fact correlates with decreased sensitivity of these cells to therapeutics compared to subtype-matched non-IBC cell lines (unpublished data). Examination of IBC and non-IBC patient tissue in a large study did not mimic the RNA changes associated with cell lines (226), while our own studies showed that increased XIAP was not due to transcriptional changes (156).

#### 1.2.3.1.2 *Translational*

After identification of the location of XIAP in both human and mouse chromosome architecture, it was revealed that the mRNA in both species contained an extraordinarily long 5' UTR. The human UTR is approximately 1.7 kb in length, while the mouse UTR is over 5 kb (243). There is very little sequence similarity in this area with the exception of a small region (350 nt) located just upstream of the initiation codon, possibly containing regulatory elements (244). Prediction of secondary structure demonstrated that XIAP might contain an IRES element, which was confirmed by the Korneluk lab using bi-cistronic mRNA constructs. In that same study, the authors narrowed down the IRES to a 162 nt region, identified a 12 nt polypyrimidine tract that was essential for IRES activity, and also ascertained that including the 5' UTR in XIAP mRNA plasmids increased resistance to apoptosis compared to plasmids with only the open reading frame (ORF) (243). With the advent of newer technologies, it was revealed that XIAP in fact has two isoforms with differing 5' UTR lengths (short-323 nt and long-1.7kb), both containing the IRES sequence (244). Work from our lab and others have shown that XIAP is continuously translated even during periods of cellular stress and

that IRES activity is critical to this process, however, the mechanism of regulation in these contexts has not been elucidated (156,243-245).

eIF4G1 has previously been shown to enhance IRES-mediated translation of cellular mRNAs in IBC (46,52) and in this study (discussed in Chapter 3), we reveal that eIF4G1 also drives XIAP expression in SUM149 IBC cells. Beyond the translational control by eIF4G1, other factors have been identified that can positively or negatively regulate its translation. These factors, termed IRES trans-acting factors (ITAFs) (246), can physically interact with XIAP and either increase mRNA stability or directly recruit ribosomes to enhance translation. After sequence characterization of the IRES, UV-crosslinking and mass spectroscopy identified the first two of these factors, the autoantigen La (247) and the heterogeneous ribonucleoprotein hnRNP (248). The autoantigen La regulates multiple aspects of RNA metabolism including processing of tRNAs (249), regulation of RNAPol II transcription (250), and translation of RNAs both viral and cellular (251-253). Interestingly, La is only necessary for IRES-mediated not cap-dependent translation of XIAP, and is specifically cleaved during apoptosis (254). This cleavage forces accumulation of La in the cytoplasm where it can enhance XIAP IRES activity. hnRNP is the most abundant RNA binding protein (RBP) in cells and exists in two forms, hnRNP1 and hnRNP2 (255). Cellular levels of hnRNP1/2 have been shown to correlate with XIAP IRES activity and similar to La, have both been shown to accumulate in the cytoplasm during apoptosis where it may enhance XIAP

translation (256). On the negative regulation side, hnRNP A1 also binds to the RBP binding site and accumulates in the cytoplasm during apoptosis; it does not, however, compete with La for binding (257). hnRNP A1 has also been shown to negatively regulate VEGF, c-myc, and Apaf-1 IRES activity, while it enhances FGF2 IRES activity (258).

While other RBPs including PTB (259), PDCD4 (260), and HuR (261) have been identified as XIAP ITAFs, the most interesting ITAF for IBC biology may be the proto-oncogene MDM2 (murine double minute 2 homolog) (245). MDM2 is deregulated in many tumor types and exerts its oncogenic effect by inhibiting p53 in most contexts, leading to therapeutic resistance, as cells cannot undergo apoptosis (262). During cell stress, when XIAP is upregulated, MDM2 is dephosphorylated and remains in the cytoplasm where it can bind to XIAP and enhance translation (263). Functionally, this binding of MDM2 to XIAP was shown to alter resistance to ionizing radiation in neuroblastoma and leukemia cell lines (245). In a recent study using lapatinib resistant cells, including the SUM190 IBC cell line, MDM2 was shown to drive lapatinib resistance in a p53 independent manner (264). This is of importance for IBC as over 50% of IBC tumors are p53 mutated. In concordance with this, MDM2 antagonization with Nutlin-3 reverses lapatinib resistance and it's interesting to speculate whether the MDM2-XIAP interaction may play a role in this.

#### 1.2.3.1.3 *Post-translational*

Identified post-translational modifications of XIAP have been revealed which increase the stability of XIAP protein by blocking autoubiquitination of the protein and subsequent degradation (177).

XIAP can be phosphorylated by two different proteins at serine 87, AKT1/2 (265) and Raf-1 (266). This phosphorylation event stabilizes XIAP protein, increasing survival from therapeutic apoptosis. These events could be potent mechanisms by which XIAP expression is increased. In IBC tumors, Her2 is commonly amplified and feeds directly into AKT, which could explain the heightened ability of IBC to resist therapeutic apoptosis.

Protein kinase C has also been possibly shown to regulate XIAP stability (267). Although it is unclear the true mechanism of this regulation, it was demonstrated that treatment with PMA, which activates PKC, can inhibit ubiquitination of XIAP by TRAIL during apoptosis. PKC-mediated stabilization of XIAP can also drive drug resistance, however, whether this is through a direct binding event or phosphorylation is unknown (268).

Another study demonstrated that the intracellular domain of Notch-1 could also enhance XIAP stability (269). Unlike AKT, this enhancement was due to a direct interaction between the transactivation domain of Notch and the RING domain of XIAP. This interaction prevented the binding of E2 ligases and inhibits the ubiquitination of XIAP both *in vitro* and *in vivo*. Notch has been shown to be

overexpressed in a multitude of cancers and its expression correlates with drug resistance (270). In IBC, a recent study revealed that targeting of Notch with a gamma secretase inhibitor significantly reduced the anchorage independent growth of SUM149 and SUM190 cells, and also enhanced the radiosensitivity of both cell lines (271). Whether this is directly due to inhibition of XIAP stability was not shown, however.

### **1.2.3.2 Caspase-independent signaling**

#### *1.2.3.2.1 NF $\kappa$ B activation*

As discussed in Section 1.2.3.1.1, XIAP can be transcriptionally activated by NF $\kappa$ B, but XIAP can also activate NF $\kappa$ B forming a feed-forward positive activation loop. Hofer-Warbinek et. al. first described increased nuclear accumulation and transcriptional activity of the NF $\kappa$ B subunit p65 (RelA) in cells with XIAP overexpression (272). Further work revealed that E3 ligase activity, mediated by the RING domain, was essential for XIAP-mediated NF $\kappa$ B activation (273). Downregulation of the negative regulator, I $\kappa$ B $\alpha$ , was also noted in cells where XIAP was overexpressed. Some follow up studies hinted at the involvement of TGF- $\beta$  associated kinase (TAK1), which is ubiquitinated by XIAP, linking this to the TGF $\beta$  pathway (274). Work in normal mouse mammary cells and 4T1 murine breast cancer cells further confirmed a role for XIAP in TGF $\beta$ -mediated NF $\kappa$ B activation, which again involved TAK1 and the RING domain of XIAP (275). In contrast to this, a 2007 study demonstrated that the RING domain was not essential for NF $\kappa$ B activation by XIAP (276). Lu et. al. revealed that XIAP has the ability to dimerize at its BIR1 domain, which leads to binding to TAK1

associated binding protein (TAB1). TAB1 physically mediates an association with TAK1 and IKK $\beta$ , a positive regulator of NF $\kappa$ B, leading to potent NF $\kappa$ B activation (277). XIAP has also been shown to ubiquitinate and regulate the expression of the copper homeostasis protein COMMD1 (278), which degrades NF $\kappa$ B subunits halting transcriptional activity (279). IBC has been shown to have an NF $\kappa$ B hyperactivation phenotype and work presented in Chapter 3 demonstrates that XIAP is critical for driving this.

#### 1.2.3.2.2 *Akt activation*

It was first noted in ovarian cancer cells that overexpression of XIAP using an adenoviral cDNA construct led to increased AKT phosphorylation, indicative of AKT activation (280). In these cells this was associated with increased resistance to therapeutic apoptosis. Our lab further confirmed this by showing that XIAP knockdown in SUM190 cells decreases p-AKT levels (135). Van Themsche et. al. elucidated that XIAP ubiquitinates phosphatase and tensin homolog (PTEN), a phosphatase that directly targets AKT (281). Ubiquitination of PTEN increases its nuclear accumulation, sequestering it from AKT, whereas loss of XIAP allows PTEN to remain in the cytoplasm and dephosphorylate AKT. This was confirmed *in vivo* in XIAP (-/-) mouse embryonic fibroblasts (MEFs), which showed higher PTEN levels, less ubiquitination, and more cytoplasmic localization.

#### 1.2.3.2.3 ROS modulation

Multiple studies have revealed that XIAP has a role to play in the inhibition of reactive oxygen species (ROS) and oxidative stress. Using XIAP null MEFs, Resch et. al. showed that antioxidants thioredoxins-2, NAD(P)H dehydrogenase quinone 1, superoxide dismutase 2, and heme oxygenase 1 were decreased compared to wild-type MEFs (282). Kairisalo et. al. (283) and Zhu et. al. (284) presented similar results in neuronal cells in culture and *in vivo*, respectively. Only Kairisalo et. al. demonstrated a mechanism for the increased antioxidant expression, through NFκB activity (283). This is of importance in IBC as our previous work revealed that cells with acquired therapeutic resistance, and XIAP overexpression, were also resistant to oxidative stress (111). If XIAP and NFκB do in fact play a role here, targeting of either may result in reversal of resistance and sensitization to therapeutics.

The regulation of COMMD1 and copper homeostasis may also modulate oxidative stress and drive redox adaptation (further discussed in Section 1.3). In addition to its ability to activate NFκB, XIAP-mediated ubiquitination of COMMD1 can also decrease intracellular free copper levels, which can generate ROS (285). XIAP also ubiquitinates CCS (copper chaperone for superoxide dismutase) enhancing its ability to activate SOD1, although the mechanism is not clear (286). XIAP is itself also regulated by copper, which induces a conformational change in XIAP protein abrogating its caspase binding abilities, and sensitizing cells to apoptosis (287).

### 1.2.3.2 XIAP as a prognostic factor

Due to its unique ability to block both the intrinsic and extrinsic pathways of apoptosis, XIAP represents a striking mechanism for cancer cells to evade apoptosis in the face of tumor microenvironment stresses as well as during therapeutic administration. Although expressed in every cell throughout the body, XIAP upregulation has been noted in many subtypes of cancer (288). Its expression has been linked to resistance to therapy, lymph node metastasis, poor clinical outcome, increased metastasis, increased risk of relapse and increased tumor recurrence (289-297). In non-small cell lung cancer, XIAP overexpression is noted (298), however, certain studies have actually correlated high expression with a more favorable prognosis (299). This has been mimicked in a prostate cancer model where XIAP deficiency promotes more aggressive tumor growth (300).

The X-linked IAP-associated factor (XAF) 1 is a negative regulator of XIAP function and anti-caspase activity, which was first identified by yeast two-hybrid screens (301). *XAF1* is located on chromosome 17p13.2, near the *p53* gene, and consists of eight exons which code for a protein with seven zinc finger domains (302). Similar to XIAP, *XAF1* is expressed ubiquitously in normal cells; however, its expression in cancer cells is extremely low (302). Confirmation of protein expression has been done in multiple cell lines and tissues (302-304). Loss of heterozygosity in the chromosomal region where *XAF1* is located led to initial hypotheses that it may be a tumor

suppressor; however, no mutations or other perturbations have been described in tissues suggesting an alternative regulatory mechanism (301,302). Multiple studies have revealed XAF1 as a prognostic biomarker and therapeutic target. These studies revealed that reintroduction of XAF1, either ectopically or endogenously, induces sensitization to various apoptotic triggers of both the intrinsic and extrinsic pathways (305,306).

### ***1.3 Redox adaptation and therapeutic resistance in cancer***

#### **1.3.1 Redox homeostasis: ROS production and elimination**

##### **1.3.1.1 Reactive species**

Reactive species (RS) include two major forms: reactive oxygen species (ROS) and reactive nitrogen species (RNS). Reactive oxygen species (ROS) are mainly comprised of neutral molecules ( $\text{H}_2\text{O}_2$ ), radicals (hydroxyl radicals), and ions (superoxide) (307,308). Superoxide anion ( $\text{O}_2^{\cdot-}$ ) is generated by a one-electron process that adds an electron to molecular oxygen ( $\text{O}_2$ ) (309,310). Superoxide is extremely unstable, short-lived, only able to act locally, and cannot readily cross cellular membranes. As such, its dismutation to hydrogen peroxide ( $\text{H}_2\text{O}_2$ ) happens very fast and can happen spontaneously or can be catalyzed by superoxide dismutase (SOD) enzymes (311-313). Superoxide can also react with nitric oxide (NO) and form the highly toxic peroxynitrite ( $\text{ONOO}^-$ ), which is not technically a free radical because it does not contain free electrons (314,315). Nitric oxide, the main form of RNS in the cell, is produced by a family of enzymes (nitric oxide synthases, NOSs), which include iNOS

(inducible), eNOS (endothelial), and nNOS (neuronal) (316). Both eNOS and nNOS are constitutively active, triggered by intracellular calcium, constantly catalyzing the reaction of L-arginine, NADPH, hydrogen, and oxygen to create citrulline and NO (317). Inducible NOS has been described as calcium-independent, but studies have shown its activation can be controlled downstream of the stress response by the NF- $\kappa$ B and JAK-STAT pathways (318,319), among others.

Hydroxyl radicals are formed when hydrogen peroxide interacts with reduced iron ( $\text{Fe}^{2+}$ ) or copper ( $\text{Cu}^+$ ) through a Fenton reaction (320-322). The reduced iron for the Fenton reaction is liberated from iron-containing proteins by superoxide and although originally demonstrated for ferritin (323), it has recently been shown to occur for proteins with Fe-S clusters (324). New evidence has shown that, in the presence of these metals, proteins are highly susceptible to damage by hydrogen peroxide by participating in Fenton-type reactions (325,326). These reactions have been shown to involve a multitude of radicals such as oxidative scissions, carbonyl groups, protein-centered alkyl molecules, and hydroxyl radicals (325). Hydroxyl radical ( $\cdot\text{OH}$ ) is a highly reactive species that has been shown modify purine and pyrimidine bases leading to DNA damage and breaks in a unique chemical pattern (327,328).

#### **1.3.1.2 Sources of ROS**

Sources of ROS include both intracellular and extracellular sources. Major cellular sources of ROS include respiration and metabolic processes; however, the main

and most prevalent source is the mitochondrial electron transport chain (mETC) (329-331). Along this chain, electrons derived from NADH and FADH can react with O<sub>2</sub> or other electron acceptors, generating ROS (332). The discovery of superoxide dismutase enzymes (SOD1 and SOD2), by Irwin Fridovich and Joe McCord in 1969, helped to solidify the generation of mitochondrial ROS (312). In addition to ROS formed in the mitochondria, both by the mETC and also by the Krebs cycle (333), low levels of reactive species can be produced by membrane-localized NADPH oxidases (NOXs), other enzymes (xanthine oxidase, nitric oxide synthetase), peroxisomes, and the cytochrome p450 system (334-336). ROS can also be produced at somewhat low levels in response to the activation of certain signaling pathways shown to be important for the proliferation, oncogenic potential, and metastatic potential of cancer cells, e.g. EGFR (337). Extracellular sources of ROS include tobacco, smoke, drugs, xenobiotics, radiation, high levels of heat, etc. most of which either activate a stress response or directly damage cellular components leading to ROS production (338).

### **1.3.1.3 Antioxidants**

Cells have natural defense systems against ROS that consists of antioxidant enzymes and scavengers. Some of these antioxidants are produced inside cells and the human body, mostly falling into the enzymatic category, as they are predominantly protein in nature. These proteins include the superoxide dismutase (SOD) enzymes (which have differential subcellular localization and dismute superoxide to H<sub>2</sub>O<sub>2</sub>),

glutathione peroxidase (GPx) and catalase (both of which clear peroxide), thioredoxins (Trxs) (reduce oxidized proteins), and glutathione synthetase (GSS) (synthesizes glutathione [GSH], an important antioxidant), among others (311,312,339). The transcriptional control of these antioxidants will be discussed in Section 1.3.2. Antioxidant scavengers are mostly obtained from nutritional sources and include ascorbic acid (vitamin A), tocopherol (vitamin E), polyphenols, carotenoids, and uric acid (340).

#### **1.3.1.4 Oxidative stress**

There exists a fine balance between the levels of ROS and antioxidants within the cell and disruption of this balance can lead cells to undergo oxidative stress. Oxidative stress occurs when the level of reactive oxygen species (ROS) outbalances the cellular capacity to remove it (341,342). This stress promotes damage to key cellular structures including DNA, proteins, lipids, which play a pivotal role in the development of multiple types of cancer (325,343,344). Arrest or induction of transcription, signaling pathways, and genomic instability are all hallmarks of cancer that are associated with oxidative damage (345,346). Cellular proliferation, evasion of apoptosis, angiogenesis, and invasion and metastasis are all processes associated with cancer that can be modulated by oxidative stress in the cell (347-349). Expression of oncogenes (e.g. Ras, myc, telomerase) and loss of tumor suppressor genes (p53, p21, Pten) can also increase

ROS leading to senescence and escape from apoptosis (350-352). These alterations can be involved in cancer from initiation to promotion to progression.

### **1.3.2 Redox control mechanisms: Nrf2 and NFκB**

Transcription factors can indirectly offset the dangerous and lethal effects of ROS through the upregulation of antioxidants. The two main factors involved in this are Nrf2 and NFκB.

The transcription factor nuclear factor erythroid 2-related factor 2 (Nrf2) is a DNA-binding protein that specifically binds to antioxidant response elements (AREs) present in the regulatory regions of antioxidant enzymes (353). These include SOD, catalase, NAD(P)H:quinone oxidoreductase 1 (NQO1), heme-oxygenase 1 (HO-1), thioredoxins, and glutathione S-transferase among others (353). Nrf2 is regulated by a partner, Keap1, that binds to Nrf2 and leads to its proteasomal degradation (354). In multiple cancer types, Nrf2 mutations, specifically in the Keap1-Nrf2 binding domain have been observed (355). Inactivating mutations in Keap1 have also been identified; all of these lead to constitutive localization of Nrf2 to the nucleus allowing it to drive transcription (356). The PI3K-Akt pathway, which is hyperactive in multiple cancers, can also activate Nrf2 (357). The effects of Nrf2 on antioxidant expression have been linked to enhanced tumorigenesis in Kras-overexpressing cells and also therapeutic resistance in myeloid leukemia (358).

Nuclear factor  $\kappa$ B, similar to Nrf2, can also enhance the expression of antioxidant enzymes. SOD, ferritin heavy chain (FHC), thioredoxins, glutathione S-transferase pi, metallothionein-3, NQO1, HO-1, and glutathione peroxidase-1(Gpx1) are some of the antioxidants driven by NF $\kappa$ B activation. Paradoxically, NF $\kappa$ B can actually augment expression of pro-oxidant enzymes such as iNOS, nNOS, NADPH oxidase NOX2, COX-2, and the cytochrome p450 enzymes. ROS itself can, however, both inactivate and activate NF $\kappa$ B in a cell-type and context specific manner (reviewed in (359)), driving home the point that redox homeostasis is a key component of cellular biology.

### **1.3.3 Oxidative stress response and adaptive mechanisms in breast cancer**

In order to compensate for increased oxidative stress, cancer cells have been identified to garner redox adaptive mechanisms that enhance their ability to detoxify ROS; exposure to constant oxidative stress selects for cells that can adapt to these conditions through a number of mechanisms. Important redox adaptive mechanisms include increased antioxidants and ROS-scavenging systems which in turn can regulate redox-sensitive transcription factors and activation of pro-survival stress response signaling, and increased expression of anti-apoptotic molecules.

A clinical study by Noh et al. analyzed 24 breast cancer samples and showed that Prx1, 2 and 3 were overexpressed in the malignant samples compared to normal tissue

(360). A more recent study by Cha et al. found that Prx1 was highly increased in breast cancer samples at both the mRNA and protein levels (361).

Increased levels of SODs in breast cancer are another mechanism of redox adaptation. *In vitro* studies have shown that overexpression of either SOD1 or SOD2 can inhibit breast cancer cell growth (362,363). *In vivo*, infection of animals with an adenovirus expressing SOD1 or SOD2 decreased xenograft growth compared to controls (363). Kattan et al. showed that there are differences in SOD2 expression between estrogen-dependent and estrogen-independent cancer cell lines, and that this expression regulates not only tumor cell growth and colony formation, but also doubling time, providing a link between SOD and the cell cycle (364). A 2004 survey of breast cancer patients in Taiwan showed that SOD2, but not SOD1, expression was higher in cancer tissue than in malignancy-free tissue (365).

GSTP1 was also upregulated in breast cancer tissue in which high levels of oxidative stress were detected (366,367); GSTP1 positivity in these tumors was associated with reduced apoptotic response to oxidative stress. Further, levels of GSH itself as well as the GSH synthase  $\gamma$ -GCS have been reported as being elevated in breast cancer tissue (367,368). In a recent study, high GSH expression was associated with metastasis in breast cancer patients receiving chemotherapy (369). Similarly, breast cancer brain metastases, which rely heavily on oxidative phosphorylation for energy generation and thus produce high levels of ROS, showed significant upregulation of

glutathione-associated enzymes including glutathione reductase (GSR) and GSTP1, which help them maintain a reduced cellular environment (370). These observations indicate that redox adaptation is crucial for metastases, as metabolic pressures such as nutrient deprivation that are associated with a foreign environment can promote oxidative stress (371).

These findings suggest that antioxidants including GSH and its associated enzymes, SOD1/2 and catalase, are all upregulated as a mechanism by which breast cancer cells adapt to a highly oxidative environment. Redox adaptation as a response to the constitutive oxidative stress that results from oncogenic changes allows for the continued survival of a population of breast cancer cells that are highly resistant to increases in cellular ROS. Many of the most common treatment regimens utilized against breast cancer work at least in part through the generation of damaging ROS and thus may be rendered ineffective in cell populations that have adapted to cope with oxidative stress. Chemotherapies widely used in breast cancer include anthracyclines (doxorubicin), taxanes (paclitaxel, docetaxel), alkylating agents and platinum compounds (cisplatin, carboplatin), as well as radiation therapy, and all of these agents rely heavily on the induction of oxidative stress-induced apoptosis for their antitumor activity (310,372,373). Thus, redox adaptation is not only involved in cancer progression and metastasis, but also in the development of drug resistance.

### **1.3.4 Targeting redox imbalances in cancer**

As previously discussed, the use of therapeutics that are either targeted to or somewhat selective for cancer cells is essential in cancer treatment to preserve function and health of normal cells. In the late 90's and early 2000's it was proposed that there existed a toxic threshold, which when crossed triggers cell death (310). If cancer cells are closer to this proposed threshold, a "gentle push" would propel them over the edge and preferentially select them out. Due to the increased ROS present in cancer cells as they rapidly proliferate and autonomously activate cellular signals, they are heavily reliant on antioxidants and redox adaptation and, therefore, possibly more susceptible to oxidative insults. Therapeutics developed against redox adaptation can be functionally separated into three classes: 1) promoting ROS production, 2) altering ROS breakdown and clearance, and 3) directly targeting resistance mechanisms.

#### **1.3.4.1 Promoting ROS production**

Arsenic trioxide ( $\text{As}_2\text{O}_3$  or ATO), an inorganic compound that can be derived from the oxidation of arsenic, has been used since the 1970s as a treatment option for hematologic malignancies (374).  $\text{As}_2\text{O}_3$ , marketed currently as Trisenox, impairs the function of the mitochondrial respiratory chain which increases the generation of superoxide radicals (375). It is currently approved for the treatment of acute promyelocytic leukemia (APL) (375), while recent work by our lab shows that ATO can sensitize hepatocellular carcinoma cells to chemotherapy (376). Other drugs such as

motexafin gadolinium and the anthracyclines can interact with cytochrome P450 reductase of NADPH to generate ROS (377,378). N-(4-hydroxyphenyl) retinamide (4HPR) elevates the p67phox subunit of NOX which can again lead to ROS generation (379). Targeting of amino acid transporters SLC6A14 and SLC1A5 by alpha-methyl-DL-tryptophan and 1,2,3-Dithiazoles, respectively, has also been shown to increase intracellular ROS by decreasing amino acid availability (380,381). Elesclomol (STA-4783) is novel small molecule that was first identified in a screen for compounds with potent pro-apoptotic efficacy (382). Elesclomol showed activity in multiple cancer types *in vitro* and enhanced the efficacy of taxanes *in vivo* (383). After a quick Phase I trial, Phase II results in malignant melanoma revealed potent activity, prolonging progression-free survival time in combination with paclitaxel (384). A follow-up study revealed that elesclomol induces significant ROS in cancer cells which is essential for its activity (385). Despite great results in Phase II, elesclomol trials were discontinued after increased mortality in Phase III trials (386).

#### **1.3.4.2 Altering ROS breakdown and clearance**

Interfering with antioxidant levels in cancer cells represents another pathway to driving these cells closer to the toxic threshold. So far compounds to antagonize superoxide dismutase (SOD), thioredoxin (Trx), and glutathione (GSH) and its upstream enzymes have been described. SOD inhibitors include 2-methoxyestradiol (387), tetrathiomolybdate (ATN-224) (388), and Mangfodipir (389) all of which have at least

advanced to Phase II clinical trials in various malignancies. In addition to its role in the ETC, arsenic trioxide can also inhibit GPx and Trx antagonizing ROS metabolism (390). PX-12 (1-methylpropyl 2-imidazolyl disulphide) is another compound that has been explored as a Trx inhibitor which has showed antineoplastic efficacy *in vivo* (391). GSH conjugators benzyl isothiocyanate (BITC), phenethyl isothiocyanate (PEITC), sulphoraphane, and imexon all deplete the intracellular GSH pool leading to oxidative insult and subsequent cell death (392-394). In terms of upstream regulators of GSH, buthionine sulphoximine (BSO) (395), an inhibitor of glutamylcystein synthetase, and sulphasalazine (396), which inhibits the cysteine/glutamate antiporter, both lead to GSH depletion by inhibiting components necessary for the synthesis of GSH.

#### **1.3.4.3 Targeting control mechanisms**

In section 1.3.2, it was revealed that control of antioxidant systems falls under the purview of two transcription factors NF $\kappa$ B and Nrf2. Inhibitors of these have been described for the, more so for NF $\kappa$ B, that could possibly be used to reverse resistance mechanisms that positively regulate these two factors. The sheer number of described NF $\kappa$ B inhibitors (well over 700), makes it almost impossible to describe the function of each one separately however, Table 1.4 classifies each of the inhibitors based on their level of action in which they antagonize NF $\kappa$ B function as reviewed in (397).

**Table 1.3 Classification of previously described NFκB inhibitors**

<b>Classification of inhibitor</b>	<b>Total number identified to date</b>
<b>Receptor/adaptor antagonists</b>	28
<b>Inhibitors of IKKα and IKKβ phosphorylation</b>	170
<b>Inhibitors of IκBα degradation/ agents that increase stability</b>	113
<b>Inhibitors of nuclear translocation of NFκB</b>	99
<b>Inhibitors of κB DNA binding</b>	206
<b>NFκB transactivation inhibitors</b>	58
<b>Antioxidants</b>	111

Nrf2 inhibitors, on the other hand, are significantly smaller in number and due to the fact that Nrf2's main function surrounds oxidative stress have enjoyed more thorough research into their mechanisms. Ascorbic acid (vitamin C), a potent natural antioxidant, was shown to sensitize imatinib-resistant BCR/ABL+ chronic myelogenous leukemia cells and reduce GSH levels by suppressing Nrf2/DNA complexing at the GCL gene promoter (398). *All-trans*-retinoic acid also decreases Nrf2 gene transcription and does so by inducing the formation of retinoic acid receptor alpha (RARα)-Nrf2 complexes decreasing DNA binding, but not nuclear translocation (399). Several plant-derived and bacterial-derived compounds including brusatol (400), luteolin (401), and

ochratoxin A (402) have been isolated and shown to reduce Nrf-2 dependent gene expression via disparate mechanisms.

## **1.4 Inflammatory breast cancer cell lines**

### **1.4.1 Patient-derived cell lines**

The first IBC model derived from a patient primary tumor is the Mary-X IBC model. Mary-X was derived by serial passaging of tumor sections in animals from which tumor cells have now been isolated (403). *In vivo*, Mary-X spheroids generate E-cadherin positive tumor emboli, which are enriched in the dermal lymphatics of immunocompromised mice (138,404). Two newer models FC-IBC01 and FC-IBC02 were derived from a thoracentesis of IBC patients and have similar characteristics to Mary-X tumor spheroids (405,406). All three of these models cannot be cultured as adherent cells and therefore are extremely hard to use for *in vitro* assessments.

In this dissertation, two cell lines, SUM149 and SUM190, both developed by Dr. Stephen Ethier and derived from IBC patients prior to chemotherapy were used (407-409). They are the only two cell lines that are commonly regarded as untreated and as such have been used for the vast majority of molecular IBC studies. Both have chromosomal abnormalities, including p53 mutations, and express cytokeratins 8, 18, and 19 (407). SUM149 is a basal-type line characterized by activation of EGFR/ErbB1 and little to no expression of ER, PR, and Her2/ErbB2 making it a triple-negative IBC cell line (408,409). SUM149 cells do not produce EGF, the common ligand for EGFR, but instead

secrete a related protein, amphiregulin, which mediates an autocrine loop to activate EGFR and downstream signaling (410). SUM149 cells have a short doubling time (~15-21 hours) (156) and have the ability to form tumor emboli *in vitro* in an environment that mimics the stresses of the lymphovascular system (411). When implanted *in vivo*, SUM149 cells rapidly form primary tumors and have demonstrated an ability to form metastases at common sites in patients, including bone, lymph node, lung, and liver (412). SUM149 cells are also characterized by a large proportion of cells with a CD44<sup>+</sup>/CD24<sup>low</sup> (ALDH<sup>+</sup>) phenotype, which are associated with stem-like characteristics (413,414). SUM190 is a Her2-positive IBC cell line also expressing high levels of cyclin-D1 (407,408). SUM190 cells have a longer doubling time (~40-45 hours) (156), also form *in vitro* tumor emboli (411), and when implanted into immunocompromised mice establish tumors which are prone to metastasis (412).

KPL-4 and MDA-IBC-3 are two other cell lines, both characterized by Her2 amplification, which have been isolated from IBC patients (415,416). KPL-4 produces significant amounts of IL-6, which *in vivo* induces cachexia (muscle wasting) and has been used to study IL-6 antagonists (415,417). KPL-4 cells do not, however, express E-cadherin and as such are not commonly used for molecular studies. MDA-IBC-3 cells have an extremely slow doubling time (~76 hours), but form *in vitro* tumor emboli (411), and are tumorigenic *in vivo* (414).

### **1.4.2 Acquired resistance models: rSUM149 and rSUM190**

It has been noted in clinic, that patients suffering from IBC are prone to developing resistance to therapies; however, a mechanism for this had not been elucidated. Using continuous exposure to the ErbB1/2 inhibitor, lapatinib, our lab developed the first models of acquired therapeutic resistance in IBC: rSUM149 and rSUM190 (156). After an ~3 month selection period, where massive cell death was first observed, the rSUM149 and rSUM190 cells demonstrated potent resistance to lapatinib at concentrations which increased cell death in parental counterparts.

Assessment of the primary mechanism of action of lapatinib, inhibition of ErbB1/2 phosphorylation, revealed that this was in fact intact. ErbB1 (rSUM149) and ErbB2 (SUM190) phosphorylation were completely abrogated similar to parental cells treated with drug. Removal of drug from the culture media of resistant cell lines led to an increase in phosphorylation further proving no change in mechanism. Apoptotic western immunoblot array revealed a stark increase in XIAP expression in both rSUM149 and rSUM190 compared to SUM149 and SUM190, respectively (unpublished data). Overexpression of XIAP in SUM149 cells led to an increase in resistance to lapatinib-mediated cell death (156), while targeting of XIAP led to a decrease confirming the mechanism of resistance (156). Further work revealed that the increased XIAP expression was due to IRES-mediated translation elucidating a possible role for the translation initiation factor, eIF4G1. Subsequent analysis of our lapatinib-resistant cell

lines uncovered a broad cross-resistance of these cells to a multitude of chemotherapeutics with various mechanisms of action, indicating the potency of XIAP upregulation (418). This indicated that targeting XIAP may represent a novel means to enhance apoptosis which was corroborated by our follow-up studies using multiple XIAP-specific antagonists, embelin and Smac mimetics, which demonstrated chemosensitization to TRAIL specifically (419,420).

Continued study of these cell lines revealed that coupled with apoptotic dysregulation mediated by XIAP overexpression, these resistant lines also exhibited stark redox adaptation compared to parental lines (111,418). Using classical ROS inducers H<sub>2</sub>O<sub>2</sub> and paraquat dichloride, which induce significant levels of ROS in parental cells, we observed suppression of ROS accumulation in both rSUM149 and rSUM190. Aird et. al. also revealed that lapatinib could induce similar levels of ROS to classical ROS inducers which was again repressed in resistant cell lines (111). To assess the mechanism of redox adaptation, cellular antioxidants were measured and rSUM149 and rSUM190 were revealed to have increases in expression for SOD1 and SOD2 as well as increases in the intracellular GSH pool. Using 2-ME and diethyldithiocarbamate, both potent redox modulators, we reversed resistance to ROS accumulation, while addition of an antioxidant decreased sensitivity of parental cells. Despite an associate between XIAP and redox adaptation, a mechanism between the two was not elucidated although this is now discussed in Chapter 4.

### **1.4.3 Resistance reversal model: rrSUM149**

Due to the observation that resistance to lapatinib was not due to mutation or epigenetic changes, and other studies showing that cells could exhibit resensitization with removal of drug (421), we sought to assess this in IBC. Removal of lapatinib from rSUM149 for an extended period of time led to the development of a resensitized population of cells, rrSUM149, which behave similar to parental cells (418). When tested against multiple chemotherapeutics, these cells were as sensitive, if not more sensitive, than parental SUM149 elucidating that apoptotic dysregulation and redox adaptation may be a reversible phenotype in IBC. Molecular analysis of these cells demonstrated decreases in XIAP expression, suggesting that lapatinib may in fact enhance resistance in a subset of cells or select for those with inherent resistance; this was coupled with changes in SOD1 and SOD2 decreasing redox adaptation.

## **1.5 Research objectives outlined in this dissertation**

After the identification of XIAP as a key factor in mediating therapeutic resistance in IBC, and correlating its expression to a potent redox adaptation, our work has been focused on the development of targeted agents that antagonize XIAP expression and function. The efficacy of these inhibitors indicates a central role for XIAP in mediating both apoptotic dysregulation and redox adaptation; however, a better mechanistic understanding of other key players that may interact with XIAP and drive these processes is essential. The studies outlined in this dissertation are intended to address our hypothesis that the anti-apoptotic protein XIAP plays a central role not only in therapeutic resistance, but also in the progression and biology of inflammatory breast cancer. Both the upstream regulators and downstream effectors of XIAP that contribute to these processes in the context of IBC pathobiology and therapeutic resistance are identified, elucidating further options for the development of targeted strategies, some of which are also reported herein.

### **1.5.1 Objective 1**

Investigation of the role of XIAP and elucidation of functional partners in IBC pathogenesis and progression (discussed in Chapter 3)

### **1.5.2 Objective 2**

Determination of the mechanism of XIAP-mediated tumor cell evasion/inhibition of immunotherapy (discussed in Chapter 4)

### **1.5.3 Objective 3**

Assessment of the therapeutic strategy of targeting XIAP-mediated redox adaptation in IBC (discussed in Chapter 5)

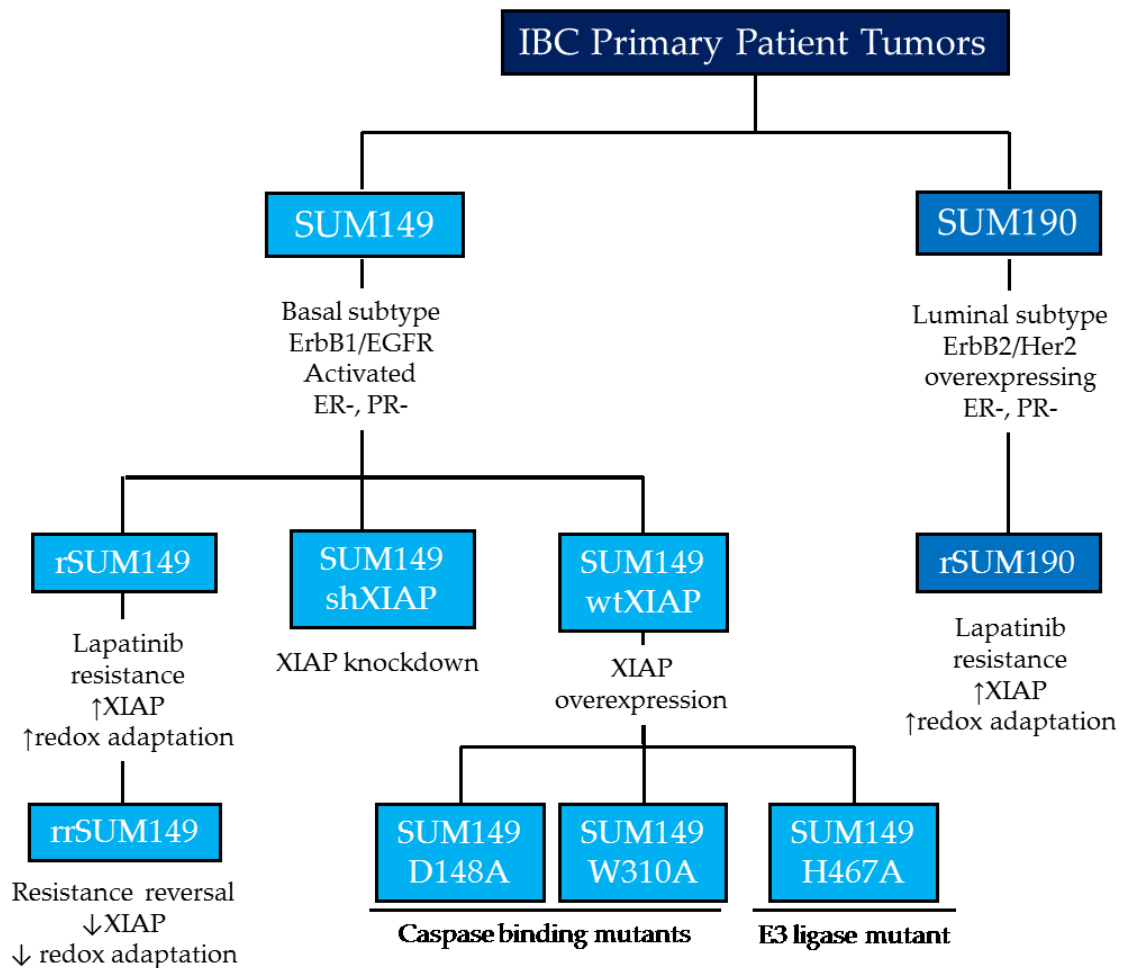


Figure 1.1 Cell lines used in this dissertation

## **2. Materials and Methods**

### **2.1 Cell Culture**

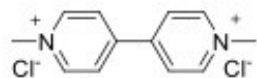
#### **2.1.1 Cell lines and reagents**

SUM149 and SUM190 cells were obtained from Asterand, Inc. (Detroit, MI). SUM149 and SUM190 cells exhibiting acquired resistance to the lapatinib analog GW583340 (referred to as rSUM149 and rSUM190) were selected by Dr. Katherine M. Aird by culturing cells in normal growth medium supplemented with increasing concentrations of GW583340 (0.25-7.5 and 0.25-2.5  $\mu$ M, respectively) (156). Although, marked cell death and growth delay were observed initially, after 2 weeks small colonies of viable cells were detected, which were cultured to confluence and placed in an increasing drug concentration. After 3 months, colonies were selected and rSUM149 and rSUM190 cell lines were routinely cultured in normal media with addition of 7.5 and 2.5  $\mu$ M GW583340, respectively. In order to generate a resistance reversal model (rrSUM149), rSUM149 were cultured in GW583340-free media for approximately 2 months. Cells were tested on a weekly basis for restored sensitivity to GW583340 by both trypan blue exclusion assay and 3-[4, 5-dimethylthiazol-yl]-2, 5 diphenyl tetrazolium bromide (MTT) assay. Interrogation of previously discovered resistance proteins (XIAP and SOD1/2) was performed by western immunoblot. Stable SUM149 variants overexpressing wild-type XIAP (wtXIAP) or the control vector (FG9) were also generated by Dr. Aird (156).

Ham's F-12 medium was purchased from Gibco (Carlsbad, CA). HEPES, hydrocortisone, sodium selenite, insulin, ethanolamine, transferrin, fetal bovine serum (FBS) and penicillin/streptomycin were all purchased from Sigma Aldrich (St. Louis, MO). SUM149 cells (and variants) were cultured in Ham's F-12 base medium supplemented with 5  $\mu\text{g}/\text{mL}$  insulin, 10 mM HEPES, 1  $\mu\text{g}/\text{mL}$  hydrocortisone, 10 units/mL penicillin, 10  $\mu\text{g}/\text{mL}$  streptomycin, and 5% FBS. SUM190 and rSUM190 cells were cultured in Ham's F-12 base medium supplemented with 5  $\mu\text{g}/\text{mL}$  insulin, 10 mM HEPES, 1  $\mu\text{g}/\text{mL}$  hydrocortisone, 5 mM ethanolamine, 5  $\mu\text{g}/\text{mL}$  transferrin, 10 nM triiodothyronine, 50 nM sodium selenite, 10 units/mL penicillin, 10  $\mu\text{g}/\text{mL}$  streptomycin, and 2% FBS. Twenty-four hours after splitting, media was changed to serum-free conditions for SUM190. All cell lines were cultured at 37 °C, 5% CO<sub>2</sub>.

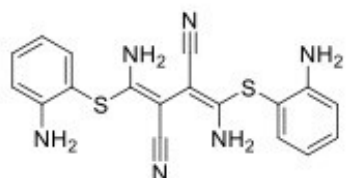
Research-grade lapatinib analog, GW583340, was purchased from Tocris Bioscience (Bristol, UK), and TNF-related apoptosis-inducing ligand (TRAIL) purchased from Enzo Life Sciences (Farmingdale, NY). Dimethyl sulfoxide (DMSO), catalase, TNF- $\alpha$ , paraquat dichloride, hydrogen peroxide (H<sub>2</sub>O<sub>2</sub>), concanamycin A (CMA), (+)-Sodium L-ascorbate, JSH-23, and CGP57380 were obtained from Sigma Aldrich. Streptolysin O (SLO) was obtained from Abcam (Cambridge, MA) and recombinant Granzyme B purchased from Enzo Life Sciences. The SOD mimetic MnTnHex-2-PyP<sup>5+</sup> was obtained from Dr. Ines Batinic-Haberle at Duke University (422), while another SOD mimetic MnTBAP was purchased from Santa Cruz Biotechnology, Inc. (Dallas, TX). Matrigel was

purchased from BD Biosciences (San Jose, CA). The MEK1/2 inhibitor U0126 and the protein kinase inhibitor staurosporine were purchased from Cell Signaling Technologies (Danvers, MA). The antibodies cetuximab (Erbix<sup>®</sup>, EGFR targeting mAb) and trastuzumab (Herceptin<sup>®</sup>, HER2 targeting mAb) were purchased from Bristol Myers Squibb (New York, NY) or Genentech (San Francisco, CA), respectively. The pan-caspase inhibitor Q-VD-OPh was purchased from Calbiochem (Billerica, MA). All cell culture plates were acquired from Corning Incorporated (Corning, NY) unless otherwise indicated. Chemical structures for lapatinib, paraquat, U0126, CGP57380, and JSH-23 can be found in Figure 2.1.



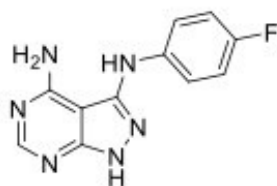
**Paraquat dichloride**

(1,1'-Dimethyl-4,4'-bipyridinium dichloride)



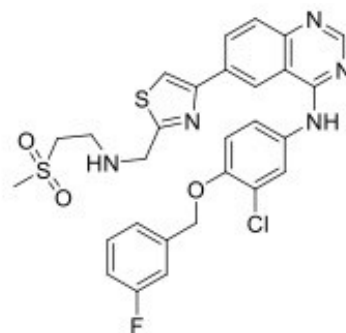
**U0126 (MEK inhibitor)**

(1,4-diamino-2,3-dicyano-1,4-bis  
(2-aminophenylthio)butadiene)



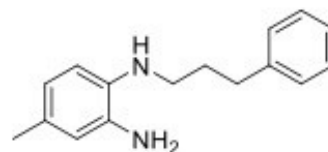
**CGP57380 (Mnk inhibitor)**

(*N*<sup>3</sup>-(4-Fluorophenyl)-1*H*-pyrazolo-  
[3,4-*d*]pyrimidine-3,4-diamine)



**GW583340 (Lapatinib)**

(*N*-[3-Chloro-4-[(3-fluorophenyl)  
methoxy]phenyl]-6-[2-[[[2-(methylsulfonyl)  
ethyl]amino]methyl]-4-thiazolyl]-4-quinazolamine)



**JSH-23 (NFκB inhibitor)**

(4-Methyl-*N*<sup>1</sup>-(3-phenylpropyl)  
benzene-1,2-diamine)

**Figure 2.1 Chemical structures of compounds used in this dissertation**

### **2.1.2 Generation of XIAP mutant cell line models**

SUM149 cells stably expressing XIAP mutant variants were generated using a lentiviral expression system (kindly provided by Dr. Colin Duckett, University of Michigan). First, endogenous XIAP expression was knocked down using an XIAP-specific shRNA and mutant XIAP re-expressed using shRNA-resistant constructs. HEK293T cells were transfected using polyethylenimine with 5 µg of pHCMV, pRRE, and pRSVrev, which drive the expression of lentiviral structural proteins, and 5 µg of pFG12 H1 shXIAP. Twenty-four hours post-transfection, media was changed. Forty-eight hours post-transfection, the virus-containing media on the HEK293T cells was collected and filtered through a 0.45 µm Millex HV PVDF filter unit (Millipore, Billerica, MA) onto cells [with 25 mM polybrene (Sigma, St. Louis, MO)]. After four hours, fresh media was added and cells were incubated for an additional forty-eight hours at 37°C, 5% CO<sub>2</sub>. As the FG12 vector contains a GFP marker, shXIAP GFP-positive cells were enriched by FACS and tested for knockdown using western immunoblot. XIAP constructs expressing mutant XIAP (pFG9 XIAP H467A or pFG9 XIAP D148A/W310A) were also provided by Dr. Colin Duckett. Virus-containing media from HEK293T cells transfected with viral packaging components and pFG9 XIAP H467A or pFG9 XIAP D148A/W310A was added to shXIAP cells to generate XIAP E3 ligase deficient (H/A) and caspase-binding (DW/AA) mutant clones, respectively. Selection for H/A and DW/AA cells was done with hygromycin B (Invitrogen, Carlsbad, CA) at 200 µg/mL. To

generate +FG9 and +wtXIAP cell lines, the appropriate viruses were added to shXIAP cells and clones selected by hygromycin addition.

### **2.1.3 shRNA-mediated knockdown of XIAP**

rSUM149 and rSUM190 cells were seeded at 150,000 cells per well into a 6 well plate and allowed to adhere. After 24 h, cells were transfected with pFG12 H1 shXIAP or the control shRNA using Mirus TransIT-2020 transfection reagent (Madison, WI) according to manufacturer's instructions. ADCC was performed using these cells 48 h post transfection according to the protocol in Section 2.11. Effective knockdown was confirmed by western immunoblot.

### **2.1.4 shRNA-mediated knockdown of eIF4G1**

SUM149 and rSUM149 were seeded at 75,000 cells per well in a 12 well plate and allowed to adhere. Cells were transfected with an eIF4G1-specific shRNA (46,423) or control shRNA using Mirus TransIT-2020. Cells were lysed at indicated time points for immunoblot or treated with TRAIL (48 h post transfection) for 24 h followed by trypan blue exclusion assay. Effective knockdown was confirmed by western immunoblot.

### **2.1.5 Transient transfection of mutant XIAP constructs**

XIAP<sup>WT</sup>, XIAP<sup>V80D</sup>, XIAP<sup>PF495A</sup>, and control pcDNA3 vectors were kindly provided by Dr. Pascal Meier (The Institute of Cancer Research, London). XIAP knockdown (shXIAP) cells were transfected with 3 µg plasmid using X-tremeGENE HP DNA transfection reagent (Roche, Indianapolis, IN) at a 3:1 DNA:reagent ratio, according to

manufacturer's instructions. Cells were analyzed for XIAP expression by immunoblot and NF $\kappa$ B localization by immunofluorescence 48 h post-transfection.

## **2.2 NRAGE peptide manufacture and use for treatment**

A 24-mer peptide, sequence (n-PPAWQTTPAWQTTPAWQTTPAWQT-c), modeled after the neurotrophin receptor-interacting MAGE protein (NRAGE) was synthesized and lyophilized by NeoBioLab (Cambridge, MA). Lyophilized powder was resuspended in DMSO at a concentration of 1 mM. The peptide was based on a previously published study (424), showing disruption of XIAP-TAB1 signaling, and has a MW of ~2740 kDa. For all *in vitro* experiments, unpurified NRAGE peptide was added to cells, for 24 h, with 6  $\mu$ M EndoPorter delivery reagent (GeneTools LLC, Philomath, OR) to facilitate intracellular transport.

## **2.3 Determination of cell viability, apoptosis, and proliferation**

### **2.3.1 Trypan blue exclusion assay**

Cell viability was determined by trypan blue exclusion assay. Cells were seeded in 12 well plates at 50,000 (SUM149 and derivatives) or 75,000 (SUM190 and derivatives) cells per well and allowed to adhere. Cells were treated with indicated agents for 24 h unless otherwise indicated. Cells were trypsinized with 0.25% Trypsin/EDTA (Sigma Aldrich) and resuspended in 1x DPBS. Equal amount of cell suspension was added to 0.4% trypan blue and 10  $\mu$ l of the mixture loaded onto a hemocytometer. Live and dead

cell numbers were recorded and percent viability calculated as the number of live cells over the total number of cells.

### **2.3.2 MTT assay**

Proliferation was determined via MTT assay. Cells were seeded in 96 well plates and allowed to reach ~80% confluency. Cells were treated with indicated agents for appropriate length of time and MTT reagent added to a final concentration of 1 mg/mL. Cells were incubated until the reaction caused the formation of granulated purple coloration. Media and MTT reagent were removed, DMSO added to each well, and absorbance read at 550 nm in a BioRad plate reader (Hercules, CA).

### **2.3.3 Clonogenic growth assay**

SUM149 and derivatives were plated in triplicate in 6 well plates at 250-500 cells/well and allowed to adhere. Cells were treated as indicated in figure legends for 24 h, after which cells were washed twice with 1x DPBS and regular growth media added. The cells were allowed to grow for approximately 12-14 days, with addition of fresh media every 4 days. Once colonies of at least 50 cells were observed, cells were washed with PBS, fixed, stained with 0.4% crystal violet, then rinsed in cold water and left to dry overnight. Colonies were counted and imaged using a ColCount (Oxford Optronix, Oxford, UK), and colonies formed per cells plated calculated. Numbers were normalized to the untreated sample.

### **2.3.4 Caspase activity assay**

Cells were seeded in 12 well plates, and the next day treated as indicated for either 4 or 24 h. After incubation, cells were lysed and 3  $\mu\text{g}$  protein (as determined by Pierce 660 assay) resuspended to 15  $\mu\text{l}$  in lysis buffer was added to a 96 well white-walled plate. An equal volume of Caspase-3/7-Glo reagent (Promega, Madison, WI) was added to the wells, and plates incubated for 30 min at RT. Luminescent signal was measured on a Veritas microplate luminometer (Turner Biosystems, Sunnyvale, CA) with a 1 s integration time. Caspase activity was normalized to the untreated sample.

### **2.3.5 TUNEL staining**

For *in vitro* experiments, cells were plated onto glass coverslips previously coated with poly-D-lysine (BD Biosciences, San Jose, CA) and allowed to adhere overnight. Cells were treated as indicated and coverslips washed 2x with media, fixed with 4% paraformaldehyde and permeabilized in a 0.1% Triton X-100 in 0.1% sodium citrate solution. Coverslips were incubated with In Situ cell death enzyme as per manufacturer's instructions (In Situ Cell Death Detection Kit, Roche, Basel, Switzerland). Coverslips were mounted with Prolong Anti-fade mounting medium with DAPI (Invitrogen). For tumor tissue, xenografts were fixed in 10% formalin, processed and embedded in paraffin. Serial sections were cut and deparaffinized in a series of 100%, 95% and 70% ethanol for 5 min each and washed in 1X PBS. Sections were incubated with 20  $\mu\text{g}/\text{mL}$  Proteinase K solution (Roche Diagnostics) for 15 min at 25  $^{\circ}\text{C}$ . After 2

washes in 1X PBS, sections were incubated with In Situ cell death enzyme as per manufacturer's instructions (In Situ Cell Death Detection Kit, Roche), and coverslipped and mounted with Prolong Anti-fade mounting medium with DAPI (Invitrogen). All images were obtained using the Zeiss Axio Imager microscope, and analyzed with Metamorph and ImageJ softwares.

### **2.3.6 Wound healing assay**

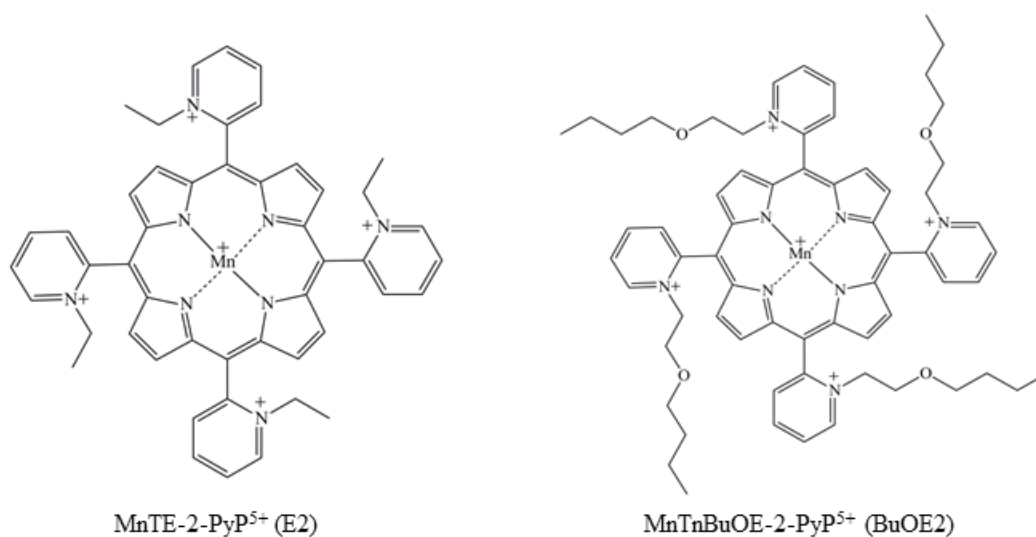
Cells were plated in 12 well plates at an optimized cell number for 100% confluency and allowed to adhere overnight. The next morning, a sterilized P200 tip was used to scratch a wound through the cells. The cells were washed with warmed 1X PBS and complete media replaced. Images were taken immediately after scratch (time point=0 h) and every 12 h for two days. Media was replaced after 24 hours. Images were imported into Tscratch, a software tool for automated analysis of wound healing assays (425). After review of parameters on 0 h images, group thresholds were applied to every image for analysis.

## **2.4 Assessment of SOD mimetics**

### **2.4.1 MnP-based SOD mimics**

Two Mn porphyrins, MnTE-2-PyP<sup>5+</sup> (AEOL10113, BMX-010) and MnTnBuOE-2-PyP<sup>5+</sup> (BMX-001), were synthesized, purified and characterized by means of thin-layer chromatography, elemental analysis, ESI-MS, and UV-Vis spectroscopy as earlier described (426,427). The structures and properties of both Mn porphyrins are presented

in Figure 2.2: catalytic rate constant for  $\text{O}_2^{\bullet-}$  dismutation,  $k_{\text{cat}}(\text{O}_2^{\bullet-})$ ; rate constant for the reduction of  $\text{O}_2$  to  $\text{O}_2^{\bullet-}$ ,  $k_{\text{red}}(\text{O}_2)$ ; metal-centered reduction potential for  $\text{Mn}^{\text{III}}\text{P}/\text{Mn}^{\text{II}}\text{P}$ ,  $E_{1/2}$  in mV vs. NHE; and lipophilicity as characterized by partition coefficient for n-octanol and water,  $\log P_{\text{ow}}$ .



Parameters	MnTE-2-PyP <sup>5+</sup>	MnTnBuOE-2-PyP <sup>5+</sup>
$k_{\text{cat}}(\text{O}_2^-)$ , $\text{M}^{-1} \text{s}^{-1}$	$5.75 \times 10^7$	$6.76 \times 10^7$
$k_{\text{red}}(\text{O}_2)$ , $\text{M}^{-1} \text{s}^{-1}$	$8 \times 10^4$	$3 \times 10^4$
$v_o [(\text{HA}^-)_{\text{ox}}]$ , $\text{M s}^{-1}$	$1.7 \times 10^{-7}$	$1.2 \times 10^{-7}$
$E_{1/2}$ , mV vs. NHE	+228	+277
$\log P_{\text{ow}}$	-7.79	-4.10

Figure 2.2 Chemical structures and physical characteristics of MnPs used

### **2.4.2 Spectrophotometrical study of the reaction of MnPs with ascorbate**

The time-dependent spectral change of MnP/ascorbate system for both E2 and BuOE2 was followed by the Batinic-Haberle lab. The time-dependent content of MnP (%) catalyst was determined based on the disappearance of the absorbance of reduced E2 at 438 nm and BuOE2 at 441.5 nm as previously reported (428-430). The oxidation/consumption of ascorbate (%) was followed spectrally at 265 nm. Also the initial rates for ascorbate oxidation were determined at 265 nm. The reduction and eventual destruction of MnPs (6  $\mu$ M) was followed in the presence of ascorbate (0.42 mM) at pH 7.8 (maintained by 0.05 M Tris buffer) on a UV-2550 PC spectrophotometer (0.5 nm resolution) (Shimadzu Instruments, Columbia, MD). While high concentrations of MnP could not have been used in aqueous system, as too high absorbance above 4 could not be measured, the ratio of MnP to ascorbate was kept the same in aqueous and cellular systems.

### **2.5 Western immunoblotting**

Cells were harvested and immediately lysed in polysome lysis buffer (100 mM KCl, 5 mM MgCl<sub>2</sub>, 20 mM Tris, 0.5% NP40, pH 7.4) with 1x Halt Protease/Phosphatase Inhibitor (Roche) and 2 mM DTT (Thermo Scientific). Protein concentration was determined by the Pierce 660 nm Protein Assay (Thermo Scientific) following manufacturer's instructions. Equal amounts of cell lysates, following boiling for

denaturation, were subjected to SDS-PAGE under reducing conditions. Protein was transferred onto Immobilon-P PVDF membrane (Millipore, Billerica, MA) previously rehydrated in methanol using the TRANS-BLOT SD semi-dry transfer cell (BioRad). After transfer, membranes were incubated with blocking buffer (either 5% dry nonfat milk or 3% BSA in 1x TBS-0.1% Tween-20) for 1 h at RT. Membranes were incubated with primary antibodies at the indicated dilutions overnight at 4 °C; a list of antibodies can be found in Table 2.1. After three washes (1x TBS-0.1% Tween-20) for 5 min each, membranes were incubated with appropriate secondary antibody conjugated with horseradish peroxidase (rabbit 1:1000, mouse 1:2000) for 1 h at RT. After final washes, bands were visualized using SuperSignal West Pico Chemiluminescent Substrate (Thermo Scientific). Signals were developed after exposure to autoradiographic film. Actin or GAPDH were used as loading controls after stripping. Stripping was accomplished in buffer [100 mM 2-mercaptoethanol, 2% SDS, 62.5 mM Tris-HCl (pH 6.7)] at 50 °C for 30 min followed by washing and blocking procedures above. Densitometric analysis was performed using NIH ImageJ software (431).

**Table 2.1 Antibodies used in this dissertation**

<b>Antibody</b>	<b>Company</b>	<b>Catalog #</b>	<b>Dilution</b>	<b>2° Ab</b>	<b>MW (kDa)</b>
<b>Bcl-2</b>	Santa Cruz	sc-7382	1:1000	mouse	26
<b>cIAP2</b>	Cell Signaling	3130	1:1000	rabbit	70
<b>c-myc</b>	Santa Cruz	sc-764	1:2000	rabbit	67
<b>EGFR/ErbB1</b>	Cell Signaling	2232	1:1000	rabbit	175
<b>eIF4E</b>	Cell Signaling	9742	1:1000	rabbit	25
<b>eIF4G1</b>	Cell Signaling	2469	1:1000	rabbit	220
<b>ERK1/2 (p44/42)</b>	Cell Signaling	9102	1:1000	rabbit	42, 44
<b>GAPDH</b>	Santa Cruz	sc-47724	1:2000	mouse	37
<b>Her2/ErbB2</b>	Cell Signaling	2242	1:1000	rabbit	185
<b>Histone H3</b>	Cell Signaling	4499	1:1000	rabbit	17
<b>IKK<math>\beta</math></b>	Cell Signaling	2678	1:1000	rabbit	87
<b>NF-<math>\kappa</math>B (p65)</b>	Cell Signaling	8242	1:1000	rabbit	65
<b>PARP</b>	Cell Signaling	9532	1:1000	rabbit	89, 116
<b>p38</b>	Cell Signaling	9212	1:1000	rabbit	43
<b>p-EGFR/ErbB1 (Tyr1068)</b>	Cell Signaling	2234	1:1000	rabbit	175
<b>p-eIF4E (Ser209)</b>	Cell Signaling	9741	1:1000	rabbit	25
<b>p-ERK1/2 (Thr202/Thr204)</b>	Cell Signaling	9101	1:1000	rabbit	42,44
<b>p-Her2/ErbB2 (Tyr877)</b>	Cell Signaling	2241	1:1000	rabbit	185
<b>p-I<math>\kappa</math>B<math>\alpha</math> (Ser32)</b>	Cell Signaling	2859	1:1000	rabbit	40
<b>p- NF-<math>\kappa</math>B (Ser536)</b>	Cell Signaling	3031	1:1000	rabbit	65
<b>p-p38 (Thr180, Tyr182)</b>	Cell Signaling	9211	1:1000	rabbit	43
<b>Smac/DIABLO</b>	Cell Signaling	2954	1:1000	mouse	21
<b>SOD1</b>	Cell Signaling	2770	1:1000	rabbit	18
<b>SOD2</b>	BD Biosciences	611580	1:1000	mouse	25
<b>Survivin</b>	Cell Signaling	2808	1:1000	rabbit	16
<b>TAB1</b>	Cell Signaling	3226	1:1000	rabbit	60
<b>XIAP</b>	BD Biosciences	610762	1:2000	mouse	57

## ***2.6 Immunoprecipitation of TAB1 and associated proteins***

Cells were seeded in 10 cm dishes and allowed to grow to ~90% confluence. Plates were transferred to ice and washed once with 1X PBS. RIPA buffer (Thermo Scientific) supplemented with HALT protease/phosphatase inhibitor cocktail (Roche) was added and cells were scraped into microcentrifuge tubes. Cells were rotated, with gentle agitation, for 1 h at 4°C and centrifuged at top speed to remove cellular debris. 50 µl of supernatant was removed for whole cell extract. TAB1 antibody (Cell Signaling Technologies) was added to the lysate at a concentration of 1:100 and incubated at 4 °C for 24 hours. Protein A/G Sepharose beads (Thermo-Fisher, Grand Island, NY) were rinsed twice in wash buffer (RIPA buffer diluted 1:5 in 1X PBS) and 60 µl of bead slurry added to pull-down lysates. Beads were incubated at 4 °C for 4 hrs. Centrifugation at top speed was followed by two washes to remove loosely bound proteins. Fifty µl 2X SDS/DTT buffer was added and beads heated to 50 °C for 10 mins to remove proteins. Protein lysates were loaded on a gel and western immunoblotting procedures followed.

## ***2.7 Preparation of nuclear and cytosolic extracts***

Nuclear and cytosolic fractionation was performed using the NE-PER™ Nuclear and Cytoplasmic Extraction Reagent kit (Thermo-Fisher) using manufacturer's instructions. Cells were plated in 10-cm dishes and allowed to grow overnight before fractionation. Histone H3 and  $\gamma$ -tubulin were used to monitor cross-contamination of fractions.

## **2.8 Flow cytometric analyses**

### **2.8.1 Annexin V**

Cells were cultured in six well plates and allowed to reach ~80% confluence. Cells were treated with the indicated agents for 4h, then harvested with 0.25% trypsin (-EDTA), washed with PBS, and incubated for five minutes with Annexin V-biotin staining solution (Immunotech, Marseilles, France) at room temperature. Cells were washed with 1% BSA/PBS and then incubated 15 min on ice with streptavidin-FITC (Zymed, San Francisco, CA). Cells were washed and analyzed by flow cytometry. At least 25,000 events were collected on a BD FACSCalibur flow cytometer and the total cell population was used for analysis. Results were analyzed using FlowJo software (Tree Star, Inc., Ashland, OR).

### **2.8.2 Measurement of intracellular reactive oxygen species**

Cells were cultured in 6 well plates to 70-80% confluence and treated as indicated for either 1 or 24 h. Cells were harvested and incubated for 30 minutes (at 37 °C) with the following dyes at 10  $\mu$ M: 2',7'-dichlorodihydrofluorescein diacetate (H<sub>2</sub>-DCFDA) or MitoSox Red (both Molecular Probes, Carlsbad, CA) to detect hydrogen peroxide-derived radicals and mitochondrial superoxides, respectively. Cells were washed twice with 1% BSA/PBS and analyzed for fluorescence by flow cytometry. Twenty-five thousand events were collected and live cells analyzed using FlowJo software. For H<sub>2</sub>-DCFDA staining, high fluorescence was calculated by setting a gate on the untreated

control cells where the peak reached a maximum, and all experimental samples were compared to this control gate. For MitoSox Red, the mean fluorescent intensity for each sample was calculated and normalized to untreated control.

### **2.8.3 Measurement of surface EGFR and Her2 levels**

Cells were trypsinized, washed and resuspended in 1% BSA/PBS. To detect surface EGFR expression, cells were incubated in rabbit anti-human EGFR antibody (2232, Cell Signaling Technologies) for 1 hour at room temperature at a concentration of 2 µg/ml. Cells were washed once and incubated with a 1:100 dilution of FITC-labeled anti-rabbit secondary (Jackson ImmunoResearch, West Grove, PA) for 1 hour at room temperature. Cells were washed twice and resuspended in 0.2 mL and immediately analyzed. To detect surface HER2 expression, mouse anti-human HER2 PE (340552, BD Biosciences) was added to the cells at a 1:50 concentration for 30 minutes at RT. Cells were washed twice before analysis. Unstained cells and appropriate IgG controls were used in all experiments. At least 25,000 events were collected on a FACSCalibur flow cytometer (BD Biosciences) and analyzed using FlowJo software.

### **2.9 Measurement of reduced glutathione content**

Reduced glutathione levels were assessed using the GSH-Glo™ Glutathione Assay (Promega) as per manufacturer's instructions. Three µg total cell lysates in 50 µl volume were incubated with an equal volume of fresh prepared GSH-Glo reagent 2X for 30 min at RT. One hundred µl of reconstituted Luciferin Detection Reagent was added,

plates mixed and incubated for 15 min at RT, and luminescence read on a BMG FLUOStar Optima (BMG Labtech, Cary, NC) with a 1 s integration time.

## **2.10 Immunofluorescence analysis**

Cells were plated on coverslips (VWR, Radnor, PA) that had previously been coated with Poly-L-Lysine (Sigma) and stored in 70% ethanol. Twenty-four hours post-plating, cells were fixed using 4% formaldehyde for 20 minutes. Blocking and permeabilization was performed with a solution of PBS containing 0.1% Triton X-100 and 5% normal goat serum. Anti-p65 antibody (8242) or anti-apoptosis inducing factor (AIF, 5318) [both Cell Signaling Technologies], diluted in blocking buffer (1:400 for both), was added to the cells overnight at 4 °C. After two washes with PBS, anti-mouse FITC secondary (Jackson ImmunoResearch, 1:200) was added for 1h. The coverslips were washed with PBS, mounted on slides with Prolong® Gold Antifade with DAPI (Invitrogen), and imaged with a Zeiss AxioObserver complete with imaging software analysis package. Merging of channels and post-processing was accomplished using ImageJ.

## **2.11 Immune assays**

### **2.11.1 Chromium based ADCC assay**

Healthy donor PBMCs (Peripheral Blood Mononuclear Cells) were isolated from leukapheresis products (HemaCare Corp., Van Nuys, CA) and stored in LN<sub>2</sub> until use. The day prior to performing an ADCC assay, PBMCs were thawed and activated with

600 IU/mL recombinant human IL-2 (Prometheus Laboratories Inc., San Diego, CA) in RPMI 1640/10% huAB serum overnight (16-18 h). Target cells were radiolabeled with <sup>51</sup>-Chromium (Perkin-Elmer, Akron, OH) for 1.5 h and washed 3 times in RPMI supplemented with huAB serum. Chromium-labeled target cells were incubated for 1 h with 10 µg/mL cetuximab or trastuzumab. Activated PBMCs were added at an effector:target (E:T) ratio of 100:1, the optimal ratio identified in preliminary assays. Plates were centrifuged at 400 rpm to initiate contact of cells. Control wells were included, which contained target cells alone (spontaneous release), target cells mixed with antibody alone, and target cells mixed with 5 % SDS (maximum release). After incubation at 37 °C for 4 h, supernatant was collected and counted for radioactive chromium release into culture media using a Microbeta Plus Scintillation Counter (Perkin-Elmer). Cytotoxicity was calculated with the following equation: %specific lysis = [(cpm of experimental release – cpm of spontaneous release) / (cpm of maximum release – cpm of spontaneous release)] x 100. Percent lysis solely due to ADCC was calculated by: %specific lysis (PBMC + antibody) - %specific lysis (PBMC alone). For concanamycin A (CMA, Sigma) treatment, 100 nM CMA was added to PBMCs 2 h prior to the start of the assay.

### **2.11.2 CytoTox-One non-radioactive ADCC assay**

A modified, non-radioactive version of our chromium-based assay was conducted using the CytoTox-ONE Homogenous Membrane Integrity assay (Promega),

which measures LDH release as a measure of cell death. Assay setup was similar to the chromium assay, excluding the chromium loading step and a 50:1 E:T ratio. After 4 h incubation of cells at 37 °C, supernatant (50 µl) was collected and mixed with 50 µl CytoTox-ONE reagent. Luminescence was measured using a BMG FLUOstar OPTIMA and percent lysis solely due to ADCC was calculated by: %specific lysis (PBMC + antibody)-%specific lysis (PBMC alone). For reversal experiments, antioxidant SOD mimetic MnTBAP (Santa Cruz Biotechnology, Dallas, TX), or caspase inhibitor qVD-OPh (EMD Millipore, Billerica, MA), alone and in combination, were added during antibody incubation.

### **2.11.3 Granzyme B loading**

Cells ( $6.0 \times 10^5$  cells) were loaded with exogenous granzyme B (gB) isolated from human lymphocytes in the presence of a sublytic dose of activated streptolysin-O, which functions as a pore-forming molecule. Cultured cells were washed once in Hank's Balanced Salt Solution (HBSS), followed by the addition of SLO at 100 ng/mL and gB at 60 ng/mL (alone or in combination) in 500 µl HBSS. Cells were incubated for 2 h at 37°C before staining with Carboxy-H<sub>2</sub>DCFDA as described.

### ***2.12 Assessment of anchorage-independent growth potential***

Cells were plated in 6 well plates at 75,000 cells per well and allowed to adhere. Indicated treatments were applied for 24 h, after which cells were harvested and live

cells counted with trypan blue exclusion dye. A base layer of 0.7% agarose in regular growth medium was poured into wells of a 12 well plate and allowed to solidify at 4 °C. Then 12,500 cells/well from each treatment were plated in triplicate in 0.45% agarose in regular growth medium on top of the base layer and allowed to solidify at 4 °C. Plates were then transferred to a 37 °C incubator with 5% CO<sub>2</sub> and allowed to grow. Once visible colonies had formed, they were counted under a microscope, and colony counts were normalized to the untreated sample. Images of representative fields were taken with 5x magnification using a Zeiss Axio Observer A1 microscope (Thornwood, NY), Hamamatsu Orca ER digital camera (Bridgewater, NJ), and MetaMorph software (Molecular Devices, Sunnyvale, CA).

### ***2.13 Assessment of intracellular ALDH activity***

ALDH enzymatic activity was evaluated using the ALDEFLUOR kit (Stem Cell Technologies, Durham, NC) according to manufacturer's instructions. Cells were incubated with provided ALDH substrate for 35 min at 37 °C. For negative control, the specific ALDH inhibitor diethylaminobenzaldehyde (DEAB) was used at a final concentration of 50 mM. ALDEFLUOR fluorescence was measured utilizing a 488 nm excitation and emission detected using a standard FITC 530/30 band pass filter. Sorting gates were established using 7-AAD for viability DEAB-treated, ALDEFLUOR-stained cells as negative controls.

## **2.14 RNA analysis**

### **2.14.1 RNA isolation**

For RNA isolation from adherent cells, cells were trypsinized, washed once with PBS, and total RNA isolated using the Ambion mirVana miRNA isolation kit (Invitrogen) following manufacturer's instructions. Tissue samples were homogenized in the provided lysis buffer and total RNA isolated following instructions. For some samples, RNA was isolated using TRI Reagent (Sigma) following manufacturer's protocol. All RNA quantification and analysis was accomplished using a NanoDrop 2000 (Thermo Scientific).

### **2.14.2 Quantitative polymerase chain reaction analysis**

Total RNA was subjected to reverse transcription using the iScript Reverse Transcription SuperMix Kit (BioRad) and oligo d(T) primers as per manufacturer's instructions. cDNA and SYBR Green were added to a custom PrimePCR plate (Bio-Rad) containing primer pairs for the NF $\kappa$ B target genes listed in Table 2.2 and  $\beta$ -actin as a loading control. The PCR was conducted on an iCycler instrument (BioRad) using the following conditions: (95 °C x 2 min, [95 °C x 5 sec, 60 °C x 30 sec] x 40 cycles) and fold changes calculated by the  $2^{-\Delta\Delta C_t}$  method.

**Table 2.2 Information for NFκB target gene qPCR primers used in Chapter 3**

Gene name	Bio-Rad Unique Assay ID	Amplicon Sequence
BCL2L1	qHsaCED0036793	GGGAAAGCTTGTAGGAGAGAAAGTCAACCACCAGCTCCCGGTTGCTCTGAGACA TTTTTATAATAGGATGGCTCAACCAGTCCATTGTCCAAAACACCTGCTCACTCA CTGAGTCTCGTCTCTGGTTAGTGATTCCTCT
NFKB1	qHsaCED0002379	CCAAGCAGCTCTGCAGCAGACCAAGGAGATGGACCTCAGCGTGGTGGCGGCTCA TGTTTACAGCTTTTCTCCGGATAGCACTGGCAGCTTCACAAGSGCCCTGGAA
FAS	qHsaCED0036301	AATGAAGCCAAAATAGATGAGATCAAGAAATGACAATGTCCAAGACACAGCAGAAC AGAAAGTTCAACTGCTTCGTAATGGCATCAACTTCATGGAAAGAAGAAGCGTAT GACACATTGATTAAGA
NQO1	qHsaCED0036869	CTCATCCTGTACCTCTTTTTTTCATTAAAGAATCCTGCCTGGAAGTTTAGGTCAAAGA GGCTGCTTGGAGCAAAATACAGTGGTGTCTCATCCCAATATTCTCCAGGCCGTT
GSTP1	qHsaCID0020557	CTCACCTGTACCAGTCCAATACCATCCTGCGTCCACCTGGCGCCACCCCTTGGG CTCTATGGGAAGGACCAGCAGGAGGCCCTGGTGACATGGTGAATGACGG CGTGGAGGACCTCC
TNFAIP3	qHsaCID0012648	GAAGCCAGAAGAACTCAACTGGTTCGAGAAAGTCCGGAAGCTTGTGGCGCTG AAACGAAACGGTGACGGCAATGCCATCATGCATGCCACTTCTCAGTACATGTGG GGCGTTCAGGACACAGACTGGTACTGAGGAAGGCGCTGTTCCAG
ICAM1	qHsaCED0004281	GCATTGCTCCTCAGTCAGATACAACAGCATTTGGGGCCATGGTACCTGCACACCTA AAACACTAGGCCACGCATCTGATCTGTAGTCACATGACTAAGCCCAAGGAAAGG AGCAAGACTCAAGACATGA
S100A6	qHsaCED0048256	TTCACCTCCTGGTCTGTTCCGGTCCAAGTCTTCCATCAGCCTTGCAATTTTCAG CATCCTGCAGCTTCGAGCCAATGGTGAGCTCCTTCTG
IL1B	qHsaCID0022272	CTGCCCTGAAGCCCTTCTGTAGTGGTGGTGGAGATTCGTAGCTGGATGCCGCC ATCCAGAGGGCAGAGGTCAGGTCCTGGAAGGAGCAGCTTCATCTGTTTAGGGCC ATCAGCTTCAAAGAACAAGTCATCCTCATTGCCACTGTAATA
HIF1A	qHsaCID0014755	TGCTGGCCCAAGCCGCTGGAGACACAATCATATCTTTAGATTTTGGCAGCAACGA CACAGAACTGATGACCAGCAACTTGAGGAAGTACCATTATATATG
MYC	qHsaCID0012921	CCGCCACACCAGCAGCAGCTCTGAGGAGGAACAAGAAGATGAGGAAGAAATC GATGTTGTTTCTGTGGAAAAGAGGCCAGCTCCTGGCAAAAAGGTCAGAGTCTGGA TCACCTTCTGCTGGAGGCCACAGCA
ACTB	qHsaCED0036269	GTGCTCGATGGGGTACTTCAGGGTGAGGATGCCCTCTCTTGTCTGGGCCCTCGTC GCCACATAGGAATCCTTCTGACCCATGCCCACTCA

### **2.14.3 Affymetrix GeneChip analysis**

RNA quality assessed using the Agilent 2100 Bioanalyzer (Agilent Technologies, Santa Clara, CA), and cDNA/aRNA was generated using the Ambion MessageAmp Premier RNA Amplification kit (Invitrogen) following manufacturer's instructions at the Duke Institute for Genome Sciences & Policy Microarray facility. Biotinlyated aRNA was fragmented according to protocol and hybridized to U133A 2.0 Human Gene microarrays (Affymetrix, Santa Clara, CA). Fluorescent images were detected in a GeneChip Scanner 3000 and expression data was extracted using the GeneChip Operating System v 1.1 (Affymetrix). Expression data were quantile-normalized and summarized using GCRMA express (432). Probe sets with a fluorescent intensity above  $\log_2(100)$  in at least 2 samples were considered informative. Expression levels were compared using generalized linear models on  $\log_2$  expression data and probe sets with nominal  $p$ -values less than 0.05 were considered significant.

#### **2.14.3.1 Expressions2Kinases analysis**

RNA quality assessed using the Agilent 2100 Bioanalyzer (Agilent Technologies, Santa Clara, CA), and cDNA/aRNA was generated using the Ambion MessageAmp Premier RNA Amplification kit (Invitrogen) following manufacturer's instructions at the Duke Institute for Genome Sciences & Policy Microarray facility. Biotinlyated aRNA was fragmented according to protocol and hybridized to U133A 2.0 Human Gene microarrays (Affymetrix, Santa Clara, CA). Fluorescent images were detected in a

GeneChip Scanner 3000 and expression data was extracted using the GeneChip Operating System v 1.1 (Affymetrix). Expression data were quantile-normalized and summarized using GCRMA express (432). Probe sets with a fluorescent intensity above  $\log_2(100)$  in at least 2 samples were considered informative. Expression levels were compared using generalized linear models on  $\log_2$  expression data and probe sets with nominal  $p$ -values less than 0.05 were considered significant.

#### **2.14.3.2 Gene set enrichment analysis**

For analysis in Chapter 3, expression data of wtXIAP (XIAP high) cells was compared to the combined parental and shXIAP cell lines (XIAP low) using default parameters with gene set level permutations and signal2noise used to rank genes. Gene set enrichment visualization was performed using Cytoscape 2.8.3 and a P-value < 0.001, Q-value cutoff 0.006, similarity cutoff of 0.5, and false discovery rate (FDR) of 0.1. For analysis in Chapter 4, gene set enrichment analysis (433) was used to compare expression data of wtXIAP and rSUM149 (ADCC-resistant) cells to parental (ADCC-sensitive) cells using default parameters with gene set level permutations and signal to noise used to rank genes. Gene sets were limited to those 300 or less in size using a nominal  $p$ -value  $\leq 0.01$ . The genes with the most significantly different expression were shown in unsupervised cluster analyses using the top 10, 15 or 30 genes depending on the size of the gene set. For both analyses, gene sets examined were from the current molecular signature (MSigDB) versions 4.0.

## **2.15 Immunohistochemistry of human tumor microarrays**

Tissue microarrays (clinical characteristics available in (434-436)) were deparaffinized in series of xylenes, then rehydrated in 95%, 85%, 70% Ethanol and washed in distilled water for 5 minutes. Antigen retrieval was performed using 1mM EDTA incubation at 95 degrees for 30 minutes. After cooling and washing in 1x Dako wash buffer, the slides were incubated with Dako peroxidase block for 5 minutes at room temperature. After washing for 5 min in wash buffer, slides were incubated overnight at 4 degrees with mouse anti-human XIAP (BD Biosciences, San Jose, CA) antibody solution at 1:60 dilution of antibody diluted in wash buffer. For the negative control, the primary antibody was omitted and the slide was incubated in buffer overnight. After incubation, slides were washed 3 times for 5 minutes with wash buffer, then incubated in the anti-mouse secondary solution (provided in the Dako anti-mouse Envision kit, Carpinteria, CA) for 30 minutes at room temperature. After washing 3 times, slides were incubated in diluted Mayer's hematoxylin (Dako, Carpinteria, CA) for 20 seconds and then washed in tap water. Scott's bluing solution was applied to each slide for 30 seconds, then slides were dehydrated in series of ethanol then incubated in xylenes for 5 minutes. Slides were then coverslipped using Invitrogen Histomount (Invitrogen Life Sciences, Grand Island, NY). Slides were imaged in the Duke Microscopy Core Facility with a Zeiss AxioObserver (Zeiss, Thornwood, NY) complete with imaging software analysis package. A board certified surgical pathologist

completed scoring of slides in a blinded manner. Staining intensity was graded on a qualitative scale (little to no staining [negative], borderline, and highly positive).

## **2.16 Human breast tumor xenograft studies**

For all studies all experiments were performed in accordance with the Duke University International Animal Care and Use Committee. In Chapter 3, female nude mice were obtained from a breeding colony maintained at the Cancer Center Isolation Facility at Duke University. SUM149, vector control (FG9/FG12), wtXIAP, shXIAP, and +XIAP cells ( $5 \times 10^6$  cells) were suspended in 50  $\mu$ l PBS and 50  $\mu$ l Matrigel and injected orthotopically, with a 28-gauge needle, into the fourth mammary fat pad, in two separate studies. Mice were monitored twice weekly and tumor volume measured using the formula  $V = (L \times W^2)/2$  where  $L$  is the length and  $W$  is the width of the tumor. Tumor doubling time was found by fitting a nonlinear regression model to the tumor volumes in GraphPad Prism. Mice were euthanized when tumors reached a humane endpoint of  $\sim 1500 \text{mm}^3$ , at the first sign of morbidity, or at end of study. Tumors were removed, and tissue harvested for RNA and western immunoblot analysis. In Chapter 4, female CB17.SCID (stock number: 001803) mice were purchased from Jackson Labs (Bar Harbor, ME). SUM149, rSUM149, and wtXIAP cells ( $5 \times 10^6$ ) were suspended in 50  $\mu$ l PBS/50  $\mu$ l Matrigel and implanted orthotopically into the fourth mammary fat pad. Once tumors were palpable (50-60  $\text{mm}^3$ ), mice were randomly assigned to treatment groups: cetuximab (200  $\mu\text{g}/\text{mouse}$  2x/week) or trastuzumab (100  $\mu\text{g}/\text{mouse}$  1x/week). Animals

were treated daily via intraperitoneal injection, and tumor volume measured using the formula  $V = (L \times W^2)/2$  where  $L$  is length and  $W$  is width of the tumor.

### ***2.17 Statistical analysis***

The statistical analyses were conducted using GraphPad Prism (GraphPad Software, Inc.) student's 2-tailed t-test, Fisher's exact test, one-way ANOVA, two-way ANOVA and Mantel-Cox log-rank test when necessary. Differences were considered significant at  $p < 0.05$ .

### **3. Investigation of the role of XIAP and identification of functional partners in IBC pathogenesis**

#### ***3.1 Introduction***

Inflammatory breast cancer (IBC) is the most lethal and metastatic variant of all subtypes of breast cancer (434,437). Further, unlike other breast cancers, IBC has a short latent period of progression and usually no solid mass or lump can be felt during a breast exam or spotted during mammography. Despite the use of multimodal treatment regimens that include chemotherapy, radiation and targeted therapies and that aim at inducing apoptosis in proliferating cancer cells, IBC patients present with a significantly elevated risk (10-15%) of tumor relapse (438), a higher incidence of recurrence (~65% compared to <50% for non-IBC), and poor long term survival outcomes (439-441)

Gene expression studies in pretreatment patient tumors have attempted to define differences in IBC patients (434), and reveal, in particular, a highly activated NFκB transcriptional profile associated with increased proliferation and estrogen receptor negativity in IBC primary tumors compared to other locally advanced breast cancers (24,26,64,69). In addition, our recent study has identified an oxidative stress metagene enriched in NFκB target genes to be highly expressed in IBC patient tumor samples when compared to not only normal breast but also to molecular subtype matched non-IBC tumors (413). Although these findings have improved our understanding of IBC, the molecular mechanisms underlying NFκB activation and its role in contributing to the hyperproliferative and cell death-resistant phenotype of IBC cells is not well

understood, leading to an unmet challenge for the development of effective targeted therapies.

We have previously reported that IBC cells overexpress an anti-apoptotic protein, the X-linked inhibitor of apoptosis protein (XIAP), as an adaptive mechanism for survival in the presence of cellular stress/death stimuli (156,418). XIAP is a member of the inhibitor of apoptosis (IAP) family and considered the most potent mammalian caspase inhibitor (442). Additionally, we identified that increased XIAP expression in IBC cells exhibiting resistance to therapy-mediated apoptosis was not due to enhanced transcription or protein stability, but was modulated at the translational level via the internal ribosome entry sites (IRES) element in the 5'UTR of *XIAP* mRNA. This is of significance as IBC patient tumors have been observed to overexpress the translation initiation factor eIF4G1 (46). eIF4G1 plays a key role in the protein synthesis machinery and can mediate increased translation of IRES-containing mRNAs, such as XIAP, as an adaptive mechanism of cell survival (443). Interestingly, a recent report identifies a link between eIF4G1 and MAPK pathway in IRES-mediated translation (444). Recent evidence now suggests that XIAP, in addition to its classical caspase binding function, acts as a signaling mediator of key survival pathways (445,446), including NF $\kappa$ B. We therefore investigated the mechanistic role of XIAP in promoting a hyperproliferative phenotype in IBC. We report that targeting MAPK pathway signals (specifically MEK and Mnk) and downstream eIF4G1 downregulates XIAP expression. Using *in vitro* and

*in vivo* IBC preclinical models, we reveal that XIAP drives activation of NF $\kappa$ B and its target genes leading to enhancement of tumor growth. This is supported by the observation of high XIAP expression in IBC patient tumor samples. In addition, a peptide that targets XIAP interaction and downstream TAB1:IKK $\beta$ -dependent mechanism NF $\kappa$ B activation caused decreased anchorage independent growth and increased sensitivity to therapeutic apoptosis.

## **3.2 Results**

### **3.2.1 XIAP translation is regulated by MAPK signaling in IBC cells**

Based on our identification of increased XIAP IRES mediated translation in apoptotic resistance in IBC cells (156) and a recent study identifying MAPK signaling in potentiating IRES-mediated protein translation of viruses (444), we sought to investigate the influence of this pathway on XIAP expression in IBC. As EGFR/HER2 overexpression and subsequent ERK activation is frequently observed in IBC patient tumors, we employed two patient-derived IBC cell lines: SUM149 – a basal type with EGFR overexpression and SUM190 – a HER2 overexpressing (only two untreated representative models that are considered true IBC-like). We targeted the MAPK pathway in these cells using two small molecule inhibitors: U0126/MEK*i* (antagonist of the MAPKKK, MEK) and CGP57380/Mnk*i* (a selective inhibitor of the MAPK, Mnk) leading to decreased ERK and eIF4E phosphorylation, respectively (Figure 3.1). Targeting MEK also decreased downstream eIF4E phosphorylation, while CGP57380 treatment decreased ERK phosphorylation, most likely due to a feedback loop. Furthermore, targeting both MEK and Mnk led to decreased XIAP expression in both SUM149 and SUM190 and also led to an inhibition eIF4G1 expression.

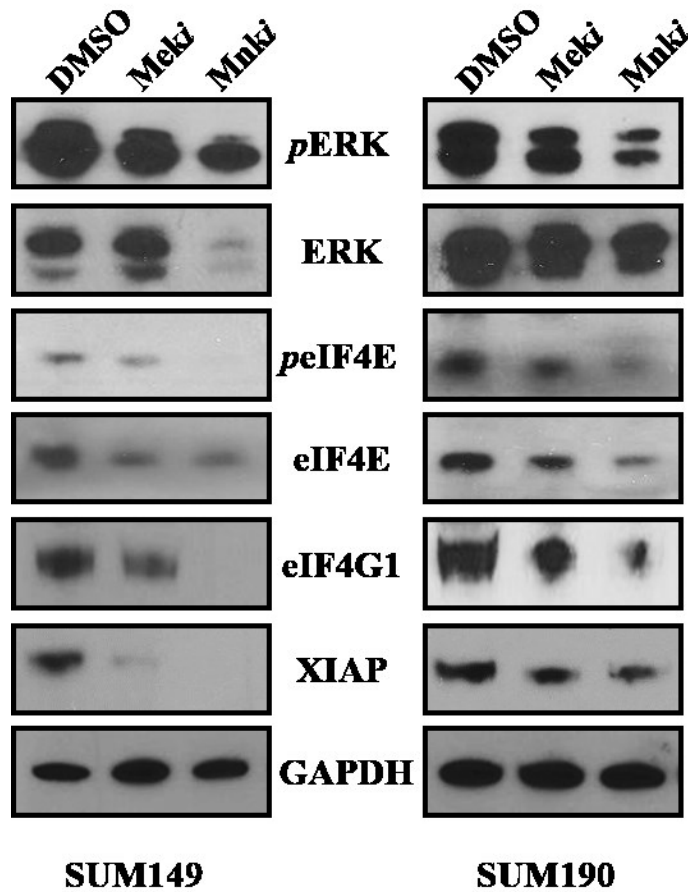


**Figure 3.1 Targeting the MAPK pathway decreases eIF4G1 and XIAP expression in parental IBC cells**

Western immunoblot expression of ERK and eIF4E phosphorylation as well as eIF4G1 and XIAP expression in SUM149 (left) and SUM190 (right) cell lines treated with vehicle, 10  $\mu$ M Meki (U0126), or 10  $\mu$ M Mnki (CGP57380).

To further evaluate the role of MAPK signaling in regulating XIAP expression in cells adapting to stress stimuli, we tested the MAPK antagonists in a drug resistant IBC cell line variant of SUM149 (rSUM149), which exhibit sustained MAPK activation and increased IRES-mediated XIAP expression (156,418). Similar to untreated cell lines, targeting the MAPK pathway in rSUM149 cells leads to decreases in ERK and eIF4E phosphorylation and also XIAP and eIF4G1 expression (Figure 3.2A). Additionally, targeting the MAPK pathway sensitized the rSUM149 cells to the classical apoptosis inducer, TNF-related apoptosis inducing ligand (TRAIL) (Figure 3.2B); we previously reported TRAIL sensitivity to be dependent on XIAP expression in IBC (419).

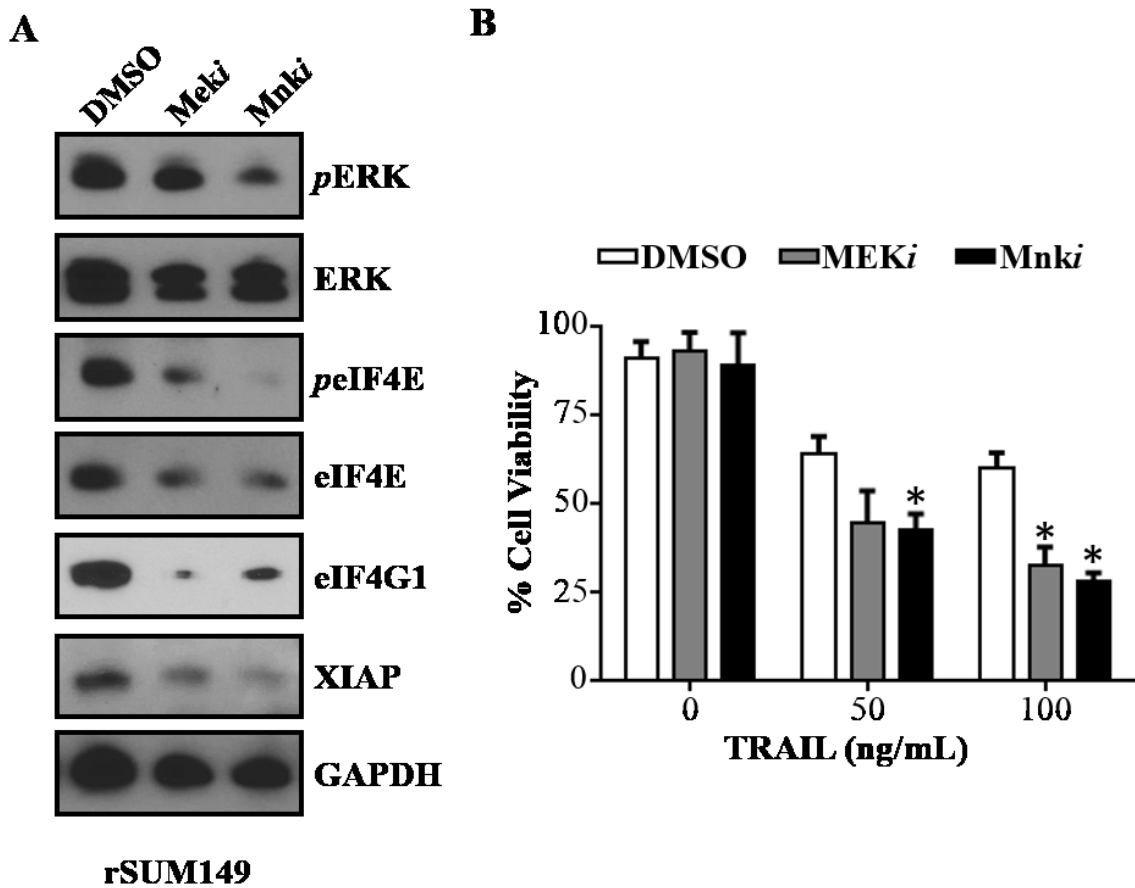
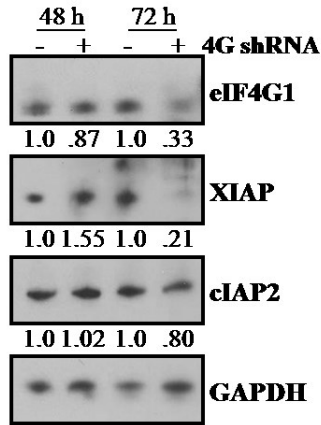


**Figure 3.2 Targeting the MAPK pathway decreases XIAP expression and sensitizes to TRAIL treatment**

A) Western immunoblot analysis of phospho- and total ERK, phospho- and total eIF4E, eIF4G1, and XIAP in cells treated with vehicle or 10  $\mu$ M U0126 (MEKi) or 10  $\mu$ M CGP57380 (Mnki). Number represent densitometric analysis. B) Cell viability of rSUM149 cells treated with vehicle or 10  $\mu$ M U0126 (MEKi) or 10  $\mu$ M CGP57380 (Mnki), alone or in combination with TRAIL. Bars represent mean $\pm$ SEM viable cells taken as a percentage of total cell number (n=2-4, \*p<0.05).

Directly targeting eIF4G1 through RNAi also led to decreased XIAP expression and increased apoptotic sensitivity to TRAIL (Figure 3.3). This XIAP decrease was specific as there was no decrease in cIAP2, a related IAP family member whose translation is not IRES-dependent. This work was part of the projects and undergraduate thesis of Courtney Edwards and M. Arianna Price in Dr. Devi's laboratory at Duke University and is included with permission from mentor and authors. Taken together, these results suggest that MAPK signaling via the protein translational pathway can regulate XIAP protein induction and apoptotic sensitivity in IBC cells.

**A**



**B**

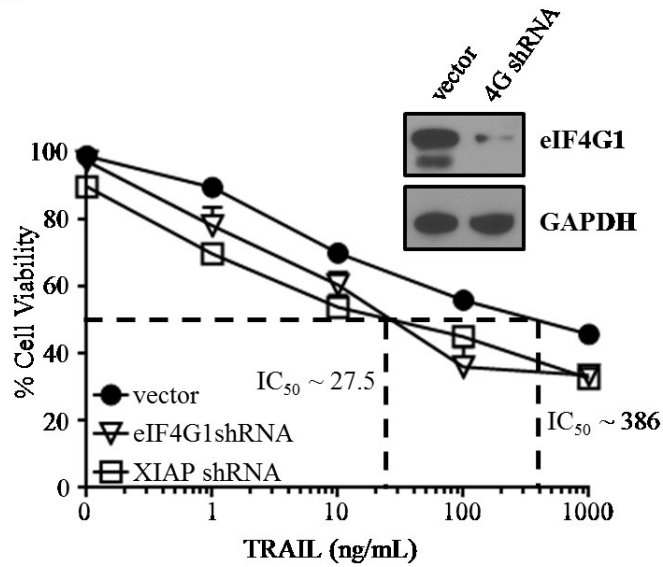


**Figure 3.3** *eIF4G1* silencing decreases XIAP expression in parental SUM149 cells and enhances sensitivity to TRAIL in resistant rSUM149

A) Western immunoblot analysis of eIF4G1, XIAP, and cIAP2 in SUM149 cells transfected with control vector or eIF4G1 shRNA. Numbers represent densitometric analysis. B) Cell viability of rSUM149 cells transfected as indicated and treated with TRAIL. Symbols represent mean±SEM viable cells taken as a percentage of total cells (n=2-3).

### **3.2.2 High XIAP expression correlates with increased expression of a proliferative cluster of genes**

Based on our above data showing regulation of XIAP levels by MAPK signaling, we evaluated XIAP protein expression in IBC patient tumor samples using a panel of breast tissue microarrays from three cohorts that included benign and malignant breast tissues from IBC and non-IBC patients (described in Chapter 2). Positive cytoplasmic staining of XIAP was selectively identified in the IBC infiltrating primary tumor samples and invasive breast tumors compared to normal tissue, low grade, and benign breast samples (Figure 3.4 and Table 3.1). Most importantly, IBC tumor cell clusters, or tumor emboli, which are a distinct histopathological hallmark of all IBC tumors and postulated to be a critical feature in increased invasion and IBC metastatic progression, showed positive XIAP staining (8/13 IBC patient samples in which we could visualize multiple tumor emboli). This work was part of projects conducted in by Arjun J. Arora, student intern at Duke Cancer Institute, and Charlotte Rypens, graduate student at University of Antwerp, in collaboration with World IBC collaboration and is included with Mentor and Authors permission. These results collectively reveal a potential correlation between high XIAP expression and aggressive characteristics of advanced breast cancer cells like IBC, which are already Stage III or higher at diagnosis.

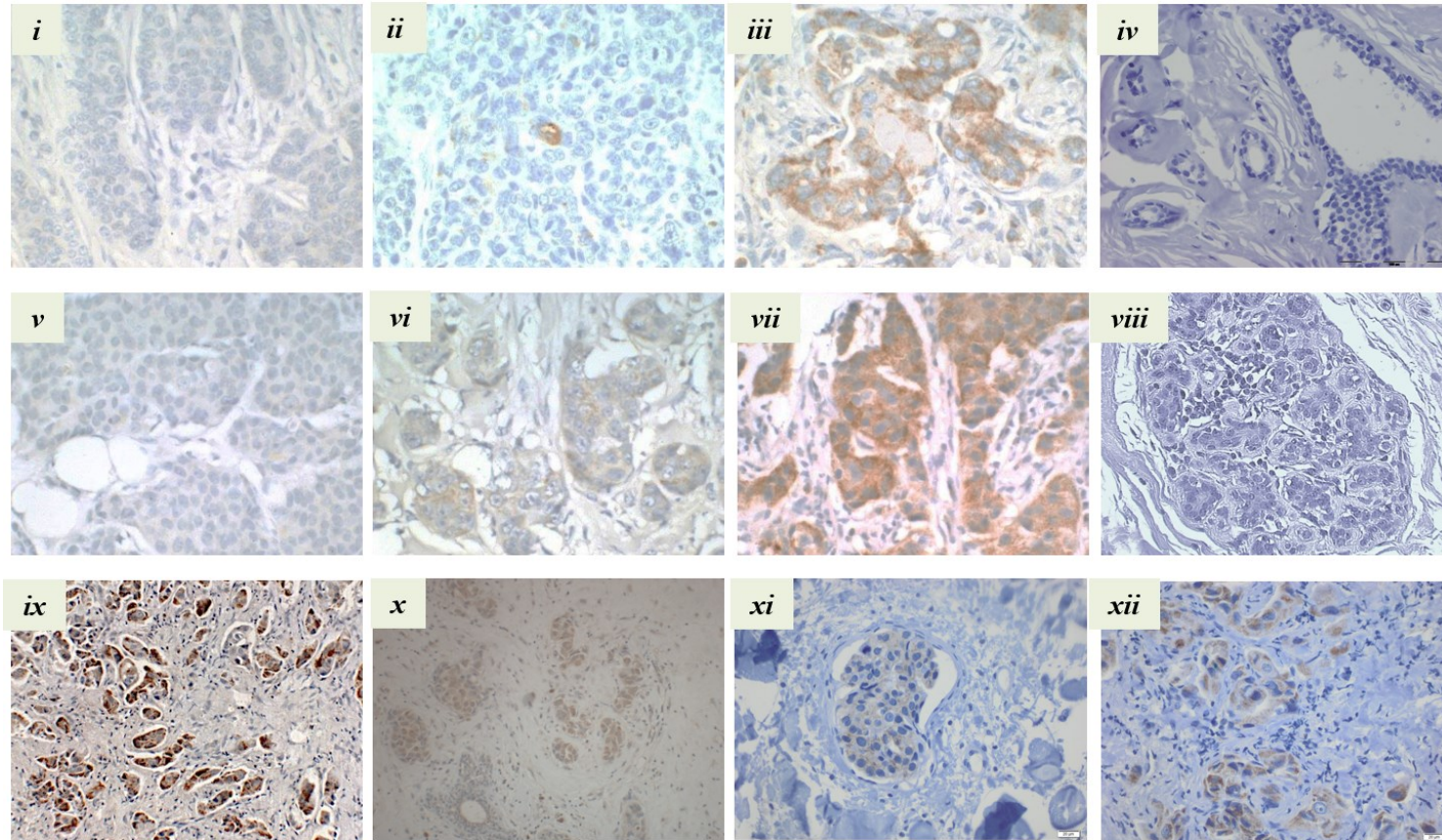


**Figure 3.4 XIAP expression in normal tissue, advanced breast cancer (non-IBC), and IBC**

Representative images of tissue stained for XIAP: (i, v) negative staining, (ii, vi) borderline positive staining, and (iii, vii) high positivity; of normal breast duct (iv) and normal breast lobule (viii); and of high XIAP expressing IBC infiltrating tumors (ix-xii): IBC tumor cell clusters (ix,x,xii) and IBC tumor emboli (xi).

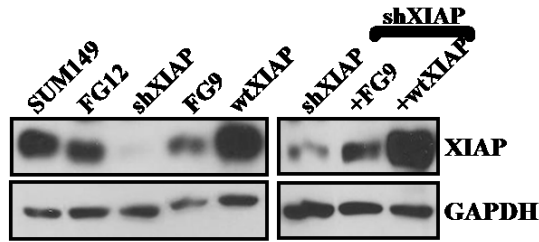
**Table 3.1 Results of XIAP staining of tumor tissue from 3 cohorts**

	Cohort 1		Cohort 2		Cohort 3		Combined	
	Negative	Positive	Negative	Positive	Negative	Positive	Negative	Positive
<i>Grade</i>								
1,2	27	23	44	18	0	1	71	42
3	3	11	23	22	1	10	27	43
p-value	0.0378		0.0442		1.0000		0.0022	
<i>Stage</i>								
1, 2	28	25	39	22	1	7	68	54
3, 4	1	6	1	5	0	2	2	13
p-value	0.1043		0.0353		1.0000		0.0021	
<i>Molecular Subtype</i>								
TNBC	4	9	3	8	0	3	7	20
Other Types	25	25	47	27	1	8	73	60
p-value	0.3494		0.0447		1.0000		0.0103	

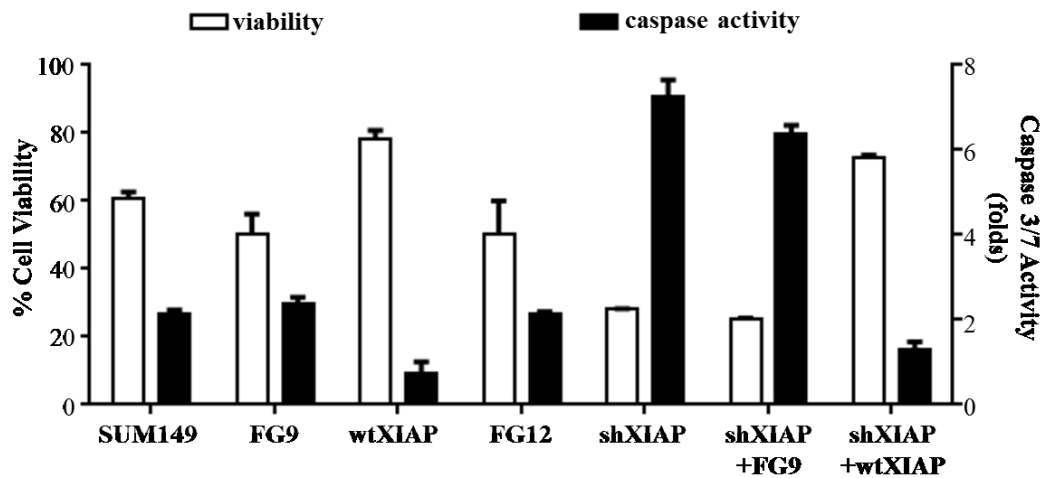
### **3.2.3 XIAP drives constitutive NFκB activity in IBC cells**

Comparative gene expression analysis of IBC and non-IBC patient tumor samples have suggested that enhanced MAPK signaling in IBC tumors is a potential link between EGFR/HER2 overexpression and increased NFκB activity in patient tumors (26). However, the molecular mechanisms underlying this link in IBC tumor cells are unknown. Our aforementioned data reveals the role of the MAPK pathway in mediating XIAP overexpression and therefore we wanted to evaluate the effect of XIAP overexpression on NFκB activation in IBC cells, as XIAP has been previously linked to NFκB both as a transcriptional target and an activator (447). We specifically overexpressed and knocked down XIAP in SUM149 cells, a patient primary tumor-derived cell line prior to any treatment and considered the only true IBC-like model of triple negative, basal type with EGFR activation (414). Validation of XIAP expression level (Figure 3.5A) and function (measured by caspase activation and cell viability post-TRAIL administration) are shown in Figure 3.5B.

**A**



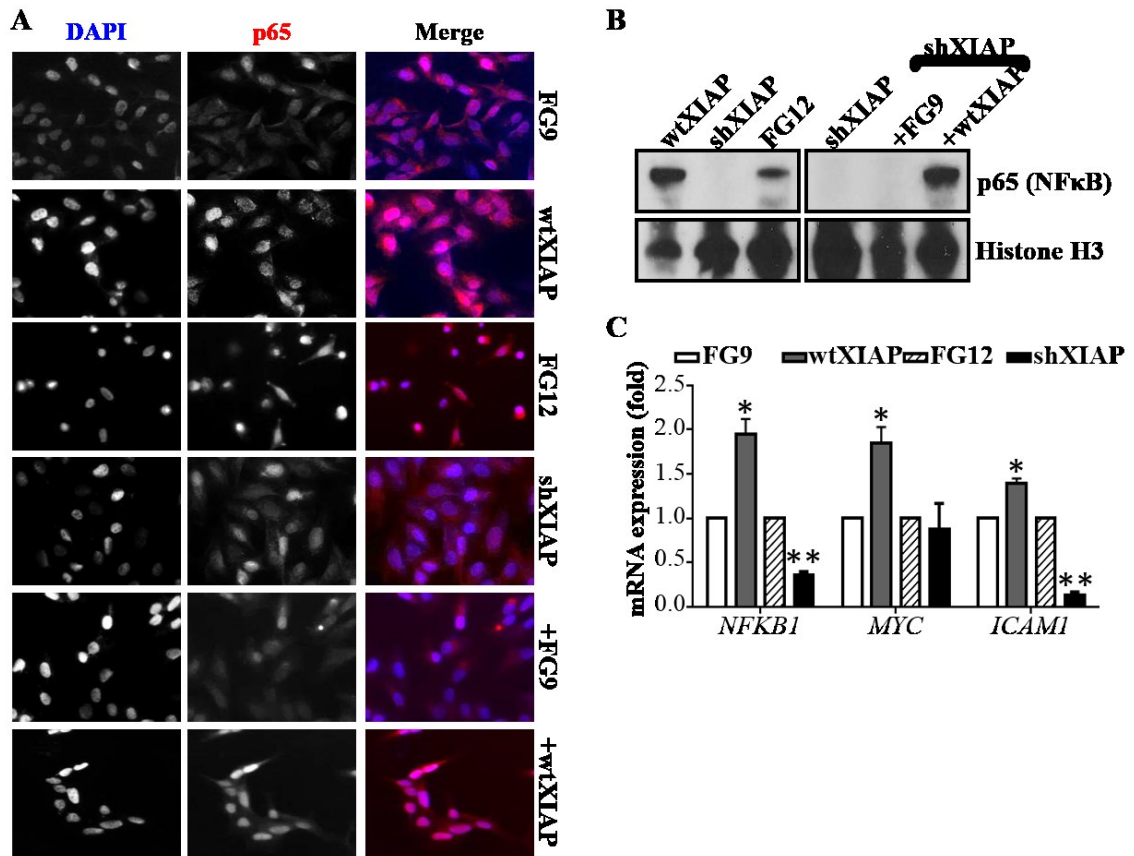
**B**



**Figure 3.5 Validation of XIAP expression and function in XIAP modulated cell lines**

A) Western immunoblot analysis of XIAP expression in FG12, shXIAP, FG9, wtXIAP, shXIAP+FG9, and shXIAP+wtXIAP cells. B) Cell viability (left axis, white bars) and caspase activity (right axis, black bars) of indicated cell lines after administration of 50 ng/mL TRAIL. For viability, bars represent mean±SEM viable cells taken as a percentage of total cell number (n=2-3). For caspase 3/7 activity, bars represent mean±SEM fold change normalized to untreated (n=2-3). All modulated cell lines significant to control vector.

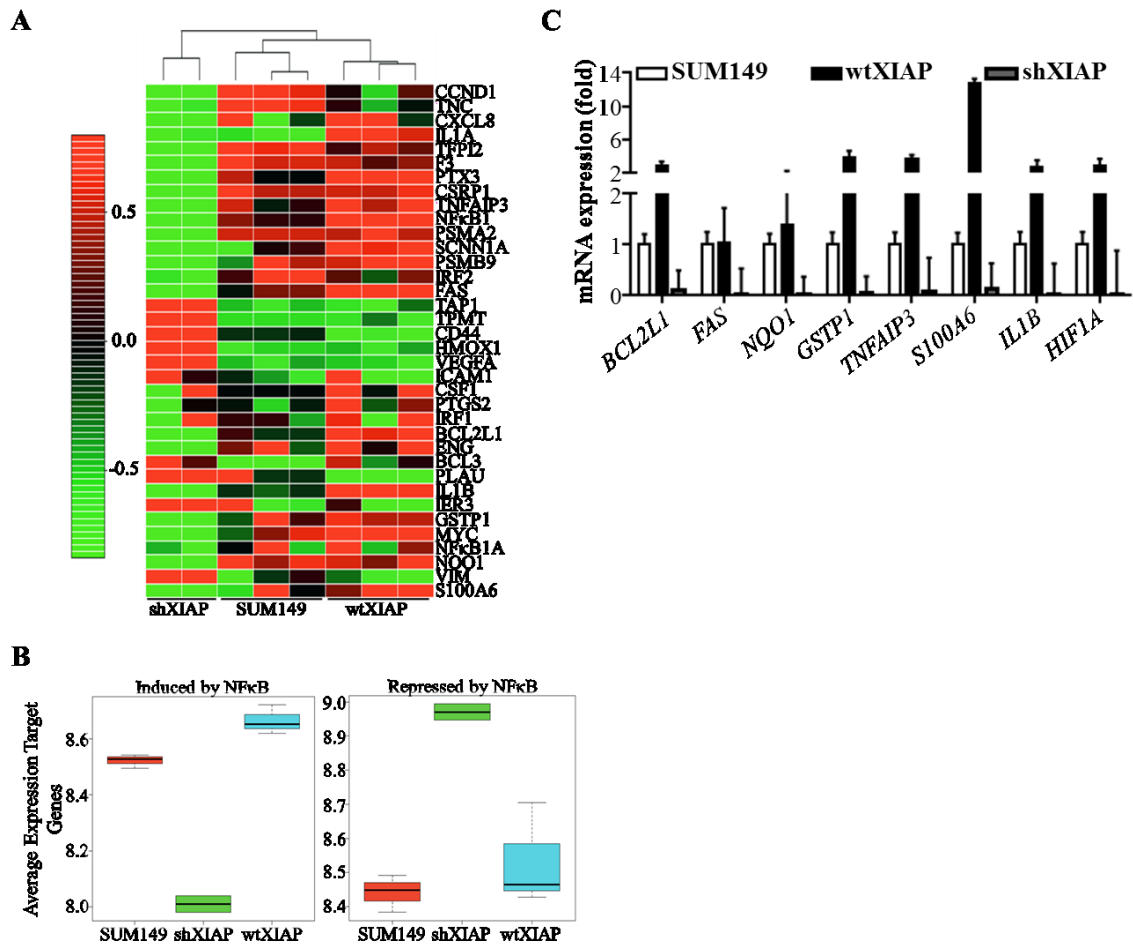
Data in Figure 3.6A show an increase in basal nuclear staining of the p65 subunit of NF $\kappa$ B in XIAP overexpressing cells, while knockdown of XIAP showed increased cytoplasmic localization compared to their respective controls (FG9 for wtXIAP and FG12 for shXIAP). We also noted slight changes in total p65 staining in XIAP-modulated cells, which is expected as p65 is a target of itself. To further support the claim that XIAP knockdown alters p65 localization, we used an siRNA against XIAP which yielded similar results (data not shown). To confirm this, we restored XIAP expression by introduction of an shRNA-resistant, full length XIAP in shXIAP cells (+XIAP) and observed an increase in NF $\kappa$ B nuclear translocation when compared to vector control (+FG9). Subcellular fractionation of cells revealed increased nuclear p65 expression in wtXIAP cells and no nuclear p65 in shXIAP cells compared to vector control. Similar to above reintroduction of XIAP into the shXIAP background increased p65 nuclear expression, while the empty vector had no effect (Figure 3.6B). Transcriptional activity of NF $\kappa$ B was confirmed by qPCR analysis of multiple NF $\kappa$ B target genes revealing significantly increased target gene expression in wtXIAP cells and decreased expression in XIAP depleted cells (Figure 3.6C).



**Figure 3.6 Modulation of XIAP expression alters NFκB localization and transcriptional activity**

A) Representative immunofluorescence images for p65 in indicated cell lines. Single color images were merged (right panels) with p65 shown in red and DAPI shown in blue, Magnification: 40x. Scale bar = 25 μm. B) Western immunoblot for p65 of nuclear lysates from a subcellular fractionation. Histone H3 as control. C) Quantitative PCR analysis of indicated NFκB target mRNAs in FG9 (white bars), wtXIAP (gray bars), FG12 (white striped bars) and shXIAP (black bars) cells. Bars represent mean±SEM calculated by the  $2^{-\Delta\Delta C_t}$  method in fold compared to SUM149 (n=2, \*p<0.05 \*\*p<0.005 compared to control).

To further characterize the transcriptional pattern associated with XIAP-mediated activation of NFκB, we evaluated the expression of >30 previously validated NFκB targets observed to be higher in IBC than non-IBC patient tumors (65) by microarray analysis in control SUM149, wtXIAP, and shXIAP cells. Unsupervised analysis clustered NFκB target gene expression profiles from SUM149 and wtXIAP together, with branch length being much shorter between SUM149 and wtXIAP, than SUM149 and shXIAP. A significant reduction of transcripts associated with cytokine signaling (*CXCL8*, *IL1A*, *IL1B*, *FAS*), inflammation (*IRF2*, *PSMA2*, *PSMB9*), and proliferation/tumor promotion (*TNC*, *CCND1*, *CSF1*, *ENG*) were noted in the shXIAP cells (Figure 3.7A). This corresponded to a high average expression of NFκB target genes in SUM149, with an increase in wtXIAP samples and a dramatic decrease in shXIAP cells (Figure 3.7B, left). This paralleled with a significant increase in expression in shXIAP samples for genes that are normally repressed by NFκB (Figure 3.7B, right). Figure 3.7C shows confirmation of this pattern of NFκB activation by quantitative PCR. Taken together, these data show not only that XIAP expression is critical for basal NFκB activation in an IBC cell line, but also that the level of XIAP expression can alter the pattern of NFκB activity and signaling associated with the hyperproliferative phenotype observed in IBC tumors.

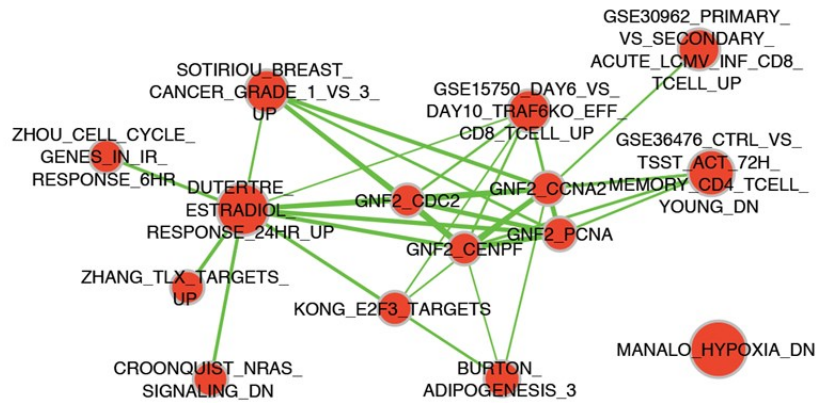
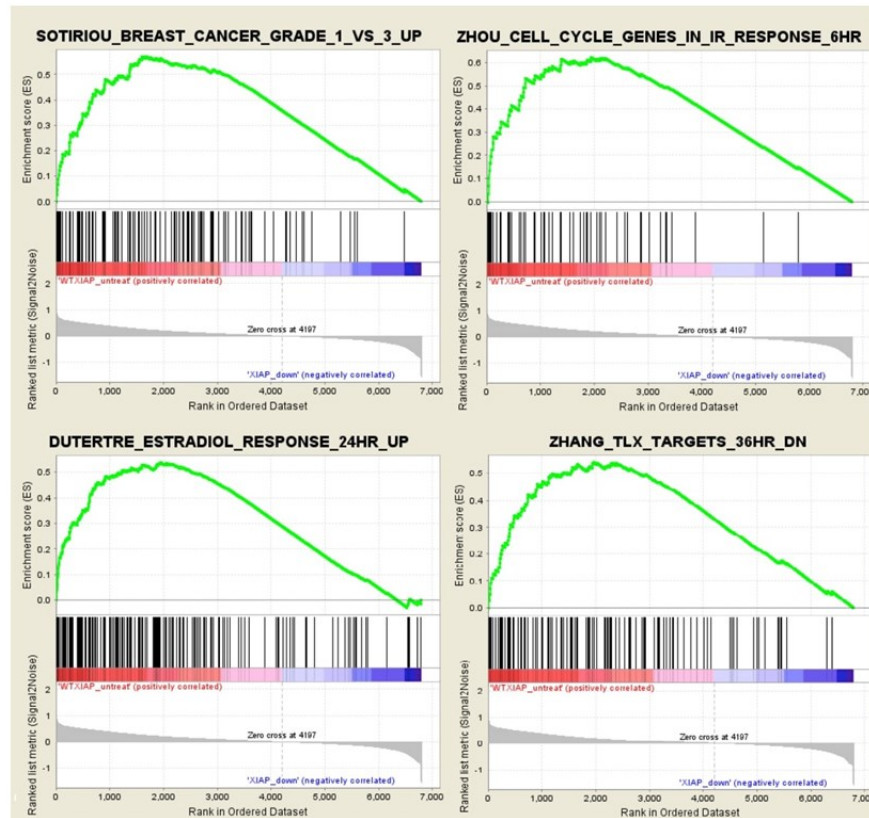


**Figure 3.7 XIAP expression is necessary for expression of and IBC-specific NFκB signature in parental SUM149 cells**

A) Heatmap of normalized gene expression for NFκB targets (genes listed on right) in indicated cell lines. B) Boxplots corresponding to genes induced (top) and repressed (bottom) by NFκB in SUM149 (red box), shXIAP (green box), or wtXIAP (blue box) cells. C) Quantitative PCR analysis of indicated NFκB target mRNAs in SUM149 (white bars), wtXIAP (black bars), and shXIAP (gray bars) cells. Bars represent mean±SEM calculated by the 2<sup>-ΔΔCt</sup> method in fold compared to SUM149 (n=2).

### **3.2.4 High XIAP expression correlates with increased expression of a proliferative cluster of genes**

We conducted a global analysis of the effects of XIAP overexpression on the transcriptomic landscape in IBC (i.e. SUM149 cells). GSEA analysis revealed a network of gene sets associated with XIAP over-expression (Figure 3.8A) including: high grade breast cancer (448), estrogen stimulated breast cancer *in vitro* (449), cervical cancer proliferation (450), cell cycle and radiation (451), markers of neuronal stem cell maintenance (452) and oligodendrocyte (453) and adipocyte (454) differentiation, and several gene sets related to primary and effector CD4 and CD8 T-cells (455,456). GNF expression atlas ontologies revealed a network of genes related to CDC2 (cyclin-dependent kinase 1), CENPF (centromere protein F), PCNA (proliferating nuclear cell antigen), RRM1 (ribonucleotide reductase M1), CCNA2 (cyclin A2), and SMC4L1 (structural maintenance of chromosomes-like 1). Selected GSEA plots are shown in Figure 3.8B. These data further suggest a possible relationship between XIAP and pathways normally associated with proliferation.

**A****B**

**Figure 3.8 XIAP expression correlates with proliferative gene expression**

A) Network graphic representative of GSEA analysis of XIAP overexpression as compared to low XIAP samples. B) Selected enrichment plots from our GSEA analysis.

### **3.2.5 Expression of XIAP correlates with an IBC-specific gene signature and is essential for in vivo tumorigenesis**

We next assessed the potential of SUM149 cells with differential XIAP expression to alter tumor growth in an orthotopic mammary fat pad xenograft murine model. XIAP modulation had no significant effect on proliferation rates of cells in culture (data not shown). Data in Figure 3.9A, however, show that while initially all mice formed tumors at similar time points, the growth in animals bearing wtXIAP cells was significantly increased compared to vector control cells (doubling time – 6.9 days-wtXIAP, 10.3 days-vector controls). In contrast, although shXIAP tumors grew to palpability, most of them either regressed (10/12) or did not increase in size compared to vector control tumors in the study period. For presentation purposes FG9 and FG12 were combined in Figure 3.9A as they had similar growth kinetics. Representative pictures from tumor bearing mice are shown in Figure 3.9B. Tumor growth related statistical analysis for all animals in these studies are presented in Table 3.2. In addition, robust tumor growth, similar to wtXIAP, was observed in mice implanted with XIAP reconstituted shXIAP cells (+XIAP) revealing the necessity for XIAP expression.

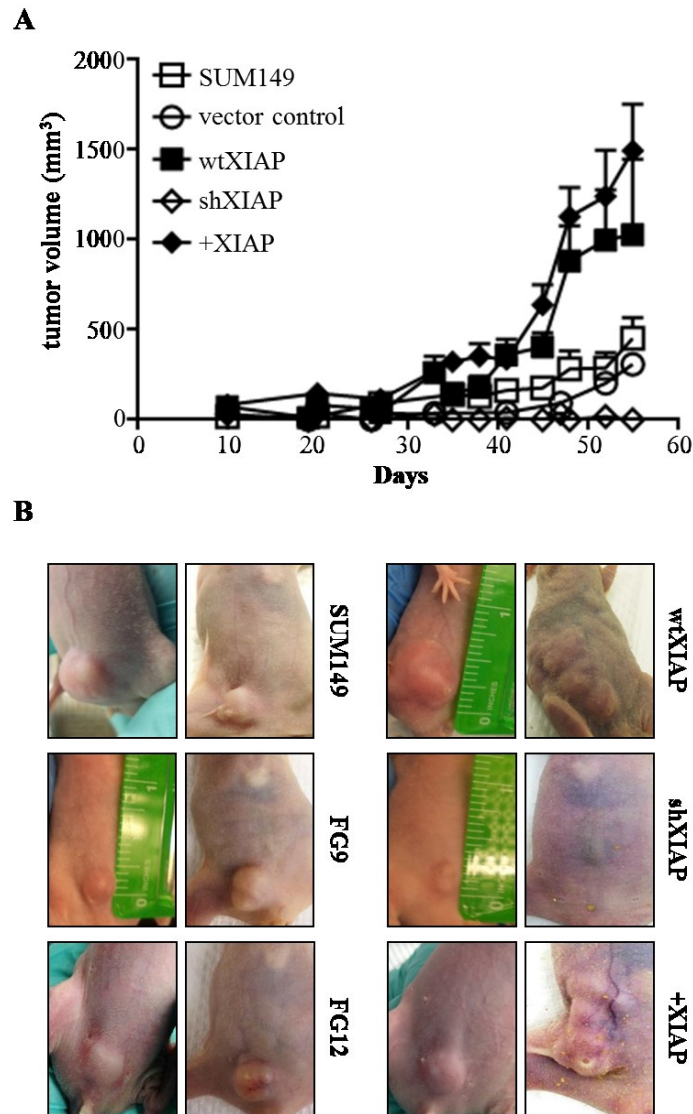


**Figure 3.9 XIAP expression is necessary for *in vivo* tumor growth of IBC cells**

A) Tumor growth curves of SUM149 (open square), vector control (open circle), wtXIAP (closed square), shXIAP (open diamond), and +XIAP (closed diamond) xenografts implanted orthotopically in nude mice. B) Representative images of mice implanted with tumors as indicated. Image on left is from approximately mid-way through the study, while image on right is at endpoint.

**Table 3.2 Statistics of mice used in XIAP modulation *in vivo* studies**

Group (n)	Mouse weight (g)		# animals with tumors	Tumor doubling (days)
	starting	ending		
SUM149 (6)	21.2±0.63	21.4±0.91	6/6	10.3±3.12
vector control (FG9/FG12) (12)	23.8±0.26	24.7±0.67	10/12	9.0±3.25
wtXIAP (12)	19.8±0.32	21.7±0.32	11/12	6.9±1.86
shXIAP (12)	19.8±0.31	22.3±0.07	2/12	N/A (lag phase)
+XIAP (6)	19.6±0.53	21.1±0.45	6/6	8.3±1.78

Tumor burden was determined by dividing tumor weight by final mouse weight; tumor doubling time was found by fitting a nonlinear regression model to tumor volumes in GraphPad Prism.

Based on our evidence of altered proliferation rates *in vivo*, but not *in vitro* we wanted to investigate if XIAP had a role in modulating cancer stem-like characteristics [observed to be high in IBC cells and patient tumors (457)] and cancer cell motility that could support the tumor growth observations. Data in Figure 3.10 show that while overexpression of XIAP (wtXIAP) increases the proportion of ALDH<sup>+</sup> cells (enzymatic marker of cancer stem-like cells), XIAP-silenced (shXIAP) cells have very low ALDH<sup>+</sup> numbers. Similar to NFκB expression analysis, reconstitution of XIAP expression in the shXIAP cells (+XIAP) showed re-emergence of high numbers of ALDH<sup>+</sup> cells. ALDH activity has been shown to be dependent on NFκB activity in basal-like cells (458) and targeting of NFκB in wtXIAP cells decreases the ALDH population further showcasing the role of XIAP-mediated NFκB activation in CSC maintenance.

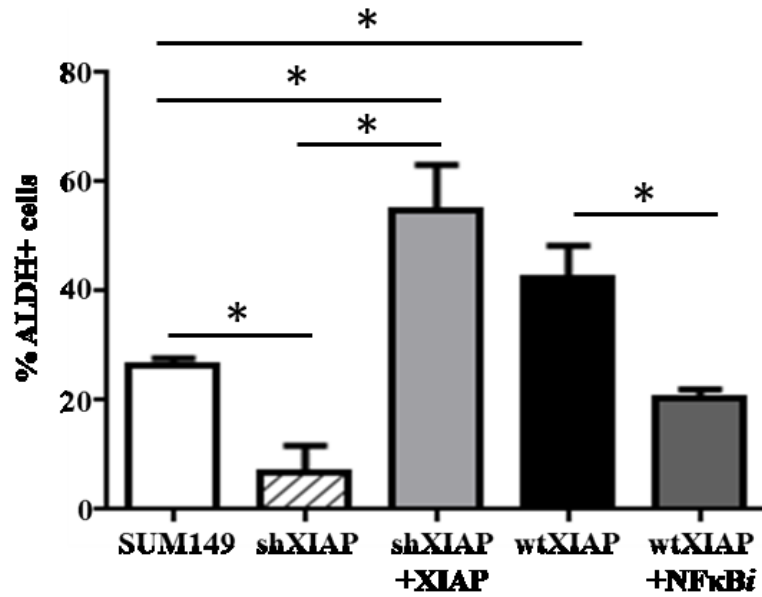


**Figure 3.10 Modulating XIAP expression alters number of ALDH+ cells and is dependent on NFκB signaling**

Flow cytometric analysis for aldehyde dehydrogenase (ALDH) activity in cell lines indicated. For NFκB inhibition, wtXIAP cells were treated with 100 μM NFκBi (JSH-23). Bars represent mean±SEM of ALDEFLUOR+ve cells as a percentage of the total number of cells analyzed, n=2-3.

Measuring cellular motility using the *in vitro* wound healing assay showed that wtXIAP cells were able to almost completely close the wound in 48 h, while shXIAP cells had a significant portion of the scratch unfilled (Figure 3.11). Additionally, restoration of XIAP expression in the XIAP silenced cells reestablished migratory capacity to a level similar to parental cells.

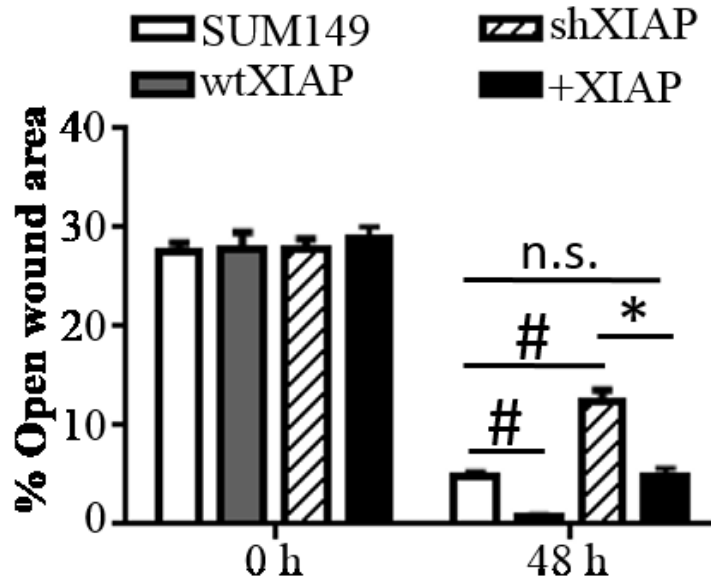


**Figure 3.11 XIAP expression strongly correlates with migratory capacity in IBC cells**

Analysis of cellular motility/wound healing in SUM149, shXIAP, wtXIAP, and +XIAP cells. Bars represent % open wound area at indicated time points as analyzed by Tscratch program as described in Chapter 2 (n=2, \*p<0.05 #p<0.001).

Next, to evaluate the clinical relevance of XIAP expression, we applied an IBC-specific 79-gene set that was identified from an integrative analysis of the largest set of untreated IBC patient tumors obtained from the World IBC Consortium when compared to stage and subtype-matched non-IBC tumors and normal breast samples (21) to the XIAP modulated SUM149 cells. Data in Figure 3.12 confirm that SUM149 cells are highly IBC-like with an average posterior probability (similarity) of 44.7% and XIAP overexpressing (wtXIAP) cells also show an increase in the posterior IBC probability (i.e. 51.5%). More importantly, knock down of XIAP completely abolishes any resemblance of the SUM149 gene expression profile to the 79-gene IBC patient gene signature (i.e. 0.05%).

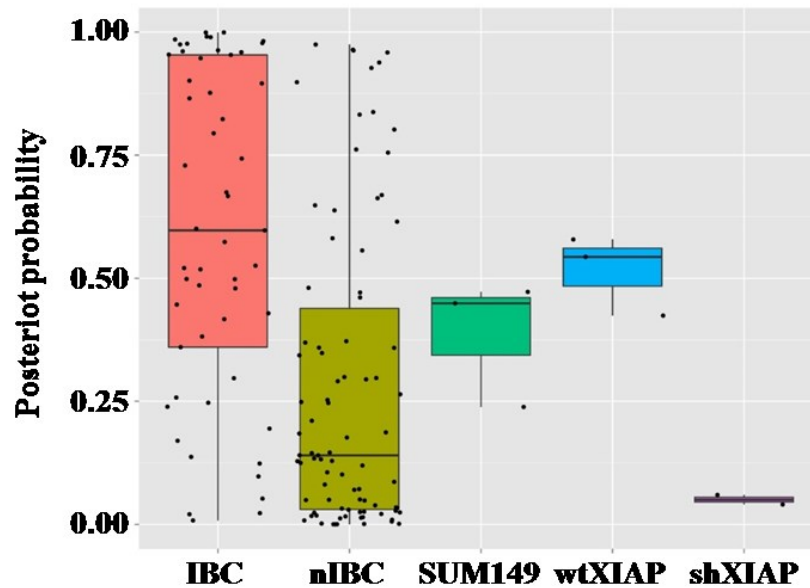


**Figure 3.12 XIAP expression correlates with an IBC patient gene signature**

Application of the IBC-specific 79 gene signature to the expression data from SUM149, wtXIAP and shXIAP cells. The figure shows, in boxplot format, the posterior IBC probability on the Y-axis for all samples including: patients with IBC (red, positive control), patients with non-IBC (moss green, negative control), SUM149 cells (green), wtXIAP (blue) and shXIAP (purple).

### **3.2.6 XIAP expression alters the transcriptomic landscape of primary tumors, correlating with high NF $\kappa$ B activation**

We further compared the gene expression profiles of SUM149 and XIAP-overexpressing primary tumors, identifying 933 differentially expressed genes. Gene ontology analysis revealed biological processes of transcription (GO:0045893/GO:1903508), RNA biosynthesis (GO:1902680), protein metabolism (GO:0051247), and cellular metabolic processes (GO:0031325) among others. Expression2Kinases (E2K) analysis revealed that this gene list was enriched for target genes of two transcription factors of the NF $\kappa$ B family (i.e. RELA and NF $\kappa$ B1). A heatmap of these target genes is shown in Figure 3.13A. In addition to target gene enrichment analysis, E2K also builds a protein-protein interaction (PPI) network that summarizes all signal transduction pathways that can theoretically explain observed gene expression differences between samples. The PPI network was analyzed for enriched pathways using the Reactome FI plugin in Cytoscape, and identified a subnetwork regulating NF $\kappa$ B activity, which is shown in Figure 3.13B.

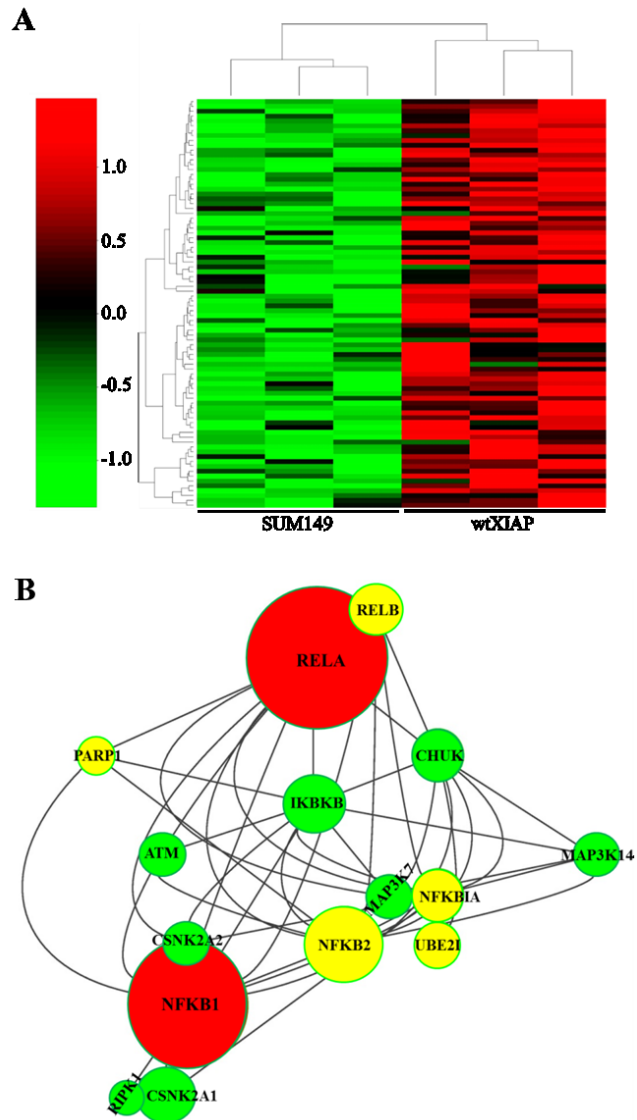


**Figure 3.13 XIAP overexpressing tumors exhibit extensive activation of NFκB signaling**

A) Heatmap of 933 differentially expressed identified between SUM149 and wtXIAP primary tumors. B) Subnetwork of the PPI network identified by E2K to regulate the gene expression profile identified by comparing SUM149 and wtXIAP primary tumors - transcription factors (red), activating kinases (green), and cytoplasmic signal transduces (yellow). The size of the nodes relates to the number of interactions each node has within the PPI network.

These data were further confirmed by qPCR analysis which revealed increased expression of NF $\kappa$ B target genes (*NFKB1*, *MYC*, and *TNFAIP3*) in wtXIAP and +XIAP tumors, while shXIAP tumors showed a loss of these transcripts (Figure 3.14A). Western immunoblot analysis of both wtXIAP and +XIAP tumors that showed enhanced activation of the nuclear transcription factor, NF $\kappa$ B (phospho-p65), and increased expression of known NF $\kappa$ B targets - anti-apoptotic protein Bcl-2, and antioxidant, SOD2 (Figure 3.14B).

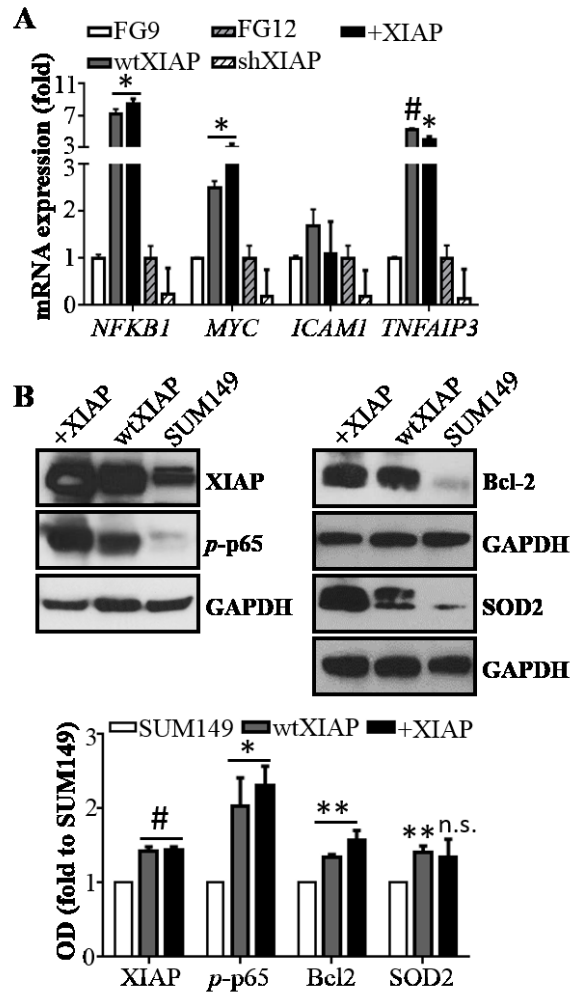


**Figure 3.14 XIAP overexpressing primary tumors have high expression of NFκB target genes and proteins**

A) Quantitative PCR analysis of indicated NFκB target mRNAs in FG9 (white bars), wtXIAP (gray bars), +XIAP (black bars) FG12 (white striped bars) and shXIAP (gray striped bars) tumors. Bars represent mean±SEM calculated by the  $2^{-\Delta\Delta C_t}$  method in fold compared to FG9 (n=2).

B) (Top) Immunoblot analysis of xenografts harvested at end of study. *Representative blots shown.* (Bottom) Densitometric analysis of multiple xenografts normalized to GAPDH. Data represent mean±SEM for arbitrary OD units relative to SUM149, n= 3-5. \*p<0.05, \*\*p<0.005, #p<0.001.

### **3.2.7 XIAP activates NF $\kappa$ B through a TAB1:IKK $\beta$ -dependent mechanism**

Based on the aforementioned data showing the ability of XIAP to drive NF $\kappa$ B activity in IBC cells and *in vivo* tumors, we sought to investigate the underlying mechanism. Data in Figure 3.15 reveals that XIAP downregulation (shXIAP) in SUM149 cells disrupts the formation of a TAB1, TAK1 and IKK $\beta$  complex demonstrated by a loss of IKK $\beta$  pulldown with TAB1, a mechanism identified to be key in NF $\kappa$ B activation (276,277). Additionally, XIAP restoration in the shXIAP cells led to normal TAB1:IKK $\beta$  complex formation. Evaluation of p-I $\kappa$ B $\alpha$  levels in whole cell extracts showed insignificant phosphorylation in shXIAP cells, while re-expression of XIAP significantly increased p-I $\kappa$ B $\alpha$  levels. These experiments suggest that constitutive activation of NF $\kappa$ B is driven in a TAB1:IKK $\beta$ -dependent manner contingent on XIAP expression in IBC cells.

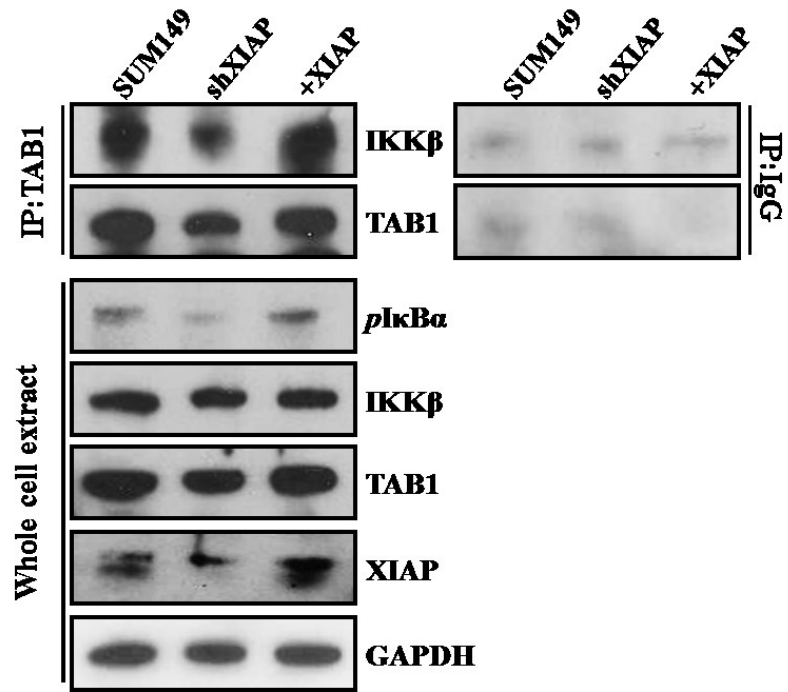


**Figure 3.15 Silencing *XIAP* reduces binding of TAB1 and IKK $\beta$  in IBC cells decreasing I $\kappa$ B $\alpha$  phosphorylation**

Immunoblot analysis for IKK $\beta$  of detergent-solubilized whole-cell extracts immunoprecipitated with either a TAB1 antibody or rabbit IgG as control. Whole-cell extracts were probed for p-I $\kappa$ B $\alpha$ , IKK $\beta$ , TAB1, XIAP, and GAPDH as indicated.

To further interrogate the role of XIAP BIR1 domain in XIAP-NF $\kappa$ B interaction in IBC cells, we first transfected shXIAP cells with a mutant XIAP construct previously shown to abrogate NF $\kappa$ B activation. Transfection of a V80D point mutant of XIAP, which antagonizes BIR1-TAB1 binding, yielded no increase in nuclear localization of p65, whereas both the full length and RING domain mutant (F495A) increased nuclear localization (Figure 3.16), confirming previously published data (276).

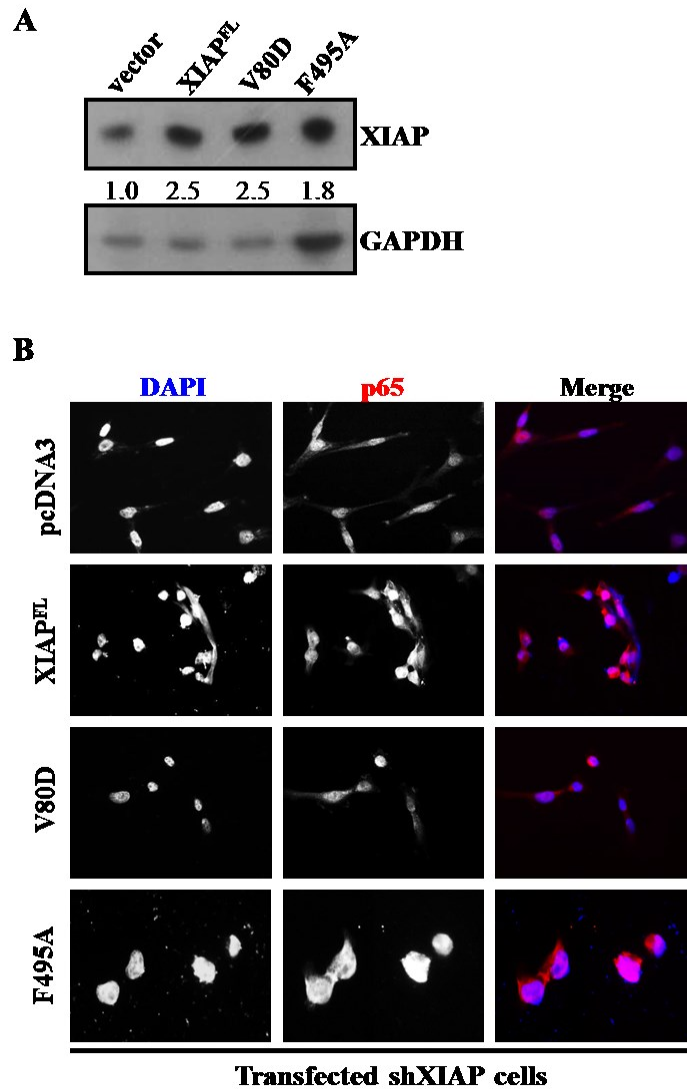


**Figure 3.16 Mutation of the oligomerization domain of XIAP inhibits NF $\kappa$ B nuclear translocation**

A) Immunoblot analysis of XIAP expression in shXIAP cells transiently transfected with XIAP expressing constructs as indicated. Numbers represent densitometric analysis. B) Representative immunofluorescence images for p65 in shXIAP cells transiently transfected with indicated constructs. Single color images were merged with p65 shown in red and DAPI shown in blue, Magnification: 40x.

Next, we targeted the XIAP:TAB1 interaction using a small peptide, modeled after the NRAGE protein, which had previously been reported to block XIAP:TAB1-driven NF $\kappa$ B activation in P19 neural progenitor cells (424). We first noted that XIAP-overexpressing wtXIAP cells exhibit increased phosphorylation of p65 when compared to FG9 vector cells which leads to increased expression of NF $\kappa$ B target, Bcl-2. Treatment of these cells with a sublethal dose of NRAGE in combination with a cargo transporter (EndoPorter) leads to a decrease in p65 phosphorylation and also a slight decrease in total p65 levels. This correlates with decreased Bcl-2 expression, while SUM149 cells showed no change in expression (Figure 3.17A). We also tested the ability of NRAGE to decrease NF $\kappa$ B phosphorylation in rSUM149 cells, which have endogenously increased XIAP expression and NF $\kappa$ B activation. NRAGE administration had a similar effect in this cell line as in wtXIAP. Figure 3.17B reveals increased cytoplasmic detection of p65 in wtXIAP cells treated with NRAGE as phosphorylation of p65 is necessary for its nuclear localization. These changes in phosphorylation and nuclear accumulation mediated by NRAGE administration correlated with decreased transcriptional activity of NF $\kappa$ B as measured by target gene expression (Figure 3.17C). Taken together, these results support the role of XIAP and in particular its BIR1 domain in the functional partnership between XIAP and NF $\kappa$ B in potentiating the hyperproliferative IBC phenotype.

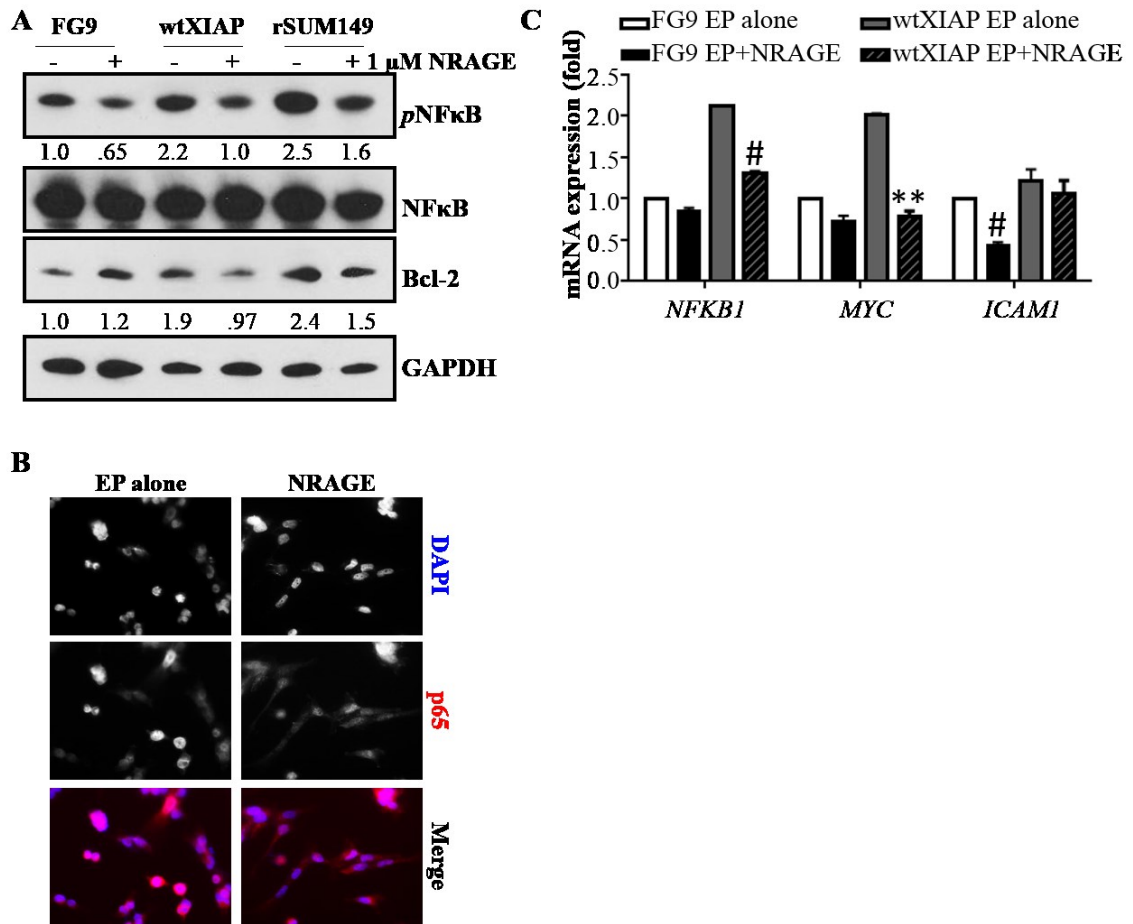


**Figure 3.17 Administration of NRAGE peptide can decrease NFκB phosphorylation and downstream signaling in IBC cells**

A) Western immunoblot analysis of phospho- and total p65 and Bcl-2 in indicated cells treated with EndoPorter alone (-) or 1 μM NRAGE peptide+EP (+). Numbers represent densitometric analysis. B) Immunofluorescence images of SUM149 and wtXIAP cells treated with EndoPorter (EP alone) or +1 μM NRAGE+EP (NRAGE). Magnification: 40x. C) Quantitative PCR analysis of indicated NFκB target mRNAs in indicated cell lines treated with EP alone or 1 μM NRAGE+EP. Bars represent mean±SEM calculated by the 2-ΔΔCt method in fold compared to FG9 (n=2, \*\*p<0.005 #p<0.001).

### **3.2.8 Targeting the XIAP:TAB1 interaction with NRAGE decreases AIG and reverses resistance to an EGFR kinase inhibitor**

In order to evaluate the therapeutic potential of targeting XIAP-BIR1 activity, we tested NRAGE for its efficacy in inhibiting anchorage independent growth (AIG), an assay considered to be a reasonably good predictor of efficacy in preclinical models and a surrogate for *in vivo* analysis of therapeutic compounds. We noted increased colony formation in wtXIAP and rSUM149 cells compared to control cell lines, similar to *in vivo* data. We observed a dose-dependent decrease in growth of NRAGE treated wt ctr, wtXIAP, and rSUM149 cells (**Figure 5E**). Of note, colonies of NRAGE treated cells were slightly larger than vehicle treated counterparts, while overall number was lowered.

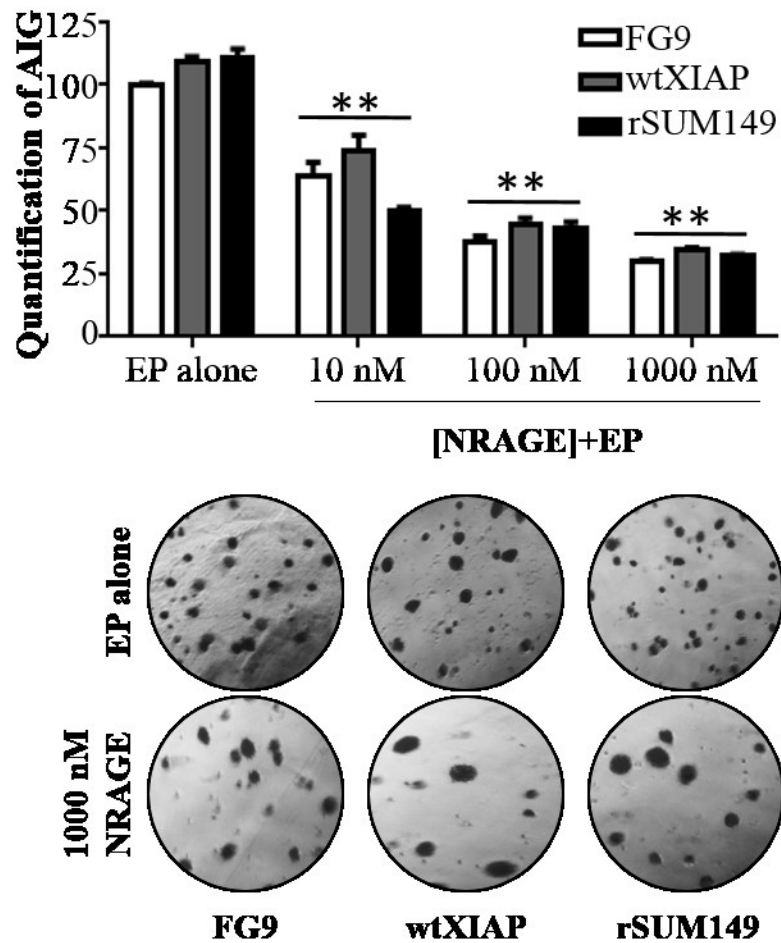


**Figure 3.18 NRAGE treatment decreases anchorage-independent growth in a dose-dependent manner**

Anchorage-independent growth assay of cells treated with EndoPorter (EP alone) or NRAGE peptide+EndoPorter. Bars represent mean±SEM colonies formed in soft agar as a percentage of untreated (n=3, \*\*p<.005 compared to EP alone). *Representative images shown below.*

Next we tested NRAGE in combination with the dual EGFR/HER2 tyrosine kinase inhibitor, lapatinib, widely used in IBC therapy due to its ability to decrease tumor cell survival by inhibiting EGFR-MAPK mitogenic signaling and also recently reported to downregulate NF $\kappa$ B phosphorylation in breast cancer cells (109). Our studies and others have previously reported the rapid development of resistance to EGFR inhibitors including lapatinib due to increased anti-apoptotic signaling (459) and in particular, XIAP overexpression as observed in rSUM149 and wtXIAP cells (156). As shown in Figure 3.19, although rSUM149 cells exhibit decreased EGFR phosphorylation, they have sustained phospho-ERK and phospho-NF $\kappa$ B along with increased XIAP expression compared to parental SUM149 cells and the lapatinib-sensitive revertant rrSUM149 cells [generated by removing lapatinib from the resistant cells (418)]. Similarly, lapatinib treatment in wtXIAP cells does not lead to decreased NF $\kappa$ B phosphorylation compared to parental lapatinib sensitive SUM149 cells and shXIAP, which similar to the above mentioned data have insignificant phosphorylation of p65 even under basal conditions (Figure 3.19B).

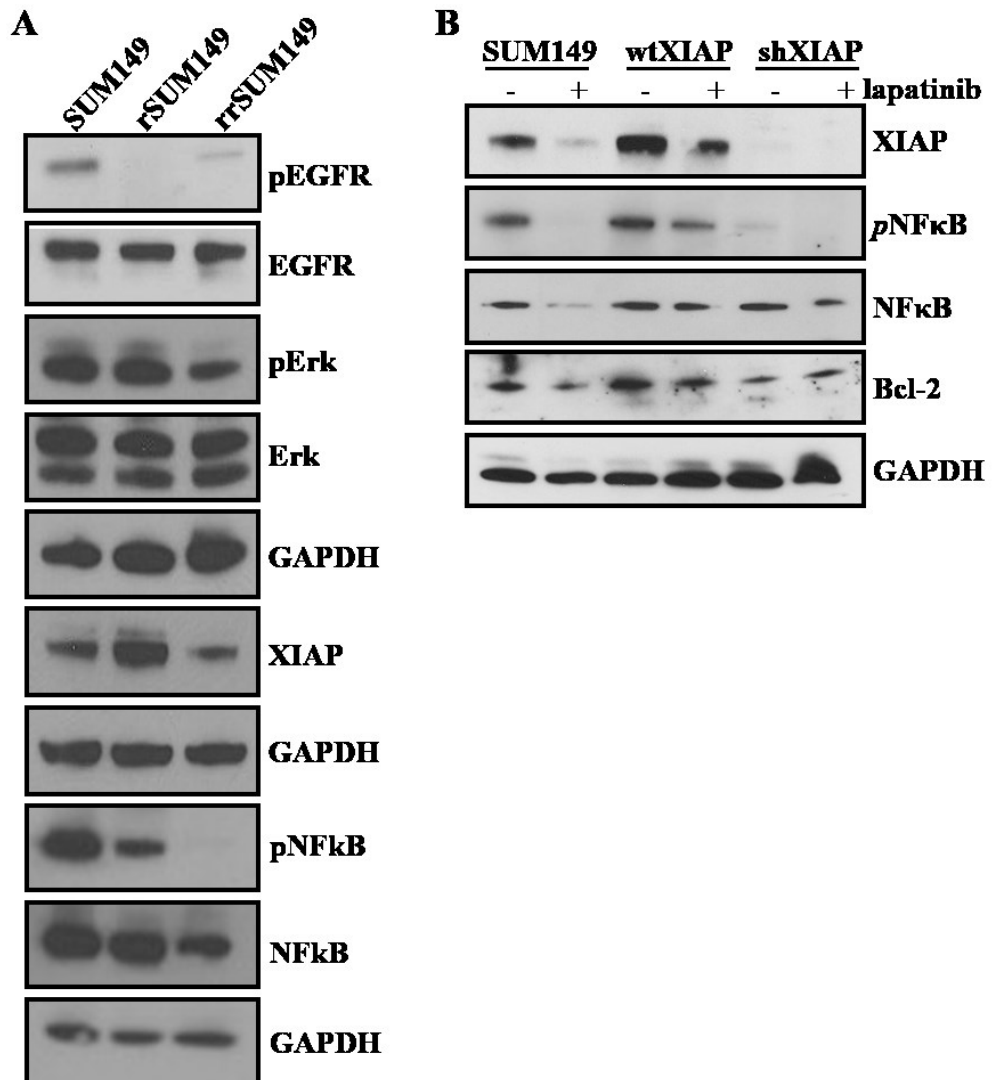


**Figure 3.19 XIAP overexpression blocks the NFκB inhibitory effects of EGFR TKI, lapatinib**

A) Immunoblot analysis of EGFR, ERK, and NFκB phosphorylation and XIAP expression in SUM149, rSUM149, and rrSUM149 cells. GAPDH as loading control. B) Immunoblot analysis of NFκB phosphorylation and target expression in SUM149, wtXIAP, and shXIAP cells untreated or treated with 7.5 μM lapatinib. GAPDH as loading control.

Furthermore, NRAGE peptide treatment potentiated the effects of lapatinib in all three cell lines, reversing resistance in rSUM149 and wtXIAP cells and further decreasing AIG in SUM149 cells. Data in Figure 3.20 show that lapatinib causes ~40% inhibition in AIG of SUM149 cells compared to no inhibition at all in wtXIAP and rSUM149 cells. These results collectively identify the potential of developing BIR1 domain antagonists that can target the XIAP-NF $\kappa$ B interaction and/or signaling to potentiate therapeutic apoptosis and overcome drug resistance in IBC cells.

Taken together, these data reveal the potential of developing BIR1 domain antagonists that can target the XIAP-NF $\kappa$ B interaction and/or signaling to potentiate therapeutic apoptosis and overcome drug resistance in IBC cells.

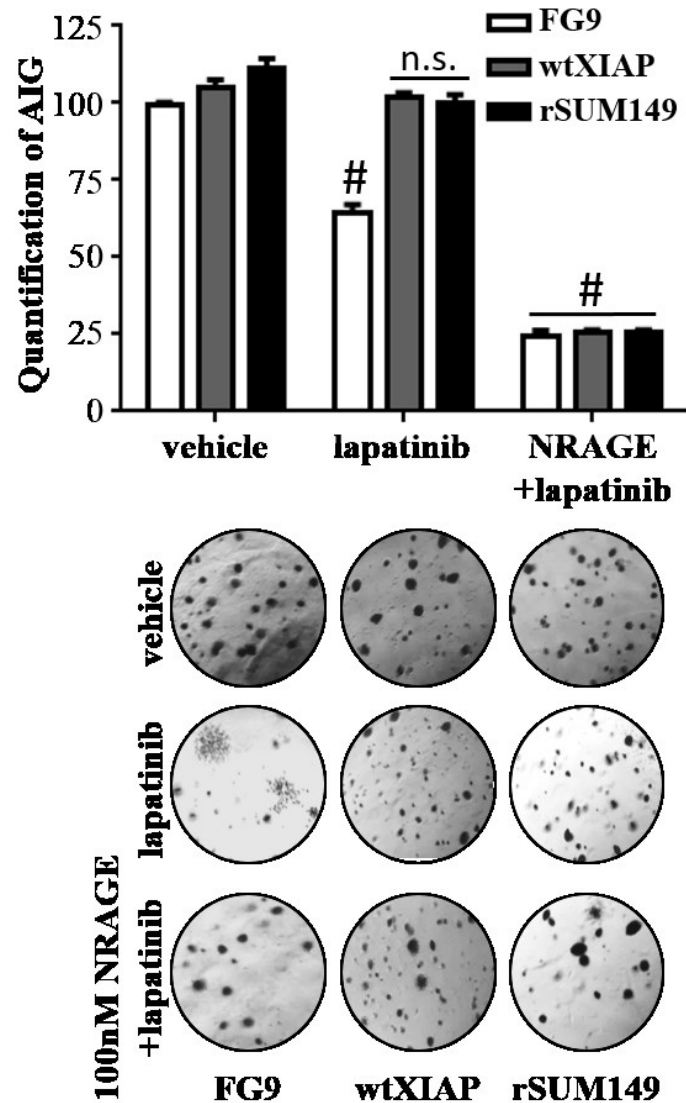


**Figure 3.20 NRAGE treatment sensitizes resistant wtXIAP and rSUM149 cells to lapatinib**

Anchorage-independent growth assay of cells treated with vehicle, lapatinib alone or in combination with 100 nM NRAGE peptide+EndoPorter. Bars represent mean±SEM colonies formed in soft agar as a percentage of untreated (n=2-3, #p<.001 lapatinib compared to vehicle & NRAGE+lapatinib compared to lapatinib alone). *Representative images shown below.*

Transcriptomic analysis of three independent cultures of the rSUM149 lapatinib-resistant (endogenous high XIAP expression) and the rrSUM149 lapatinib-sensitive cells (decreased endogenous XIAP) demonstrate increased expression of genes related to: 1) the NIK/NF $\kappa$ B cascade and 2) MAPK regulated genes during apoptosis induction (Figure 3.21) in rSUM149 as compared to both SUM149 and rrSUM149. This is similar to the correlation between high XIAP expression and increased proliferative and NF $\kappa$ B gene signatures as described in our abovementioned results with the XIAP modulated IBC variants, supporting the role of XIAP in conferring survival benefits to IBC cells.

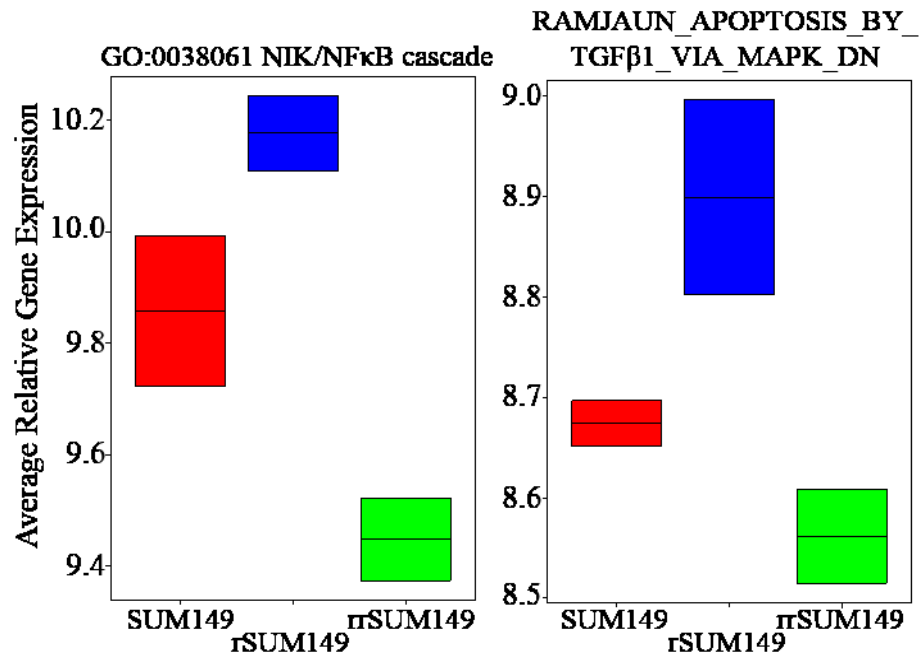


**Figure 3.21 Lapatinib resistance correlates with increased expression of genes related to NFκB and MAPK**

Boxplots corresponding to genes regulated by NIK/NFκB (left) and by MAPK (right) in SUM149 (red), rSUM149 (blue), rrSUM149 (green).

### **3.3 Discussion**

The key findings of the current study provide new insights into the important role of XIAP as a mechanistic link between the observed hyperactivation of MAPK and NF $\kappa$ B pathways in IBC patient tumors and preclinical models. Our studies identify that the MAPK pathway, specifically ERK and Mnk, have the ability to modulate XIAP protein expression in estrogen negative IBC cells with EGFR activation or HER2 overexpression, most common molecular subtypes in IBC patients. Furthermore, we demonstrate that XIAP expression is necessary for the constitutive activation of the NF $\kappa$ B pathway associated with IBC. This is mediated by coupling of the XIAP BIR1 domain with TAB1/TAK1:IKK $\beta$  signals leading to downstream NF $\kappa$ B transcriptional activity, corresponding with increased proliferation and resistance to therapeutic apoptosis. Most importantly, we demonstrate for the first time that this XIAP-NF $\kappa$ B axis directly correlates with tumor growth rate *in vivo*, thereby revealing a functional necessity for XIAP expression during IBC tumor progression (Figure 3.22).

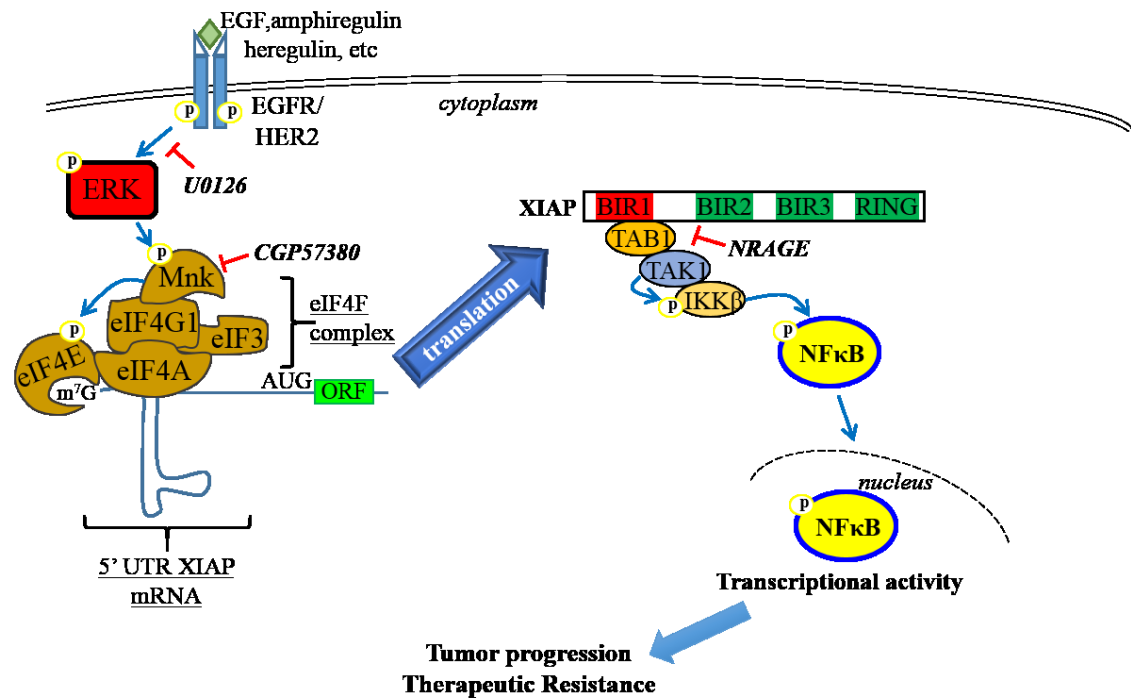


**Figure 3.22 Schematic of MAPK pathway-mediated XIAP translation induction and subsequent NFκB activation**

Activation of the epidermal growth factor by exogenous ligand can lead to phosphorylation of the kinase, ERK. ERK in turn phosphorylates its substrate Mnk leading to enhanced translation of the X-linked inhibitor of apoptosis protein (XIAP) through an IRES-mediated mechanism. The BIR1 domain of XIAP facilitates a physical interaction with the TGFβ-associated binding protein, TAB1, and its cognate kinase, TAK1. This binding event leads to the phosphorylation of the NFκB activation kinase, IKKβ, which goes on to induce the degradation of IκBα, allowing NFκB to translocate to the nucleus and increase target gene expression. In IBC cells, these target genes modulate proliferation, tumorigenesis, therapeutic resistance, and disease progression.

The X-linked inhibitor of apoptosis protein is ubiquitously expressed in most normal cells (460), although the level of expression is heterogeneous throughout tissues and within primary tumors (461). Our previous work also revealed differential expression of *XIAP* in IBC cell lines when compared to subtype-matched non-IBC lines (135). Interestingly, *XIAP* deletion is not toxic to normal cells and *XIAP* knockout mice do not show lethal defects in development or in the regulation of apoptosis (462). Studies overwhelmingly show that *XIAP* antagonism in established tumors *in vivo* or in cell lines *in vitro* can sensitize tumor cells to therapy-mediated cell death, thereby identifying *XIAP* as a chemoresistance factor with many *XIAP* antagonists currently in clinical development (463). However, there are also reports that show that in some tumors *XIAP* expression correlates with a favorable clinical outcome (295,299) and *XIAP* deficiency instead of increasing apoptosis can promote aggressive tumor growth as reported in a prostate cancer model (300). It is therefore increasingly clear that in addition to the classical caspase-inhibitory function, understanding the caspase-independent role of *XIAP* in subsequent activation of cell survival signaling pathways (446) specific to cancer types will be essential in optimizing therapies that target this protein. Indeed, our finding that the *XIAP* BIR1 domain, which does not bind caspases, as necessary for initiating TAB1:IKK $\beta$  complex formation leading to NF $\kappa$ B activation in IBC cells underscores the recent mounting evidence of the non-apoptotic function of *XIAP* as a signaling intermediate (445,446). The majority of therapeutics that have been

developed targeting XIAP are directed towards the BIR2 and BIR3 domains, leading to increased activation of caspases to enhance therapeutic apoptosis (464). However, clinically relevant strategies targeting the XIAP BIR1 domain are lacking. Although the second mitochondria-derived activator of caspases (SMAC) protein, an endogenous protein that antagonizes IAP function, can bind XIAP and inhibit interaction with TAB1 through steric hindrance (276), small molecule SMAC peptidomimetics have not been observed to induce this same inhibition (465) and in our previous study were not effective as single agents in SUM149 IBC cells (420). This coupling of XIAP to NF $\kappa$ B and the inability of currently developed therapeutics to inhibit this interaction may be a reason they show no greater clinical efficacy. Our data herein, using a small molecule mimicking the NRAGE protein which blocks the XIAP:TAB1 interaction (424), showing decreased NF $\kappa$ B translocation, inhibition of anchorage-independent growth and increased sensitivity to an EGFR small molecule inhibitor lapatinib may represent a novel means of targeting this interaction and needs further evaluation in *in vivo* models.

Another significant finding of our studies is the immunohistochemical analysis of breast cancer patient tumor samples, which uncovered a high XIAP expression profile in invasive, infiltrating tumor cells including IBC and associated tumor embolic structures. We also noted strong staining for NF $\kappa$ B in the IBC samples compared to normal and benign tissue corroborating our *in vitro* data (data not shown). These observations are also strengthened by previous studies reporting a significant difference

in XIAP expression between breast cancer and matched normal tissue (461), with a non-significant trend towards an association between increased XIAP expression and poor disease-free and overall survival in basal-like, HER-2 positive disease, and lymph node negative patients. It has been postulated that in the case of fast growing tumors like IBC there is a delicate balance between cellular proliferation, the ability of cancer stem cells to self-renew while creating progeny, and the ability of said progeny to “self-metastasize” and migrate away freeing up space for continued tumor expansion (466,467). Our results showing that XIAP expression directly correlates with the number of ALDH+ cells and cell motility in IBC cells warrants further investigation of the role of XIAP in IBC metastatic progression.

In summary, the present study delineates the role of XIAP in the NF $\kappa$ B-mediated proliferative phenotype present in IBC and suggests an upstream regulation by MAPK signaling. These findings of a strong correlation between XIAP expression in untreated IBC tumors with MAPK and NF $\kappa$ B gene signatures suggests an important role of XIAP in IBC pathobiology. In addition to identifying a targeted approach to disrupt the pro-survival signaling mediated by XIAP and NF $\kappa$ B, our data reveal the potential of MAPK-XIAP-NF $\kappa$ B as a druggable pathway in developing promising therapeutic strategies for patients with IBC.

## **4. Elucidation of the mechanism of XIAP-mediated tumor cell evasion/inhibition of immunotherapy**

### ***4.1 Introduction***

Immunotherapy has demonstrated promise for preventing recurrences, reducing tumor burden, and lengthening survival of breast cancer patients reviewed in (468). Elements necessary for successful immunotherapy are well described and include – 1) tumor expression of immunogenic targets (e.g., HER2, HER3, EGFR, CEA, MAGE, MUC-1, survivin, and NY-ESO-1 (469-472)), 2) presence of immune effectors [e.g., cytolytic T cells (CTL), natural killer (NK) cells, and antibodies that can recognize and destroy tumors expressing these antigens], and 3) potent strategies for activating or delivering immune effectors [e.g., vaccines, antibody administration, T cell transfer, immune modulatory agents (reviewed in (468))]. However, the broad application of immunotherapy to the treatment of breast cancer has been challenging due to the ability of tumors to evade immune effectors. Diverse explanations for immune evasion include failure to achieve a high frequency, potency, and durability of CTLs (caused by T cell-expressed immune checkpoint molecules such CTLA4 or PD-1, regulatory T cells, and myeloid derived suppressor cells) or cloaking of the tumor from effectors (caused by loss of MHC class I and/or tumor antigen expression) reviewed in (473). Although these mechanisms are operative to varying extents in most tumors, because immune effectors destroy cancer cells by activating common intrinsic and extrinsic apoptotic pathways,

we hypothesized that a critical means of immune evasion is dysregulation of the apoptotic signaling pathway.

Inflammatory breast cancer (IBC) is the most aggressive subtype of breast cancer, often presenting with lymphatic involvement and metastatic disease (12). Despite an aggressive multidisciplinary treatment approach that includes chemotherapy and when still localized, surgery and radiation therapy; clinical outcomes remain poor (474). Immunohistochemical studies have revealed that a large proportion of IBC tumors have amplification/overexpression of the oncogene HER2 (36-42% compared to 17% for non-IBC (25,26)) or the related family member EGFR (~30% compared to 18% for non-IBC (23,24)), suggesting possible therapeutic utility for the monoclonal antibodies trastuzumab (anti-HER2) or cetuximab (anti-EGFR). *De novo* or acquired therapeutic resistance is rapid and commonly observed in IBC limiting the clinical utility of these antibodies (103,104). Our long-term goal is to study the mechanisms of resistance to these therapies in IBC in order to identify strategies that would increase the effectiveness of these treatments.

Induction of apoptotic signaling through both the intrinsic (cytotoxic granule [perforin, granzyme B] exocytosis) and extrinsic (engagement of death receptors [FAS, TNFR and TRAILR]) cell death pathways is key to both natural killer (NK) cell-mediated antibody-dependent cellular cytotoxicity (ADCC) and cytotoxic T lymphocyte (CTL)-mediated lysis of tumor cells (475,476). These pathways primarily converge at the point

of activation of effector caspases-3 and -7, the chief executioners of apoptosis (475-478). X-linked inhibitor of apoptosis protein (XIAP), a member of the inhibitor of apoptosis protein (IAP) family, is considered the most potent caspase binding protein and inhibitor of both extrinsic and intrinsic death pathways (479). XIAP overexpression in tumor cells is a well-described mediator of resistance to chemotherapy and targeted therapy in breast cancer and other malignancies and has been linked to tumor aggressiveness (110,111,156,295,480,481). Indeed, we have observed stress-mediated induction of XIAP at the protein translational level in IBC cells (156), leading to suppression of apoptosis mediated by chemotherapy, targeted therapy and CTLs (418,482). Additionally, recent reports support roles for XIAP and other IAP family members in the regulation of inflammation and innate immunity (483-485).

In the present study, using cellular models of IBC with high expression of either EGFR or HER2, we demonstrate that XIAP expression modulates IBC cell susceptibility to NK-mediated ADCC when challenged with the anti-EGFR antibody cetuximab or the anti-HER2 antibody trastuzumab, respectively. Our results reveal that cells with acquired therapeutic resistance are insensitive to ADCC, which can be reversed by specific downregulation of XIAP expression. Further, we provide evidence for two distinct functions of XIAP in suppressing cell death in response to ADCC, inhibition of caspase activity and suppression of reactive oxygen species (ROS) accumulation. This study uncovers a unique mechanism for evasion of ADCC and highlights XIAP as a

novel target for the enhancement of immunotherapy. This work was recently published by our lab (486).

## **4.2 Results**

### **4.2.1 IBC cells with apoptotic dysregulation are resistant to ADCC**

To study the role of anti-apoptotic signaling in ADCC-mediated cell lysis, we utilized two inflammatory breast cancer cell lines: the basal type, EGFR-activated SUM149 and the HER2-overexpressing SUM190. Both cell lines have been derived from patient primary tumors prior to treatment and are considered true IBC-like primary cell models (414). In addition, we also used two isotype-matched, multi-drug resistant variants (rSUM149 and rSUM190), which we have previously characterized and identified to exhibit resistance to apoptosis-inducing agents due to stress-mediated XIAP induction (156,418). We co-cultured these tumor cells with human peripheral blood mononuclear cells (PBMCs) with and without addition of the monoclonal antibodies, cetuximab, which binds to EGFR, or trastuzumab, which binds to HER2. Data in Figure 1 show that parental cell lines [SUM149 (1A) and SUM190 (1B)] were sensitive to cetuximab- or trastuzumab- mediated ADCC, respectively. ADCC response was significantly attenuated in therapy-resistant rSUM149 and rSUM190 cells, with rSUM190 cells showing no cellular lysis.

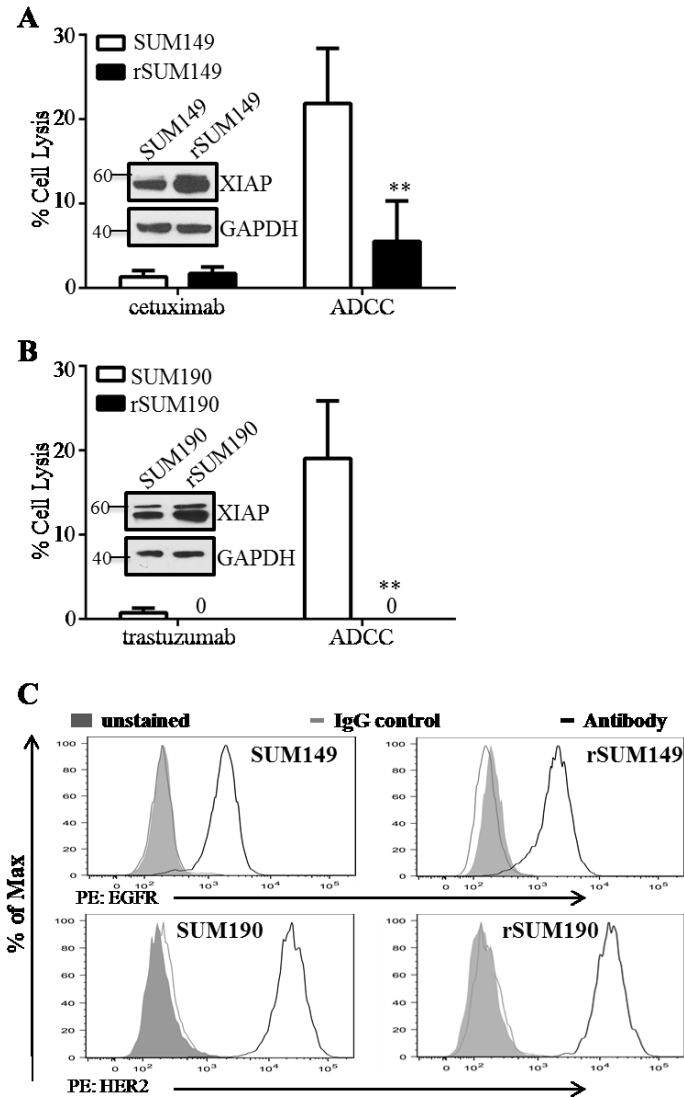


**Figure 4.1 Apoptotic dysregulation inhibits antibody-dependent cell cytotoxicity (ADCC) in breast cancer cells**

Percent cell lysis of A) SUM149 and rSUM149 cells or B) SUM190 and rSUM190 incubated with antibody alone or ADCC conditions for 4 h. Bars represent mean±SEM calculated percent lysis, n=3-6, \*\*p<0.005. C) Surface expression of EGFR in SUM149 and rSUM149 (top) and HER2 in SUM190 and rSUM190 (bottom) as measured by flow cytometry. *Inset: Labeling of axes, representative of n=3 experiments.*

The differential responses of the parental and resistant cells to cetuximab- and trastuzumab- mediated ADCC were not attributable to differences in surface expression of the receptors EGFR or HER2 (Figure 4.1C). We observed that the ADCC -sensitive and -resistant cells had similar basal surface expression of these receptors, and that any changes in surface expression of HER2 or EGFR due to internalization of the antibody-receptor complex were similar between cell lines (Figure 4.2A). Additionally, evaluation of the growth inhibitory effects of each antibody showed that cetuximab alone had little to no effect on SUM149 and rSUM149 cell proliferation and trastuzumab inhibited proliferation of SUM190 and rSUM190 only at higher concentrations than those used (10  $\mu\text{g/ml}$ ) for the ADCC assay (Figure 4.2B). Experiments using human PBMCs from different donors revealed qualitatively similar results, further suggesting intrinsic tumor cell-dependent effects (data not shown). These data suggest that differential responses of these cell lines to ADCC is not attributable to differences in surface expression of the antigen or ligand-receptor internalization, but a tumor cell specific effect.

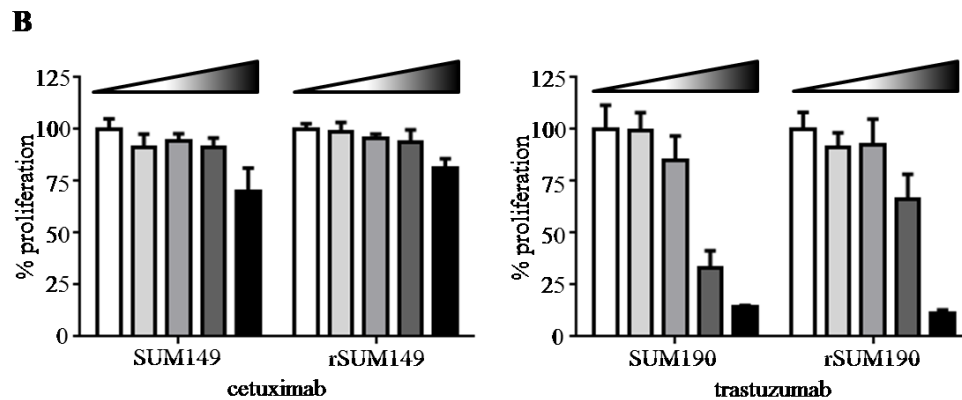
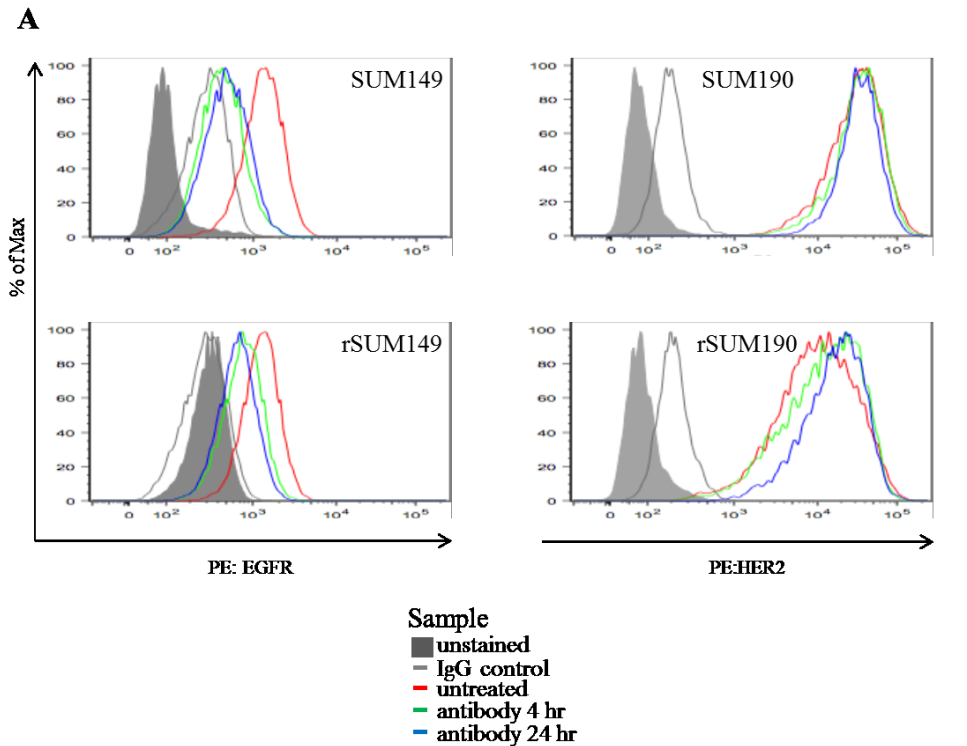


**Figure 4.2 Antibody administration alone does not have differential effects on receptor internalization or inhibition of proliferation**

A) Surface EGFR (left) and HER2 (right) expression post-antibody administration for indicated times in indicated cells. Representative histogram from n=3 experiments. B) Cellular proliferation of indicated cells treated with vehicle or increasing doses of antibody (1, 10, 100, 1000  $\mu\text{g}/\text{mL}$ ) measured by MTT assay. Bars represent mean $\pm$ SEM proliferation, n=4-8.

### **4.2.2 Caspase dependent apoptosis is inhibited in ADCC-resistant cells**

In order to confirm the mechanism of cell death during ADCC, we performed TUNEL staining and measured caspase 3/7 activity. ADCC-resistant rSUM149 cells had very few TUNEL positive cells (Figures 4.3A and 4.3B) and show decreased caspase -3/7 activation (Figure 4.3C) when co-cultured with PBMCs+cetuximab compared to the ADCC-sensitive SUM149 cells, indicating the need for apoptotic signaling for a potent ADCC response.

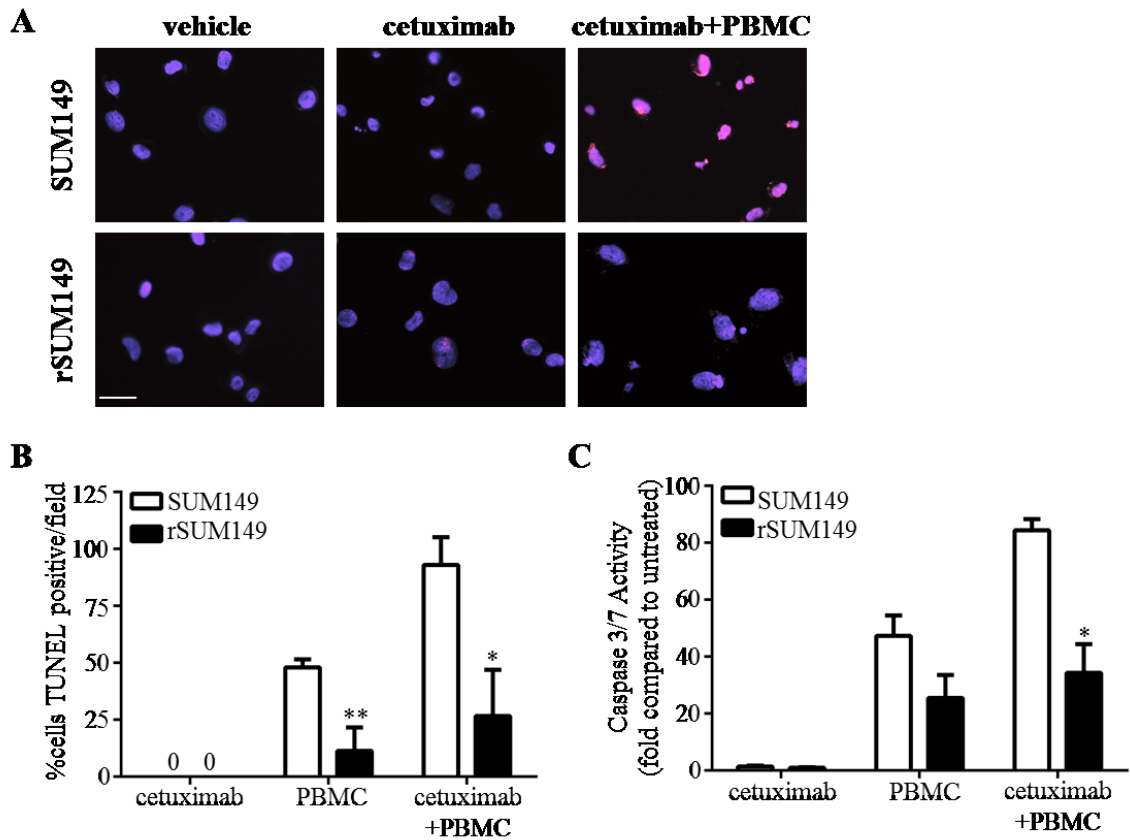


**Figure 4.3 Apoptosis caused by ADCC is caspase-dependent and inhibited in rSUM149 cells**

A) TUNEL staining of SUM149 and rSUM149 cells treated with vehicle, cetuximab alone, or cetuximab plus PBMCs. DAPI is shown in blue and TUNEL in red. *Representative of n=2, scale bar=25  $\mu$ m.* B) Quantification of TUNEL+ cells in A. Bars represent %positive out of the total number of cells in each field/condition, n=3. C) Caspase activity of SUM149 and rSUM149 cells treated as indicated for 4h. Bars represent mean $\pm$ SEM fold relative light units compared to untreated, n=2-3. \*p<0.05, \*\*p<0.005 (comparison of rSUM149 to SUM149).

### **4.2.3 The caspase-binding function of XIAP contributes to ADCC resistance**

The aforementioned data indicated that caspase activity correlates with ADCC-mediated cell death, which is attenuated in XIAP-overexpressing, ADCC-resistant rSUM149 and rSUM190 cells. To directly assess the role of XIAP in resistance to ADCC, we stably overexpressed the full-length protein in SUM149 cells (referred to as wtXIAP). Data in Figure 4.4A show that wtXIAP cells exhibit suppressed response to both PBMCs alone and PBMCs in combination with cetuximab compared to control vector (FG9) cells. To specifically evaluate the caspase inhibitory function of XIAP in suppression of ADCC, we knocked down endogenous XIAP in SUM149 cells and reconstituted expression (to levels similar to wtXIAP) using a construct bearing two point mutations in the BIR domains, D148A and W310A, referred to as DW/AA (Figure 4.4B). This double mutation is known to abrogate binding to executioner caspases - 3 and -7 as well as initiator caspase 9 (446). The role of the caspase binding function of XIAP was further confirmed by using another mutant, H467A (H/A) in the RING domain, known to inhibit the ubiquitination function of XIAP but does not affect caspase binding function of XIAP (depicted in Figure 2B) (446,487). Immunoblots in Figure 2C confirm higher XIAP expression levels in cell expressing the wtXIAP, DW/AA or H/A mutants compared to control vector FG9 cells. Furthermore, knockdown of endogenous XIAP in SUM149 cells led to increased caspase-3/7 activation and higher susceptibility to cell death when exposed to the classical apoptosis inducing agent, TNF-related apoptosis-

inducing ligand (TRAIL) compared to FG9 cells (Figures 4.4D and 4.4E). Conversely, overexpression of XIAP in SUM149 cells (wtXIAP) resulted in decreased caspase-3/7 activity and reduced cell death. The mutant DW/AA cells showed similar caspase activation and TRAIL-mediated cell death to shXIAP cells, while the H/A mutant cells behaved like wtXIAP cells.

Comparison of ADCC response in these XIAP modulated cell lines (Figure 4.4F) shows that DW/AA mutant cells have significantly increased lysis when exposed to antibody and immune effector cells compared to wtXIAP and H/A cells. The results presented thus far reveal a caspase-dependent function of XIAP in suppressing an ADCC-activated apoptotic response.

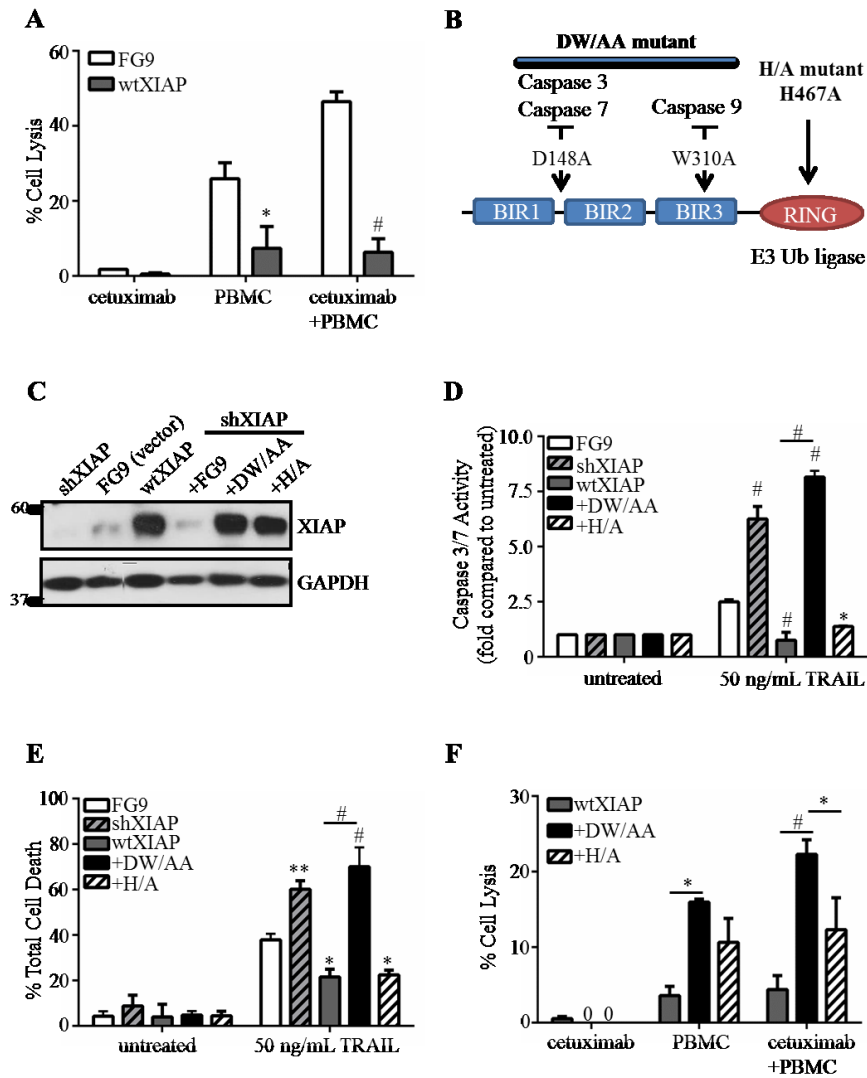


**Figure 4.4 XIAP overexpression inhibits ADCC response in SUM149 cells through caspase inhibition**

A) Percent cell lysis of SUM149 FG9 and wtXIAP cells treated as indicated for 4 h, n=2-3.

B) Schematic of XIAP mutants used in this study. C) Western immunoblot of XIAP expression in cell lines transduced as indicated. D) Caspase activity and E) viability of cell lines  $\pm$  TRAIL. Bars

represent fold change in luminescence (d) or mean $\pm$ SEM % cell death (e), n=2-3. F) Percent cell lysis of wtXIAP, +DW/AA, and +H/A cells treated as indicated for 4 h, n=2-3. \*p<0.05, \*\*p<0.005,

#p<0.001 (compared to FG9 unless otherwise indicated).

#### **4.2.4 Reactive oxygen species generation is required for granzyme-mediated ADCC response**

One of the key mechanisms of ADCC-mediated cell death is perforin/granzyme delivery to target cells and subsequent activation of apoptotic cell death (136). We confirmed this by using the perforin inhibitor (concanamycin A, CMA), which causes a significant reversal of cytotoxicity in ADCC-sensitive cell lines (SUM149-Figure 4.5A, SUM190-4.5B), indicating that granzyme accumulation in tumor cells is essential for ADCC response in this breast cancer subtype.

Recent studies have identified that granzyme B, in addition to directly activating caspases (488), can cleave mitochondrial subunits (in a caspase-independent manner) leading to accumulation of reactive oxygen species (ROS) (489); however, the contribution of this mechanism to ADCC has not been fully elucidated. To test if increased ROS levels contribute to ADCC-mediated apoptosis in the IBC cells, we used the superoxide dismutase (SOD) mimetic and  $O_2^-$  scavenger, MnTBAP, which has previously been shown to antagonize ROS accumulation (490). Data in Figure 4.5C revealed that treatment with MnTBAP causes a significant decrease in lysis (~80%) in the ADCC-sensitive SUM149 cells, indicating the necessity for ROS accumulation for ADCC response.

To support the importance of caspase activation in ADCC-mediated lysis shown in Figure 4.4F, we utilized a pan-caspase inhibitor, QVD-OPh, which yields a similar level of decreased ADCC response (~80%) while a combination of QVD-OPh and

MnTBAP further inhibits ADCC response (>95%). These observations indicate that ROS accumulation or caspase activation can each independently cause ADCC-mediated apoptosis. In addition, most likely there is also some overlap between these two events, as combination treatment with QVD-OPh and MnTBAP led to an increase (16%) in inhibition of cytotoxicity compared to each inhibitor alone.

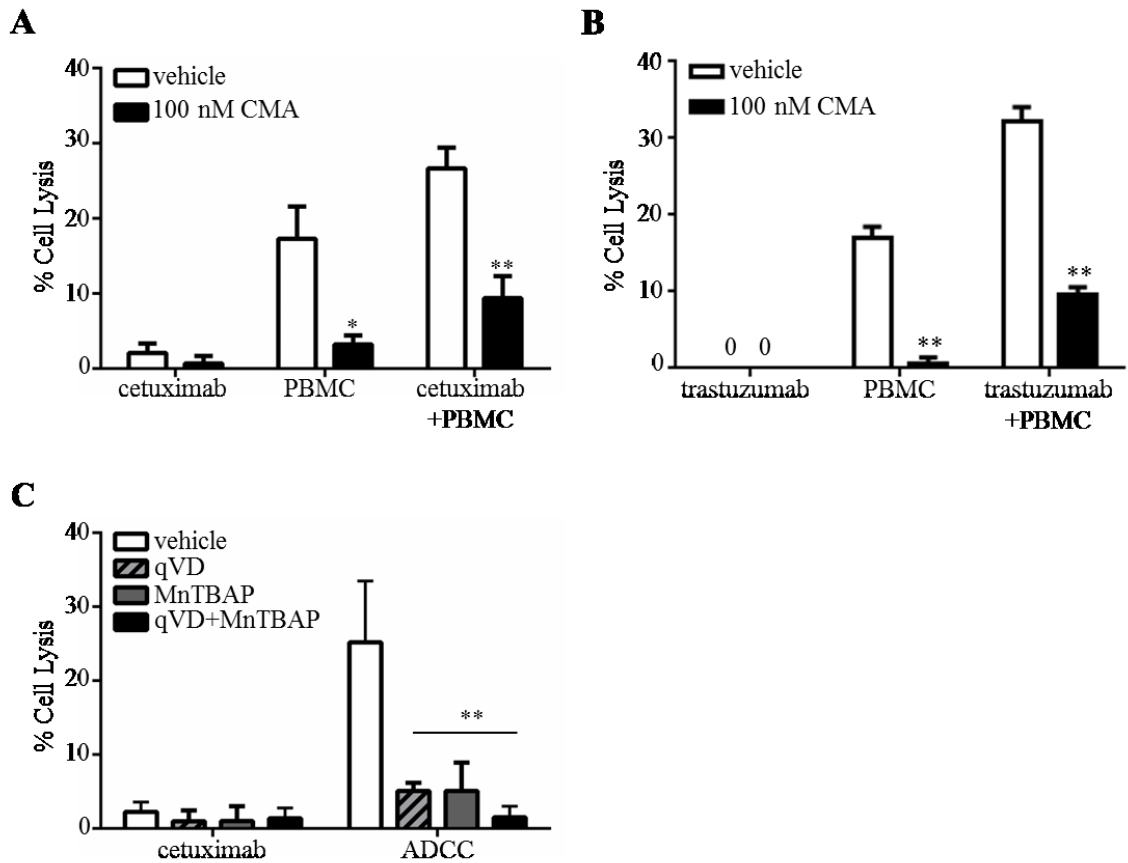


**Figure 4.5 Inhibition of granzyme accumulation prevents ROS- and caspase-dependent ADCC**

Percent cell lysis of A) SUM149 and B) SUM190 cells incubated with antibody, PBMC alone, or the combination in the presence or absence of concanamycin A (CMA), a perforin inhibitor. Bars represent mean±SEM calculated percent lysis, n=2-3. B) Percent cell lysis of SUM149 cells incubated with cetuximab alone or in ADCC conditions in the presence or absence of qVD (pan-caspase inhibitor), MnTBAP (antioxidant), or the combination. Bars represent mean±SEM calculated percent lysis, n=2-3. \*p<0.05, \*\*p<0.005.

#### **4.2.5 XIAP overexpression inhibits granzyme B-mediated ROS generation**

Considering that cells with XIAP overexpression inhibit ADCC response, and mutation of the caspase binding domain (using the DW/AA XIAP mutant) only partially reverses resistance, we wanted to evaluate the effect of XIAP overexpression on granzyme B-mediated ROS generation. We loaded target cells with granzyme B and measured ROS levels in ADCC-sensitive (SUM149) and ADCC-resistant cells (rSUM149 and wtXIAP) cells using carboxy-H<sub>2</sub>DCFDA, a well-established dye for the quantification of H<sub>2</sub>O<sub>2</sub>-derived radicals. Streptolysin O (SLO), a bacterially-derived molecule that permeabilizes cell membranes, was used in combination with granzyme B, to mimic perforin/granzyme lytic granules. Figure 4.6 shows that SUM149 cells treated with SLO and granzyme B (green line) exhibited a 41.6% increase in ROS levels compared to untreated (black line). In contrast, granzyme-mediated ROS accumulation was significantly blunted in the XIAP overexpressing rSUM149 and wtXIAP cells (2.7% and 11.5% increase in ROS, respectively). Taken together, the data presented thus far demonstrate that high levels of XIAP expression can inhibit both granzyme B-mediated ROS generation and caspase activation.

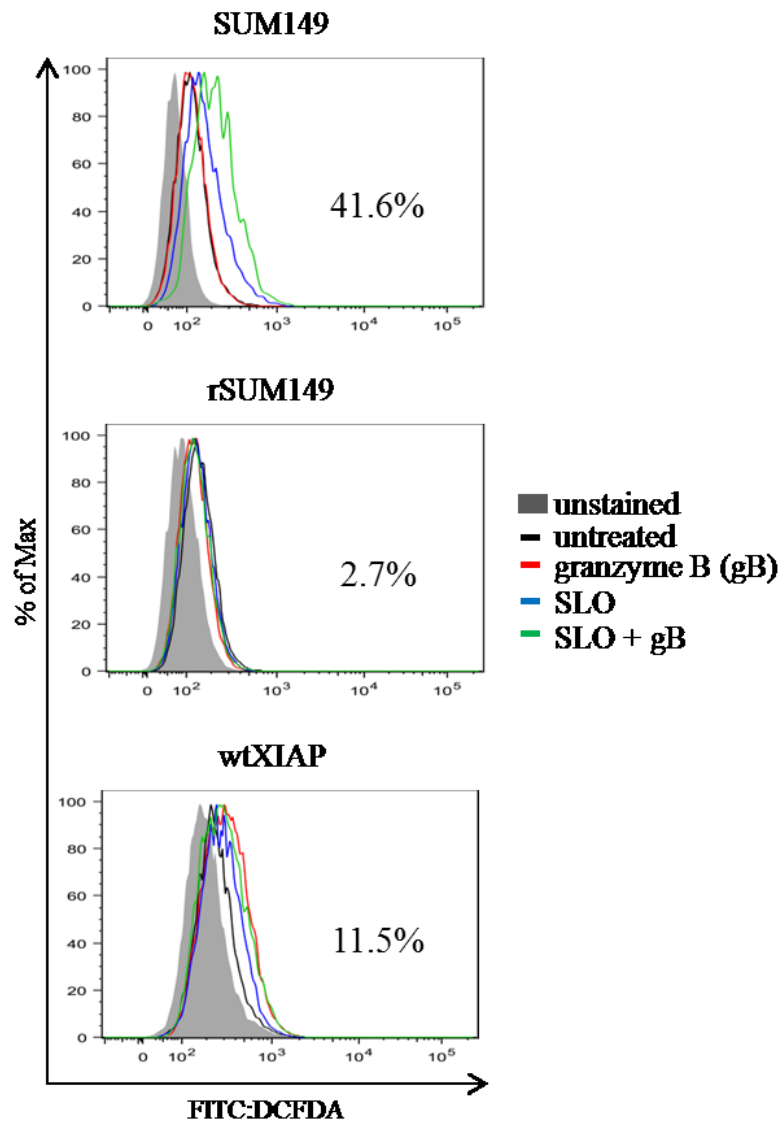


**Figure 4.6 Granzyme B-mediated ROS accumulation is inhibited in XIAP overexpressing cells**

A) Representative histograms of cells treated with: granzyme B (gB) alone (red line), streptolysin-O (SLO) alone (blue line), or the combination of SLO+gB (green line) compared to untreated (black line). Number represents %positive for SLO+gB condition. Inset: Labeling of axes and diagram of sample colors, representative of n=2 experiments.

#### **4.2.6 XIAP suppresses ROS accumulation in a caspase-independent manner by increasing the antioxidant pool**

In order to further understand the effect of XIAP levels on ROS accumulation, we challenged cells with two classical ROS-inducing agents, hydrogen peroxide and paraquat dichloride and measured peroxy radical or superoxide accumulation, respectively. Compared to parental SUM149, the ADCC-resistant, XIAP-overexpressing (wtXIAP, rSUM149) cells show little to no increase in peroxy radical or superoxide accumulation when treated with the ROS inducers (Figures 4.7A and 4.7B). The XIAP mutants, DW/AA and H/A, similarly showed little to no increase in ROS accumulation, indicating that the ability of XIAP to suppress ROS accumulation is independent of both caspase binding and ubiquitination functions. The suppression of ROS accumulation observed in the XIAP overexpressing cell lines correlated with increased expression of antioxidant enzymes, superoxide dismutases 1 and 2 (SOD1/SOD2) (Figure 4.7C). Increased expression of transcripts related to oxidoreductase activity (GO:0016491) were observed in the XIAP overexpressing lines, including plasma glutathione peroxidase (GPX3), which metabolizes H<sub>2</sub>O<sub>2</sub>, the leukotriene-B<sub>4</sub> degrading enzyme CYP4F3, the tryptophan-hydroxylating enzyme KMO, and two hydrogenases involved in steroid synthesis of dihydrotestosterone (SRD5A1) and dihydroxyprogesterone (DHRS9) (all  $p \leq 0.01$ ; Figure 4.7D). The results so far support the role of ROS in ADCC-mediated cell death in IBC cells and further identify a caspase-independent, ROS-suppressive function of XIAP that along with its caspase inhibitory function can attenuate ADCC response.

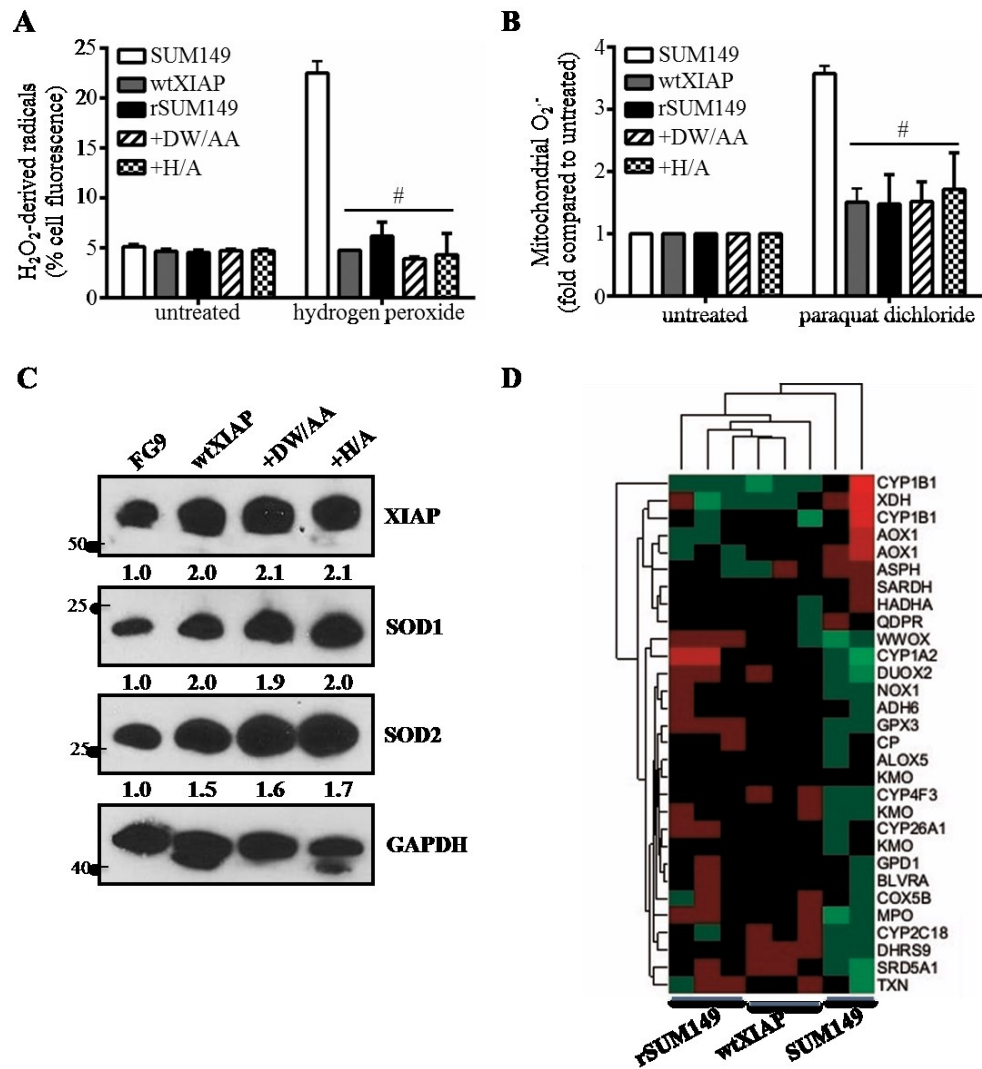


**Figure 4.7 XIAP overexpression inhibits ROS accumulation through upregulation of antioxidant capacity**

A) Fold induction of mitochondrial superoxides and B) percentage of cells with high H<sub>2</sub>O<sub>2</sub>-derived radicals in cells treated as indicated. Bars represent mean±SEM relative to untreated cells. n=2-3, #p<0.001. C) Western immunoblot analysis of XIAP, SOD1 and SOD2 levels in indicated cells. Numbers represent densitometric analysis. D) Normalized expression of the most significantly differentially expressed genes in the oxidoreductase activity (GO:001649) GSEA category (red-over, green-under expressed).

### **4.2.7 XIAP-mediated suppression of ROS is dependent on NFκB signaling**

Transcriptional control of key antioxidants, including the ones shown in Figure 4.7, can be directly upregulated by the nuclear transcription factor κB (NFκB) activity as discussed in Section 1.3.2. Furthermore, XIAP itself has also been shown to enhance NFκB transcriptional activity in multiple cell types (275,276,447), including IBC as shown in Chapter 3. Therefore, to assess the involvement of NFκB in XIAP-mediated ROS suppression we treated wtXIAP cells with JSH-23, a cell-permeable diamino compound that specifically inhibits NFκB translocation to the nucleus, thereby barring its transcriptional activity (491). Data in Figure 4.8A demonstrate that JSH-23 treatment can reverse the ROS-suppressive effects of XIAP overexpression after H<sub>2</sub>O<sub>2</sub> administration. We also observed that JSH-23 alone also causes an increase in ROS accumulation. This enhanced ROS accumulation coincided with decreased colony formation, reversing the effects of XIAP overexpression (Figure 4.8B).

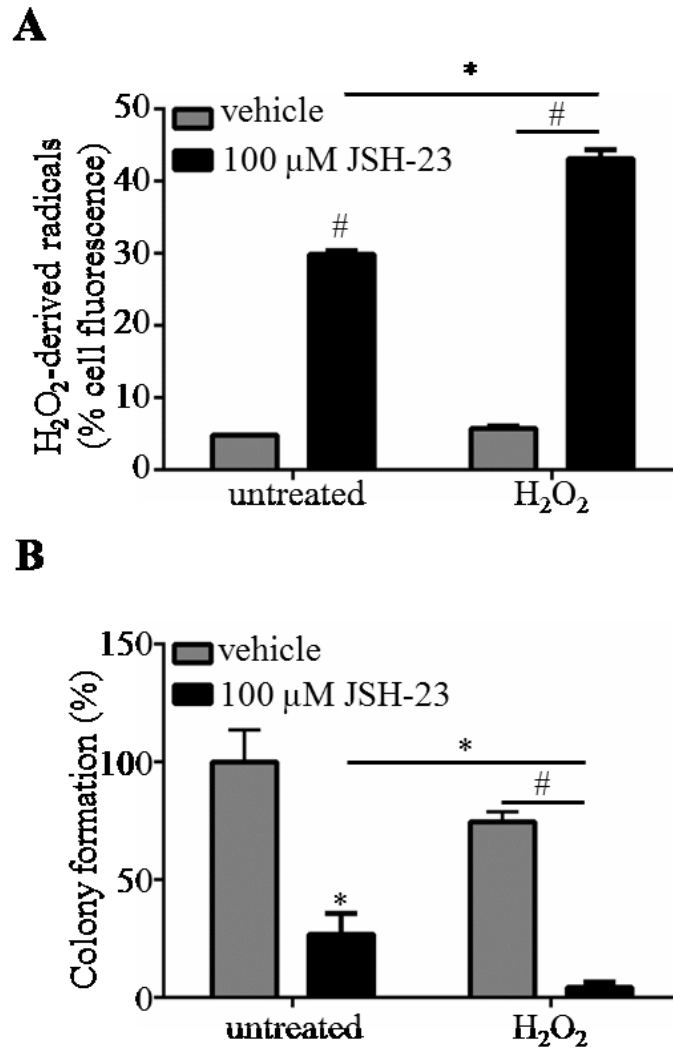


**Figure 4.8 Inhibition of NFκB nuclear translocation reverses resistance to ROS accumulation**

A) Percentage of cells with high hydrogen peroxide-derived radicals in cells treated as indicated. Bars represent mean±SEM relative to untreated cells, n=2-3. B) Clonogenic growth assay in cells treated as indicated. Bars represent mean±SEM colonies formed/cells plated as a percentage of the untreated sample, n=2-3. \*p<0.05, #p<0.001.

To directly block XIAP-mediated NF $\kappa$ B activation, we utilized the NRAGE peptide again as described in Chapter 3. The ability of NRAGE to decrease XIAP-mediated NF $\kappa$ B activation (Figure 4.9A) also led to an increase in ADCC response compared to vehicle control (Figure 4.9B), similar to the effect seen after mutation of the caspase-binding domains. This further corroborates that two different functional domains mediate the full effect of XIAP-driven suppression of ADCC.

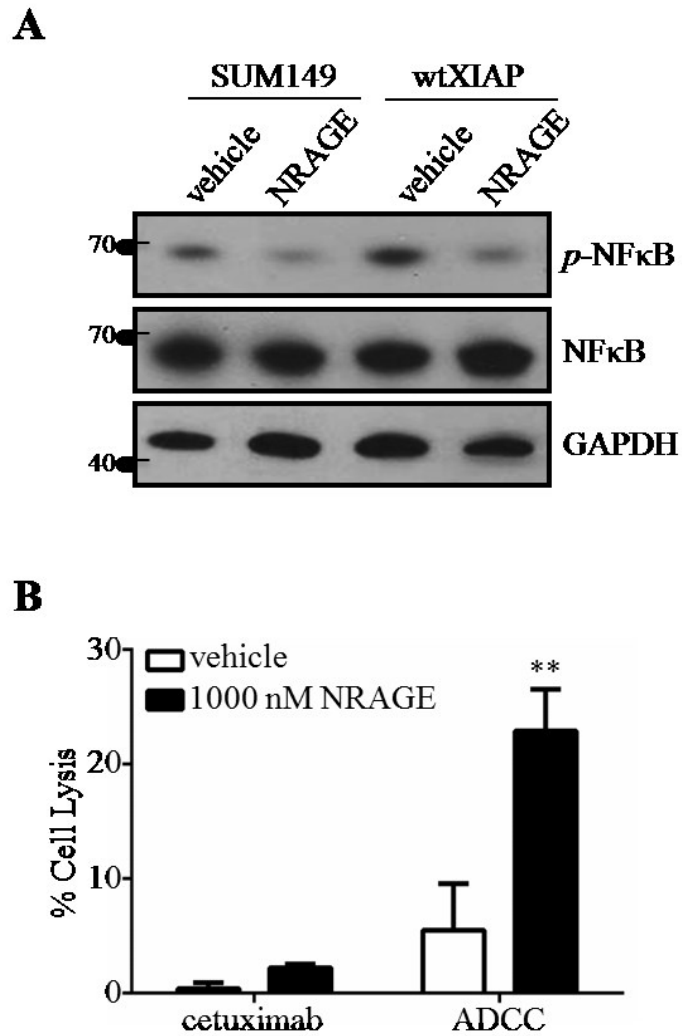


**Figure 4.9 Administration of NRAGE inhibits NFκB phosphorylation in IBC cells and reverses resistance to ADCC**

A) Western immunoblotting for phospho-p65 (p-NFκB), total p65 (NFκB), and GAPDH as loading control in SUM149 and wtXIAP cells treated with vehicle or 1 μM NRAGE. B) Percent cell lysis of wtXIAP cells incubated with cetuximab alone or in ADCC conditions in the presence or absence of NRAGE peptide. Bars represent mean±SEM calculated percent lysis, n=2-3. \*\*p<0.005.

#### **4.2.8 RNAi-mediated targeting of XIAP enhances sensitivity to ADCC-mediated apoptosis**

Finally, to confirm the relevance of XIAP in resistance to ADCC and suggest future therapeutic directions to restore ADCC sensitivity, we targeted XIAP expression directly using RNAi in the acquired therapy resistant rSUM149 and rSUM190 cells. XIAP downregulation increased sensitivity of both rSUM149 (Figure 4.10A) and rSUM190 (Figure 4.10B) to ADCC-mediated apoptosis, suggesting that both inhibitors and targeted downregulation of XIAP can restore ADCC response in therapy-resistant cells, supporting the development of combinatorial strategies that target both the ROS-suppressive and caspase-binding functions of XIAP.

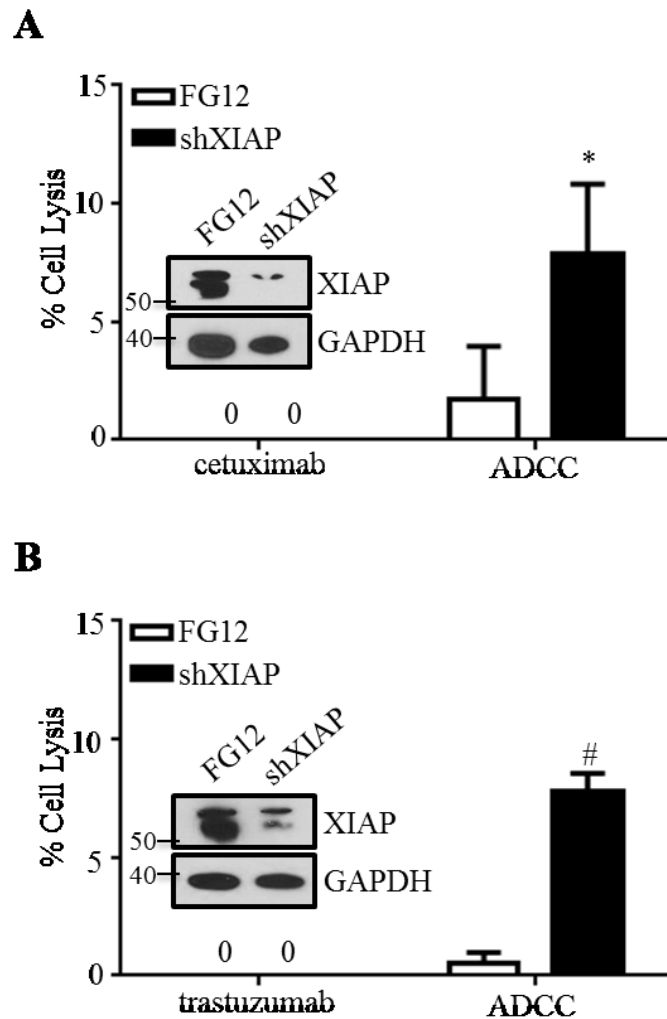


**Figure 4.10 Targeted inhibition of XIAP by RNAi sensitizes ADCC-resistant cells to apoptosis**

Percent cell lysis of FG12 (control) or XIAP shRNA transfected A) rSUM149 cells and B) rSUM190 cells incubated with antibody alone or ADCC conditions for 4 h. Bars represent mean±SEM calculated percent lysis, n=4-5, \*p<0.05, #p<0.001. Inset: Western immunoblot of XIAP expression at time of ADCC experiment.

### **4.3 Discussion**

A key challenge to successful cancer immunotherapy is the ability of tumors to evade killing by immune effectors (T cells, NK cells, monocytes, etc.). This has largely been attributed to impaired effector function in cancer-bearing individuals (492). It is also well recognized that the ability of immune effectors to induce cancer cell cytotoxicity is dependent on activation of the intrinsic and extrinsic apoptotic pathways (463). Therefore, we hypothesized that a critical means by which tumors evade killing by immune effectors is due to downregulation of apoptotic signaling. This is highly relevant in a hyperproliferative cancer that rapidly acquires apoptotic resistance such as IBC (493). The role of XIAP in reducing tumor cell sensitivity to immune-mediated killing was suggested by our recent studies in which apoptosis-resistant IBC cells, expressing XIAP through a translational stress response mechanism during acquisition of a drug-resistant phenotype (156,418), were resistant to killing by antigen-specific cytolytic T cells compared to isotype-matched parental cells (482). In the present study, we show for the first time that ADCC-mediated cancer cell death, facilitated by monoclonal antibodies targeting epidermal growth factor receptors, is suppressed by tumor cell upregulation of XIAP.

Our results identify two distinct mechanisms (Figure 4.11) by which XIAP attenuates ADCC-mediated lysis in inflammatory breast cancer cells: one dependent on the ability of XIAP to bind caspases and the other mediated by the inhibition of ROS

accumulation. We observed decreased ADCC-mediated lysis of apoptotic-insensitive IBC cell line variants that either endogenously express high XIAP or were engineered to exogenously overexpress wild-type XIAP. IBC cells expressing a variant of XIAP, with mutations at key amino acids necessary for caspase-binding, demonstrated resensitization to ADCC, while treatment of ADCC-sensitive SUM149 cells with a caspase inhibitor decreased sensitivity. These data demonstrate that direct binding of effector caspases by XIAP plays a significant role in decreased ADCC-mediated apoptosis. Nonetheless, caspase binding did not account for the totality of XIAP's ability to reduce the sensitivity of tumor cells to ADCC.

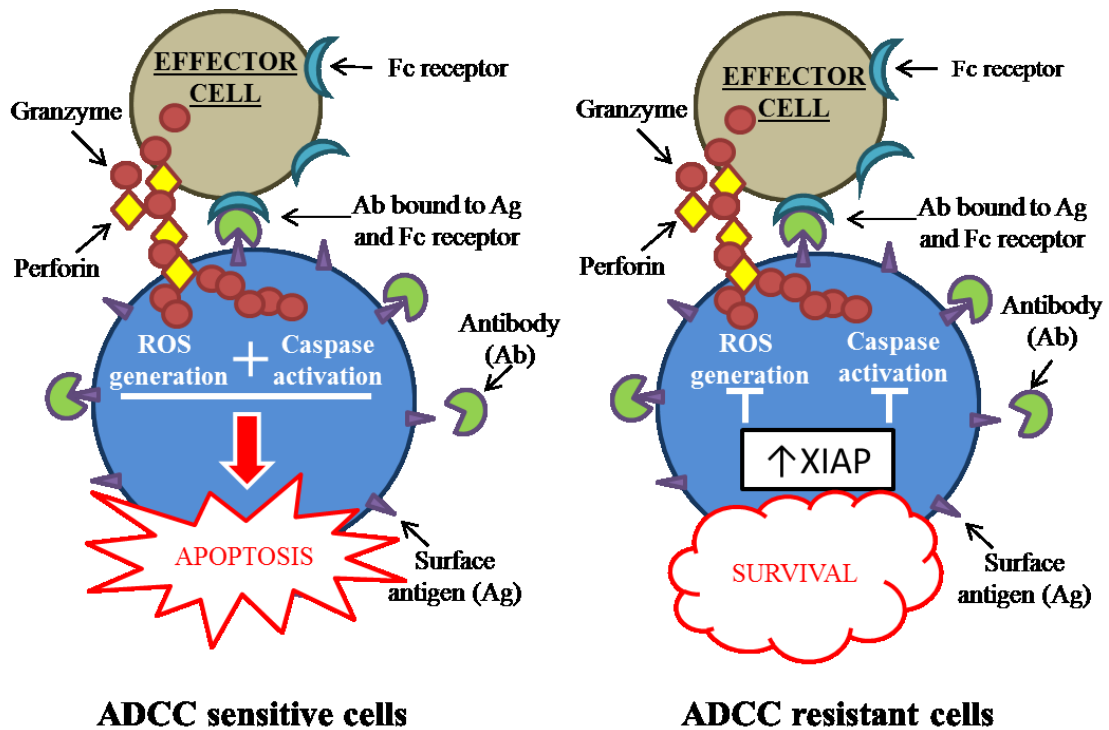


**Figure 4.11 Schematic of XIAP effect on immune effector cell-mediated antibody-dependent cellular cytotoxicity**

Schematic of XIAP-mediated inhibition of ADCC. In ADCC-sensitive cells, antibody binding to surface antigen bridges tumor cells to effector cells, leading to subsequent release of lytic granules containing perforin and granzymes. Granzymes enter target cells through perforin channels, inducing both ROS generation and activating effector caspases leading to efficient apoptosis in tumor cells. In cells with XIAP overexpression, however, this process is abrogated through caspase -dependent and -independent mechanisms leading to tumor cell survival.

We also identified another mechanism for XIAP's attenuation of tumor cell immune responsiveness when we noted that granzyme-mediated ADCC required ROS generation and that this was suppressed in XIAP overexpressing cells, contributing to ADCC resistance. We further showed that introduction of an exogenous antioxidant in ADCC-sensitive cells caused decreased ADCC, while a combination of this antioxidant and a caspase inhibitor almost completely abolished ADCC response, revealing a role for ROS induction in the response to ADCC. Concordantly, IBC cells with high XIAP levels, including XIAP with mutations in the caspase binding domains, exhibited suppressed ROS accumulation triggered by both granzyme B released during ADCC and classical ROS inducers, revealing a caspase-independent mechanism. Further, gene set enrichment analysis identified that ADCC-resistant cells show an enrichment of genes implicated in the oxidative stress response, independent of known roles of XIAP in apoptosis and proliferation, and corresponding with an increase in the antioxidant pool identified both by gene and protein expression analysis. In XIAP overexpressing, ADCC-resistant IBC cells, inhibition of NF $\kappa$ B activation by JSH-23 led to increased ROS accumulation both basally and in the presence of H<sub>2</sub>O<sub>2</sub>. This further supported the role of XIAP-mediated NF $\kappa$ B activation as a means of blunting ROS generation. Using NRAGE to specifically inhibit XIAP-mediated NF $\kappa$ B activation, we reveal this axis can be targeted to enhance ADCC response in an ADCC-resistant cell line. This targeting approach is supported by studies from our lab and others that have reported a caspase-

independent role for XIAP in mediating survival signaling and ROS suppression, in particular through activation of NF $\kappa$ B and its target genes (e.g. antioxidant enzymes SOD1 and SOD2 among others) (111,447,494). These data support this additional mechanism of XIAP in modulating redox response in cancer cells and this study is the first to observe that XIAP can abrogate ADCC-mediated cell death in a caspase-independent manner.

In addition to the roles identified for XIAP in directly promoting tumor resistance to immune therapy, it is also likely that it is associated with the induction of a more immunosuppressive tumor microenvironment. Among the immune genes identified in our gene set enrichment analysis of ADCC-resistant IBC cells (Figures S5 and S6), CSF2 induces myeloid-derived suppressor cell (MDSC) generation and subsequent immunosuppressive activities (495), and IFN $\gamma$  induces PD-L1 expression in cancer cell lines, which can suppress the cytotoxicity of both NK cells and CTLs (496-498). Chemokine (CC) ligand 13 (CCL13) is a chemoattractant factor for monocytes and lymphocytes and downregulation could limit ADCC and T cell-mediated killing. CCL21 leads to a tolerogenic tumor microenvironment and promotes survival of tumor xenografts (499). CCL21 can also promote differentiation into Treg cells and induce effector T cell senescence (500). CXCL13/bca-1 can promote eosinophil and naïve T cell accumulation, suppressing immune response (501). IL-25 has been shown to polarize ILC2s creating an immunosuppressive environment (502). Upregulation of kynurenine

4-monooxygenase (KMO) diverts catabolism of tryptophan, an essential element for T cell proliferation, to create a specific metabolite, 3-hydroxykynurenine (3-HK), which has roles in redox homeostasis (503) and can suppress T cell function directly (504). Although alterations in the levels of these molecules may not affect *in vitro* assessment of ADCC and immune-mediated apoptosis, they do suggest an immunosuppressive phenotype that may be present *in vivo* in tumors with high XIAP expression.

In conclusion, our data reveal not only the significance of anti-apoptotic signaling but also a redox adaptive mechanism that allows cancer cells to suppress ROS, which can in turn modulate immune-mediated cell death. Monoclonal antibodies mediating ADCC are important components of cancer therapy and resistance to them limits therapeutic options for patients with advanced cancer. These data suggest that continued sensitivity to the ADCC-mediating functions of these antibodies may be achieved by targeting XIAP in two manners: the anti-apoptotic function-mediated by binding caspases, and/or the caspase-independent ROS suppressive function. The IAPs (including XIAP) are inhibited endogenously by Smac/DIABLO (230,505), which is released from mitochondria along with cytochrome c during apoptosis and promotes caspase activation by competitively binding to the IAPs. There is growing evidence from our laboratory and others of the ability of Smac mimetics, many of which are in clinical development (506), to potentiate therapeutic apoptosis (420,507,508). This highlights the potential for the therapeutic utility of these Smac mimetics in sensitizing tumors to

immune therapies, as well. In summary, these data provide a strong rationale for testing strategies that combine antibody therapeutics with pro-apoptotic agents, such as XIAP antagonists or ROS modulators to overcome the frequent problem of resistance by directly inducing apoptosis or by lowering the apoptotic threshold and increasing specific tumor cytotoxicity.

## **5. Development and characterization of a novel combination therapy to antagonize redox imbalance in IBC**

### ***5.1 Introduction***

At physiological low levels, reactive oxygen species (ROS) function as “redox messengers” in intracellular signaling and homeostatic regulation. In contrast, oxidative modification of cellular macromolecules, inhibition of protein function, and cell death can occur when cells are exposed to or accumulate high levels of ROS in submicro- and micro- molar concentrations (309,342,509,510). Therefore, increased accumulation of ROS leading to cancer cell death is a prominent mechanism of radiotherapy and many commonly used chemotherapeutics (511-514). Both normal and cancer cells, however, have the innate ability to regulate ROS and modulate apoptosis using various redox systems which operate on multiple levels, including but not limited to reduced glutathione (GSH), glutathione peroxidase, thioredoxin, peroxiredoxin, catalase and superoxide dismutases (SODs). The fine balance between these two systems (ROS and antioxidants) keeps ROS below a specific threshold, above which cell death is induced (515,516). In cancer cells however, ROS accumulation has been shown to increase as mutations in key pathways such as the epidermal growth factor receptor (EGFR) (337), which is extremely important for the proliferation and metastatic potential of IBC cells, accumulate and drive oncogenesis. It is observed that in cancer cells, a robust redox adaptation often evolves as a survival mechanism, leading to an upregulation of

antioxidant capacity and a shift of redox dynamics, resulting in low generation and high elimination of ROS to maintain ROS levels below the threshold needed to induce cell death (310,517). We recently reported this mechanism to be highly prevalent in our therapy-resistant IBC cell lines, significantly suppressing oxidative stress-associated cell death and leading to multi-drug resistance in these cells (111). Our previously published evidence with 2-methoxyestradiol (2-ME), sodium diethyldithiocarbamate trihydrate (DETC), and embelin revealed evidence that redox modulators that can act as pro-oxidants have the potential to enhance cytotoxicity and induce oxidative stress in IBC cells (111,419). Data presented in Chapter 4, showing evidence for XIAP- and NF $\kappa$ B-mediated regulation of this redox adaptation also elucidates pathways that can be targeted by these pro-oxidant therapies.

Superoxide dismutase (SOD) is the first line of cellular antioxidative defense (518). Therefore, small molecules mimicking its function have been developed in order to augment cellular antioxidant ability. Cationic manganese porphyrins (MnPs) are among the most potent synthetic SOD mimics identified to date (422,519-521). They target both cytoplasmic and mitochondrial compartments, where they catalyze the dismutation of O<sub>2</sub><sup>-</sup> at similar efficacy to the endogenous SOD protein (522). They can also function as pro-oxidants, depending upon the redox status of the cell, the species they encounter, and their location within the cell. These SOD mimetics have also been

shown to induce oxidation of the p50 subunit (523-527) and glutathionylation of the p65 subunit of NF $\kappa$ B (528,529), leading to specific downregulation of transcriptional activity.

In the work presented in this chapter, two MnPs of different properties were assessed alone and in combination with ascorbate (asc), which is catalyzed by MnP leading to massive production of peroxide, for their ability to induce cell death in multiple IBC cell lines (both therapy -sensitive and -resistant). The combination of MnP +asc decreased the viability and proliferation of two patient-derived, therapy-sensitive IBC cell lines, an isotype matched drug-resistant cell line, and an exogenous model of XIAP overexpression. These decreases were shown to be dependent on ROS accumulation, leading to the downregulation of GSH levels, and subsequent blockade of NF $\kappa$ B and ERK survival signaling. Further analysis revealed a caspase-independent mode of cell death that was seemingly specific for tumor cells and not normal cells. Taken together, these data provide the rationale for the use of this novel combination for targeting and treating IBC. This work was previously published by our lab (530).

## 5.2 Results

### 5.2.1 Combination of MnP+asc decreases cell viability and proliferation in therapy –sensitive and –resistant IBC cells

We evaluated two MnPs, MnTE-2-PyP<sup>5+</sup> (E2) and MnTnBuOE-2-PyP<sup>5+</sup> (BuOE2) (whose distinct physical and chemical characteristics are shown in Figure 2.2), in cellular models of IBC, a highly aggressive breast cancer subtype with increased deregulation in apoptotic and oxidative response gene signaling (52,111,135,419). We first characterized cell viability with increasing doses (0-50  $\mu$ M) of the two MnPs in combination with ascorbate by trypan blue exclusion assay (Figure 5.1). Neither of the MnPs or ascorbate alone had a significant effect on viability in any of the cell lines. Data in Figure 5.1 show that both E2 and BuOE2 in combination with ascorbate caused decreased viability in all three cell lines. The E2 compound, however, decreased viability at lower concentrations (EC<sub>50</sub> of 10  $\mu$ M for E2 as compared to 30  $\mu$ M of BuOE2). Table 5.1 lists the approximate, calculated EC<sub>50</sub> values for each combination across the cell lines.

**Table 5.1 Approximate EC<sub>50</sub> values for each MnP+asc in cell lines tested**

	SUM149	rSUM149	SUM190
MnTE-2-PyP <sup>5+</sup> (E2)	11.3 $\pm$ 1.1	12.5 $\pm$ 1.5	10.2 $\pm$ 1.8
MnTnBuOE-2-PyP <sup>5+</sup> (BuOE2)	30.0 $\pm$ 1.3	39.9 $\pm$ 2.2	17.1 $\pm$ 1.5

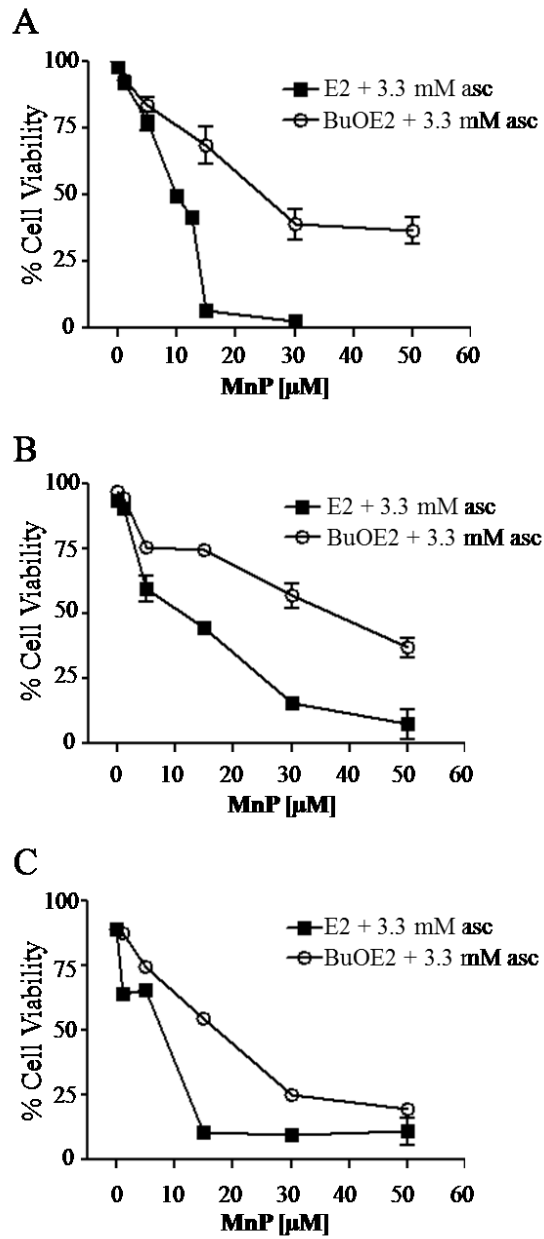


**Figure 5.1 Combining MnP and ascorbate induces significant cell death in IBC cells**

Cell viability of A) SUM149, B) rSUM149, and C) SUM190 viability as determined by trypan blue exclusion of cells treated with E2 or BuOE2 (0-50  $\mu$ M) in the presence of ascorbate (3.3 mM) measured after 24 hours. Data represent mean $\pm$ SEM viable cells taken as a percentage of total cells (n=2-3).

In three cell lines tested, ascorbate alone increased formation of formazan (the purple colored reduced tetrazolium MTT reagent measured as explained in Methods section) (~30-50% over untreated) which is commonly used to measure the cellular reducing potential as well as proliferation (Figure 5.2) (531). E2 alone also increased the reduction of MTT dye to formazan in both SUM149 and SUM190 cell lines (~40% over untreated), but not in the therapy-resistant rSUM149 line, while BuOE2 alone caused no significant increase in any of the three cell lines. When combined with ascorbate, E2 induced a significant decrease when compared to E2 alone (~ 70-120% decrease), while BuOE2 yielded a lower decrease (~30-45%). We also assessed increased proliferation by total cell counts; the administration of MnPs decreased the growth rate for cells ~4 hours, bringing the SUM149 line doubling time from 22.5 hours to 17.5 hours. The cytotoxic pro-oxidative effects were not seen with either of the MnPs as single agents at given concentrations.

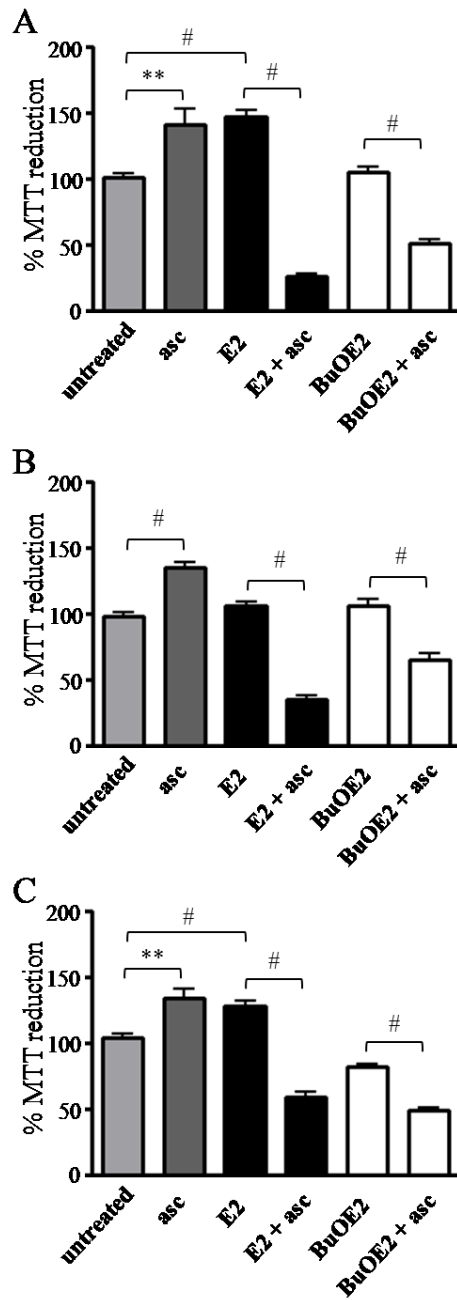


**Figure 5.2 MnP+asc treatment reduces cellular proliferation of IBC cells**

Cellular proliferation of A) SUM149, B) rSUM149, and C) SUM190 cells treated with E2 or BuOE2 (50  $\mu$ M) or ascorbate (3.3 mM), alone and in combination. Bars represent mean $\pm$ SEM (n=8-16, \*\*p<0.005, #p<0.001).

### **5.2.2 E2+asc induces significant ROS accumulation in IBC cells**

We next measured changes in mitochondrial superoxide and hydrogen peroxide-derived radicals using MitoSox Red and Carboxy-H<sub>2</sub>DCFDA flow cytometric analysis respectively in the SUM149 (Fig. 5.3A) and rSUM149 (Fig. 5.3B) cells. The MnP compounds, E2 and BuOE2, did not increase ROS accumulation as single agents in either cell line tested. In both cell lines, however, ascorbate alone caused a modest decrease in ROS accumulation. Comparison of respective combinations of E2 and BuOE2 with ascorbate revealed that the E2 compound was more efficacious in inducing both mitochondrial superoxide (~3 fold increase) and H<sub>2</sub>O<sub>2</sub>-derived radicals (~20% cell fluorescence increase) in the parental SUM149 cell line. Comparison of the two cell line models revealed that in the rSUM149 model, which has insignificant ROS accumulation in the presence of classical ROS generating agents (paraquat and H<sub>2</sub>O<sub>2</sub>) and therapeutic ROS inducing agents (lapatinib and TRAIL) (111,419), the E2+ascorbate combination treatment induced significant ROS accumulation, albeit at lower levels (~2 fold mitochondrial superoxides and 10% H<sub>2</sub>O<sub>2</sub>-derived radical increase) compared to the parental therapy-sensitive SUM149 cells. Taken together these results indicate that E2, which is less stable than BuOE2 in the presence of ascorbate, is more potent in inducing ROS accumulation and decreasing cell viability than BuOE2. The combination is also able to induce ROS accumulation in a cell line that shows little to no accumulation when challenged with classical or therapeutic ROS inducers.

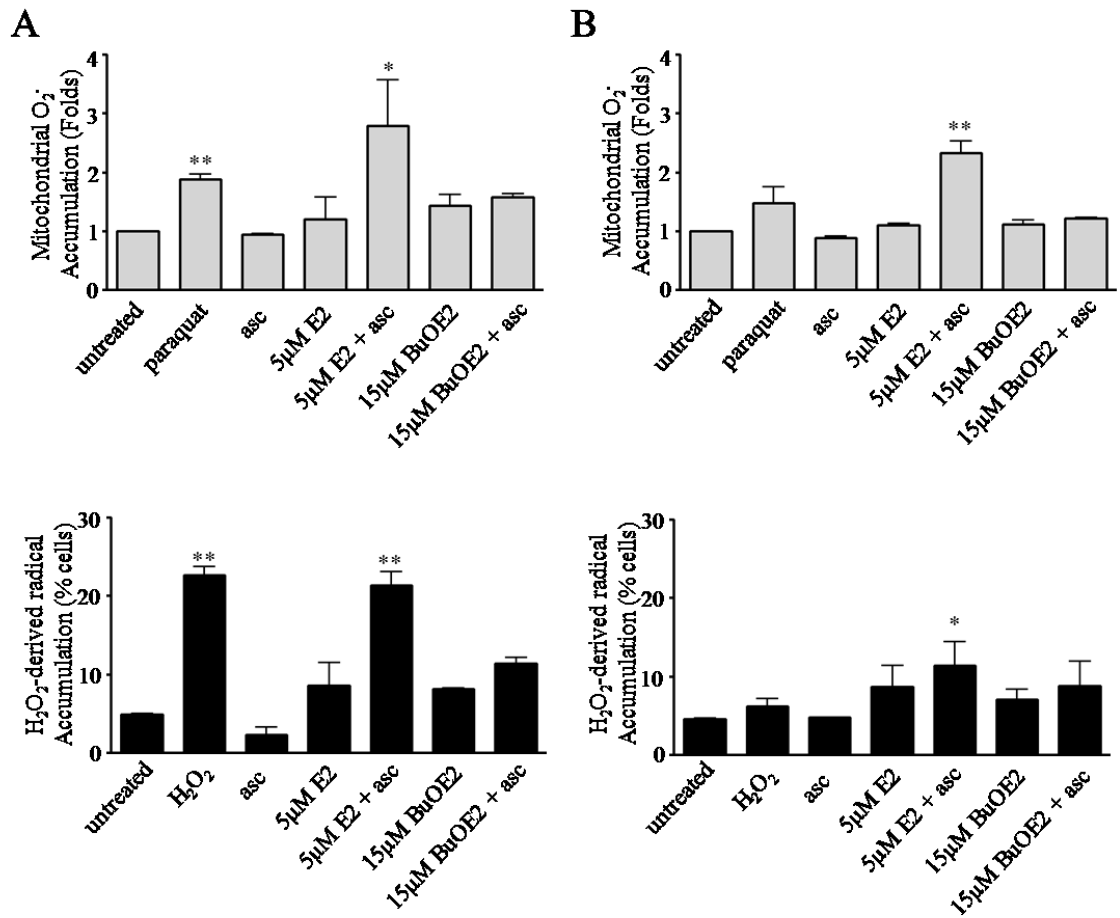


**Figure 5.3 Combination of MnP and ascorbate induces ROS accumulation and overcomes redox adaptation in rSUM149 cells**

Fold induction of mitochondrial superoxides (top, gray bars) and percentage of cells with high H<sub>2</sub>O<sub>2</sub>-derived radicals (bottom, black bars) in A) SUM149 and B) rSUM149 cells treated as indicated. Bars represent mean±SEM relative to untreated cells, (n=2-3). \*p<.05, \*\*p<.005.

### **5.2.3 Peroxide is essential for MnP+asc cytotoxicity, consuming the reduced glutathione pool**

As our data above shows the induction of ROS with the combination of MnP+asc, we tested the levels of endogenous antioxidant defenses in the cells after treatment. Western immunoblot of SOD1 and SOD2 show that in SUM149 cells, addition of excess ascorbate, either alone or in combination with MnPs actually caused increased SOD1 expression (Figure 5.3A). E2 and BuOE2 alone also produced a slight increase in SOD1 expression. This slight upregulation is most likely a response to ROS accumulation in the cell. SOD2 expression showed no significant changes under any of the indicated conditions. We also assessed levels of glutathione (GSH) in the cells after treatment. Neither ascorbate nor E2 alone had any effect on GSH levels, however, the combination of E2+asc significantly depleted GSH levels in the SUM149 cells, which correlates with oxidant accumulation (Figure 5.3B).

In order to prove H<sub>2</sub>O<sub>2</sub> involvement in MnP+asc cytotoxicity, we examined whether the administration of exogenous catalase, an H<sub>2</sub>O<sub>2</sub> scavenger, would reverse the cell death. Data in Figure 5.3C show that the treatment of cells with E2+asc and BuOE2+asc in the presence of catalase provided protection against the H<sub>2</sub>O<sub>2</sub>-mediated cell death and significantly increased the cellular viability ( $p < .01$  and  $p < .05$ , respectively) (Figure 5.3C).

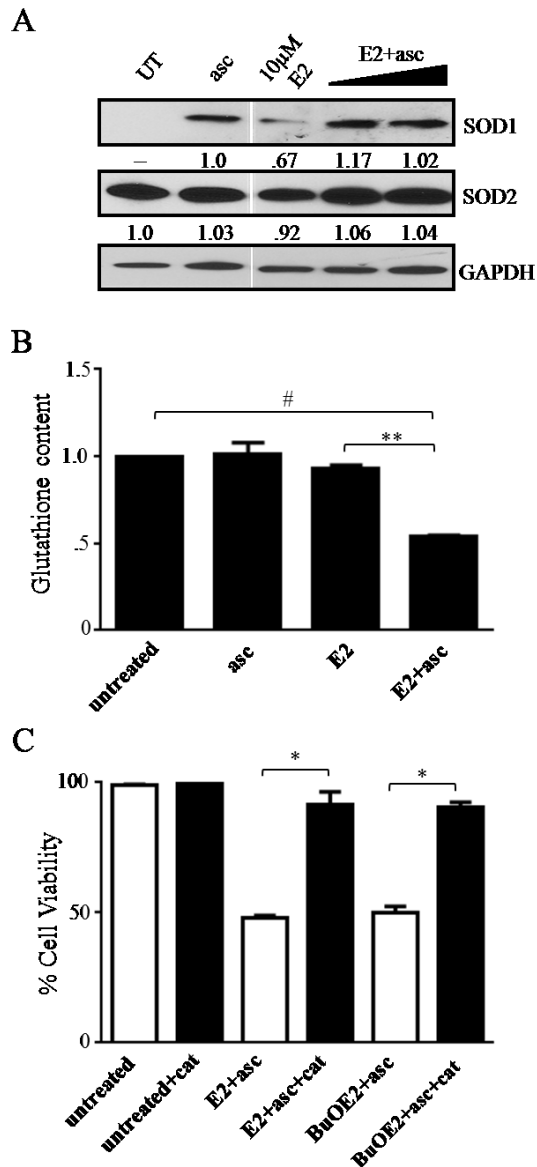


**Figure 5.4 MnP+asc induced cytotoxicity is reversible by administration of catalase**

A) Western immunoblot analysis of SOD1 and SOD2. E2 doses in combination with 3.3 mM ascorbate: 1  $\mu$ M and 10  $\mu$ M. Numbers represent densitometric analysis. B) GSH content of cells treated as indicated for 4 hours. Bars represent mean $\pm$ SEM fold content (n=2-3). C) Viability of SUM149 cells treated with the combination of E2+asc (10  $\mu$ M) or BuOE2+asc (30  $\mu$ M) in the presence or absence of catalase. Bars represent mean $\pm$ SEM viable cells (n=2-3). \*p<0.05, \*\*p<0.005

#### **5.2.4 MnP+asc antagonizes pro-survival NFκB and ERK signals**

Since the MnP+asc combination leads to excessive H<sub>2</sub>O<sub>2</sub> production and in turn decreased cell viability, western immunoblot was carried out to elucidate the expression of proteins involved in ROS and cell survival signaling. Immunoblots in Figure 5.4 show a dose-dependent decrease in ERK1/2 [p44/42] and NFκB phosphorylation, but no significant changes in p38 MAPK phosphorylation in treated lysates, respectively, which is consistent with the increased ROS production and decreased viability.

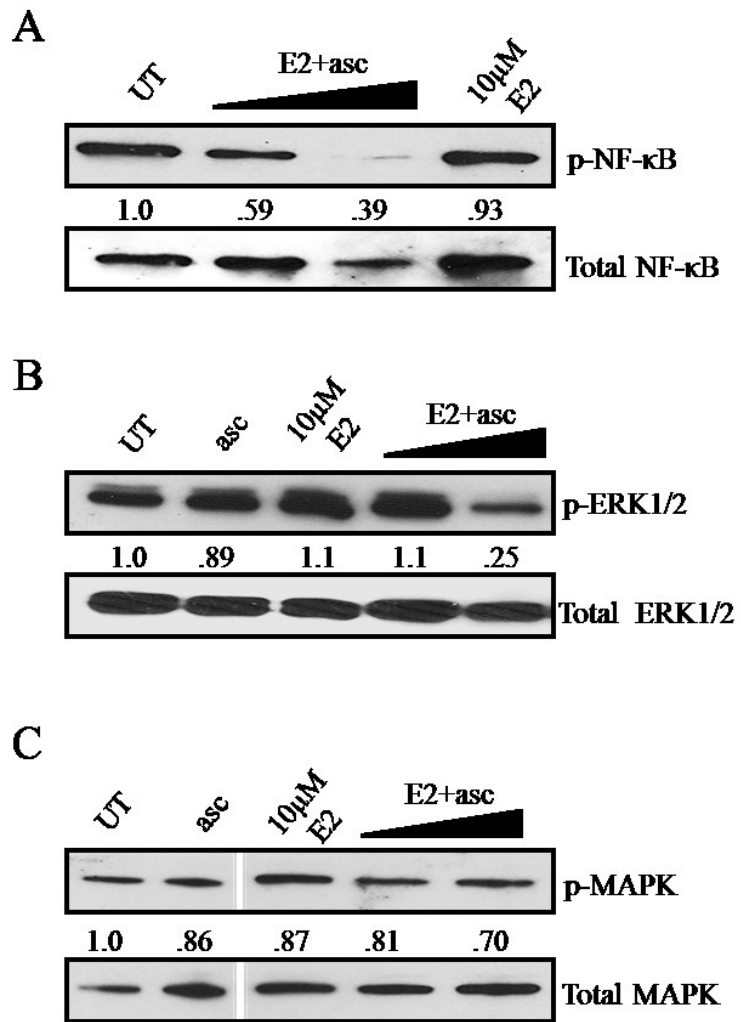


**Figure 5.5 Peroxide generated by MnP+asc treatment reduces pro-survival signaling**

Western immunoblot analysis of A) phospho- and total ERK1/2, B) phospho- and total NF-κB, and C) phospho- and total MAPK in SUM149 cells treated with ascorbate or E2, alone and in combination. E2 doses in combination with 3.3 mM ascorbate: 1 μM and 10 μM. *Numbers represent densitometric analysis.*

### **5.2.5 Apoptosis induced by this combination is caspase independent**

As the MnP+asc combination exhibited high cytotoxicity, Annexin V staining was carried out with E2 and BuOE2, alone and in combination with ascorbate to gain further insight into the mechanism of cell death. Figure 5.5A shows a dose-dependent increase in the number of Annexin V positive cells in the SUM149 cells. Analysis of X-linked inhibitor of apoptosis (XIAP) expression, the most potent cellular inhibitor of apoptosis, in SUM149 cells showed a decrease in XIAP expression with the combination of E2+asc; BuOE2+asc, however, had little to no effect (Figure 5.5B top). A cleavage product of XIAP was also observed in E2+asc treated cells at both doses, while BuOE2+asc showed negligible cleavage. PARP cleavage is another marker of apoptosis that was measured to elucidate the mechanism of cell death. Combination of E2/BuOE2 and ascorbate at lower doses led to a decrease in total PARP expression and as the concentration of the combination increased to a dose corresponding to the EC<sub>50</sub>, PARP cleavage as well as a laddering effect was observed (Figure 5.5B middle).

Interestingly, E2+asc mediated cell death was not reversed when cells were pre-treated with a pan-caspase inhibitor (QVD-OPh). Staurosporine, a known apoptosis inducer that is semi-dependent on the caspase activity (532), was used as a control, and pre-treatment with QVD-OPh significantly reversed staurosporine-mediated cell death, while having no significant effects on cell death mediated by E2+asc combination (Figure 5.5C).

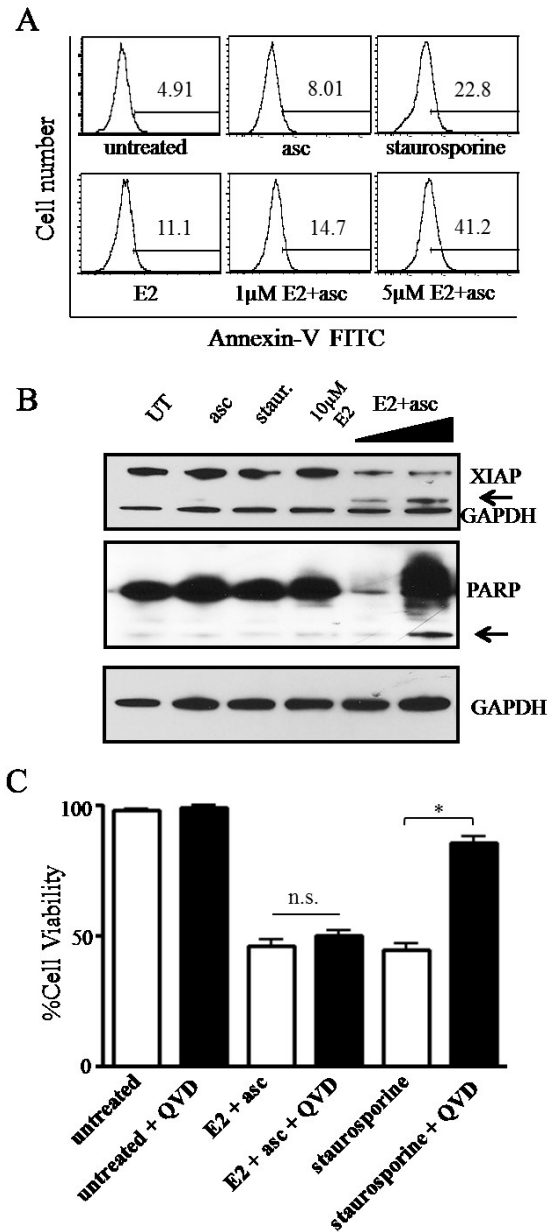


**Figure 5.6 Cell death induced by MnP+asc is caspase-independent**

A) Representative histograms of Annexin V staining for SUM149 cells treated as indicated for 4h, representative of n=2-3. B) Western immunoblot analysis of XIAP and PARP in SUM149 cells treated as indicated, arrows denote cleavage products. C) Cell viability of cells treated as indicated for 24 h. Bars represent mean±SEM viable cells (n=2-3). \*p<0.05.

### **5.2.6 MnP+asc leads to translocation of apoptosis-inducing factor (AIF) to the nucleus**

Given that caspase inhibition did not reverse the cell death seen with combination treatment, we sought to investigate the possibility of a caspase-independent mechanism of apoptosis. To further characterize the cell death mechanism, cells were treated and immunofluorescently labeled for apoptosis inducing factor (AIF) following treatment with MnP+asc. Translocation to the nucleus was indicated by the overlap of the AIF fluorescent signal (FITC) with DAPI nuclear staining. H<sub>2</sub>O<sub>2</sub> was used as a positive control, as it has been previously linked to caspase-independent cell death and AIF translocation (533,534). In untreated cells (Figure 5.6 top panel), AIF was seen to surround the nucleus in a pattern consistent with the normal mitochondrial localization of the protein. However, upon treatment with H<sub>2</sub>O<sub>2</sub> or MnP+asc, AIF translocated into the nucleus, and staining overlapped with DAPI (Figure 5.6 bottom panel).

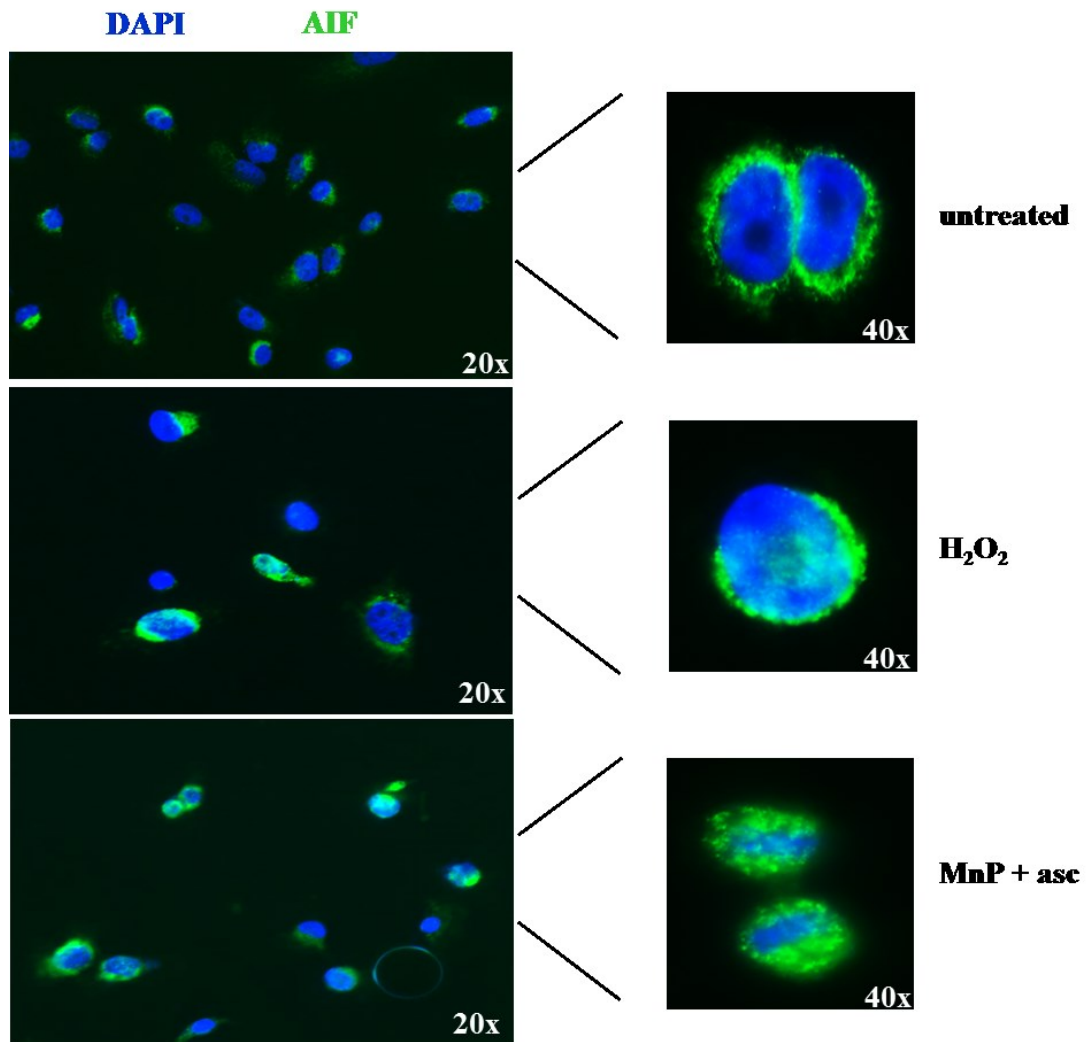


**Figure 5.7 MnP+asc treatment induces translocation of mitochondrial protein, AIF, to the nucleus**

Representative immunofluorescence images of SUM149 cells for AIF after treatment as indicated to the right of each image. AIF shown in green and DAPI shown in blue, Magnification: 40x, representative of n=2.

### 5.2.7 Ascorbate oxidation/consumption is catalyzed by E2 at faster rate

In order to further understand the differences in cytotoxicity and ROS production between E2 and BuOE2, we spectrophotometrically measured the loss of MnP at 438 nm for E2 and 441.5 nm for BuOE2, which correspond to Soret bands of reduced Mn<sup>II</sup>P (Figure 5.7A). The data in Figure 5.7A only relate to the presence of reduced Mn<sup>II</sup>P in solution, but did not account for species which bear Mn in +3, +4, and +5 oxidation states. With ascorbate in solution only reduced Mn<sup>II</sup>P was detected (Figure 5.7B). Once ascorbate is fully consumed (detected as disappearance of HA<sup>-</sup> absorption band at 265 nm), we saw the appearance of Mn<sup>III</sup>P at 90 min for E2 and 125 min for BuOE2 (Figure 5.7B). The H<sub>2</sub>O<sub>2</sub>, which is produced as a consequence of MnP/ascorbate cycling, oxidizes Mn<sup>III</sup>P to (O)<sub>2</sub>Mn<sup>V</sup>P [49,50,51]. Mn in (O)<sub>2</sub>Mn<sup>V</sup>P then oxidizes the porphyrin ring which in turn falls apart (535). Aside from Mn<sup>II</sup>P and Mn<sup>III</sup>P, which were clearly detected spectrally, other features of a complicated spectrum relate to the high-valent Mn oxo species (Figure 5.7B). We also assessed the oxidation/consumption of ascorbate (HA<sup>-</sup>) spectrally as the disappearance of its absorption band at 265 nm (Figure 5.7C) *via* initial rates approach. The initial rates,  $v_0(\text{HA}^-)_{\text{ox}}$  are given in Figure 1B. The differences in initial rates of ~30% between E2 ( $v_0(\text{HA}^-)_{\text{ox}} = 1.7 \times 10^{-7} \text{ M s}^{-1}$ ) and BuOE2 ( $v_0(\text{HA}^-)_{\text{ox}} = 1.2 \times 10^{-7} \text{ M s}^{-1}$ ) (Figure 5.7B). The  $E_{1/2}$  of BuOE2, relative to E2, is ~50 mV more positive; this indicates that it is more electron-deficient than E2 and likes accepting electron. Therefore, the BuOE2 is stabilized in the Mn +2 oxidation state more than E2. In

turn, it would be less prone to re-oxidation with O<sub>2</sub> and peroxide formation than E2, thus to peroxide-driven oxidative degradation. Based on the estimated rate constant for Mn<sup>III</sup>P re-oxidation with O<sub>2</sub> to Mn<sup>IV</sup>P,  $k_{\text{red}}(\text{O}_2)$  (Figure 1B) (536), presumably the rate-limiting step in peroxide production, the ~2.6-fold faster H<sub>2</sub>O<sub>2</sub> production by E2 than by BuOE2 may be anticipated. Yet, the data on the metabolic activity and cell viability agree well with such estimation; they indicate that: (i) 10 μM E2+asc inflicts equal loss of cell viability as 30 μM BuOE2+asc; and (ii) 30 μM BuOE2+asc is up to few-fold less cytotoxic than 30 μM E2+asc.

*The ascorbate oxidation, H<sub>2</sub>O<sub>2</sub> production and subsequent MnP degradation.* The favorable properties of the catalyst would involve not only the rate of ascorbate oxidation and in turn H<sub>2</sub>O<sub>2</sub> production, but also the rate of its oxidative degradation. As long as it is present in solution, ascorbate supports Mn<sup>III</sup>P/Mn<sup>II</sup>P and suppresses Mn<sup>III</sup>P/(O)<sub>2</sub>Mn<sup>V</sup>P redox (Figures 5.7A and B). Once ascorbate is oxidized/consumed (at ~90 or 125 min, respectively for E2 and BuOE2) (Figure 5.7C), the Mn<sup>III</sup>P starts undergoing oxidation to (O)<sub>2</sub>Mn<sup>V</sup>P with subsequent porphyrin ring degradation (Figures 5.7A and B) (535). The (O)<sub>2</sub>Mn<sup>V</sup>P was identified as two-electron oxidized species based on the H<sub>2</sub>O<sub>2</sub>/MnP kinetic studies of a very similar MnTDE-2-ImP<sup>5+</sup> analog (521,537,538). The (O)<sub>2</sub>Mn<sup>V</sup>P readily decays to O=Mn<sup>IV</sup>P (539,540). *In vitro* and *in vivo* the high-valent Mn oxo species cycles back to Mn<sup>III</sup>P with cellular reductants [49]. Once ascorbate is consumed, thus H<sub>2</sub>O<sub>2</sub> accumulated, the spectral scans show similar spectral

profiles to those obtained in MnP+ H<sub>2</sub>O<sub>2</sub> system. The MnP degradation in the presence of MnP/asc and MnP/H<sub>2</sub>O<sub>2</sub> shows the same spectrophotometrical profile (426,428,429), which is additional proof that peroxide is produced in the reaction of MnP with ascorbate (428,430,521,541). The BuOE2 is less prone to re-oxidation from Mn<sup>II</sup>P to Mn<sup>III</sup>P than E2. Therefore, within same time period its catalytic action upon ascorbate oxidation results in lower peroxide levels than with E2. Thus, oxidative degradation of BuOE2 begins with certain delay (~30 min), which gives impression that it appears more resistant in the reaction mixture than E2. More studies are needed to gain further insight into its resistance towards oxidative degradation with H<sub>2</sub>O<sub>2</sub> relative to other Mn(III) *N*-substituted pyridylporphyrins. This analysis was performed by the Batinic-Haberle lab at Duke University.

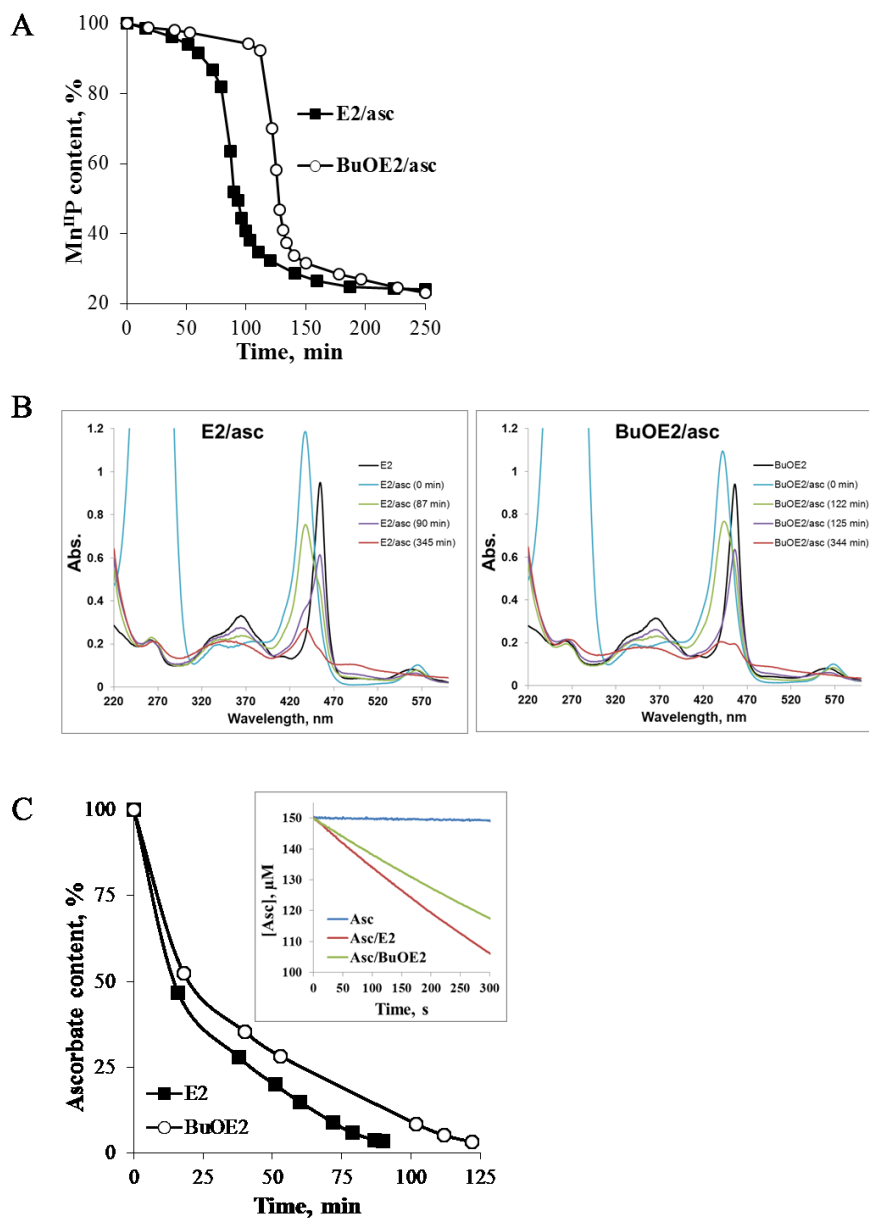


**Figure 5.8 H<sub>2</sub>O<sub>2</sub>-driven degradation of MnPs in the presence of ascorbate, and consumption of ascorbate**

A) Spectrophotometric analysis of MnP content after addition of ascorbate. B) Time-dependent spectral change of MnPs in the presence of ascorbate. C) Time-dependent oxidation/consumption of ascorbate after addition of MnP. *Inset, Initial rates of ascorbate oxidation by MnPs.*

### 5.3 Discussion

We report herein the assessment of the cytotoxic effects of two MnPs in combination with ascorbate on inflammatory breast cancer cells and the pathways involved in cell death mediated by this combination. Two MnPs of different physical and chemical properties listed in Figure 2.2 were explored in order to understand their ability to act as catalysts for ascorbate oxidation and peroxide formation. We have previously reported the reducibility of cationic Mn(III) *N*-substituted pyridylporphyrins with cellular reductants and our data suggest that the MnP+asc system may represent a prospective anticancer treatment for aggressive inflammatory breast cancer (426,521-523,537).

Earlier reports on the cellular studies showed that extracellular peroxide, formed as a consequence of MnP/ascorbate interactions, is the cause of cell death (518,542,543). Similar to our previous report (430), the ~5,000-fold difference in the lipophilicity of E2 and BuOE2 (Figure 2.2) is of no great importance in this cellular model of IBC. However, shape, planarity, lipophilicity, and in turn bioavailability will likely play a significant role in animal models and clinical settings. We have already shown that the lipophilic BuOE2 distributes to mitochondria (relative to cytosol) and crosses the blood brain barrier to a higher extent than E2 (521,537). A most dramatic example how lipophilicity can compensate for insufficient reactivity of Mn porphyrin has been the aerobic growth of SOD-deficient *E. coli* (544). The *meta* isomeric MnTE-3-PyP<sup>5+</sup> (E3), which has 10-fold

lower  $k_{\text{cat}}(\text{O}_2^{\bullet-})$ , exhibits identical protection to aerobic growth of SOD-deficient *E. coli* as the *ortho* isomeric E2 due to its 10-fold higher lipophilicity (544).

Our data show that the rapid production of  $\text{H}_2\text{O}_2$  led to decreased pro-survival ERK and NF- $\kappa$ B signaling (Figure 5.9, 2) and decreased mitochondrial integrity (Figure 5.9, 3). The cell death was dependent on ROS, specifically  $\text{H}_2\text{O}_2$ , as addition of exogenous catalase, effectively reversed cell death. Increased accumulation of ROS decreased *p*-NF- $\kappa$ B and *p*-ERK levels. This is of particular interest in IBC as high NF- $\kappa$ B activity is a feature of IBC pathogenesis (26,64). Another group has shown that, under conditions of increased  $\text{H}_2\text{O}_2$  as a consequence of glucocorticoid treatment, and in the presence of glutathione, MnTE-2-PyP<sup>5+</sup> would glutathionylate the p65 subunit of NF- $\kappa$ B and deplete GSH preventing its anti-apoptotic activity (528,545). Similar to our study, GSH levels were depleted with combination treatment.

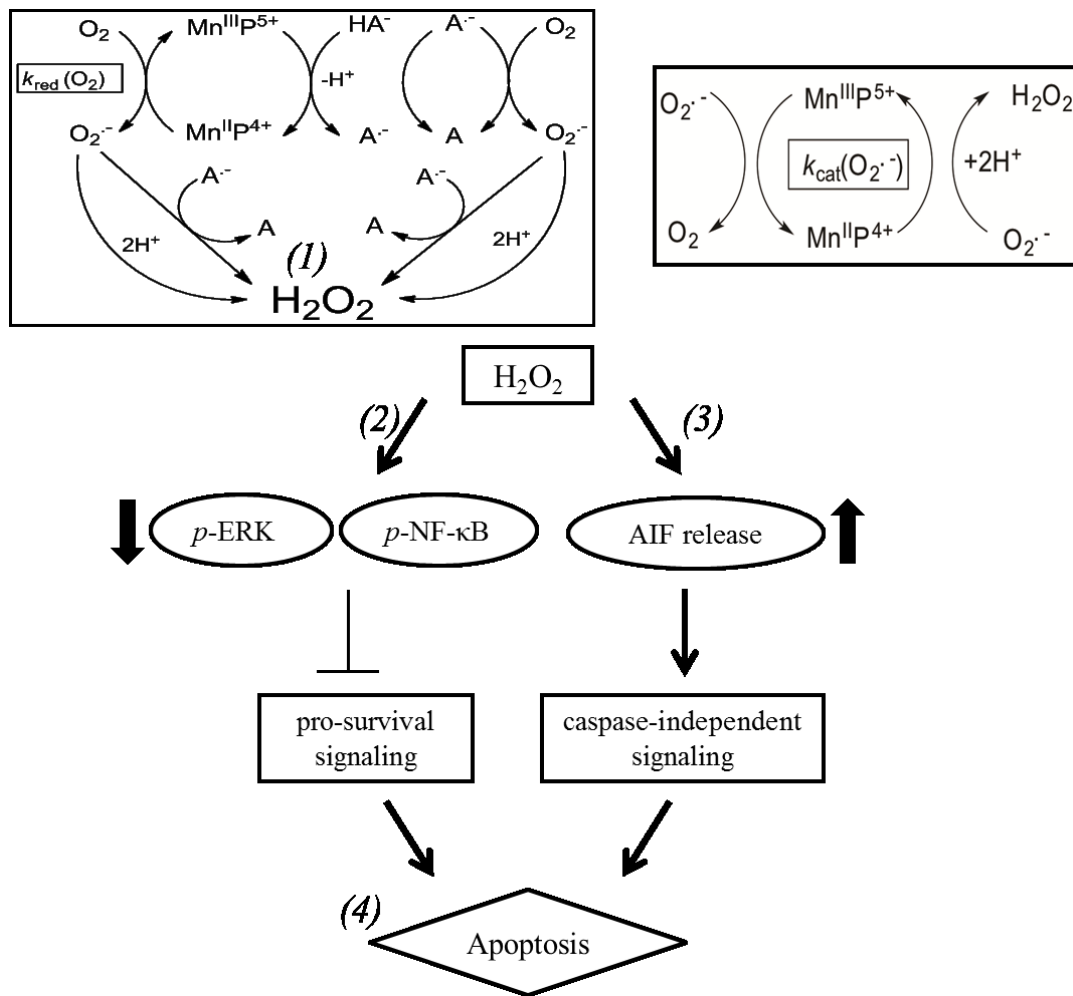


**Figure 5.9 Schematic of the interaction between MnP and ascorbate and the cellular effects**

Mn<sup>III</sup>P reacts with ascorbate (HA<sup>-</sup>), to form ascorbyl radical (A<sup>•-</sup>) and Mn<sup>II</sup>P. Mn<sup>II</sup>P undergoes re-oxidation with oxygen to form superoxide (O<sub>2</sub><sup>•-</sup>), which readily dismutates into H<sub>2</sub>O<sub>2</sub> (1). Mn<sup>II</sup>P can also undergo a reaction with to form H<sub>2</sub>O<sub>2</sub>. Subsequently, the increased H<sub>2</sub>O<sub>2</sub> production leads to dephosphorylation of ERK and NF-κB (2). Increased ROS leads to permeabilization of mitochondria and release of AIF from the mitochondria (3). Upon release, AIF translocates to the nucleus, and can mediate caspase-independent cell death (4).

Cell death parameters assayed in the E2+asc treated cells showed increased Annexin V positivity, decreased XIAP, and cleavage of the caspase substrate PARP, revealing apoptosis-mediated cytotoxicity in cells. Remarkably, addition of a potent pan-caspase inhibitor (Q-VD-OPh) did not reverse the cell death mediated by E2+asc. Correspondent with this inability to reverse cell death with a caspase inhibitor, we observed that in these treated cells, apoptosis inducing factor (AIF) was translocated to the nucleus (Figure 5.9, 4). AIF is a 67 kDa, mitochondria-localized flavoprotein that is known to activate caspase-independent cell death upon mitochondrial damage (546). After cellular insult, AIF translocates to the nucleus and can cause cell death while also inducing classical apoptotic features such as phosphatidylserine exposure and chromatin condensation; this cell death mechanism has been shown to be PARP1-dependent in some systems, consistent with findings in Figure 5 (546-548). This phenomenon of AIF induction after H<sub>2</sub>O<sub>2</sub> treatment has been reported in various cell types including B cells, myoblasts, and neurons, among others (548,549). Continuous influx of H<sub>2</sub>O<sub>2</sub> was seen to induce caspase-independent cell death in Jurkat T cells (550). Indeed, data in the current study show that the interaction between MnPs and ascorbate can continuously produce superoxide and hydrogen peroxide (until all ascorbate is consumed) (Figure 5.9, 1), which is most likely the cause for AIF-mediated, caspase-independent cell death in this pro-oxidant model. Conversely, in a model of cardiomyocytes, AIF nuclear translocation *via* doxorubicin-driven mitochondrial lipid

peroxidation was attenuated by the administration of various MnPs alone (551). The differential effects, pro-oxidative (with cancer cells) *vs.* anti-oxidative with cardiomyocytes (normal cell), are at least in part a consequence of differences in the cell types. These studies, along with our observations, support a caspase-independent mechanism of cell death induced by E2+ascorbate.

Earlier work has shown the efficacy of pharmacological administration of ascorbate in treating cancer cells *in vitro* and *in vivo* (542,552,553) and paved the way to clinical trials. Ascorbate administration for 8 weeks increased both progression-free survival and overall survival in these clinical trials (554,555).

Based on present understanding of anticancer therapy the most promising strategies would combine several approaches. We have already shown that MnTE-2-PyP<sup>5+</sup> enhances radiation (422,519,521,537,556) and glucocorticoid therapy (528,545). For the latter, the evidence was provided that it occurs via glutathionylation of NF- $\kappa$ B, catalyzed by MnP in the presence of H<sub>2</sub>O<sub>2</sub> and GSH system. Future studies would clarify if the radiotherapy enhancement shares the same apoptotic pathways. In order to correctly predict which cancer cell type would be responsive to any of these strategies alone or combined, and at what ratio of MnP to ascorbate the system would be therapeutic, one would need to explore the ability of the cell to handle excess of peroxide. This would include the determination of the cellular redox environment,

which would include the measurements of the levels and activities of cellular antioxidants.

The peroxide generating system MnP+ascorbate leads to cellular apoptosis in inflammatory breast cancer. Moreover, it overcame the high antioxidant-mediated apoptosis resistance in the rSUM149 aggressive breast cancer cellular model. Reduction of NF- $\kappa$ B and ERK pro-survival signaling as well as caspase-independent apoptosis was observed with MnP+ascorbate administration. The current study substantiates the therapeutic potential of a system where the metal-based catalyst favors redox cycling with ascorbate, producing peroxide, which along with its progeny, causes cell death. Further optimization of the system may be necessary to move forward with its development as anticancer treatment. Studies are needed to explore the redox status of each cancer type to be treated in order to correctly predict which one would be responsive to excessive levels of peroxide. This system may be combined with other therapeutic strategies that kill cancer cells *via* enhanced oxidative stress.

## 6. Conclusions and Implications

In conclusion, the data presented in this dissertation describe novel roles for the anti-apoptotic protein, XIAP, in regulating multiple aspects of inflammatory breast cancer (IBC) pathobiology and therapeutic resistance. While our previous work identified XIAP as a central player in acquired therapeutic resistance in IBC, the exact mechanisms for how XIAP mediated these processes was unknown. Preliminary evidence also suggested a possible role for XIAP in the pathogenesis and pathology of IBC, which had yet to be fully investigated.

In Chapter 3 of this dissertation:

- We demonstrated for the first time that the MAPK pathway controls XIAP expression in cancer cells
- We reveal that XIAP directly influences the activation profile of NF $\kappa$ B in IBC cells, altering both subcellular localization and transcriptional activity
- We determined the necessity for XIAP expression in IBC tumor growth *in vivo*, where modulating XIAP expression affects the number of ALDH<sup>+</sup> cancer stem cells and cellular motility

- Finally, after determining the mechanism of XIAP-mediated NF $\kappa$ B activation, we demonstrate that targeting of this axis can reverse therapeutic resistance in 2D and 3D culture.

In Chapter 4:

- We demonstrate that the resistance to chemotherapy previously identified in our rSUM cell lines applies to resistance to immunotherapy, specifically antibody-dependent cellular cytotoxicity (ADCC)
- We reveal that XIAP-mediated inhibition of ADCC relies on both caspase –dependent and –independent functions of XIAP, determining that XIAP overexpression increases the antioxidant pool reducing reactive oxygen species-mediated cellular damage
- We functionally elucidate that the inhibition of ROS mediated by XIAP overexpression is dependent on NF $\kappa$ B activation, allowing us to again show the efficacy of our peptide from Chapter 3
- Finally, we show that direct targeting of XIAP can reverse resistance to ADCC-mediated apoptosis in IBC cells

In Chapter 5:

- We demonstrate again the efficacy of targeting XIAP and NF $\kappa$ B in IBC by utilizing a novel combination of manganese porphyrins and ascorbate

- We determined that this combination generates significant ROS, overcoming the increased antioxidant pool in IBC cells possibly through downregulation of NF $\kappa$ B
- Finally, we show that this combination induces caspase-independent cell death most likely through damage to the mitochondria as we observed translocation of a pro-apoptotic protein, localized to the mitochondria under normal conditions, to the nucleus after treatment with combination

The rest of this chapter will discuss these results in the context of current literature and expound on future experiments.

The translation initiation factor eIF4G1 has been shown to be overexpressed in IBC (46) and to mediate cap-independent translation of IRES-containing mRNAs, *p120 catenin* and *VEGF* (46,52). XIAP is another cellular mRNA containing an IRES element and it has been interesting to speculate if eIF4G1 could enhance XIAP translation. In Chapter 3, we present data revealing that knockdown of eIF4G1 in parental IBC cells leads to an almost complete loss of XIAP expression. This is the first finding of an upstream regulator of XIAP expression specifically in IBC. Elucidating eIF4G1 does not, however, rule out the impact of identified *XIAP* ITAFs, which could also play a role (discussed in Section 1.2.3.1.3); determining their involvement will be essential to define the mechanistic role of all proteins. In our previous work we determined that XIAP overexpression in our resistant IBC cell lines was due to post-translational upregulation via its IRES element (156), but we were unable to determine the mechanism driving this enhancement. Utilizing RNAi, we demonstrate that eIF4G1 silencing can reverse resistance to the apoptotic inducer TRAIL at levels strikingly similar to direct knockdown of XIAP. These data yield answers to multiple lines of questions surrounding eIF4G1 and the XIAP IRES in IBC biology. Although identification of eIF4G1 is salient, it is a poor molecular target as its expression and function is not cancer-cell specific. Using targeted agents towards the MAPK pathway, which is being targeted in multiple forms of cancer, we reveal a possible further upstream control of XIAP IRES-mediated translation. A recent study showed a role for the MAPK pathway

in viral IRES translation (557) and previous work has demonstrated that MAPK hyperactivation is a key feature in IBC (26), making our findings highly relevant for the field. A multitude of MAPK pathway inhibitors have been tested in pre-clinical and clinical trials (558) and may be available for use in IBC in combination with approved treatment regimens.

As mentioned earlier in Section 1.1.2.8.2, the MAPK pathway (downstream of EGFR/Her2) has been correlated with NF $\kappa$ B activation in IBC, but no mechanistic explanation directly linking the two could be found at the time. Our work presented here reveals that MAPK-mediated control of XIAP expression may in turn regulate the NF $\kappa$ B activated phenotype associated with IBC. These findings link the commonly overexpressed ErbB receptors to a transcription factor and delineate a pathway that may be targetable at multiple points to enhance therapeutic efficacy in patients diagnosed with IBC. Whole-genome sequencing of *XIAP*-silenced cells uncovered numerous changes across the genome, which according to our analyses can be pinpointed to modulation of the MAPK and NF $\kappa$ B pathways. These changes abolish the tumorigenic capacity of IBC cells in mouse models, furthering the idea that targeting this pathway will be potent in eradicating tumors *in vivo*. Elucidation of the TAB1:TAK1-dependent mechanism for XIAP-mediated NF $\kappa$ B activation is highly interesting and may explain the poor effectiveness of current XIAP-targeting drugs in clinic. The majority of these drugs are directed towards the BIR2 and BIR3 domains (464,559,560), where XIAP binds

caspases, while only one compound outside of our NRAGE peptide (described in Chapter 3), the recently identified NF023 (561), has been observed to disrupt XIAP:TAB1 binding. Further work will be necessary with both of these compounds to determine if they can be utilized as therapeutic agents as well as the identification of other targeted agents that specifically antagonize this binding.

Using our resistant cell line, rSUM149 we also demonstrated the potency of the XIAP-NF $\kappa$ B interaction in driving the progression of IBC. According to one thought, drug resistance does not exist *de novo*, but rather is acquired by a subset of cells under some sort of selective pressure and is a reversible change that can revert with removal (421). This seems to be the case in IBC based on our previously published efforts (418), showing the reversible nature of increased XIAP expression and therapeutic resistance. It is postulated that these cells represent the true cancer stem cells (CSCs), as CSCs have been shown to more drug resistant than other cells in tumors and can reseed after therapeutic intervention (562-564). Our results are concordant with this hypothesis as our rSUM149 cells have a higher population of ALDH1 positive cells, a marker of CSCs in breast cancer. Additionally, we reveal that overexpression of XIAP in parental cells can mimic this increase in ALDH positive cells, which can be decreased by specific targeting of NF $\kappa$ B. This confirms the original hypothesis with XIAP being the factor that is regulated by selective pressure (i.e. a non-mutational increased IRES activity), which increases NF $\kappa$ B activation and the population of CSCs, thereby increasing drug

resistance. A still-standing future direction is the confirmation of these mechanisms in patient tissue. Pre-treatment samples support our conclusions, however, analysis of the above molecules in post-treatment samples will be critical to evaluate our proposed mechanisms *in vivo*.

In Chapter 4, we take a novel approach to IBC therapy in understanding the inhibition of immunotherapy. Immunotherapy has been steadily increasing in treatment regimens for multiple types of cancer, as it represents a systemic, but targeted approach to eradicate tumor cells. As mentioned in Section 1.1.3.3.1, only a few studies in the vein of immunotherapy have been in IBC, but none have at all assessed the inhibition of immunotherapy of which there are a multitude of reported mechanisms. Our earlier works had been largely focused on chemotherapy (156,418-420), while one paper published by our lab reveals that the apoptotic dysregulation in resistant cells leads to the inhibition of T-cell mediated killing (482). This spurred a thought that XIAP may be inhibiting immune-mediated killing and targeting XIAP may enhance the efficacy of immunotherapy. We reveal that XIAP overexpression does decrease immune-mediated cytotoxicity using antibody-dependent cellular cytotoxicity, mediated by NK cells, as proof of principle. We chose this as the use of monoclonal antibodies, particularly trastuzumab, has steadily increased in IBC although all patients seemingly reach a plateau where treatment is no longer efficacious (103,104); however, no explanation has been investigated. Using caspase-binding mutants, we observed that the ability of XIAP

to regulate caspase activation was only partially responsible for the inhibition of apoptosis. The activity of granzyme B has been shown in biochemical assays to have two effects: direct cleavage of caspase-3 (488) and direct cleavage of mitochondrial subunits leading to the generation of ROS (489). Further in-depth analysis elucidated a novel role for XIAP in this process: the inhibition of oxidative stress through activation of NF $\kappa$ B and subsequent redox adaptation. This finding was extremely fortuitous and may explain the effects of our earlier tested compounds that antagonize XIAP function and alter redox adaptation (413,419,420): embelin, which is known to block procaspases-9 binding to XIAP, can also antagonize NF $\kappa$ B activation; Smac mimetics can interfere with NF $\kappa$ B survival signaling through multiple mechanisms involving other IAPs; and disulfiram has been shown in multiple reports to block NF $\kappa$ B. Utilizing Smac mimetics, our NRAGE peptide, and RNAi we demonstrate that targeting of XIAP can enhance immunotherapy efficacy, which merits further testing of IAP inhibitors and redox modulators for their ability to sensitize cells to apoptosis. This study represents the first study to date to: 1) assess the therapeutic efficacy of cetuximab to mediate ADCC in IBC cells with EGFR expression, which comprises a significant portion of tumors; 2) define a mechanism for resistance to ADCC in IBC, predicated on the expression and function of XIAP; and 3) elucidate the mechanisms by which XIAP mediates the inhibition of oxidative stress in IBC. Finally, although not published in this dissertation, our lab recently developed and optimized an *in vivo* ADCC system using CB.17SCID mice,

which retain functional NK cells. This animal model revealed that rSUM149 and wtXIAP cells maintain resistance in tumors and will be useful to test compounds identified in *in vitro* screens.

The finding in Chapter 4 that XIAP-mediated NF $\kappa$ B activation is the mechanism for redox adaptation and subsequent drug resistance was crucial in designing other novel agents that can antagonize these particular targets. Experiments in Chapter 5 utilized a novel combination of two antioxidants, manganese porphyrins (MnPs) and ascorbate, which when combined function as pro-oxidants inducing a significant amount of ROS (530). This combination was able to reverse resistance in both rSUM149 and wtXIAP, correlating with decreased GSH levels, an antioxidant controlled by NF $\kappa$ B. Manganese porphyrins have been revealed to decrease NF $\kappa$ B activation, which was observed in our studies. It is interesting to speculate whether the MnPs directly antagonize NF $\kappa$ B or overwhelm the cell through the continual production of hydrogen peroxide, which can indirectly lead to the dephosphorylation of NF $\kappa$ B (359). No matter the mechanism, these results reveal that interfering with redox adaptation in IBC is a potent way to reverse acquired therapeutic resistance and enhance tumor cell death. In assessing the mechanism of cell death cause by this combination, we observed that inhibition of caspase activity does not decrease the efficacy of this combination. Combined with other data showing Annexin V staining and PARP laddering this led us to look at caspase-independent mechanisms of cell death. Using TMRE staining as a

measure of mitochondrial polarization, we observed significant hyperpolarization of the mitochondrial membrane (unpublished data), which can lead to the release of apoptogenic factors from the inner membrane space (565). One such factor, AIF was seen to translocate to the nucleus, where it has been suggested to have an active role in cell death (566). Further work using RNAi or *AIF* knockout cells could better answer whether AIF is passive or active in this process. Disregarding mechanism, the MnP+ascorbate combination has been shown to selectively target cancer cells while sparing normal cells which is an important consideration in further developing it as a therapeutic strategy (567). *In vivo* work did not show significant decreases in tumor growth with one of the MnP+ascorbate combinations in a 4T1 model (430); however, further work with other MnPs and an IBC model may demonstrate significant changes.

Our identification of redox adaptation as a potent pro-survival mechanism and the elucidation of multiple strategies that target this to enhance apoptosis beg the simple question: can this be seen in patient tissue? We had previously noted that after acute exposure to  $H_2O_2$ , a subset of tumor cells survive and proliferate; analysis of these cells revealed increased NF $\kappa$ B activation at both the gene and protein level suggesting redox adaptation may occur early (unpublished data). Using a whole-genome approach we identified an oxidative stress response metagene, which comprised a number of genes upregulated or downregulated in these surviving cells. Applying this metagene to patient tissue revealed increased redox adaptation in breast cancer samples, with the

highest levels seen in IBC tissue. We were able to recapitulate this data using a commercially available metagene set, furthering our results. This represents the first time redox adaptation has been seen in patient tissue corroborating all of our *in vitro* work to date. Concordant with the “threshold model” (310), we determined from this that IBC tumor cells would be particularly sensitive to redox modulation.

In a recent paper published by our lab, we utilized the FDA approved, anti-alcoholism drug disulfiram (DSF) to determine the feasibility of targeting redox adaptation with a clinically relevant compound (413). *In vitro* studies reported that complexing DSF with exogenous copper could effectively target redox adaptation and NFκB, both of which we have shown to be critical mediators of therapeutic resistance. As the time from preclinical development of a novel drug to FDA approval can be anywhere from 8-10 years, finding activities of already approved drugs (repurposing) in other diseases is attractive. Disulfiram/Antabuse, a drug approved for alcohol abuse management since the 1920s with extensive pharmacokinetic and safety data (568)], showed potent efficacy both *in vitro* and *in vivo* in IBC cells and xenografts when combined with copper (413). Unpublished data from our lab demonstrates that DSF can also enhance the effectiveness of approved chemotherapeutics both *in vitro* and *in vivo*. Current work is ongoing in our laboratory to understand the mechanisms of IBC metastatic progression and to use this information in developing novel combination strategies that can prolong drug sensitivity.

Inflammatory breast cancer is an understudied disease leading to extremely poor outcomes for patients diagnosed and suffering from the disease. The studies here provide a central and essential role for XIAP in key aspects of IBC pathobiology and redox adaptation, both of which contribute to the aggressive nature of the disease. This work not only adds to the basic mechanistic knowledge of key molecules involved in IBC, but also reports novel targeted strategies that can be incorporated to increase patient survival. Further work using patient tissue, other cell line models, and more *in vivo* study will hopefully expedite the awareness of XIAP in IBC and accelerate the introduction of targeted agents into clinical trials to improve patient outcomes.

## References

1. Lee B, Tannenbaum N. Inflammatory carcinoma of the breast: a report of twenty-eight cases from the breast clinic of Memorial Hospital. *Surg Gynecol Obstet* 1924;39:580-95.
2. Anderson WF, Chu KC, Chang S. Inflammatory breast carcinoma and noninflammatory locally advanced breast carcinoma: distinct clinicopathologic entities? *J Clin Oncol* 2003;21(12):2254-9.
3. Anderson WF, Schairer C, Chen BE, Hance KW, Levine PH. Epidemiology of inflammatory breast cancer (IBC). *Breast Dis* 2005;22:9-23.
4. Hance KW, Anderson WF, Devesa SS, Young HA, Levine PH. Trends in inflammatory breast carcinoma incidence and survival: the surveillance, epidemiology, and end results program at the National Cancer Institute. *J Natl Cancer Inst* 2005;97(13):966-75.
5. Chang S, Parker SL, Pham T, Buzdar AU, Hursting SD. Inflammatory breast carcinoma incidence and survival: the surveillance, epidemiology, and end results program of the National Cancer Institute, 1975-1992. *Cancer* 1998;82(12):2366-72.
6. Schmoll H-J, F.L. Greene, D.L. Page, I.D. Fleming et al. (eds). *AJCC Cancer Staging Manual*, 6th edition. *Annals of Oncology* 2003;14(2):345-46.
7. Dawood S, Cristofanilli M. Inflammatory breast cancer: what progress have we made? *Oncology (Williston Park, NY)* 2011;25(3):264-70, 73.
8. Bozzetti F, Saccozzi R, De Lena M, Salvadori B. Inflammatory cancer of the breast: analysis of 114 cases. *Journal of surgical oncology* 1981;18(4):355-61.
9. Zucali R, Uslenghi C, Kenda R, Bonadonna G. Natural history and survival of inoperable breast cancer treated with radiotherapy and radiotherapy followed by radical mastectomy. *Cancer* 1976;37(3):1422-31.
10. Baldini E, Gardin G, Evagelista G, Prochilo T, Collecchi P, Lionetto R. Long-term results of combined-modality therapy for inflammatory breast carcinoma. *Clinical breast cancer* 2004;5(5):358-63.

11. Bonnier P, Charpin C, Lejeune C, Romain S, Tubiana N, Beedassy B, et al. Inflammatory carcinomas of the breast: a clinical, pathological, or a clinical and pathological definition? *International journal of cancer Journal international du cancer* 1995;62(4):382-5.
12. Robertson FM, Bondy M, Yang W, Yamauchi H, Wiggins S, Kamrudin S, et al. Inflammatory breast cancer: the disease, the biology, the treatment. *CA Cancer J Clin* 2010;60(6):351-75.
13. Yamauchi H, Cristofanilli M, Nakamura S, Hortobagyi GN, Ueno NT. Molecular targets for treatment of inflammatory breast cancer. *Nat Rev Clin Oncol* 2009.
14. Giordano SH, Hortobagyi GN. Inflammatory breast cancer: clinical progress and the main problems that must be addressed. *Breast Cancer Res* 2003;5(6):284-8.
15. Walshe JM, Swain SM. Clinical aspects of inflammatory breast cancer. *Breast Dis* 2005;22:35-44.
16. Labidi SI, Mrad K, Mezlini A, Ouarda MA, Combes JD, Ben Abdallah M, et al. Inflammatory breast cancer in Tunisia in the era of multimodality therapy. *Annals of oncology : official journal of the European Society for Medical Oncology / ESMO* 2008;19(3):473-80.
17. Wingo PA, Jamison PM, Young JL, Gargiullo P. Population-based statistics for women diagnosed with inflammatory breast cancer (United States). *Cancer causes & control : CCC* 2004;15(3):321-8.
18. Levine PH, Veneroso C. The epidemiology of inflammatory breast cancer. *Semin Oncol* 2008;35(1):11-6.
19. Chang S, Buzdar AU, Hursting SD. Inflammatory breast cancer and body mass index. *J Clin Oncol* 1998;16(12):3731-5.
20. Comprehensive molecular portraits of human breast tumours. *Nature* 2012;490(7418):61-70.
21. Van Laere SJ, Ueno NT, Finetti P, Vermeulen P, Lucci A, Robertson FM, et al. Uncovering the molecular secrets of inflammatory breast cancer biology: an integrated analysis of three distinct affymetrix gene expression datasets. *Clinical*

cancer research : an official journal of the American Association for Cancer Research 2013;19(17):4685-96.

22. Ross JS, Ali SM, Wang K, Khaira D, Palma NA, Chmielecki J, et al. Comprehensive genomic profiling of inflammatory breast cancer cases reveals a high frequency of clinically relevant genomic alterations. *Breast cancer research and treatment* 2015;154(1):155-62.
23. Rimawi MF, Shetty PB, Weiss HL, Schiff R, Osborne CK, Chamness GC, et al. Epidermal growth factor receptor expression in breast cancer association with biologic phenotype and clinical outcomes. *Cancer* 2010;116(5):1234-42.
24. Cabioglu N, Gong Y, Islam R, Broglio KR, Sneige N, Sahin A, et al. Expression of growth factor and chemokine receptors: new insights in the biology of inflammatory breast cancer. *Annals of oncology : official journal of the European Society for Medical Oncology / ESMO* 2007;18(6):1021-9.
25. Prost S, Le MG, Douc-Rasy S, Ahomadegbe JC, Spielmann M, Guerin M, et al. Association of c-erbB2-gene amplification with poor prognosis in non-inflammatory breast carcinomas but not in carcinomas of the inflammatory type. *International journal of cancer Journal international du cancer* 1994;58(6):763-8.
26. Van Laere SJ, Van der Auwera I, Van den Eynden GG, van Dam P, Van Marck EA, Vermeulen PB, et al. NF-kappaB activation in inflammatory breast cancer is associated with oestrogen receptor downregulation, secondary to EGFR and/or ErbB2 overexpression and MAPK hyperactivation. *British journal of cancer* 2007;97(5):659-69.
27. Zell JA, Tsang WY, Taylor TH, Mehta RS, Anton-Culver H. Prognostic impact of human epidermal growth factor-like receptor 2 and hormone receptor status in inflammatory breast cancer (IBC): analysis of 2,014 IBC patient cases from the California Cancer Registry. *Breast Cancer Res* 2009;11(1):R9.
28. Harvey HA, Lipton A, Lawrence BV, White DS, Wells SA, Blumenschein G, et al. Estrogen receptor status in inflammatory breast carcinoma. *Journal of surgical oncology* 1982;21(1):42-4.
29. McCarthy NJ, Yang X, Linnoila IR, Merino MJ, Hewitt SM, Parr AL, et al. Microvessel density, expression of estrogen receptor alpha, MIB-1, p53, and c-

- erbB-2 in inflammatory breast cancer. *Clinical cancer research : an official journal of the American Association for Cancer Research* 2002;8(12):3857-62.
30. Boyle P. Triple-negative breast cancer: epidemiological considerations and recommendations. *Annals of oncology : official journal of the European Society for Medical Oncology / ESMO* 2012;23 Suppl 6:vi7-12.
  31. Li J, Gonzalez-Angulo AM, Allen PK, Yu TK, Woodward WA, Ueno NT, et al. Triple-negative subtype predicts poor overall survival and high locoregional relapse in inflammatory breast cancer. *The oncologist* 2011;16(12):1675-83.
  32. Masuda H, Baggerly KA, Wang Y, Iwamoto T, Brewer T, Pusztai L, et al. Comparison of molecular subtype distribution in triple-negative inflammatory and non-inflammatory breast cancers. *Breast Cancer Res* 2013;15(6):R112.
  33. Masuda H, Zhang D, Bartholomeusz C, Doihara H, Hortobagyi GN, Ueno NT. Role of epidermal growth factor receptor in breast cancer. *Breast cancer research and treatment* 2012;136(2):331-45.
  34. Lo HW, Hsu SC, Hung MC. EGFR signaling pathway in breast cancers: from traditional signal transduction to direct nuclear translocalization. *Breast cancer research and treatment* 2006;95(3):211-8.
  35. Yarden Y. The EGFR family and its ligands in human cancer. signalling mechanisms and therapeutic opportunities. *Eur J Cancer* 2001;37 Suppl 4:S3-8.
  36. Yarden Y. Biology of HER2 and its importance in breast cancer. *Oncology* 2001;61 Suppl 2:1-13.
  37. Bertucci F, Finetti P, Birnbaum D. Basal breast cancer: a complex and deadly molecular subtype. *Current molecular medicine* 2012;12(1):96-110.
  38. Ben Hamida A, Labidi IS, Mrad K, Charafe-Jauffret E, Ben Arab S, Esterni B, et al. Markers of subtypes in inflammatory breast cancer studied by immunohistochemistry: prominent expression of P-cadherin. *BMC cancer* 2008;8:28.
  39. Charafe-Jauffret E, Tarpin C, Bardou VJ, Bertucci F, Ginestier C, Braud AC, et al. Immunophenotypic analysis of inflammatory breast cancers: identification of an 'inflammatory signature'. *The Journal of pathology* 2004;202(3):265-73.

40. Nguyen DM, Sam K, Tsimelzon A, Li X, Wong H, Mohsin S, et al. Molecular heterogeneity of inflammatory breast cancer: a hyperproliferative phenotype. *Clinical cancer research : an official journal of the American Association for Cancer Research* 2006;12(17):5047-54.
41. Paradiso A, Tommasi S, Brandi M, Marzullo F, Simone G, Lorusso V, et al. Cell kinetics and hormonal receptor status in inflammatory breast carcinoma. Comparison with locally advanced disease. *Cancer* 1989;64(9):1922-7.
42. Gingras AC, Raught B, Sonenberg N. mTOR signaling to translation. *Current topics in microbiology and immunology* 2004;279:169-97.
43. Ramirez-Valle F, Braunstein S, Zavadil J, Formenti SC, Schneider RJ. eIF4GI links nutrient sensing by mTOR to cell proliferation and inhibition of autophagy. *The Journal of cell biology* 2008;181(2):293-307.
44. Jang SK, Krausslich HG, Nicklin MJ, Duke GM, Palmenberg AC, Wimmer E. A segment of the 5' nontranslated region of encephalomyocarditis virus RNA directs internal entry of ribosomes during in vitro translation. *Journal of virology* 1988;62(8):2636-43.
45. Pelletier J, Sonenberg N. Internal initiation of translation of eukaryotic mRNA directed by a sequence derived from poliovirus RNA. *Nature* 1988;334(6180):320-5.
46. Silvera D, Arju R, Darvishian F, Levine PH, Zolfaghari L, Goldberg J, et al. Essential role for eIF4GI overexpression in the pathogenesis of inflammatory breast cancer. *Nature cell biology* 2009;11(7):903-8.
47. Colpaert CG, Vermeulen PB, Benoy I, Soubry A, van Roy F, van Beest P, et al. Inflammatory breast cancer shows angiogenesis with high endothelial proliferation rate and strong E-cadherin expression. *British journal of cancer* 2003;88(5):718-25.
48. Keirsebilck A, Bonne S, Staes K, van Hengel J, Nollet F, Reynolds A, et al. Molecular cloning of the human p120ctn catenin gene (CTNND1): expression of multiple alternatively spliced isoforms. *Genomics* 1998;50(2):129-46.

49. Bryant DM, Stow JL. The ins and outs of E-cadherin trafficking. *Trends in cell biology* 2004;14(8):427-34.
50. Xiao K, Oas RG, Chiasson CM, Kowalczyk AP. Role of p120-catenin in cadherin trafficking. *Biochimica et biophysica acta* 2007;1773(1):8-16.
51. Höckel M, Vaupel P. Tumor Hypoxia: Definitions and Current Clinical, Biologic, and Molecular Aspects. *Journal of the National Cancer Institute* 2001;93(4):266-76.
52. Silvera D, Schneider RJ. Inflammatory breast cancer cells are constitutively adapted to hypoxia. *Cell Cycle* 2009;8(19):3091-6.
53. Bieche I, Lerebours F, Tozlu S, Espie M, Marty M, Lidereau R. Molecular profiling of inflammatory breast cancer: identification of a poor-prognosis gene expression signature. *Clinical cancer research : an official journal of the American Association for Cancer Research* 2004;10(20):6789-95.
54. Braunstein S, Karpisheva K, Pola C, Goldberg J, Hochman T, Yee H, et al. A hypoxia-controlled cap-dependent to cap-independent translation switch in breast cancer. *Mol Cell* 2007;28(3):501-12.
55. McMahon G. VEGF receptor signaling in tumor angiogenesis. *The oncologist* 2000;5 Suppl 1:3-10.
56. Levine PH, Portera CC, Hoffman HJ, Yang SX, Takikita M, Duong QN, et al. Evaluation of lymphangiogenic factors, vascular endothelial growth factor D and E-cadherin in distinguishing inflammatory from locally advanced breast cancer. *Clinical breast cancer* 2012;12(4):232-9.
57. Sato Y. VEGFR1 for Lymphangiogenesis: An Alternative Signaling Pathway? *Arteriosclerosis, Thrombosis, and Vascular Biology* 2008;28(4):604-05.
58. Plate KH. From angiogenesis to lymphangiogenesis. *Nat Med* 2001;7(2):151-52.
59. Van der Auwera I, Van Laere SJ, Van den Eynden GG, Benoy I, van Dam P, Colpaert CG, et al. Increased angiogenesis and lymphangiogenesis in inflammatory versus noninflammatory breast cancer by real-time reverse transcriptase-PCR gene expression quantification. *Clinical cancer research : an*

official journal of the American Association for Cancer Research  
2004;10(23):7965-71.

60. Shirakawa K, Kobayashi H, Heike Y, Kawamoto S, Brechbiel MW, Kasumi F, et al. Hemodynamics in vasculogenic mimicry and angiogenesis of inflammatory breast cancer xenograft. *Cancer research* 2002;62(2):560-6.
61. Shirakawa K, Kobayashi H, Sobajima J, Hashimoto D, Shimizu A, Wakasugi H. Inflammatory breast cancer: vasculogenic mimicry and its hemodynamics of an inflammatory breast cancer xenograft model. *Breast Cancer Res* 2003;5(3):136-9.
62. Bertucci F, Finetti P, Rougemont J, Charafe-Jauffret E, Nasser V, Loriod B, et al. Gene expression profiling for molecular characterization of inflammatory breast cancer and prediction of response to chemotherapy. *Cancer research* 2004;64(23):8558-65.
63. Van Laere S, Van der Auwera I, Van den Eynden GG, Fox SB, Bianchi F, Harris AL, et al. Distinct molecular signature of inflammatory breast cancer by cDNA microarray analysis. *Breast cancer research and treatment* 2005;93(3):237-46.
64. Van Laere SJ, Van der Auwera I, Van den Eynden GG, Elst HJ, Weyler J, Harris AL, et al. Nuclear factor-kappaB signature of inflammatory breast cancer by cDNA microarray validated by quantitative real-time reverse transcription-PCR, immunohistochemistry, and nuclear factor-kappaB DNA-binding. *Clinical cancer research : an official journal of the American Association for Cancer Research* 2006;12(11 Pt 1):3249-56.
65. Lerebours F, Vacher S, Andrieu C, Espie M, Marty M, Lidereau R, et al. NF-kappa B genes have a major role in inflammatory breast cancer. *BMC cancer* 2008;8:41.
66. Wu CJ, Qian X, O'Rourke DM. Sustained mitogen-activated protein kinase activation is induced by transforming erbB receptor complexes. *DNA and cell biology* 1999;18(10):731-41.
67. Dhillon AS, Hagan S, Rath O, Kolch W. MAP kinase signalling pathways in cancer. *Oncogene* 2007;26(22):3279-90.

68. Santarpia L, Lippman SM, El-Naggar AK. Targeting the MAPK-RAS-RAF signaling pathway in cancer therapy. *Expert opinion on therapeutic targets* 2012;16(1):103-19.
69. van Golen KL, Bao LW, Pan Q, Miller FR, Wu ZF, Merajver SD. Mitogen activated protein kinase pathway is involved in RhoC GTPase induced motility, invasion and angiogenesis in inflammatory breast cancer. *Clinical & experimental metastasis* 2002;19(4):301-11.
70. Clark EA, Golub TR, Lander ES, Hynes RO. Genomic analysis of metastasis reveals an essential role for RhoC. *Nature* 2000;406(6795):532-5.
71. Ridley AJ. The GTP-binding protein Rho. *The international journal of biochemistry & cell biology* 1997;29(11):1225-9.
72. van Golen KL, Davies S, Wu ZF, Wang Y, Bucana CD, Root H, et al. A novel putative low-affinity insulin-like growth factor-binding protein, LIBC (lost in inflammatory breast cancer), and RhoC GTPase correlate with the inflammatory breast cancer phenotype. *Clinical cancer research : an official journal of the American Association for Cancer Research* 1999;5(9):2511-9.
73. van Golen KL, Wu ZF, Qiao XT, Bao LW, Merajver SD. RhoC GTPase, a novel transforming oncogene for human mammary epithelial cells that partially recapitulates the inflammatory breast cancer phenotype. *Cancer research* 2000;60(20):5832-8.
74. Caponigro F, Casale M, Bryce J. Farnesyl transferase inhibitors in clinical development. *Expert opinion on investigational drugs* 2003;12(6):943-54.
75. van Golen KL, Bao L, DiVito MM, Wu Z, Prendergast GC, Merajver SD. Reversion of RhoC GTPase-induced inflammatory breast cancer phenotype by treatment with a farnesyl transferase inhibitor. *Molecular cancer therapeutics* 2002;1(8):575-83.
76. Creighton CJ, Hilger AM, Murthy S, Rae JM, Chinnaiyan AM, El-Ashry D. Activation of mitogen-activated protein kinase in estrogen receptor alpha-positive breast cancer cells in vitro induces an in vivo molecular phenotype of estrogen receptor alpha-negative human breast tumors. *Cancer research* 2006;66(7):3903-11.

77. Biswas DK, Cruz AP, Gansberger E, Pardee AB. Epidermal growth factor-induced nuclear factor kappa B activation: A major pathway of cell-cycle progression in estrogen-receptor negative breast cancer cells. *Proceedings of the National Academy of Sciences of the United States of America* 2000;97(15):8542-7.
78. Biswas DK, Dai SC, Cruz A, Weiser B, Graner E, Pardee AB. The nuclear factor kappa B (NF-kappa B): a potential therapeutic target for estrogen receptor negative breast cancers. *Proceedings of the National Academy of Sciences of the United States of America* 2001;98(18):10386-91.
79. Hanahan D, Weinberg RA. The hallmarks of cancer. *Cell* 2000;100(1):57-70.
80. Cristofanilli M, Buzdar AU, Hortobagyi GN. Update on the management of inflammatory breast cancer. *The oncologist* 2003;8(2):141-8.
81. Sinclair S, Swain SM. Primary systemic chemotherapy for inflammatory breast cancer. *Cancer* 2010;116(11 Suppl):2821-8.
82. Rowinsky EK. The development and clinical utility of the taxane class of antimicrotubule chemotherapy agents. *Annual review of medicine* 1997;48:353-74.
83. Horwitz SB. Taxol (paclitaxel): mechanisms of action. *Annals of oncology : official journal of the European Society for Medical Oncology / ESMO* 1994;5 Suppl 6:S3-6.
84. Sparano JA. Taxanes for breast cancer: an evidence-based review of randomized phase II and phase III trials. *Clinical breast cancer* 2000;1(1):32-40; discussion 41-2.
85. Pal SK, Sonpavde G. Cabazitaxel for the therapy of metastatic castration-resistant prostate cancer in the aftermath of the CHAARTED trial. *BJU international* 2015;116(6):839-40.
86. Pommier Y, Leo E, Zhang H, Marchand C. DNA topoisomerases and their poisoning by anticancer and antibacterial drugs. *Chemistry & biology* 2010;17(5):421-33.

87. Schott B, Robert J. Comparative cytotoxicity, DNA synthesis inhibition and drug incorporation of eight anthracyclines in a model of doxorubicin-sensitive and -resistant rat glioblastoma cells. *Biochemical pharmacology* 1989;38(1):167-72.
88. Gouspillou G, Scheede-Bergdahl C, Spendiff S, Vuda M, Meehan B, Mlynarski H, et al. Anthracycline-containing chemotherapy causes long-term impairment of mitochondrial respiration and increased reactive oxygen species release in skeletal muscle. *Scientific reports* 2015;5:8717.
89. Pang B, Qiao X, Janssen L, Velds A, Groothuis T, Kerkhoven R, et al. Drug-induced histone eviction from open chromatin contributes to the chemotherapeutic effects of doxorubicin. *Nature communications* 2013;4:1908.
90. Minotti G, Menna P, Salvatorelli E, Cairo G, Gianni L. Anthracyclines: molecular advances and pharmacologic developments in antitumor activity and cardiotoxicity. *Pharmacological reviews* 2004;56(2):185-229.
91. Yang CH, Cristofanilli M. Systemic treatments for inflammatory breast cancer. *Breast Dis* 2005;22:55-65.
92. Kell MR, Morrow M. Surgical aspects of inflammatory breast cancer. *Breast Dis* 2005;22:67-73.
93. Curcio LD, Rupp E, Williams WL, Chu DZ, Clarke K, Odom-Maryon T, et al. Beyond palliative mastectomy in inflammatory breast cancer--a reassessment of margin status. *Annals of surgical oncology* 1999;6(3):249-54.
94. Dushkin H, Cristofanilli M. Inflammatory breast cancer. *Journal of the National Comprehensive Cancer Network : JNCCN* 2011;9(2):233-40; quiz 41.
95. Liao Z, Strom EA, Buzdar AU, Singletary SE, Hunt K, Allen PK, et al. Locoregional irradiation for inflammatory breast cancer: effectiveness of dose escalation in decreasing recurrence. *Int J Radiat Oncol Biol Phys* 2000;47(5):1191-200.
96. Hudis CA. Trastuzumab--mechanism of action and use in clinical practice. *The New England journal of medicine* 2007;357(1):39-51.

97. Cho HS, Mason K, Ramyar KX, Stanley AM, Gabelli SB, Denney DW, Jr., et al. Structure of the extracellular region of HER2 alone and in complex with the Herceptin Fab. *Nature* 2003;421(6924):756-60.
98. Sliwkowski MX, Lofgren JA, Lewis GD, Hotaling TE, Fendly BM, Fox JA. Nonclinical studies addressing the mechanism of action of trastuzumab (Herceptin). *Semin Oncol* 1999;26(4 Suppl 12):60-70.
99. Albanell J, Codony J, Rovira A, Mellado B, Gascon P. Mechanism of action of anti-HER2 monoclonal antibodies: scientific update on trastuzumab and 2C4. *Advances in experimental medicine and biology* 2003;532:253-68.
100. Le XF, Pruefer F, Bast RC, Jr. HER2-targeting antibodies modulate the cyclin-dependent kinase inhibitor p27Kip1 via multiple signaling pathways. *Cell Cycle* 2005;4(1):87-95.
101. Clynes RA, Towers TL, Presta LG, Ravetch JV. Inhibitory Fc receptors modulate in vivo cytotoxicity against tumor targets. *Nat Med* 2000;6(4):443-6.
102. Gianni L, Eiermann W, Semiglazov V, Manikhas A, Lluch A, Tjulandin S, et al. Neoadjuvant chemotherapy with trastuzumab followed by adjuvant trastuzumab versus neoadjuvant chemotherapy alone, in patients with HER2-positive locally advanced breast cancer (the NOAH trial): a randomised controlled superiority trial with a parallel HER2-negative cohort. *Lancet* 2010;375(9712):377-84.
103. Esteva FJ, Valero V, Booser D, Guerra LT, Murray JL, Puztai L, et al. Phase II study of weekly docetaxel and trastuzumab for patients with HER-2-overexpressing metastatic breast cancer. *J Clin Oncol* 2002;20(7):1800-8.
104. Slamon DJ, Leyland-Jones B, Shak S, Fuchs H, Paton V, Bajamonde A, et al. Use of chemotherapy plus a monoclonal antibody against HER2 for metastatic breast cancer that overexpresses HER2. *The New England journal of medicine* 2001;344(11):783-92.
105. LoRusso PM, Weiss D, Guardino E, Girish S, Sliwkowski MX. Trastuzumab emtansine: a unique antibody-drug conjugate in development for human epidermal growth factor receptor 2-positive cancer. *Clinical cancer research : an official journal of the American Association for Cancer Research* 2011;17(20):6437-47.

106. Verma S, Miles D, Gianni L, Krop IE, Welslau M, Baselga J, et al. Trastuzumab emtansine for HER2-positive advanced breast cancer. *The New England journal of medicine* 2012;367(19):1783-91.
107. Burris HA, 3rd. Dual kinase inhibition in the treatment of breast cancer: initial experience with the EGFR/ErbB-2 inhibitor lapatinib. *The oncologist* 2004;9 Suppl 3:10-5.
108. Nelson MH, Dolder CR. Lapatinib: a novel dual tyrosine kinase inhibitor with activity in solid tumors. *The Annals of pharmacotherapy* 2006;40(2):261-9.
109. Ma C, Zuo W, Wang X, Wei L, Guo Q, Song X. Lapatinib inhibits the activation of NF-kappaB through reducing phosphorylation of IkappaB-alpha in breast cancer cells. *Oncology reports* 2013;29(2):812-8.
110. Xia W, Bisi J, Strum J, Liu L, Carrick K, Graham KM, et al. Regulation of survivin by ErbB2 signaling: therapeutic implications for ErbB2-overexpressing breast cancers. *Cancer research* 2006;66(3):1640-7.
111. Aird KM, Allensworth JL, Batinic-Haberle I, Lysterly HK, Dewhirst MW, Devi GR. ErbB1/2 tyrosine kinase inhibitor mediates oxidative stress-induced apoptosis in inflammatory breast cancer cells. *Breast cancer research and treatment* 2012;132(1):109-19.
112. Dai CL, Tiwari AK, Wu CP, Su XD, Wang SR, Liu DG, et al. Lapatinib (Tykerb, GW572016) reverses multidrug resistance in cancer cells by inhibiting the activity of ATP-binding cassette subfamily B member 1 and G member 2. *Cancer research* 2008;68(19):7905-14.
113. Polli JW, Humphreys JE, Harmon KA, Castellino S, O'Mara MJ, Olson KL, et al. The role of efflux and uptake transporters in [N-(3-chloro-4-[(3-fluorobenzyl)oxy]phenyl)-6-[5-((2-(methylsulfonyl)ethyl)amino)methyl]-2-furyl]-4-quinazolinamine (GW572016, lapatinib) disposition and drug interactions. *Drug Metab Dispos* 2008;36(4):695-701.
114. Johnston S, Trudeau M, Kaufman B, Boussen H, Blackwell K, LoRusso P, et al. Phase II study of predictive biomarker profiles for response targeting human epidermal growth factor receptor 2 (HER-2) in advanced inflammatory breast cancer with lapatinib monotherapy. *J Clin Oncol* 2008;26(7):1066-72.

115. Blackwell KL, Burstein HJ, Storniolo AM, Rugo HS, Sledge G, Aktan G, et al. Overall survival benefit with lapatinib in combination with trastuzumab for patients with human epidermal growth factor receptor 2-positive metastatic breast cancer: final results from the EGF104900 Study. *J Clin Oncol* 2012;30(21):2585-92.
116. Bousсен H, Cristofanilli M, Zaks T, DeSilvio M, Salazar V, Spector N. Phase II study to evaluate the efficacy and safety of neoadjuvant lapatinib plus paclitaxel in patients with inflammatory breast cancer. *J Clin Oncol* 2010;28(20):3248-55.
117. Geyer CE, Forster J, Lindquist D, Chan S, Romieu CG, Pienkowski T, et al. Lapatinib plus capecitabine for HER2-positive advanced breast cancer. *The New England journal of medicine* 2006;355(26):2733-43.
118. Johnston S, Pippen J, Jr., Pivot X, Lichinitser M, Sadeghi S, Dieras V, et al. Lapatinib combined with letrozole versus letrozole and placebo as first-line therapy for postmenopausal hormone receptor-positive metastatic breast cancer. *J Clin Oncol* 2009;27(33):5538-46.
119. Chen FL, Xia W, Spector NL. Acquired resistance to small molecule ErbB2 tyrosine kinase inhibitors. *Clinical cancer research : an official journal of the American Association for Cancer Research* 2008;14(21):6730-4.
120. Shih T, Lindley C. Bevacizumab: an angiogenesis inhibitor for the treatment of solid malignancies. *Clinical therapeutics* 2006;28(11):1779-802.
121. Wedam SB, Low JA, Yang SX, Chow CK, Choyke P, Danforth D, et al. Antiangiogenic and antitumor effects of bevacizumab in patients with inflammatory and locally advanced breast cancer. *J Clin Oncol* 2006;24(5):769-77.
122. Hamberg P, Verweij J, Sleijfer S. (Pre-)clinical pharmacology and activity of pazopanib, a novel multikinase angiogenesis inhibitor. *The oncologist* 2010;15(6):539-47.
123. Pick AM, Nystrom KK. Pazopanib for the treatment of metastatic renal cell carcinoma. *Clinical therapeutics* 2012;34(3):511-20.
124. Verweij J, Sleijfer S. Pazopanib, a new therapy for metastatic soft tissue sarcoma. *Expert opinion on pharmacotherapy* 2013;14(7):929-35.

125. Mahner S, Woelber L, Mueller V, Witzel I, Prieske K, Grimm D, et al. Beyond Bevacizumab: An Outlook to New Anti-Angiogenics for the Treatment of Ovarian Cancer. *Frontiers in oncology* 2015;5:211.
126. Cristofanilli M, Johnston SR, Manikhas A, Gomez HL, Gladkov O, Shao Z, et al. A randomized phase II study of lapatinib + pazopanib versus lapatinib in patients with HER2+ inflammatory breast cancer. *Breast cancer research and treatment* 2013;137(2):471-82.
127. Overmoyer B, Fu P, Hoppel C, Radivoyevitch T, Shenk R, Persons M, et al. Inflammatory breast cancer as a model disease to study tumor angiogenesis: results of a phase IB trial of combination SU5416 and doxorubicin. *Clinical cancer research : an official journal of the American Association for Cancer Research* 2007;13(19):5862-8.
128. Wiseman C, Jessup JM, Smith TL, Hersh E, Bowen J, Blumenshein G. Inflammatory breast cancer treated with surgery, chemotherapy and allogeneic tumor cell/BCG immunotherapy. *Cancer* 1982;49(6):1266-71.
129. Crispen R. History of BCG and its substrains. *Progress in clinical and biological research* 1989;310:35-50.
130. Liu J, Tran V, Leung AS, Alexander DC, Zhu B. BCG vaccines: their mechanisms of attenuation and impact on safety and protective efficacy. *Human vaccines* 2009;5(2):70-8.
131. Freyne B, Marchant A, Curtis N. BCG-associated heterologous immunity, a historical perspective: experimental models and immunological mechanisms. *Transactions of the Royal Society of Tropical Medicine and Hygiene* 2015;109(1):46-51.
132. Wiseman CL. Inflammatory breast cancer: 10-year follow-up of a trial of surgery, chemotherapy, and allogeneic tumor cell/BCG immunotherapy. *Cancer investigation* 1995;13(3):267-71.
133. Pluzanska A, Stempczynska J, Wolska H, Szmigielski S, Jeljaszewicz J, Pulverer G. Beneficial response of local immunotherapy with *Propionibacterium granulosum* KP-45 in combined treatment of inflammatory breast carcinoma. *J Cancer Res Clin Oncol* 1988;114(4):432-37.

134. Eibl B, Schwaighofer H, Nachbaur D, Marth C, Gachter A, Knapp R, et al. Evidence for a graft-versus-tumor effect in a patient treated with marrow ablative chemotherapy and allogeneic bone marrow transplantation for breast cancer. *Blood* 1996;88(4):1501-8.
135. Aird KM, Ding X, Baras A, Wei J, Morse MA, Clay T, et al. Trastuzumab signaling in ErbB2-overexpressing inflammatory breast cancer correlates with X-linked inhibitor of apoptosis protein expression. *Molecular cancer therapeutics* 2008;7(1):38-47.
136. Seidel UJ, Schlegel P, Lang P. Natural killer cell mediated antibody-dependent cellular cytotoxicity in tumor immunotherapy with therapeutic antibodies. *Frontiers in immunology* 2013;4:76.
137. Dawood S, Merajver SD, Viens P, Vermeulen PB, Swain SM, Buchholz TA, et al. International expert panel on inflammatory breast cancer: consensus statement for standardized diagnosis and treatment. *Annals of Oncology* 2010.
138. Tomlinson JS, Alpaugh ML, Barsky SH. An intact overexpressed E-cadherin/alpha,beta-catenin axis characterizes the lymphovascular emboli of inflammatory breast carcinoma. *Cancer research* 2001;61(13):5231-41.
139. Sparano JA, Moulder S, Kazi A, Coppola D, Negassa A, Vahdat L, et al. Phase II trial of tipifarnib plus neoadjuvant doxorubicin-cyclophosphamide in patients with clinical stage IIB-IIIC breast cancer. *Clinical cancer research : an official journal of the American Association for Cancer Research* 2009;15(8):2942-8.
140. Schmid P, Kuhnhardt D, Kiewe P, Lehenbauer-Dehm S, Schippinger W, Greil R, et al. A phase I/II study of bortezomib and capecitabine in patients with metastatic breast cancer previously treated with taxanes and/or anthracyclines. *Annals of oncology : official journal of the European Society for Medical Oncology / ESMO* 2008;19(5):871-6.
141. Scaltriti M, Rojo F, Ocana A, Anido J, Guzman M, Cortes J, et al. Expression of p95HER2, a truncated form of the HER2 receptor, and response to anti-HER2 therapies in breast cancer. *J Natl Cancer Inst* 2007;99(8):628-38.
142. Nagy P, Friedlander E, Tanner M, Kapanen AI, Carraway KL, Isola J, et al. Decreased accessibility and lack of activation of ErbB2 in JIMT-1, a herceptin-

- resistant, MUC4-expressing breast cancer cell line. *Cancer research* 2005;65(2):473-82.
143. Lu Y, Zi X, Zhao Y, Mascarenhas D, Pollak M. Insulin-like growth factor-I receptor signaling and resistance to trastuzumab (Herceptin). *J Natl Cancer Inst* 2001;93(24):1852-7.
  144. Nagata Y, Lan KH, Zhou X, Tan M, Esteva FJ, Sahin AA, et al. PTEN activation contributes to tumor inhibition by trastuzumab, and loss of PTEN predicts trastuzumab resistance in patients. *Cancer cell* 2004;6(2):117-27.
  145. Nahta R, Takahashi T, Ueno NT, Hung MC, Esteva FJ. P27(kip1) down-regulation is associated with trastuzumab resistance in breast cancer cells. *Cancer research* 2004;64(11):3981-6.
  146. Zhang S, Huang WC, Li P, Guo H, Poh SB, Brady SW, et al. Combating trastuzumab resistance by targeting SRC, a common node downstream of multiple resistance pathways. *Nat Med* 2011;17(4):461-9.
  147. Berns K, Horlings HM, Hennessy BT, Madiredjo M, Hijmans EM, Beelen K, et al. A functional genetic approach identifies the PI3K pathway as a major determinant of trastuzumab resistance in breast cancer. *Cancer cell* 2007;12(4):395-402.
  148. Xia W, Husain I, Liu L, Bacus S, Saini S, Spohn J, et al. Lapatinib antitumor activity is not dependent upon phosphatase and tensin homologue deleted on chromosome 10 in ErbB2-overexpressing breast cancers. *Cancer research* 2007;67(3):1170-5.
  149. Xia W, Liu LH, Ho P, Spector NL. Truncated ErbB2 receptor (p95ErbB2) is regulated by heregulin through heterodimer formation with ErbB3 yet remains sensitive to the dual EGFR/ErbB2 kinase inhibitor GW572016. *Oncogene* 2004;23(3):646-53.
  150. Spector NL, Xia W, Burris H, 3rd, Hurwitz H, Dees EC, Dowlati A, et al. Study of the biologic effects of lapatinib, a reversible inhibitor of ErbB1 and ErbB2 tyrosine kinases, on tumor growth and survival pathways in patients with advanced malignancies. *J Clin Oncol* 2005;23(11):2502-12.

151. Hegde PS, Rusnak D, Bertiaux M, Alligood K, Strum J, Gagnon R, et al. Delineation of molecular mechanisms of sensitivity to lapatinib in breast cancer cell lines using global gene expression profiles. *Molecular cancer therapeutics* 2007;6(5):1629-40.
152. Garrett JT, Olivares MG, Rinehart C, Granja-Ingram ND, Sanchez V, Chakrabarty A, et al. Transcriptional and posttranslational up-regulation of HER3 (ErbB3) compensates for inhibition of the HER2 tyrosine kinase. *Proceedings of the National Academy of Sciences of the United States of America* 2011;108(12):5021-6.
153. Xia W, Bacus S, Husain I, Liu L, Zhao S, Liu Z, et al. Resistance to ErbB2 tyrosine kinase inhibitors in breast cancer is mediated by calcium-dependent activation of RelA. *Molecular cancer therapeutics* 2010;9(2):292-9.
154. Bailey ST, Miron PL, Choi YJ, Kochupurakkal B, Maulik G, Rodig SJ, et al. NF-kappaB activation-induced anti-apoptosis renders HER2-positive cells drug resistant and accelerates tumor growth. *Molecular cancer research : MCR* 2014;12(3):408-20.
155. Martin AP, Miller A, Emad L, Rahmani M, Walker T, Mitchell C, et al. Lapatinib resistance in HCT116 cells is mediated by elevated MCL-1 expression and decreased BAK activation and not by ERBB receptor kinase mutation. *Molecular pharmacology* 2008;74(3):807-22.
156. Aird KM, Ghanayem RB, Peplinski S, Lyerly HK, Devi GR. X-linked inhibitor of apoptosis protein inhibits apoptosis in inflammatory breast cancer cells with acquired resistance to an ErbB1/2 tyrosine kinase inhibitor. *Molecular cancer therapeutics* 2010;9(5):1432-42.
157. Elmore S. Apoptosis: a review of programmed cell death. *Toxicologic pathology* 2007;35(4):495-516.
158. Kerr JF, Wyllie AH, Currie AR. Apoptosis: a basic biological phenomenon with wide-ranging implications in tissue kinetics. *British journal of cancer* 1972;26(4):239-57.
159. Cohen GM. Caspases: the executioners of apoptosis. *The Biochemical journal* 1997;326 ( Pt 1):1-16.

160. Joza N, Susin SA, Daugas E, Stanford WL, Cho SK, Li CY, et al. Essential role of the mitochondrial apoptosis-inducing factor in programmed cell death. *Nature* 2001;410(6828):549-54.
161. Ashkenazi A, Dixit VM. Death receptors: signaling and modulation. *Science* 1998;281(5381):1305-8.
162. Locksley RM, Killeen N, Lenardo MJ. The TNF and TNF receptor superfamilies: integrating mammalian biology. *Cell* 2001;104(4):487-501.
163. Hsu H, Xiong J, Goeddel DV. The TNF receptor 1-associated protein TRADD signals cell death and NF-kappa B activation. *Cell* 1995;81(4):495-504.
164. Wajant H. The Fas signaling pathway: more than a paradigm. *Science* 2002;296(5573):1635-6.
165. Kischkel FC, Hellbardt S, Behrmann I, Germer M, Pawlita M, Krammer PH, et al. Cytotoxicity-dependent APO-1 (Fas/CD95)-associated proteins form a death-inducing signaling complex (DISC) with the receptor. *The EMBO journal* 1995;14(22):5579-88.
166. Ozoren N, El-Deiry WS. Defining characteristics of Types I and II apoptotic cells in response to TRAIL. *Neoplasia* 2002;4(6):551-7.
167. Decaudin D, Marzo I, Brenner C, Kroemer G. Mitochondria in chemotherapy-induced apoptosis: a prospective novel target of cancer therapy (review). *International journal of oncology* 1998;12(1):141-52.
168. Green DR, Kroemer G. The pathophysiology of mitochondrial cell death. *Science* 2004;305(5684):626-9.
169. Saelens X, Festjens N, Vande Walle L, van Gurp M, van Loo G, Vandenabeele P. Toxic proteins released from mitochondria in cell death. *Oncogene* 2004;23(16):2861-74.
170. Cain K, Bratton SB, Langlais C, Walker G, Brown DG, Sun XM, et al. Apaf-1 oligomerizes into biologically active approximately 700-kDa and inactive approximately 1.4-MDa apoptosome complexes. *The Journal of biological chemistry* 2000;275(9):6067-70.

171. Chinnaiyan AM. The apoptosome: heart and soul of the cell death machine. *Neoplasia* 1999;1(1):5-15.
172. Hill MM, Adrain C, Duriez PJ, Creagh EM, Martin SJ. Analysis of the composition, assembly kinetics and activity of native Apaf-1 apoptosomes. *The EMBO journal* 2004;23(10):2134-45.
173. Reed JC, Zha H, Aime-Sempe C, Takayama S, Wang HG. Structure-function analysis of Bcl-2 family proteins. Regulators of programmed cell death. *Advances in experimental medicine and biology* 1996;406:99-112.
174. Cory S, Adams JM. The Bcl2 family: regulators of the cellular life-or-death switch. *Nature reviews Cancer* 2002;2(9):647-56.
175. Birnbaum MJ, Clem RJ, Miller LK. An apoptosis-inhibiting gene from a nuclear polyhedrosis virus encoding a polypeptide with Cys/His sequence motifs. *Journal of virology* 1994;68(4):2521-8.
176. Crook NE, Clem RJ, Miller LK. An apoptosis-inhibiting baculovirus gene with a zinc finger-like motif. *Journal of virology* 1993;67(4):2168-74.
177. Yang Y, Fang S, Jensen JP, Weissman AM, Ashwell JD. Ubiquitin protein ligase activity of IAPs and their degradation in proteasomes in response to apoptotic stimuli. *Science* 2000;288(5467):874-7.
178. Vaux DL, Silke J. IAPs, RINGs and ubiquitylation. *Nature reviews Molecular cell biology* 2005;6(4):287-97.
179. Deveraux QL, Roy N, Stennicke HR, Van Arsdale T, Zhou Q, Srinivasula SM, et al. IAPs block apoptotic events induced by caspase-8 and cytochrome c by direct inhibition of distinct caspases. *The EMBO journal* 1998;17(8):2215-23.
180. Eckelman BP, Salvesen GS, Scott FL. Human inhibitor of apoptosis proteins: why XIAP is the black sheep of the family. *EMBO reports* 2006;7(10):988-94.
181. Huang H, Joazeiro CA, Bonfoco E, Kamada S, Levrson JD, Hunter T. The inhibitor of apoptosis, cIAP2, functions as a ubiquitin-protein ligase and promotes in vitro monoubiquitination of caspases 3 and 7. *The Journal of biological chemistry* 2000;275(35):26661-4.

182. Suzuki Y, Nakabayashi Y, Takahashi R. Ubiquitin-protein ligase activity of X-linked inhibitor of apoptosis protein promotes proteasomal degradation of caspase-3 and enhances its anti-apoptotic effect in Fas-induced cell death. *Proceedings of the National Academy of Sciences of the United States of America* 2001;98(15):8662-7.
183. Feltham R, Khan N, Silke J. IAPs and ubiquitylation. *IUBMB life* 2012;64(5):411-8.
184. Muschen M, Rajewsky K, Kronke M, Kuppers R. The origin of CD95-gene mutations in B-cell lymphoma. *Trends in immunology* 2002;23(2):75-80.
185. Bennett MW, O'Connell J, O'Sullivan GC, Brady C, Roche D, Collins JK, et al. The Fas counterattack in vivo: apoptotic depletion of tumor-infiltrating lymphocytes associated with Fas ligand expression by human esophageal carcinoma. *Journal of immunology* 1998;160(11):5669-75.
186. O'Connell J, O'Sullivan GC, Collins JK, Shanahan F. The Fas counterattack: Fas-mediated T cell killing by colon cancer cells expressing Fas ligand. *The Journal of experimental medicine* 1996;184(3):1075-82.
187. Ozoren N, Fisher MJ, Kim K, Liu CX, Genin A, Shifman Y, et al. Homozygous deletion of the death receptor DR4 gene in a nasopharyngeal cancer cell line is associated with TRAIL resistance. *International journal of oncology* 2000;16(5):917-25.
188. Shin MS, Kim HS, Lee SH, Park WS, Kim SY, Park JY, et al. Mutations of tumor necrosis factor-related apoptosis-inducing ligand receptor 1 (TRAIL-R1) and receptor 2 (TRAIL-R2) genes in metastatic breast cancers. *Cancer research* 2001;61(13):4942-6.
189. Tourneur L, Buzyn A, Chiocchia G. FADD adaptor in cancer. *Medical immunology (London, England)* 2005;4(1):1.
190. Zhang X, Jin TG, Yang H, DeWolf WC, Khosravi-Far R, Olumi AF. Persistent c-FLIP(L) expression is necessary and sufficient to maintain resistance to tumor necrosis factor-related apoptosis-inducing ligand-mediated apoptosis in prostate cancer. *Cancer research* 2004;64(19):7086-91.
191. Tourneur L, Delluc S, Levy V, Valensi F, Radford-Weiss I, Legrand O, et al. Absence or low expression of fas-associated protein with death domain in acute

- myeloid leukemia cells predicts resistance to chemotherapy and poor outcome. *Cancer research* 2004;64(21):8101-8.
192. Korkolopoulou P, Saetta AA, Levidou G, Gigelou F, Lazaris A, Thymara I, et al. c-FLIP expression in colorectal carcinomas: association with Fas/FasL expression and prognostic implications. *Histopathology* 2007;51(2):150-6.
  193. Fulda S, Meyer E, Debatin KM. Metabolic inhibitors sensitize for CD95 (APO-1/Fas)-induced apoptosis by down-regulating Fas-associated death domain-like interleukin 1-converting enzyme inhibitory protein expression. *Cancer research* 2000;60(14):3947-56.
  194. Soengas MS, Capodici P, Polsky D, Mora J, Esteller M, Opitz-Araya X, et al. Inactivation of the apoptosis effector Apaf-1 in malignant melanoma. *Nature* 2001;409(6817):207-11.
  195. Sun Y, Orrenius S, Pervaiz S, Fadeel B. Plasma membrane sequestration of apoptotic protease-activating factor-1 in human B-lymphoma cells: a novel mechanism of chemoresistance. *Blood* 2005;105(10):4070-7.
  196. Hajra KM, Liu JR. Apoptosome dysfunction in human cancer. *Apoptosis : an international journal on programmed cell death* 2004;9(6):691-704.
  197. Hinds MG, Day CL. Regulation of apoptosis: uncovering the binding determinants. *Current opinion in structural biology* 2005;15(6):690-9.
  198. Rampino N, Yamamoto H, Ionov Y, Li Y, Sawai H, Reed JC, et al. Somatic frameshift mutations in the BAX gene in colon cancers of the microsatellite mutator phenotype. *Science* 1997;275(5302):967-9.
  199. Meijerink JP, Smetsers TF, Sloetjes AW, Linders EH, Mensink EJ. Bax mutations in cell lines derived from hematological malignancies. *Leukemia* 1995;9(11):1828-32.
  200. Yamamoto H, Sawai H, Perucho M. Frameshift somatic mutations in gastrointestinal cancer of the microsatellite mutator phenotype. *Cancer research* 1997;57(19):4420-6.

201. Krajewska M, Moss SF, Krajewski S, Song K, Holt PR, Reed JC. Elevated expression of Bcl-X and reduced Bak in primary colorectal adenocarcinomas. *Cancer research* 1996;56(10):2422-7.
202. Zong WX, Lindsten T, Ross AJ, MacGregor GR, Thompson CB. BH3-only proteins that bind pro-survival Bcl-2 family members fail to induce apoptosis in the absence of Bax and Bak. *Genes & development* 2001;15(12):1481-6.
203. Shivapurkar N, Reddy J, Matta H, Sathyanarayana UG, Huang CX, Toyooka S, et al. Loss of expression of death-inducing signaling complex (DISC) components in lung cancer cell lines and the influence of MYC amplification. *Oncogene* 2002;21(55):8510-4.
204. Teitz T, Wei T, Valentine MB, Vanin EF, Grenet J, Valentine VA, et al. Caspase 8 is deleted or silenced preferentially in childhood neuroblastomas with amplification of MYCN. *Nat Med* 2000;6(5):529-35.
205. Zuzak TJ, Steinhoff DF, Sutton LN, Phillips PC, Eggert A, Grotzer MA. Loss of caspase-8 mRNA expression is common in childhood primitive neuroectodermal brain tumour/medulloblastoma. *Eur J Cancer* 2002;38(1):83-91.
206. Fulda S, Meyer E, Friesen C, Susin SA, Kroemer G, Debatin KM. Cell type specific involvement of death receptor and mitochondrial pathways in drug-induced apoptosis. *Oncogene* 2001;20(9):1063-75.
207. Krueger A, Baumann S, Krammer PH, Kirchhoff S. FLICE-inhibitory proteins: regulators of death receptor-mediated apoptosis. *Molecular and cellular biology* 2001;21(24):8247-54.
208. Fulda S, Debatin KM. IFN $\gamma$  sensitizes for apoptosis by upregulating caspase-8 expression through the Stat1 pathway. *Oncogene* 2002;21(15):2295-308.
209. Kagawa S, Gu J, Honda T, McDonnell TJ, Swisher SG, Roth JA, et al. Deficiency of caspase-3 in MCF7 cells blocks Bax-mediated nuclear fragmentation but not cell death. *Clinical cancer research : an official journal of the American Association for Cancer Research* 2001;7(5):1474-80.
210. Reed JC. Bcl-2 family proteins: regulators of apoptosis and chemoresistance in hematologic malignancies. *Seminars in hematology* 1997;34(4 Suppl 5):9-19.

211. Tsujimoto Y, Cossman J, Jaffe E, Croce CM. Involvement of the bcl-2 gene in human follicular lymphoma. *Science* 1985;228(4706):1440-3.
212. Hanada M, Delia D, Aiello A, Stadtmauer E, Reed JC. bcl-2 gene hypomethylation and high-level expression in B-cell chronic lymphocytic leukemia. *Blood* 1993;82(6):1820-8.
213. Verdoodt B, Neid M, Vogt M, Kuhn V, Liffers ST, Palisaar RJ, et al. MicroRNA-205, a novel regulator of the anti-apoptotic protein Bcl2, is downregulated in prostate cancer. *International journal of oncology* 2013;43(1):307-14.
214. Reed JC. Regulation of apoptosis by bcl-2 family proteins and its role in cancer and chemoresistance. *Current opinion in oncology* 1995;7(6):541-6.
215. Foreman KE, Wrone-Smith T, Boise LH, Thompson CB, Polverini PJ, Simonian PL, et al. Kaposi's sarcoma tumor cells preferentially express Bcl-xL. *The American journal of pathology* 1996;149(3):795-803.
216. Tu Y, Renner S, Xu F, Fleishman A, Taylor J, Weisz J, et al. BCL-X expression in multiple myeloma: possible indicator of chemoresistance. *Cancer research* 1998;58(2):256-62.
217. Castilla C, Congregado B, Chinchon D, Torrubia FJ, Japon MA, Saez C. Bcl-xL is overexpressed in hormone-resistant prostate cancer and promotes survival of LNCaP cells via interaction with proapoptotic Bak. *Endocrinology* 2006;147(10):4960-7.
218. Vucic D, Fairbrother WJ. The inhibitor of apoptosis proteins as therapeutic targets in cancer. *Clinical cancer research : an official journal of the American Association for Cancer Research* 2007;13(20):5995-6000.
219. Tamm I, Wang Y, Sausville E, Scudiero DA, Vigna N, Oltersdorf T, et al. IAP-family protein survivin inhibits caspase activity and apoptosis induced by Fas (CD95), Bax, caspases, and anticancer drugs. *Cancer research* 1998;58(23):5315-20.
220. Altieri DC. Validating survivin as a cancer therapeutic target. *Nature reviews Cancer* 2003;3(1):46-54.

221. Imoto I, Yang ZQ, Pimkhaokham A, Tsuda H, Shimada Y, Imamura M, et al. Identification of cIAP1 as a candidate target gene within an amplicon at 11q22 in esophageal squamous cell carcinomas. *Cancer research* 2001;61(18):6629-34.
222. Zender L, Spector MS, Xue W, Flemming P, Cordon-Cardo C, Silke J, et al. Identification and validation of oncogenes in liver cancer using an integrative oncogenomic approach. *Cell* 2006;125(7):1253-67.
223. Vega F, Medeiros LJ. Marginal-zone B-cell lymphoma of extranodal mucosa-associated lymphoid tissue type: molecular genetics provides new insights into pathogenesis. *Advances in anatomic pathology* 2001;8(6):313-26.
224. Zhou H, Du MQ, Dixit VM. Constitutive NF-kappaB activation by the t(11;18)(q21;q21) product in MALT lymphoma is linked to deregulated ubiquitin ligase activity. *Cancer cell* 2005;7(5):425-31.
225. Sanna MG, da Silva Correia J, Luo Y, Chuang B, Paulson LM, Nguyen B, et al. ILPIP, a novel anti-apoptotic protein that enhances XIAP-mediated activation of JNK1 and protection against apoptosis. *The Journal of biological chemistry* 2002;277(34):30454-62.
226. Iwamoto T, Bianchini G, Qi Y, Cristofanilli M, Lucci A, Woodward WA, et al. Different gene expressions are associated with the different molecular subtypes of inflammatory breast cancer. *Breast cancer research and treatment* 2011;125(3):785-95.
227. Bharti AC, Aggarwal BB. Nuclear factor-kappa B and cancer: its role in prevention and therapy. *Biochemical pharmacology* 2002;64(5-6):883-8.
228. Gyrd-Hansen M, Meier P. IAPs: from caspase inhibitors to modulators of NF-kappaB, inflammation and cancer. *Nature reviews Cancer* 2010;10(8):561-74.
229. Scott FL, Denault JB, Riedl SJ, Shin H, Renatus M, Salvesen GS. XIAP inhibits caspase-3 and -7 using two binding sites: evolutionarily conserved mechanism of IAPs. *The EMBO journal* 2005;24(3):645-55.
230. Srinivasula SM, Hegde R, Saleh A, Datta P, Shiozaki E, Chai J, et al. A conserved XIAP-interaction motif in caspase-9 and Smac/DIABLO regulates caspase activity and apoptosis. *Nature* 2001;410(6824):112-6.

231. Huang Y, Park YC, Rich RL, Segal D, Myszka DG, Wu H. Structural basis of caspase inhibition by XIAP: differential roles of the linker versus the BIR domain. *Cell* 2001;104(5):781-90.
232. Farahani R, Fong WG, Korneluk RG, MacKenzie AE. Genomic organization and primary characterization of miap-3: the murine homologue of human X-linked IAP. *Genomics* 1997;42(3):514-8.
233. Liston P, Roy N, Tamai K, Lefebvre C, Baird S, Cherton-Horvat G, et al. Suppression of apoptosis in mammalian cells by NAIP and a related family of IAP genes. *Nature* 1996;379(6563):349-53.
234. Cao Z, Li X, Li J, Luo W, Huang C, Chen J. X-linked inhibitor of apoptosis protein (XIAP) lacking RING domain localizes to the nuclear and promotes cancer cell anchorage-independent growth by targeting the E2F1/Cyclin E axis. *Oncotarget* 2014;5(16):7126-37.
235. Duckett CS, Nava VE, Gedrich RW, Clem RJ, Van Dongen JL, Gilfillan MC, et al. A conserved family of cellular genes related to the baculovirus iap gene and encoding apoptosis inhibitors. *The EMBO journal* 1996;15(11):2685-94.
236. Stehlik C, de Martin R, Kumabashiri I, Schmid JA, Binder BR, Lipp J. Nuclear factor (NF)-kappaB-regulated X-chromosome-linked iap gene expression protects endothelial cells from tumor necrosis factor alpha-induced apoptosis. *The Journal of experimental medicine* 1998;188(1):211-6.
237. Mohapatra S, Chu B, Wei S, Djeu J, Epling-Burnette PK, Loughran T, et al. Roscovitine inhibits STAT5 activity and induces apoptosis in the human leukemia virus type 1-transformed cell line MT-2. *Cancer research* 2003;63(23):8523-30.
238. Wang S, Patsis C, Koromilas AE. Stat1 stimulates cap-independent mRNA translation to inhibit cell proliferation and promote survival in response to antitumor drugs. *Proceedings of the National Academy of Sciences of the United States of America* 2015;112(17):E2149-55.
239. Lee TJ, Jung EM, Lee JT, Kim S, Park JW, Choi KS, et al. Mithramycin A sensitizes cancer cells to TRAIL-mediated apoptosis by down-regulation of XIAP gene promoter through Sp1 sites. *Molecular cancer therapeutics* 2006;5(11):2737-46.

240. Mohapatra S, Chu B, Zhao X, Pledger WJ. Accumulation of p53 and reductions in XIAP abundance promote the apoptosis of prostate cancer cells. *Cancer research* 2005;65(17):7717-23.
241. Sasaki H, Sheng Y, Kotsuji F, Tsang BK. Down-regulation of X-linked inhibitor of apoptosis protein induces apoptosis in chemoresistant human ovarian cancer cells. *Cancer research* 2000;60(20):5659-66.
242. Dixit V, Mak TW. NF-kappaB signaling. Many roads lead to madrid. *Cell* 2002;111(5):615-9.
243. Holcik M, Lefebvre C, Yeh C, Chow T, Korneluk RG. A new internal-ribosome-entry-site motif potentiates XIAP-mediated cytoprotection. *Nat Cell Biol* 1999;1(3):190-2.
244. Riley A, Jordan LE, Holcik M. Distinct 5' UTRs regulate XIAP expression under normal growth conditions and during cellular stress. *Nucleic acids research* 2010;38(14):4665-74.
245. Gu L, Zhu N, Zhang H, Durden DL, Feng Y, Zhou M. Regulation of XIAP translation and induction by MDM2 following irradiation. *Cancer cell* 2009;15(5):363-75.
246. Komar AA, Hatzoglou M. Cellular IRES-mediated translation: the war of ITAFs in pathophysiological states. *Cell Cycle* 2011;10(2):229-40.
247. Holcik M, Korneluk RG. Functional characterization of the X-linked inhibitor of apoptosis (XIAP) internal ribosome entry site element: role of La autoantigen in XIAP translation. *Molecular and cellular biology* 2000;20(13):4648-57.
248. Holcik M, Gordon BW, Korneluk RG. The internal ribosome entry site-mediated translation of antiapoptotic protein XIAP is modulated by the heterogeneous nuclear ribonucleoproteins C1 and C2. *Molecular and cellular biology* 2003;23(1):280-8.
249. Fan H, Goodier JL, Chamberlain JR, Engelke DR, Maraia RJ. 5' processing of tRNA precursors can be modulated by the human La antigen phosphoprotein. *Molecular and cellular biology* 1998;18(6):3201-11.

250. Gottlieb E, Steitz JA. Function of the mammalian La protein: evidence for its action in transcription termination by RNA polymerase III. *The EMBO journal* 1989;8(3):851-61.
251. Ali N, Siddiqui A. The La antigen binds 5' noncoding region of the hepatitis C virus RNA in the context of the initiator AUG codon and stimulates internal ribosome entry site-mediated translation. *Proceedings of the National Academy of Sciences of the United States of America* 1997;94(6):2249-54.
252. Kim YK, Jang SK. La protein is required for efficient translation driven by encephalomyocarditis virus internal ribosomal entry site. *The Journal of general virology* 1999;80 ( Pt 12):3159-66.
253. Meerovitch K, Svitkin YV, Lee HS, Lejbkowitz F, Kenan DJ, Chan EK, et al. La autoantigen enhances and corrects aberrant translation of poliovirus RNA in reticulocyte lysate. *Journal of virology* 1993;67(7):3798-807.
254. Rutjes SA, Utz PJ, van der Heijden A, Broekhuis C, van Venrooij WJ, Pruijn GJ. The La (SS-B) autoantigen, a key protein in RNA biogenesis, is dephosphorylated and cleaved early during apoptosis. *Cell death and differentiation* 1999;6(10):976-86.
255. Krecic AM, Swanson MS. hnRNP complexes: composition, structure, and function. *Current opinion in cell biology* 1999;11(3):363-71.
256. Waterhouse N, Kumar S, Song Q, Strike P, Sparrow L, Dreyfuss G, et al. Heteronuclear ribonucleoproteins C1 and C2, components of the spliceosome, are specific targets of interleukin 1beta-converting enzyme-like proteases in apoptosis. *The Journal of biological chemistry* 1996;271(46):29335-41.
257. Lewis SM, Veyrier A, Hosszu Ungureanu N, Bonnal S, Vagner S, Holcik M. Subcellular relocalization of a trans-acting factor regulates XIAP IRES-dependent translation. *Molecular biology of the cell* 2007;18(4):1302-11.
258. Bonnal S, Pileur F, Orsini C, Parker F, Pujol F, Prats AC, et al. Heterogeneous nuclear ribonucleoprotein A1 is a novel internal ribosome entry site trans-acting factor that modulates alternative initiation of translation of the fibroblast growth factor 2 mRNA. *The Journal of biological chemistry* 2005;280(6):4144-53.

259. Baird SD, Lewis SM, Turcotte M, Holcik M. A search for structurally similar cellular internal ribosome entry sites. *Nucleic acids research* 2007;35(14):4664-77.
260. Liwak U, Thakor N, Jordan LE, Roy R, Lewis SM, Pardo OE, et al. Tumor suppressor PDCD4 represses internal ribosome entry site-mediated translation of antiapoptotic proteins and is regulated by S6 kinase 2. *Molecular and cellular biology* 2012;32(10):1818-29.
261. Durie D, Lewis SM, Liwak U, Kisilewicz M, Gorospe M, Holcik M. RNA-binding protein HuR mediates cytoprotection through stimulation of XIAP translation. *Oncogene* 2011;30(12):1460-9.
262. Wade M, Li YC, Wahl GM. MDM2, MDMX and p53 in oncogenesis and cancer therapy. *Nature reviews Cancer* 2013;13(2):83-96.
263. Okamoto K, Li H, Jensen MR, Zhang T, Taya Y, Thorgeirsson SS, et al. Cyclin G recruits PP2A to dephosphorylate Mdm2. *Mol Cell* 2002;9(4):761-71.
264. Kurokawa M, Kim J, Geradts J, Matsuura K, Liu L, Ran X, et al. A network of substrates of the E3 ubiquitin ligases MDM2 and HUWE1 control apoptosis independently of p53. *Science signaling* 2013;6(274):ra32.
265. Dan HC, Sun M, Kaneko S, Feldman RI, Nicosia SV, Wang HG, et al. Akt phosphorylation and stabilization of X-linked inhibitor of apoptosis protein (XIAP). *The Journal of biological chemistry* 2004;279(7):5405-12.
266. Tian S, Mewani RR, Kumar D, Li B, Danner MT, Ahmad I, et al. Interaction and stabilization of X-linked inhibitor of apoptosis by Raf-1 protein kinase. *International journal of oncology* 2006;29(4):861-7.
267. Kato K, Tanaka T, Sadik G, Baba M, Maruyama D, Yanagida K, et al. Protein kinase C stabilizes X-linked inhibitor of apoptosis protein (XIAP) through phosphorylation at Ser(87) to suppress apoptotic cell death. *Psychogeriatrics : the official journal of the Japanese Psychogeriatric Society* 2011;11(2):90-7.
268. Shi RX, Ong CN, Shen HM. Protein kinase C inhibition and x-linked inhibitor of apoptosis protein degradation contribute to the sensitization effect of luteolin on tumor necrosis factor-related apoptosis-inducing ligand-induced apoptosis in cancer cells. *Cancer research* 2005;65(17):7815-23.

269. Liu WH, Hsiao HW, Tsou WI, Lai MZ. Notch inhibits apoptosis by direct interference with XIAP ubiquitination and degradation. *The EMBO journal* 2007;26(6):1660-9.
270. Allenspach EJ, Maillard I, Aster JC, Pear WS. Notch signaling in cancer. *Cancer biology & therapy* 2002;1(5):466-76.
271. Debeb BG, Cohen EN, Boley K, Freiter EM, Li L, Robertson FM, et al. Pre-clinical studies of Notch signaling inhibitor RO4929097 in inflammatory breast cancer cells. *Breast cancer research and treatment* 2012;134(2):495-510.
272. Hofer-Warbinek R, Schmid JA, Stehlik C, Binder BR, Lipp J, de Martin R. Activation of NF-kappa B by XIAP, the X chromosome-linked inhibitor of apoptosis, in endothelial cells involves TAK1. *The Journal of biological chemistry* 2000;275(29):22064-8.
273. Birkey Reffey S, Wurthner JU, Parks WT, Roberts AB, Duckett CS. X-linked inhibitor of apoptosis protein functions as a cofactor in transforming growth factor-beta signaling. *The Journal of biological chemistry* 2001;276(28):26542-9.
274. Kaur S, Wang F, Venkatraman M, Arsur M. X-linked inhibitor of apoptosis (XIAP) inhibits c-Jun N-terminal kinase 1 (JNK1) activation by transforming growth factor beta1 (TGF-beta1) through ubiquitin-mediated proteosomal degradation of the TGF-beta1-activated kinase 1 (TAK1). *The Journal of biological chemistry* 2005;280(46):38599-608.
275. Neil JR, Tian M, Schiemann WP. X-linked inhibitor of apoptosis protein and its E3 ligase activity promote transforming growth factor- $\beta$ -mediated nuclear factor- $\kappa$ B activation during breast cancer progression. *The Journal of biological chemistry* 2009;284(32):21209-17.
276. Lu M, Lin SC, Huang Y, Kang YJ, Rich R, Lo YC, et al. XIAP induces NF-kappaB activation via the BIR1/TAB1 interaction and BIR1 dimerization. *Molecular cell* 2007;26(5):689-702.
277. Neil JR, Schiemann WP. Altered TAB1:I kappaB kinase interaction promotes transforming growth factor beta-mediated nuclear factor-kappaB activation during breast cancer progression. *Cancer research* 2008;68(5):1462-70.

278. Maine GN, Mao X, Muller PA, Komarck CM, Klomp LW, Burstein E. COMMD1 expression is controlled by critical residues that determine XIAP binding. *The Biochemical journal* 2009;417(2):601-9.
279. Maine GN, Mao X, Komarck CM, Burstein E. COMMD1 promotes the ubiquitination of NF-kappaB subunits through a cullin-containing ubiquitin ligase. *The EMBO journal* 2007;26(2):436-47.
280. Asselin E, Mills GB, Tsang BK. XIAP regulates Akt activity and caspase-3-dependent cleavage during cisplatin-induced apoptosis in human ovarian epithelial cancer cells. *Cancer research* 2001;61(5):1862-8.
281. Van Themsche C, Leblanc V, Parent S, Asselin E. X-linked inhibitor of apoptosis protein (XIAP) regulates PTEN ubiquitination, content, and compartmentalization. *The Journal of biological chemistry* 2009;284(31):20462-6.
282. Resch U, Schichl YM, Sattler S, de Martin R. XIAP regulates intracellular ROS by enhancing antioxidant gene expression. *Biochemical and biophysical research communications* 2008;375(1):156-61.
283. Kairisalo M, Korhonen L, Blomgren K, Lindholm D. X-linked inhibitor of apoptosis protein increases mitochondrial antioxidants through NF-kappaB activation. *Biochemical and biophysical research communications* 2007;364(1):138-44.
284. Zhu C, Xu F, Fukuda A, Wang X, Fukuda H, Korhonen L, et al. X chromosome-linked inhibitor of apoptosis protein reduces oxidative stress after cerebral irradiation or hypoxia-ischemia through up-regulation of mitochondrial antioxidants. *The European journal of neuroscience* 2007;26(12):3402-10.
285. Sarkar B, Roberts EA. The puzzle posed by COMMD1, a newly discovered protein binding Cu(II). *Metallomics : integrated biometal science* 2011;3(1):20-7.
286. Brady GF, Galban S, Liu X, Basrur V, Gitlin JD, Elenitoba-Johnson KS, et al. Regulation of the copper chaperone CCS by XIAP-mediated ubiquitination. *Molecular and cellular biology* 2010;30(8):1923-36.
287. Mufti AR, Burstein E, Csomos RA, Graf PC, Wilkinson JC, Dick RD, et al. XIAP Is a copper binding protein deregulated in Wilson's disease and other copper toxicosis disorders. *Mol Cell* 2006;21(6):775-85.

288. Obexer P, Ausserlechner MJ. X-linked inhibitor of apoptosis protein - a critical death resistance regulator and therapeutic target for personalized cancer therapy. *Frontiers in oncology* 2014;4:197.
289. Burstein DE, Idrees MT, Li G, Wu M, Kalir T. Immunohistochemical detection of the X-linked inhibitor of apoptosis protein (XIAP) in cervical squamous intraepithelial neoplasia and squamous carcinoma. *Annals of diagnostic pathology* 2008;12(2):85-9.
290. Gu LQ, Li FY, Zhao L, Liu Y, Chu Q, Zang XX, et al. Association of XIAP and P2X7 receptor expression with lymph node metastasis in papillary thyroid carcinoma. *Endocrine* 2010;38(2):276-82.
291. Hussain AR, Uddin S, Ahmed M, Bu R, Ahmed SO, Abubaker J, et al. Prognostic significance of XIAP expression in DLBCL and effect of its inhibition on AKT signalling. *The Journal of pathology* 2010;222(2):180-90.
292. Ibrahim AM, Mansour IM, Wilson MM, Mokhtar DA, Helal AM, Al Wakeel HM. Study of survivin and X-linked inhibitor of apoptosis protein (XIAP) genes in acute myeloid leukemia (AML). *Laboratory hematology : official publication of the International Society for Laboratory Hematology* 2012;18(1):1-10.
293. Kim MA, Lee HE, Lee HS, Yang HK, Kim WH. Expression of apoptosis-related proteins and its clinical implication in surgically resected gastric carcinoma. *Virchows Archiv : an international journal of pathology* 2011;459(5):503-10.
294. Kluger HM, McCarthy MM, Alvero AB, Sznol M, Ariyan S, Camp RL, et al. The X-linked inhibitor of apoptosis protein (XIAP) is up-regulated in metastatic melanoma, and XIAP cleavage by Phenoxodiol is associated with Carboplatin sensitization. *Journal of translational medicine* 2007;5:6.
295. Seligson DB, Hongo F, Huerta-Yepez S, Mizutani Y, Miki T, Yu H, et al. Expression of X-linked inhibitor of apoptosis protein is a strong predictor of human prostate cancer recurrence. *Clinical cancer research : an official journal of the American Association for Cancer Research* 2007;13(20):6056-63.
296. Yang XH, Feng ZE, Yan M, Hanada S, Zuo H, Yang CZ, et al. XIAP is a predictor of cisplatin-based chemotherapy response and prognosis for patients with advanced head and neck cancer. *PloS one* 2012;7(3):e31601.

297. Zhang Y, Zhu J, Tang Y, Li F, Zhou H, Peng B, et al. X-linked inhibitor of apoptosis positive nuclear labeling: a new independent prognostic biomarker of breast invasive ductal carcinoma. *Diagnostic pathology* 2011;6:49.
298. Krepela E, Dankova P, Moravcikova E, Krepelova A, Prochazka J, Cermak J, et al. Increased expression of inhibitor of apoptosis proteins, survivin and XIAP, in non-small cell lung carcinoma. *International journal of oncology* 2009;35(6):1449-62.
299. Ferreira CG, van der Valk P, Span SW, Ludwig I, Smit EF, Kruyt FA, et al. Expression of X-linked inhibitor of apoptosis as a novel prognostic marker in radically resected non-small cell lung cancer patients. *Clinical cancer research : an official journal of the American Association for Cancer Research* 2001;7(8):2468-74.
300. Hwang C, Oetjen KA, Kosoff D, Wojno KJ, Albertelli MA, Dunn RL, et al. X-linked inhibitor of apoptosis deficiency in the TRAMP mouse prostate cancer model. *Cell death and differentiation* 2008;15(5):831-40.
301. Liston P, Fong WG, Kelly NL, Toji S, Miyazaki T, Conte D, et al. Identification of XAF1 as an antagonist of XIAP anti-Caspase activity. *Nat Cell Biol* 2001;3(2):128-33.
302. Fong WG, Liston P, Rajcan-Separovic E, St Jean M, Craig C, Korneluk RG. Expression and genetic analysis of XIAP-associated factor 1 (XAF1) in cancer cell lines. *Genomics* 2000;70(1):113-22.
303. Ma TL, Ni PH, Zhong J, Tan JH, Qiao MM, Jiang SH. Low expression of XIAP-associated factor 1 in human colorectal cancers. *Chinese journal of digestive diseases* 2005;6(1):10-4.
304. Ng KC, Campos EI, Martinka M, Li G. XAF1 expression is significantly reduced in human melanoma. *The Journal of investigative dermatology* 2004;123(6):1127-34.
305. Leaman DW, Chawla-Sarkar M, Vyas K, Reheman M, Tamai K, Toji S, et al. Identification of X-linked inhibitor of apoptosis-associated factor-1 as an interferon-stimulated gene that augments TRAIL Apo2L-induced apoptosis. *The Journal of biological chemistry* 2002;277(32):28504-11.

306. Perrelet D, Perrin FE, Liston P, Korneluk RG, MacKenzie A, Ferrer-Alcon M, et al. Motoneuron resistance to apoptotic cell death in vivo correlates with the ratio between X-linked inhibitor of apoptosis proteins (XIAPs) and its inhibitor, XIAP-associated factor 1. *The Journal of neuroscience : the official journal of the Society for Neuroscience* 2004;24(15):3777-85.
307. Azad MB, Chen Y, Gibson SB. Regulation of autophagy by reactive oxygen species (ROS): implications for cancer progression and treatment. *Antioxidants & redox signaling* 2009;11(4):777-90.
308. Mates JM, Sanchez-Jimenez F. Antioxidant enzymes and their implications in pathophysiologic processes. *Frontiers in bioscience : a journal and virtual library* 1999;4:D339-45.
309. Adler V, Yin Z, Tew KD, Ronai Z. Role of redox potential and reactive oxygen species in stress signaling. *Oncogene* 1999;18(45):6104-11.
310. Trachootham D, Alexandre J, Huang P. Targeting cancer cells by ROS-mediated mechanisms: a radical therapeutic approach? *Nature reviews Drug discovery* 2009;8(7):579-91.
311. McCord JM, Fridovich I. Superoxide dismutase. An enzymic function for erythrocuprein (hemocuprein). *The Journal of biological chemistry* 1969;244(22):6049-55.
312. McCord JM, Fridovich I. The utility of superoxide dismutase in studying free radical reactions. I. Radicals generated by the interaction of sulfite, dimethyl sulfoxide, and oxygen. *The Journal of biological chemistry* 1969;244(22):6056-63.
313. Sies H, de Groot H. Role of reactive oxygen species in cell toxicity. *Toxicology letters* 1992;64-65 Spec No:547-51.
314. Beckman JS, Beckman TW, Chen J, Marshall PA, Freeman BA. Apparent hydroxyl radical production by peroxynitrite: implications for endothelial injury from nitric oxide and superoxide. *Proceedings of the National Academy of Sciences of the United States of America* 1990;87(4):1620-4.
315. Pacher P, Beckman JS, Liaudet L. Nitric oxide and peroxynitrite in health and disease. *Physiological reviews* 2007;87(1):315-424.

316. Knowles RG, Moncada S. Nitric oxide synthases in mammals. *The Biochemical journal* 1994;298 ( Pt 2):249-58.
317. Stuehr DJ. Mammalian nitric oxide synthases. *Biochimica et biophysica acta* 1999;1411(2-3):217-30.
318. Janssen-Heininger YM, Macara I, Mossman BT. Cooperativity between oxidants and tumor necrosis factor in the activation of nuclear factor (NF)-kappaB: requirement of Ras/mitogen-activated protein kinases in the activation of NF-kappaB by oxidants. *American journal of respiratory cell and molecular biology* 1999;20(5):942-52.
319. Kleinert H, Wallerath T, Fritz G, Ihrig-Biedert I, Rodriguez-Pascual F, Geller DA, et al. Cytokine induction of NO synthase II in human DLD-1 cells: roles of the JAK-STAT, AP-1 and NF-kappaB-signaling pathways. *British journal of pharmacology* 1998;125(1):193-201.
320. Halliwell B, Gutteridge JM. Role of free radicals and catalytic metal ions in human disease: an overview. *Methods in enzymology* 1990;186:1-85.
321. Halliwell B, Gutteridge JM. Biologically relevant metal ion-dependent hydroxyl radical generation. An update. *FEBS letters* 1992;307(1):108-12.
322. Wardman P, Candeias LP. Fenton chemistry: an introduction. *Radiation research* 1996;145(5):523-31.
323. Biemond P, Swaak AJ, van Eijk HG, Koster JF. Superoxide dependent iron release from ferritin in inflammatory diseases. *Free radical biology & medicine* 1988;4(3):185-98.
324. Imlay JA. Cellular defenses against superoxide and hydrogen peroxide. *Annual review of biochemistry* 2008;77:755-76.
325. Valko M, Rhodes CJ, Moncol J, Izakovic M, Mazur M. Free radicals, metals and antioxidants in oxidative stress-induced cancer. *Chemico-biological interactions* 2006;160(1):1-40.
326. Vineis P, Husgafvel-Pursiainen K. Air pollution and cancer: biomarker studies in human populations. *Carcinogenesis* 2005;26(11):1846-55.

327. Aruoma OI, Halliwell B, Gajewski E, Dizdaroglu M. Damage to the bases in DNA induced by hydrogen peroxide and ferric ion chelates. *The Journal of biological chemistry* 1989;264(34):20509-12.
328. Dizdaroglu M, Jaruga P, Birincioglu M, Rodriguez H. Free radical-induced damage to DNA: mechanisms and measurement. *Free radical biology & medicine* 2002;32(11):1102-15.
329. Balaban RS, Nemoto S, Finkel T. Mitochondria, oxidants, and aging. *Cell* 2005;120(4):483-95.
330. Chen Y, Gibson SB. Is mitochondrial generation of reactive oxygen species a trigger for autophagy? *Autophagy* 2008;4(2):246-8.
331. Han D, Williams E, Cadenas E. Mitochondrial respiratory chain-dependent generation of superoxide anion and its release into the intermembrane space. *The Biochemical journal* 2001;353(Pt 2):411-6.
332. Orrenius S, Gogvadze V, Zhivotovsky B. Mitochondrial oxidative stress: implications for cell death. *Annual review of pharmacology and toxicology* 2007;47:143-83.
333. Starkov AA, Fiskum G, Chinopoulos C, Lorenzo BJ, Browne SE, Patel MS, et al. Mitochondrial alpha-ketoglutarate dehydrogenase complex generates reactive oxygen species. *The Journal of neuroscience : the official journal of the Society for Neuroscience* 2004;24(36):7779-88.
334. Bonekamp NA, Volkl A, Fahimi HD, Schrader M. Reactive oxygen species and peroxisomes: struggling for balance. *BioFactors (Oxford, England)* 2009;35(4):346-55.
335. Ushio-Fukai M. Localizing NADPH oxidase-derived ROS. *Science's STKE : signal transduction knowledge environment* 2006;2006(349):re8.
336. Zangar RC, Davydov DR, Verma S. Mechanisms that regulate production of reactive oxygen species by cytochrome P450. *Toxicology and applied pharmacology* 2004;199(3):316-31.

337. Nitta M, Kozono D, Kennedy R, Stommel J, Ng K, Zinn PO, et al. Targeting EGFR induced oxidative stress by PARP1 inhibition in glioblastoma therapy. *PloS one* 2010;5(5):e10767.
338. Ziech D, Franco R, Georgakilas AG, Georgakila S, Malamou-Mitsi V, Schoneveld O, et al. The role of reactive oxygen species and oxidative stress in environmental carcinogenesis and biomarker development. *Chemico-biological interactions* 2010;188(2):334-9.
339. Droge W. Free radicals in the physiological control of cell function. *Physiological reviews* 2002;82(1):47-95.
340. Samoylenko A, Hossain JA, Mennerich D, Kellokumpu S, Hiltunen JK, Kietzmann T. Nutritional Countermeasures Targeting Reactive Oxygen Species in Cancer: From Mechanisms to Biomarkers and Clinical Evidence. *Antioxidants & redox signaling* 2013.
341. Chen Y, McMillan-Ward E, Kong J, Israels SJ, Gibson SB. Oxidative stress induces autophagic cell death independent of apoptosis in transformed and cancer cells. *Cell death and differentiation* 2008;15(1):171-82.
342. Ott M, Gogvadze V, Orrenius S, Zhivotovsky B. Mitochondria, oxidative stress and cell death. *Apoptosis : an international journal on programmed cell death* 2007;12(5):913-22.
343. Khandrika L, Kumar B, Koul S, Maroni P, Koul HK. Oxidative stress in prostate cancer. *Cancer letters* 2009;282(2):125-36.
344. Wells PG, McCallum GP, Chen CS, Henderson JT, Lee CJ, Perstin J, et al. Oxidative stress in developmental origins of disease: teratogenesis, neurodevelopmental deficits, and cancer. *Toxicological sciences : an official journal of the Society of Toxicology* 2009;108(1):4-18.
345. Cooke MS, Evans MD, Dizdaroglu M, Lunec J. Oxidative DNA damage: mechanisms, mutation, and disease. *FASEB journal : official publication of the Federation of American Societies for Experimental Biology* 2003;17(10):1195-214.
346. Marnett LJ. Oxyradicals and DNA damage. *Carcinogenesis* 2000;21(3):361-70.

347. Matsuzawa A, Ichijo H. Redox control of cell fate by MAP kinase: physiological roles of ASK1-MAP kinase pathway in stress signaling. *Biochimica et biophysica acta* 2008;1780(11):1325-36.
348. Maulik N. Redox signaling of angiogenesis. *Antioxidants & redox signaling* 2002;4(5):805-15.
349. Yang W, Zou L, Huang C, Lei Y. Redox regulation of cancer metastasis: molecular signaling and therapeutic opportunities. *Drug development research* 2014;75(5):331-41.
350. Indran IR, Hande MP, Pervaiz S. hTERT overexpression alleviates intracellular ROS production, improves mitochondrial function, and inhibits ROS-mediated apoptosis in cancer cells. *Cancer research* 2011;71(1):266-76.
351. Matoba S, Kang JG, Patino WD, Wragg A, Boehm M, Gavrilova O, et al. p53 regulates mitochondrial respiration. *Science* 2006;312(5780):1650-3.
352. Yagoda N, von Rechenberg M, Zaganjor E, Bauer AJ, Yang WS, Fridman DJ, et al. RAS-RAF-MEK-dependent oxidative cell death involving voltage-dependent anion channels. *Nature* 2007;447(7146):864-8.
353. Lee JM, Johnson JA. An important role of Nrf2-ARE pathway in the cellular defense mechanism. *Journal of biochemistry and molecular biology* 2004;37(2):139-43.
354. Kansanen E, Kuosmanen SM, Leinonen H, Levonen AL. The Keap1-Nrf2 pathway: Mechanisms of activation and dysregulation in cancer. *Redox biology* 2013;1:45-9.
355. Shibata T, Ohta T, Tong KI, Kokubu A, Odogawa R, Tsuta K, et al. Cancer related mutations in NRF2 impair its recognition by Keap1-Cul3 E3 ligase and promote malignancy. *Proceedings of the National Academy of Sciences of the United States of America* 2008;105(36):13568-73.
356. Hast BE, Cloer EW, Goldfarb D, Li H, Siesser PF, Yan F, et al. Cancer-derived mutations in KEAP1 impair NRF2 degradation but not ubiquitination. *Cancer research* 2014;74(3):808-17.

357. Ding Y, Choi KJ, Kim JH, Han X, Piao Y, Jeong JH, et al. Endogenous hydrogen peroxide regulates glutathione redox via nuclear factor erythroid 2-related factor 2 downstream of phosphatidylinositol 3-kinase during muscle differentiation. *The American journal of pathology* 2008;172(6):1529-41.
358. DeNicola GM, Karreth FA, Humpton TJ, Gopinathan A, Wei C, Frese K, et al. Oncogene-induced Nrf2 transcription promotes ROS detoxification and tumorigenesis. *Nature* 2011;475(7354):106-9.
359. Morgan MJ, Liu ZG. Crosstalk of reactive oxygen species and NF-kappaB signaling. *Cell research* 2011;21(1):103-15.
360. Noh DY, Ahn SJ, Lee RA, Kim SW, Park IA, Chae HZ. Overexpression of peroxiredoxin in human breast cancer. *Anticancer research* 2001;21(3B):2085-90.
361. Cha MK, Suh KH, Kim IH. Overexpression of peroxiredoxin I and thioredoxin1 in human breast carcinoma. *Journal of experimental & clinical cancer research : CR* 2009;28:93.
362. Liu R, Oberley TD, Oberley LW. Transfection and expression of MnSOD cDNA decreases tumor malignancy of human oral squamous carcinoma SCC-25 cells. *Human gene therapy* 1997;8(5):585-95.
363. Weydert CJ, Waugh TA, Ritchie JM, Iyer KS, Smith JL, Li L, et al. Overexpression of manganese or copper-zinc superoxide dismutase inhibits breast cancer growth. *Free radical biology & medicine* 2006;41(2):226-37.
364. Kattan Z, Minig V, Leroy P, Dauca M, Becuwe P. Role of manganese superoxide dismutase on growth and invasive properties of human estrogen-independent breast cancer cells. *Breast cancer research and treatment* 2008;108(2):203-15.
365. Er TK, Hou MF, Tsa EM, Lee JN, Tsai LY. Differential expression of manganese containing superoxide dismutase in patients with breast cancer in Taiwan. *Annals of clinical and laboratory science* 2004;34(2):159-64.
366. Huang J, Tan PH, Tan BK, Bay BH. GST-pi expression correlates with oxidative stress and apoptosis in breast cancer. *Oncol Rep* 2004;12(4):921-5.
367. Balendiran GK, Dabur R, Fraser D. The role of glutathione in cancer. *Cell Biochem Funct* 2004;22(6):343-52.

368. Perry RR, Mazetta JA, Levin M, Barranco SC. Glutathione levels and variability in breast tumors and normal tissue. *Cancer* 1993;72(3):783-7.
369. Jardim BV, Moschetta MG, Leonel C, Gelaleti GB, Regiani VR, Ferreira LC, et al. Glutathione and glutathione peroxidase expression in breast cancer: An immunohistochemical and molecular study. *Oncology reports* 2013.
370. Chen EI, Hewel J, Krueger JS, Tiraby C, Weber MR, Kralli A, et al. Adaptation of energy metabolism in breast cancer brain metastases. *Cancer research* 2007;67(4):1472-86.
371. Singh B, Tai K, Madan S, Raythatha MR, Cady AM, Braunlin M, et al. Selection of metastatic breast cancer cells based on adaptability of their metabolic state. *PLoS One* 2012;7(5):e36510. doi: 10.1371/journal.pone.0036510. Epub 2012 May 3.
372. Brown NS, Bicknell R. Hypoxia and oxidative stress in breast cancer. *Oxidative stress: its effects on the growth, metastatic potential and response to therapy of breast cancer. Breast Cancer Res* 2001;3(5):323-7.
373. Manda G, Nechifor MT, Neagu T. Reactive Oxygen Species, Cancer and Anti-Cancer Therapies. *Current Chemical Biology* 2009;3:342-66.
374. Rao Y, Li R, Zhang D. A drug from poison: how the therapeutic effect of arsenic trioxide on acute promyelocytic leukemia was discovered. *Science China Life sciences* 2013;56(6):495-502.
375. Pelicano H, Feng L, Zhou Y, Carew JS, Hileman EO, Plunkett W, et al. Inhibition of mitochondrial respiration: a novel strategy to enhance drug-induced apoptosis in human leukemia cells by a reactive oxygen species-mediated mechanism. *The Journal of biological chemistry* 2003;278(39):37832-9.
376. Rangwala F, Williams KP, Smith GR, Thomas Z, Allensworth JL, Lyerly HK, et al. Differential effects of arsenic trioxide on chemosensitization in human hepatic tumor and stellate cell lines. *BMC cancer* 2012;12:402.
377. Magda D, Miller RA. Motexafin gadolinium: a novel redox active drug for cancer therapy. *Seminars in cancer biology* 2006;16(6):466-76.

378. Vasquez-Vivar J, Martasek P, Hogg N, Masters BS, Pritchard KA, Jr., Kalyanaraman B. Endothelial nitric oxide synthase-dependent superoxide generation from adriamycin. *Biochemistry* 1997;36(38):11293-7.
379. Kim HJ, Oridate N, Lotan R. Increased level of the p67phox subunit of NADPH oxidase by 4HPR in head and neck squamous carcinoma cells. *International journal of oncology* 2005;27(3):787-90.
380. Karunakaran S, Ramachandran S, Coothankandaswamy V, Elangovan S, Babu E, Periyasamy-Thandavan S, et al. SLC6A14 (ATB0,+) protein, a highly concentrative and broad specific amino acid transporter, is a novel and effective drug target for treatment of estrogen receptor-positive breast cancer. *The Journal of biological chemistry* 2011;286(36):31830-8.
381. Oppedisano F, Catto M, Koutentis PA, Nicolotti O, Pochini L, Koyioni M, et al. Inactivation of the glutamine/amino acid transporter ASCT2 by 1,2,3-dithiazoles: proteoliposomes as a tool to gain insights in the molecular mechanism of action and of antitumor activity. *Toxicology and applied pharmacology* 2012;265(1):93-102.
382. Chen S, Sun L, Koya K, Tatsuta N, Xia Z, Korbut T, et al. Syntheses and antitumor activities of N'1,N'3-dialkyl-N'1,N'3-di-(alkylcarbonothioyl) malonohydrazide: the discovery of elesclomol. *Bioorganic & medicinal chemistry letters* 2013;23(18):5070-6.
383. Koya K, Sun L, Chen S, Tatsuta N, Korbut T, Zhou D, et al. STA-4783, a novel HSP70 inducer, enhances the anti-cancer activity of Paclitaxel without increasing toxicity in preclinical studies. *Cancer research* 2004;64(7 Supplement):346.
384. Tuma RS. Reactive oxygen species may have antitumor activity in metastatic melanoma. *J Natl Cancer Inst* 2008;100(1):11-2.
385. Kirshner JR, He S, Balasubramanyam V, Kepros J, Yang CY, Zhang M, et al. Elesclomol induces cancer cell apoptosis through oxidative stress. *Molecular cancer therapeutics* 2008;7(8):2319-27.
386. O'Day SJ, Eggermont AM, Chiarion-Sileni V, Kefford R, Grob JJ, Mortier L, et al. Final results of phase III SYMMETRY study: randomized, double-blind trial of elesclomol plus paclitaxel versus paclitaxel alone as treatment for chemotherapy-naive patients with advanced melanoma. *J Clin Oncol* 2013;31(9):1211-8.

387. Huang P, Feng L, Oldham EA, Keating MJ, Plunkett W. Superoxide dismutase as a target for the selective killing of cancer cells. *Nature* 2000;407(6802):390-5.
388. Juarez JC, Manuia M, Burnett ME, Betancourt O, Boivin B, Shaw DE, et al. Superoxide dismutase 1 (SOD1) is essential for H<sub>2</sub>O<sub>2</sub>-mediated oxidation and inactivation of phosphatases in growth factor signaling. *Proceedings of the National Academy of Sciences of the United States of America* 2008;105(20):7147-52.
389. Alexandre J, Nicco C, Chereau C, Laurent A, Weill B, Goldwasser F, et al. Improvement of the therapeutic index of anticancer drugs by the superoxide dismutase mimic mangafodipir. *J Natl Cancer Inst* 2006;98(4):236-44.
390. Lu J, Chew EH, Holmgren A. Targeting thioredoxin reductase is a basis for cancer therapy by arsenic trioxide. *Proceedings of the National Academy of Sciences of the United States of America* 2007;104(30):12288-93.
391. Welsh SJ, Williams RR, Birmingham A, Newman DJ, Kirkpatrick DL, Powis G. The thioredoxin redox inhibitors 1-methylpropyl 2-imidazolyl disulfide and pleurotin inhibit hypoxia-induced factor 1 alpha and vascular endothelial growth factor formation. *Molecular cancer therapeutics* 2003;2(3):235-43.
392. Dvorakova K, Payne CM, Tome ME, Briehl MM, McClure T, Dorr RT. Induction of oxidative stress and apoptosis in myeloma cells by the aziridine-containing agent imexon. *Biochemical pharmacology* 2000;60(6):749-58.
393. Xu K, Thornalley PJ. Involvement of glutathione metabolism in the cytotoxicity of the phenethyl isothiocyanate and its cysteine conjugate to human leukaemia cells in vitro. *Biochemical pharmacology* 2001;61(2):165-77.
394. Zhang Y, Talalay P. Anticarcinogenic activities of organic isothiocyanates: chemistry and mechanisms. *Cancer research* 1994;54(7 Suppl):1976s-81s.
395. Griffith OW, Meister A. Potent and specific inhibition of glutathione synthesis by buthionine sulfoximine (S-n-butyl homocysteine sulfoximine). *The Journal of biological chemistry* 1979;254(16):7558-60.

396. Narang VS, Pauletti GM, Gout PW, Buckley DJ, Buckley AR. Sulfasalazine-induced reduction of glutathione levels in breast cancer cells: enhancement of growth-inhibitory activity of Doxorubicin. *Chemotherapy* 2007;53(3):210-7.
397. Gilmore TD, Herscovitch M. Inhibitors of NF-kappaB signaling: 785 and counting. *Oncogene* 2006;25(51):6887-99.
398. Tarumoto T, Nagai T, Ohmine K, Miyoshi T, Nakamura M, Kondo T, et al. Ascorbic acid restores sensitivity to imatinib via suppression of Nrf2-dependent gene expression in the imatinib-resistant cell line. *Experimental hematology* 2004;32(4):375-81.
399. Wang XJ, Hayes JD, Henderson CJ, Wolf CR. Identification of retinoic acid as an inhibitor of transcription factor Nrf2 through activation of retinoic acid receptor alpha. *Proceedings of the National Academy of Sciences of the United States of America* 2007;104(49):19589-94.
400. Olayanju A, Copple IM, Bryan HK, Edge GT, Sison RL, Wong MW, et al. Brusatol provokes a rapid and transient inhibition of Nrf2 signaling and sensitizes mammalian cells to chemical toxicity-implications for therapeutic targeting of Nrf2. *Free radical biology & medicine* 2015;78:202-12.
401. Tang X, Wang H, Fan L, Wu X, Xin A, Ren H, et al. Luteolin inhibits Nrf2 leading to negative regulation of the Nrf2/ARE pathway and sensitization of human lung carcinoma A549 cells to therapeutic drugs. *Free radical biology & medicine* 2011;50(11):1599-609.
402. Boesch-Saadatmandi C, Wagner AE, Graeser AC, Hundhausen C, Wolfram S, Rimbach G. Ochratoxin A impairs Nrf2-dependent gene expression in porcine kidney tubulus cells. *Journal of animal physiology and animal nutrition* 2009;93(5):547-54.
403. Alpaugh ML, Tomlinson JS, Shao ZM, Barsky SH. A novel human xenograft model of inflammatory breast cancer. *Cancer research* 1999;59(20):5079-84.
404. Mahooti S, Porter K, Alpaugh ML, Ye Y, Xiao Y, Jones S, et al. Breast carcinomatous tumoral emboli can result from encircling lymphovascuogenesis rather than lymphovascular invasion. *Oncotarget* 2010;1(2):131-47.

405. Chu K, Mu Z, Alpaugh K, Fernandez S, Freiter E, Wu H, et al. P4-03-06: Development and Comparative Characterization of Metastasis in Newly Developed Pre-Clinical Models of Inflammatory Breast Cancer. *Cancer research* 2011;71(24 Supplement):P4-03-06.
406. Fernandez SV, Mu Z, Aburto L, Dong X, Chu K, Boley K, et al. Abstract 5342: FC-IBC-02: A new in vitro-in vivo model of inflammatory breast cancer (IBC). *Cancer research* 2012;72(8 Supplement):5342.
407. Forozan F, Veldman R, Ammerman CA, Parsa NZ, Kallioniemi A, Kallioniemi OP, et al. Molecular cytogenetic analysis of 11 new breast cancer cell lines. *British journal of cancer* 1999;81(8):1328-34.
408. Ignatoski KM, Ethier SP. Constitutive activation of pp125fak in newly isolated human breast cancer cell lines. *Breast cancer research and treatment* 1999;54(2):173-82.
409. Neve RM, Chin K, Fridlyand J, Yeh J, Baehner FL, Fevr T, et al. A collection of breast cancer cell lines for the study of functionally distinct cancer subtypes. *Cancer cell* 2006;10(6):515-27.
410. Willmarth NE, Ethier SP. Autocrine and juxtacrine effects of amphiregulin on the proliferative, invasive, and migratory properties of normal and neoplastic human mammary epithelial cells. *The Journal of biological chemistry* 2006;281(49):37728-37.
411. Lehman HL, Dashner EJ, Lucey M, Vermeulen P, Dirix L, Van Laere S, et al. Modeling and characterization of inflammatory breast cancer emboli grown in vitro. *International journal of cancer Journal international du cancer* 2013;132(10):2283-94.
412. Klee CG, van Golen KL, Merajver SD. Molecular biology of breast cancer metastasis. Inflammatory breast cancer: clinical syndrome and molecular determinants. *Breast Cancer Res* 2000;2(6):423-9.
413. Allensworth JL, Evans MK, Bertucci F, Aldrich AJ, Festa RA, Finetti P, et al. Disulfiram (DSF) acts as a copper ionophore to induce copper-dependent oxidative stress and mediate anti-tumor efficacy in inflammatory breast cancer. *Molecular oncology* 2015;9(6):1155-68.

414. Robertson FM, Chu K, Fernandez SV, Mu Z, Zhang X, Liu H, et al. Genomic Profiling of Pre-Clinical Models of Inflammatory Breast Cancer Identifies a Signature of Epithelial Plasticity and Suppression of TGF $\beta$  Signaling. *J Clin Exp Pathol* 2012;2(5):2161-0681.1000119.
415. Kurebayashi J, Otsuki T, Tang CK, Kurosumi M, Yamamoto S, Tanaka K, et al. Isolation and characterization of a new human breast cancer cell line, KPL-4, expressing the Erb B family receptors and interleukin-6. *British journal of cancer* 1999;79(5-6):707-17.
416. Klopp AH, Lacerda L, Gupta A, Debeb BG, Solley T, Li L, et al. Mesenchymal stem cells promote mammosphere formation and decrease E-cadherin in normal and malignant breast cells. *PloS one* 2010;5(8):e12180.
417. Kurebayashi J. Regulation of interleukin-6 secretion from breast cancer cells and its clinical implications. *Breast cancer* 2000;7(2):124-9.
418. Williams KP, Allensworth JL, Ingram SM, Smith GR, Aldrich AJ, Sexton JZ, et al. Quantitative high-throughput efficacy profiling of approved oncology drugs in inflammatory breast cancer models of acquired drug resistance and re-sensitization. *Cancer letters* 2013;337(1):77-89.
419. Allensworth JL, Aird KM, Aldrich AJ, Batinic-Haberle I, Devi GR. XIAP inhibition and generation of reactive oxygen species enhances TRAIL sensitivity in inflammatory breast cancer cells. *Molecular cancer therapeutics* 2012;11(7):1518-27.
420. Allensworth JL, Sauer SJ, Lyerly HK, Morse MA, Devi GR. Smac mimetic Birinapant induces apoptosis and enhances TRAIL potency in inflammatory breast cancer cells in an IAP-dependent and TNF-alpha-independent mechanism. *Breast cancer research and treatment* 2013;137(2):359-71.
421. Sharma SV, Lee DY, Li B, Quinlan MP, Takahashi F, Maheswaran S, et al. A chromatin-mediated reversible drug-tolerant state in cancer cell subpopulations. *Cell* 2010;141(1):69-80.
422. Batinic-Haberle I, Rajic Z, Tovmasyan A, Reboucas JS, Ye X, Leong KW, et al. Diverse functions of cationic Mn(III)N-substituted pyridylporphyrins, recognized as SOD mimics. *Free radical biology & medicine* 2011;51(5):1035-53.

423. Dobrikov MI, Shveygert M, Brown MC, Gromeier M. Mitotic phosphorylation of eukaryotic initiation factor 4G1 (eIF4G1) at Ser1232 by Cdk1: cyclin B inhibits eIF4A helicase complex binding with RNA. *Molecular and cellular biology* 2014;34(3):439-51.
424. Rochira JA, Matluk NN, Adams TL, Karaczyn AA, Oxburgh L, Hess ST, et al. A small peptide modeled after the NRAGE repeat domain inhibits XIAP-TAB1-TAK1 signaling for NF-kappaB activation and apoptosis in P19 cells. *PloS one* 2011;6(7):e20659.
425. Geback T, Schulz MM, Koumoutsakos P, Detmar M. TScratch: a novel and simple software tool for automated analysis of monolayer wound healing assays. *BioTechniques* 2009;46(4):265-74.
426. Batinic-Haberle I, Spasojevic I, Hambright P, Benov L, Crumbliss AL, Fridovich I. Relationship among Redox Potentials, Proton Dissociation Constants of Pyrrolic Nitrogens, and in Vivo and in Vitro Superoxide Dismutating Activities of Manganese(III) and Iron(III) Water-Soluble Porphyrins. *Inorganic Chemistry* 1999;38(18):4011-22.
427. Rajic Z, Tovmasyan A, Spasojevic I, Sheng H, Lu M, Li AM, et al. A new SOD mimic, Mn(III) ortho N-butoxyethylpyridylporphyrin, combines superb potency and lipophilicity with low toxicity. *Free radical biology & medicine* 2012;52(9):1828-34.
428. Spasojevic I, Colvin OM, Warshany KR, Batinic-Haberle I. New approach to the activation of anti-cancer pro-drugs by metalloporphyrin-based cytochrome P450 mimics in all-aqueous biologically relevant system. *Journal of inorganic biochemistry* 2006;100(11):1897-902.
429. Tovmasyan AG, Rajic Z, Spasojevic I, Reboucas JS, Chen X, Salvemini D, et al. Methoxy-derivatization of alkyl chains increases the in vivo efficacy of cationic Mn porphyrins. Synthesis, characterization, SOD-like activity, and SOD-deficient *E. coli* study of meta Mn(III) N-methoxyalkylpyridylporphyrins. *Dalton transactions (Cambridge, England : 2003)* 2011;40(16):4111-21.
430. Ye X, Fels D, Tovmasyan A, Aird KM, Dedeugd C, Allensworth JL, et al. Cytotoxic effects of Mn(III) N-alkylpyridylporphyrins in the presence of cellular reductant, ascorbate. *Free radical research* 2011;45(11-12):1289-306.

431. Abramoff MD, Magalhaes, P.J., Ram, S.J. . Image Processing with ImageJ. *Biophotonics International* 2004;11(7):36-42.
432. Irizarry RA, Bolstad BM, Collin F, Cope LM, Hobbs B, Speed TP. Summaries of Affymetrix GeneChip probe level data. *Nucleic acids research* 2003;31(4):e15.
433. Subramanian A, Tamayo P, Mootha VK, Mukherjee S, Ebert BL, Gillette MA, et al. Gene set enrichment analysis: a knowledge-based approach for interpreting genome-wide expression profiles. *Proceedings of the National Academy of Sciences of the United States of America* 2005;102(43):15545-50.
434. Bertucci F, Ueno NT, Finetti P, Vermeulen P, Lucci A, Robertson FM, et al. Gene expression profiles of inflammatory breast cancer: correlation with response to neoadjuvant chemotherapy and metastasis-free survival. *Annals of oncology : official journal of the European Society for Medical Oncology / ESMO* 2014;25(2):358-65.
435. Heller G, Geradts J, Ziegler B, Newsham I, Filipits M, Markis-Ritzinger EM, et al. Downregulation of TSLC1 and DAL-1 expression occurs frequently in breast cancer. *Breast cancer research and treatment* 2007;103(3):283-91.
436. Sood AK, Saxena R, Groth J, Desouki MM, Cheewakriangkrai C, Rodabaugh KJ, et al. Expression characteristics of prostate-derived Ets factor support a role in breast and prostate cancer progression. *Human pathology* 2007;38(11):1628-38.
437. Dawood S, Lei X, Dent R, Gupta S, Sirohi B, Cortes J, et al. Survival of women with inflammatory breast cancer: a large population-based study. *Annals of oncology : official journal of the European Society for Medical Oncology / ESMO* 2014;25(6):1143-51.
438. Cristofanilli M, Valero V, Buzdar AU, Kau SW, Broglio KR, Gonzalez-Angulo AM, et al. Inflammatory breast cancer (IBC) and patterns of recurrence: understanding the biology of a unique disease. *Cancer* 2007;110(7):1436-44.
439. Masuda H, Brewer TM, Liu DD, Iwamoto T, Shen Y, Hsu L, et al. Long-term treatment efficacy in primary inflammatory breast cancer by hormonal receptor- and HER2-defined subtypes. *Annals of oncology : official journal of the European Society for Medical Oncology / ESMO* 2014;25(2):384-91.

440. Rueth NM, Lin HY, Bedrosian I, Shaitelman SF, Ueno NT, Shen Y, et al. Underuse of trimodality treatment affects survival for patients with inflammatory breast cancer: an analysis of treatment and survival trends from the national cancer database. *J Clin Oncol* 2014;32(19):2018-24.
441. Saigal K, Hurley J, Takita C, Reis IM, Zhao W, Rodgers SE, et al. Risk factors for locoregional failure in patients with inflammatory breast cancer treated with trimodality therapy. *Clinical breast cancer* 2013;13(5):335-43.
442. Deveraux QL, Reed JC. IAP family proteins--suppressors of apoptosis. *Genes & development* 1999;13(3):239-52.
443. Holcik M, Sonenberg N. Translational control in stress and apoptosis. *Nature reviews Molecular cell biology* 2005;6(4):318-27.
444. Brown MC, Bryant JD, Dobrikova EY, Shveygert M, Bradrick SS, Chandramohan V, et al. Induction of viral, 7-methyl-guanosine cap-independent translation and oncolysis by mitogen-activated protein kinase-interacting kinase-mediated effects on the serine/arginine-rich protein kinase. *Journal of virology* 2014;88(22):13135-48.
445. Huang X, Wu Z, Mei Y, Wu M. XIAP inhibits autophagy via XIAP-Mdm2-p53 signalling. *The EMBO journal* 2013;32(16):2204-16.
446. Lewis J, Burstein E, Reffey SB, Bratton SB, Roberts AB, Duckett CS. Uncoupling of the signaling and caspase-inhibitory properties of X-linked inhibitor of apoptosis. *The Journal of biological chemistry* 2004;279(10):9023-9.
447. Galban S, Duckett CS. XIAP as a ubiquitin ligase in cellular signaling. *Cell death and differentiation* 2010;17(1):54-60.
448. Sotiriou C, Wirapati P, Loi S, Harris A, Fox S, Smeds J, et al. Gene expression profiling in breast cancer: understanding the molecular basis of histologic grade to improve prognosis. *J Natl Cancer Inst* 2006;98(4):262-72.
449. Dutertre M, Gratadou L, Dardenne E, Germann S, Samaan S, Lidereau R, et al. Estrogen regulation and physiopathologic significance of alternative promoters in breast cancer. *Cancer research* 2010;70(9):3760-70.

450. Rosty C, Sheffer M, Tsafrir D, Stransky N, Tsafrir I, Peter M, et al. Identification of a proliferation gene cluster associated with HPV E6/E7 expression level and viral DNA load in invasive cervical carcinoma. *Oncogene* 2005;24(47):7094-104.
451. Zhou T, Chou J, Mullen TE, Elkon R, Zhou Y, Simpson DA, et al. Identification of primary transcriptional regulation of cell cycle-regulated genes upon DNA damage. *Cell Cycle* 2007;6(8):972-81.
452. Zhang CL, Zou Y, He W, Gage FH, Evans RM. A role for adult TLX-positive neural stem cells in learning and behaviour. *Nature* 2008;451(7181):1004-7.
453. Gobert RP, Joubert L, Curchod ML, Salvat C, Foucault I, Jorand-Lebrun C, et al. Convergent functional genomics of oligodendrocyte differentiation identifies multiple autoinhibitory signaling circuits. *Molecular and cellular biology* 2009;29(6):1538-53.
454. Burton GR, Nagarajan R, Peterson CA, McGehee RE, Jr. Microarray analysis of differentiation-specific gene expression during 3T3-L1 adipogenesis. *Gene* 2004;329:167-85.
455. Pearce EL, Walsh MC, Cejas PJ, Harms GM, Shen H, Wang LS, et al. Enhancing CD8 T-cell memory by modulating fatty acid metabolism. *Nature* 2009;460(7251):103-7.
456. Yu M, Li G, Lee WW, Yuan M, Cui D, Weyand CM, et al. Signal inhibition by the dual-specific phosphatase 4 impairs T cell-dependent B-cell responses with age. *Proceedings of the National Academy of Sciences of the United States of America* 2012;109(15):E879-88.
457. Charafe-Jauffret E, Ginestier C, Iovino F, Tarpin C, Diebel M, Esterni B, et al. Aldehyde dehydrogenase 1-positive cancer stem cells mediate metastasis and poor clinical outcome in inflammatory breast cancer. *Clinical cancer research : an official journal of the American Association for Cancer Research* 2010;16(1):45-55.
458. Yamamoto M, Taguchi Y, Ito-Kureha T, Semba K, Yamaguchi N, Inoue J. NF-kappaB non-cell-autonomously regulates cancer stem cell populations in the basal-like breast cancer subtype. *Nature communications* 2013;4:2299.
459. Xia W, Bacus S, Hegde P, Husain I, Strum J, Liu L, et al. A model of acquired autoresistance to a potent ErbB2 tyrosine kinase inhibitor and a therapeutic

strategy to prevent its onset in breast cancer. *Proceedings of the National Academy of Sciences of the United States of America* 2006;103(20):7795-800.

460. Hunter AM, LaCasse EC, Korneluk RG. The inhibitors of apoptosis (IAPs) as cancer targets. *Apoptosis : an international journal on programmed cell death* 2007;12(9):1543-68.
461. Jaffer S, Orta L, Sunkara S, Sabo E, Burstein DE. Immunohistochemical detection of antiapoptotic protein X-linked inhibitor of apoptosis in mammary carcinoma. *Human pathology* 2007;38(6):864-70.
462. Harlin H, Reffey SB, Duckett CS, Lindsten T, Thompson CB. Characterization of XIAP-deficient mice. *Molecular and cellular biology* 2001;21(10):3604-8.
463. Kashkar H. X-linked inhibitor of apoptosis: a chemoresistance factor or a hollow promise. *Clinical cancer research : an official journal of the American Association for Cancer Research* 2010;16(18):4496-502.
464. de Almagro MC, Vucic D. The inhibitor of apoptosis (IAP) proteins are critical regulators of signaling pathways and targets for anti-cancer therapy. *Experimental oncology* 2012;34(3):200-11.
465. Wang L, Du F, Wang X. TNF-alpha induces two distinct caspase-8 activation pathways. *Cell* 2008;133(4):693-703.
466. Enderling H, Hlatky L, Hahnfeldt P. Migration rules: tumours are conglomerates of self-metastases. *British journal of cancer* 2009;100(12):1917-25.
467. Vermeulen PB, Van Laere SJ, Dirix LY. Inflammatory breast carcinoma as a model of accelerated self-metastatic expansion by intravascular growth. *British journal of cancer* 2009;101(6):1028-9; author reply 30.
468. Wright SE. Immunotherapy of breast cancer. *Expert opinion on biological therapy* 2012;12(4):479-90.
469. Spears M, Pederson HC, Lyttle N, Gray C, Quintayo MA, Brogan L, et al. Expression of activated type I receptor tyrosine kinases in early breast cancer. *Breast cancer research and treatment* 2012;134(2):701-8.

470. Janku F, Srovnal J, Korinkova G, Novotny J, Petruzelka L, Power D, et al. Molecular detection of disseminated breast cancer cells in the bone marrow of early breast cancer patients using quantitative RT PCR for CEA. *Neoplasma* 2008;55(4):317-22.
471. Otte M, Zafrakas M, Riethdorf L, Pichlmeier U, Loning T, Janicke F, et al. MAGE-A gene expression pattern in primary breast cancer. *Cancer research* 2001;61(18):6682-7.
472. Singh R, Bandyopadhyay D. MUC1: a target molecule for cancer therapy. *Cancer biology & therapy* 2007;6(4):481-6.
473. Topfer K, Kempe S, Muller N, Schmitz M, Bachmann M, Cartellieri M, et al. Tumor evasion from T cell surveillance. *Journal of biomedicine & biotechnology* 2011;2011:918471.
474. Ueno NT, Buzdar AU, Singletary SE, Ames FC, McNeese MD, Holmes FA, et al. Combined-modality treatment of inflammatory breast carcinoma: twenty years of experience at M. D. Anderson Cancer Center. *Cancer chemotherapy and pharmacology* 1997;40(4):321-9.
475. Chavez-Galan L, Arenas-Del Angel MC, Zenteno E, Chavez R, Lascurain R. Cell death mechanisms induced by cytotoxic lymphocytes. *Cellular & molecular immunology* 2009;6(1):15-25.
476. Cullen SP, Brunet M, Martin SJ. Granzymes in cancer and immunity. *Cell death and differentiation* 2010;17(4):616-23.
477. Afonina IS, Cullen SP, Martin SJ. Cytotoxic and non-cytotoxic roles of the CTL/NK protease granzyme B. *Immunological reviews* 2010;235(1):105-16.
478. Perl M, Denk S, Kalbitz M, Huber-Lang M. Granzyme B: a new crossroad of complement and apoptosis. *Advances in experimental medicine and biology* 2012;946:135-46.
479. Holcik M, Korneluk RG. XIAP, the guardian angel. *Nature reviews Molecular cell biology* 2001;2(7):550-6.
480. Fulda S. Tumor resistance to apoptosis. *International journal of cancer Journal international du cancer* 2009;124(3):511-5.

481. LaCasse EC. Pulling the plug on a cancer cell by eliminating XIAP with AEG35156. *Cancer letters* 2013;332(2):215-24.
482. Nair S, Aldrich AJ, McDonnell E, Cheng Q, Aggarwal A, Patel P, et al. Immunologic targeting of FOXP3 in inflammatory breast cancer cells. *PloS one* 2013;8(1):e53150.
483. Beug ST, Cheung HH, LaCasse EC, Korneluk RG. Modulation of immune signalling by inhibitors of apoptosis. *Trends in immunology* 2012;33(11):535-45.
484. Damgaard RB, Gyrd-Hansen M. Inhibitor of apoptosis (IAP) proteins in regulation of inflammation and innate immunity. *Discovery medicine* 2011;11(58):221-31.
485. Varfolomeev E, Goncharov T, Maecker H, Zobel K, Komuves LG, Deshayes K, et al. Cellular inhibitors of apoptosis are global regulators of NF-kappaB and MAPK activation by members of the TNF family of receptors. *Science signaling* 2012;5(216):ra22.
486. Evans MK, Sauer SJ, Nath S, Robinson TJ, Morse MA, Devi GR. X-linked Inhibitor of Apoptosis Protein Mediates Tumor Cell Resistance to Antibody-Dependent Cellular Cytotoxicity. *Cell Death Dis* 2016;in press.
487. Schile AJ, Garcia-Fernandez M, Steller H. Regulation of apoptosis by XIAP ubiquitin-ligase activity. *Genes & development* 2008;22(16):2256-66.
488. Goping IS, Barry M, Liston P, Sawchuk T, Constantinescu G, Michalak KM, et al. Granzyme B-induced apoptosis requires both direct caspase activation and relief of caspase inhibition. *Immunity* 2003;18(3):355-65.
489. Jacquemin G, Margiotta D, Kasahara A, Bassoy EY, Walch M, Thiery J, et al. Granzyme B-induced mitochondrial ROS are required for apoptosis. *Cell death and differentiation* 2015;22(5):862-74.
490. Day BJ, Fridovich I, Crapo JD. Manganic porphyrins possess catalase activity and protect endothelial cells against hydrogen peroxide-mediated injury. *Archives of biochemistry and biophysics* 1997;347(2):256-62.

491. Shin HM, Kim MH, Kim BH, Jung SH, Kim YS, Park HJ, et al. Inhibitory action of novel aromatic diamine compound on lipopolysaccharide-induced nuclear translocation of NF-kappaB without affecting IkappaB degradation. *FEBS letters* 2004;571(1-3):50-4.
492. Pardoll DM. The blockade of immune checkpoints in cancer immunotherapy. *Nature reviews Cancer* 2012;12(4):252-64.
493. Perez-Sanchez V, Maldonado-Martinez H, Juarez-Sanchez P, Meneses-Garcia A. Pathology of Inflammatory Breast Cancer. In: de la Garza-Salazar JG, Meneses-Garcia A, Arce-Salinas C, editors. *Inflammatory Breast Cancer*: Springer London; 2013. p 29-50.
494. Jin HS, Lee DH, Kim DH, Chung JH, Lee SJ, Lee TH. cIAP1, cIAP2, and XIAP act cooperatively via nonredundant pathways to regulate genotoxic stress-induced nuclear factor-kappaB activation. *Cancer research* 2009;69(5):1782-91.
495. Marigo I, Bosio E, Solito S, Mesa C, Fernandez A, Dolcetti L, et al. Tumor-induced tolerance and immune suppression depend on the C/EBPbeta transcription factor. *Immunity* 2010;32(6):790-802.
496. Maio M, Altomonte M, Tataka R, Zeff RA, Ferrone S. Reduction in susceptibility to natural killer cell-mediated lysis of human FO-1 melanoma cells after induction of HLA class I antigen expression by transfection with B2m gene. *The Journal of clinical investigation* 1991;88(1):282-9.
497. Pena J, Alonso C, Solana R, Serrano R, Carracedo J, Ramirez R. Natural killer susceptibility is independent of HLA class I antigen expression on cell lines obtained from human solid tumors. *European journal of immunology* 1990;20(11):2445-8.
498. Soliman H, Khalil F, Antonia S. PD-L1 expression is increased in a subset of basal type breast cancer cells. *PloS one* 2014;9(2):e88557.
499. Shields JD, Kourtis IC, Tomei AA, Roberts JM, Swartz MA. Induction of lymphoidlike stroma and immune escape by tumors that express the chemokine CCL21. *Science* 2010;328(5979):749-52.
500. Forster R, Davalos-Misslitz AC, Rot A. CCR7 and its ligands: balancing immunity and tolerance. *Nature reviews Immunology* 2008;8(5):362-71.

501. Mantovani A, Sica A, Sozzani S, Allavena P, Vecchi A, Locati M. The chemokine system in diverse forms of macrophage activation and polarization. *Trends in immunology* 2004;25(12):677-86.
502. Bie Q, Zhang P, Su Z, Zheng D, Ying X, Wu Y, et al. Polarization of ILC2s in peripheral blood might contribute to immunosuppressive microenvironment in patients with gastric cancer. *Journal of immunology research* 2014;2014:923135.
503. Reyes Ocampo J, Lugo Huitron R, Gonzalez-Esquivel D, Ugalde-Muniz P, Jimenez-Anguiano A, Pineda B, et al. Kynurenines with neuroactive and redox properties: relevance to aging and brain diseases. *Oxidative medicine and cellular longevity* 2014;2014:646909.
504. Zaher SS, Germain C, Fu H, Larkin DF, George AJ. 3-hydroxykynurenine suppresses CD4+ T-cell proliferation, induces T-regulatory-cell development, and prolongs corneal allograft survival. *Investigative ophthalmology & visual science* 2011;52(5):2640-8.
505. Verhagen AM, Ekert PG, Pakusch M, Silke J, Connolly LM, Reid GE, et al. Identification of DIABLO, a mammalian protein that promotes apoptosis by binding to and antagonizing IAP proteins. *Cell* 2000;102(1):43-53.
506. Fulda S. Smac mimetics as IAP antagonists. *Seminars in cell & developmental biology* 2014.
507. Brinkmann K, Hombach A, Seeger JM, Wagner-Stippich D, Klubertz D, Kronke M, et al. Second mitochondria-derived activator of caspase (SMAC) mimetic potentiates tumor susceptibility toward natural killer cell-mediated killing. *Leukemia & lymphoma* 2014;55(3):645-51.
508. Beug ST, Tang VA, LaCasse EC, Cheung HH, Beauregard CE, Brun J, et al. Smac mimetics and innate immune stimuli synergize to promote tumor death. *Nature biotechnology* 2014;32(2):182-90.
509. Rada B, Leto TL. Oxidative innate immune defenses by Nox/Duox family NADPH oxidases. *Contributions to microbiology* 2008;15:164-87.
510. Toure F, Fritz G, Li Q, Rai V, Daffu G, Zou YS, et al. Formin mDia1 mediates vascular remodeling via integration of oxidative and signal transduction pathways. *Circulation research* 2012;110(10):1279-93.

511. Agostinelli E, Seiler N. Non-irradiation-derived reactive oxygen species (ROS) and cancer: therapeutic implications. *Amino Acids* 2006;31(3):341-55.
512. Fuchs-Tarlovsky V. Role of antioxidants in cancer therapy. *Nutrition (Burbank, Los Angeles County, Calif)* 2013;29(1):15-21.
513. Fang J, Nakamura H, Iyer AK. Tumor-targeted induction of oxystress for cancer therapy. *Journal of drug targeting* 2007;15(7-8):475-86.
514. Fang J, Seki T, Maeda H. Therapeutic strategies by modulating oxygen stress in cancer and inflammation. *Advanced drug delivery reviews* 2009;61(4):290-302.
515. Sies H. Strategies of antioxidant defense. *European journal of biochemistry / FEBS* 1993;215(2):213-9.
516. Di Mascio P, Murphy ME, Sies H. Antioxidant defense systems: the role of carotenoids, tocopherols, and thiols. *The American journal of clinical nutrition* 1991;53(1 Suppl):194S-200S.
517. Gius D, Spitz DR. Redox signaling in cancer biology. *Antioxidants & redox signaling* 2006;8(7-8):1249-52.
518. Halliwell B, Gutteridge JM. *Free radicals in biology and medicine*. 4th ed. New York: Oxford University Press; 2007.
519. Batinic-Haberle I, Reboucas JS, Spasojevic I. Superoxide dismutase mimics: chemistry, pharmacology, and therapeutic potential. *Antioxidants & redox signaling* 2010;13(6):877-918.
520. Miriyala S, Spasojevic I, Tovmasyan A, Salvemini D, Vujaskovic Z, St Clair D, et al. Manganese superoxide dismutase, MnSOD and its mimics. *Biochimica et biophysica acta* 2012;1822(5):794-814.
521. Batinic-Haberle I, Tovmasyan A, Roberts E, Vujaskovic Z, Leong KW, Spasojevic I. SOD therapeutics: Latest insights into the structure-activity relationships and cellular redox-based pathways - lessons from cancer and radiation studeis. *Antioxidants & redox signaling* 2013;Under Revision.
522. Batinic-Haberle I, Spasojevic I, Stevens RD, Hambright P, Neta P, Okado-Matsumoto A, et al. New class of potent catalysts of O<sub>2</sub>·-dismutation. *Mn(III)*

ortho-methoxyethylpyridyl- and di-ortho-methoxyethylimidazolylporphyrins. Dalton transactions (Cambridge, England : 2003) 2004(11):1696-702.

523. Batinic-Haberle I, Spasojevic I, Tse HM, Tovmasyan A, Rajic Z, St Clair DK, et al. Design of Mn porphyrins for treating oxidative stress injuries and their redox-based regulation of cellular transcriptional activities. *Amino Acids* 2012;42(1):95-113.
524. Bottino R, Balamurugan AN, Tse H, Thirunavukkarasu C, Ge X, Profozich J, et al. Response of human islets to isolation stress and the effect of antioxidant treatment. *Diabetes* 2004;53(10):2559-68.
525. Sheng H, Spasojevic I, Tse HM, Jung JY, Hong J, Zhang Z, et al. Neuroprotective efficacy from a lipophilic redox-modulating Mn(III) N-Hexylpyridylporphyrin, MnTnHex-2-PyP: rodent models of ischemic stroke and subarachnoid hemorrhage. *The Journal of pharmacology and experimental therapeutics* 2011;338(3):906-16.
526. Sheng H, Yang W, Fukuda S, Tse HM, Paschen W, Johnson K, et al. Long-term neuroprotection from a potent redox-modulating metalloporphyrin in the rat. *Free radical biology & medicine* 2009;47(7):917-23.
527. Tse HM, Milton MJ, Piganelli JD. Mechanistic analysis of the immunomodulatory effects of a catalytic antioxidant on antigen-presenting cells: implication for their use in targeting oxidation-reduction reactions in innate immunity. *Free radical biology & medicine* 2004;36(2):233-47.
528. Jaramillo MC, Briehl MM, Tome ME. Manganese Porphyrin Glutathionylates the p65 Subunit of NF- $\kappa$ B to Potentiate Glucocorticoid-induced Apoptosis in Lymphoma. *Free radical biology & medicine* 2010;49:S63-S63.
529. Jaramillo MC, Frye JB, Crapo JD, Briehl MM, Tome ME. Increased manganese superoxide dismutase expression or treatment with manganese porphyrin potentiates dexamethasone-induced apoptosis in lymphoma cells. *Cancer research* 2009;69(13):5450-7.
530. Evans MK, Tovmasyan A, Batinic-Haberle I, Devi GR. Mn porphyrin in combination with ascorbate acts as a pro-oxidant and mediates caspase-independent cancer cell death. *Free radical biology & medicine* 2014;68:302-14.

531. Mosmann T. Rapid colorimetric assay for cellular growth and survival: application to proliferation and cytotoxicity assays. *Journal of immunological methods* 1983;65(1-2):55-63.
532. Chae HJ, Kang JS, Byun JO, Han KS, Kim DU, Oh SM, et al. Molecular mechanism of staurosporine-induced apoptosis in osteoblasts. *Pharmacological research : the official journal of the Italian Pharmacological Society* 2000;42(4):373-81.
533. Son YO, Jang YS, Heo JS, Chung WT, Choi KC, Lee JC. Apoptosis-inducing factor plays a critical role in caspase-independent, pyknotic cell death in hydrogen peroxide-exposed cells. *Apoptosis : an international journal on programmed cell death* 2009;14(6):796-808.
534. Gallego MA, Joseph B, Hemstrom TH, Tamiji S, Mortier L, Kroemer G, et al. Apoptosis-inducing factor determines the chemoresistance of non-small-cell lung carcinomas. *Oncogene* 2004;23(37):6282-91.
535. Spasojević I, Batinić-Haberle I. Manganese(III) complexes with porphyrins and related compounds as catalytic scavengers of superoxide. *Inorganica Chimica Acta* 2001;317(1-2):230-42.
536. Spasojevic I, Batinic-Haberle I, Fridovich I. Nitrosylation of manganese(II) tetrakis(N-ethylpyridinium-2-yl)porphyrin: a simple and sensitive spectrophotometric assay for nitric oxide. *Nitric Oxide* 2000;4(5):526-33.
537. Batinic-Haberle I, Tovmasyan A, Roberts E, Vujaskovic Z, Leong KW, Spasojevic I. SOD therapeutics: Latest insights into their structure-activity relationships and impact upon the cellular redox-based pathways. *Antioxidants & redox signaling* 2013.
538. Jin N, Lahaye DE, Groves JT. A "push-pull" mechanism for heterolytic o-o bond cleavage in hydroperoxo manganese porphyrins. *Inorg Chem* 2010;49(24):11516-24.
539. Ferrer-Sueta G, Quijano C, Alvarez B, Radi R. Reactions of manganese porphyrins and manganese-superoxide dismutase with peroxynitrite. *Methods in enzymology* 2002;349:23-37.

540. Groves JT, Lee J, Marla SS. Detection and Characterization of an Oxomanganese(V) Porphyrin Complex by Rapid-Mixing Stopped-Flow Spectrophotometry. *Journal of the American Chemical Society* 1997;119(27):6269-73.
541. Tovmasyan A, Sheng H, Weitner T, Arulpragasam A, Lu M, Warner DS, et al. Design, mechanism of action, bioavailability and therapeutic effects of mn porphyrin-based redox modulators. *Medical principles and practice : international journal of the Kuwait University, Health Science Centre* 2013;22(2):103-30.
542. Chen Q, Espey MG, Sun AY, Pooput C, Kirk KL, Krishna MC, et al. Pharmacologic doses of ascorbate act as a prooxidant and decrease growth of aggressive tumor xenografts in mice. *Proceedings of the National Academy of Sciences of the United States of America* 2008;105(32):11105-9.
543. Ranzato E, Biffo S, Burlando B. Selective ascorbate toxicity in malignant mesothelioma: a redox Trojan mechanism. *American journal of respiratory cell and molecular biology* 2011;44(1):108-17.
544. Kos I, Benov L, Spasojevic I, Reboucas JS, Batinic-Haberle I. High lipophilicity of meta Mn(III) N-alkylpyridylporphyrin-based superoxide dismutase mimics compensates for their lower antioxidant potency and makes them as effective as ortho analogues in protecting superoxide dismutase-deficient *Escherichia coli*. *Journal of medicinal chemistry* 2009;52(23):7868-72.
545. Jaramillo MC, Briehl MM, Crapo JD, Batinic-Haberle I, Tome ME. Manganese porphyrin, MnTE-2-PyP5+, Acts as a pro-oxidant to potentiate glucocorticoid-induced apoptosis in lymphoma cells. *Free radical biology & medicine* 2012;52(8):1272-84.
546. Lorenzo HK, Susin SA, Penninger J, Kroemer G. Apoptosis inducing factor (AIF): a phylogenetically old, caspase-independent effector of cell death. *Cell death and differentiation* 1999;6(6):516-24.
547. Loeffler M, Daugas E, Susin SA, Zamzami N, Metivier D, Nieminen AL, et al. Dominant cell death induction by extramitochondrially targeted apoptosis-inducing factor. *FASEB journal : official publication of the Federation of American Societies for Experimental Biology* 2001;15(3):758-67.

548. Yu SW, Wang H, Poitras MF, Coombs C, Bowers WJ, Federoff HJ, et al. Mediation of poly(ADP-ribose) polymerase-1-dependent cell death by apoptosis-inducing factor. *Science* 2002;297(5579):259-63.
549. Qiu XZ, Yu L, Lai GH, Wang LY, Chen B, Ouyang J. Mitochondrial AIF protein involved in skeletal muscle regeneration. *Cell Biochem Funct* 2008;26(5):598-602.
550. Barbouti A, Doulias PT, Nouis L, Tenopoulou M, Galaris D. DNA damage and apoptosis in hydrogen peroxide-exposed Jurkat cells: bolus addition versus continuous generation of H<sub>2</sub>O<sub>2</sub>. *Free radical biology & medicine* 2002;33(5):691-702.
551. Miriyala S, Thipakkom C, Xu Y, Prachayasittikul V, Noel T, St Clair D. 4-hydroxy-2-nonenal Mediates AIFm2 Release from Mitochondria: An Insight into the Mechanism of Oxidative Stress Mediated Retrograde Signaling. *Free radical biology & medicine* 2010;49:S170-S70.
552. Chen Q, Espey MG, Krishna MC, Mitchell JB, Corpe CP, Buettner GR, et al. Pharmacologic ascorbic acid concentrations selectively kill cancer cells: action as a pro-drug to deliver hydrogen peroxide to tissues. *Proceedings of the National Academy of Sciences of the United States of America* 2005;102(38):13604-9.
553. Chen Q, Espey MG, Sun AY, Lee JH, Krishna MC, Shacter E, et al. Ascorbate in pharmacologic concentrations selectively generates ascorbate radical and hydrogen peroxide in extracellular fluid in vivo. *Proceedings of the National Academy of Sciences of the United States of America* 2007;104(21):8749-54.
554. Welsh JL, Wagner BA, van't Erve TJ, Zehr PS, Berg DJ, Halfdanarson TR, et al. Pharmacological ascorbate with gemcitabine for the control of metastatic and node-positive pancreatic cancer (PACMAN): results from a phase I clinical trial. *Cancer chemotherapy and pharmacology* 2013;71(3):765-75.
555. Monti DA, Mitchell E, Bazzan AJ, Littman S, Zabrecky G, Yeo CJ, et al. Phase I evaluation of intravenous ascorbic acid in combination with gemcitabine and erlotinib in patients with metastatic pancreatic cancer. *PloS one* 2012;7(1):e29794.
556. Moeller BJ, Batinic-Haberle I, Spasojevic I, Rabbani ZN, Anscher MS, Vujaskovic Z, et al. A manganese porphyrin superoxide dismutase mimetic enhances tumor radioresponsiveness. *Int J Radiat Oncol Biol Phys* 2005;63(2):545-52.

557. Brown MC, Dobrikov MI, Gromeier M. Mitogen-activated protein kinase-interacting kinase regulates mTOR/AKT signaling and controls the serine/arginine-rich protein kinase-responsive type 1 internal ribosome entry site-mediated translation and viral oncolysis. *Journal of virology* 2014;88(22):13149-60.
558. Roberts PJ, Der CJ. Targeting the Raf-MEK-ERK mitogen-activated protein kinase cascade for the treatment of cancer. *Oncogene* 2007;26(22):3291-310.
559. Schimmer AD, Welsh K, Pinilla C, Wang Z, Krajewska M, Bonneau MJ, et al. Small-molecule antagonists of apoptosis suppressor XIAP exhibit broad antitumor activity. *Cancer cell* 2004;5(1):25-35.
560. Wang Z, Cuddy M, Samuel T, Welsh K, Schimmer A, Hanai F, et al. Cellular, biochemical, and genetic analysis of mechanism of small molecule IAP inhibitors. *The Journal of biological chemistry* 2004;279(46):48168-76.
561. Cossu F, Milani M, Grassi S, Malvezzi F, Corti A, Bolognesi M, et al. NF023 binding to XIAP-BIR1: searching drugs for regulation of the NF-kappaB pathway. *Proteins* 2015;83(4):612-20.
562. Abdullah LN, Chow EK. Mechanisms of chemoresistance in cancer stem cells. *Clinical and translational medicine* 2013;2(1):3.
563. Huang CP, Tsai MF, Chang TH, Tang WC, Chen SY, Lai HH, et al. ALDH-positive lung cancer stem cells confer resistance to epidermal growth factor receptor tyrosine kinase inhibitors. *Cancer letters* 2013;328(1):144-51.
564. Januchowski R, Wojtowicz K, Zabel M. The role of aldehyde dehydrogenase (ALDH) in cancer drug resistance. *Biomedicine & pharmacotherapy = Biomedecine & pharmacotherapie* 2013;67(7):669-80.
565. Tait SW, Green DR. Mitochondria and cell death: outer membrane permeabilization and beyond. *Nature reviews Molecular cell biology* 2010;11(9):621-32.
566. Cheung EC, Joza N, Steenaart NA, McClellan KA, Neuspiel M, McNamara S, et al. Dissociating the dual roles of apoptosis-inducing factor in maintaining mitochondrial structure and apoptosis. *The EMBO journal* 2006;25(17):4061-73.

567. Batinic-Haberle I, Tovmasyan A, Spasojevic I. An educational overview of the chemistry, biochemistry and therapeutic aspects of Mn porphyrins - From superoxide dismutation to HO-driven pathways. *Redox biology* 2015;5:43-65.
568. Johansson B. A review of the pharmacokinetics and pharmacodynamics of disulfiram and its metabolites. *Acta psychiatrica Scandinavica Supplementum* 1992;369:15-26.

## Biography

Myron K. Evans II was born on December 12<sup>th</sup>, 1988 in Ft. Campbell, Kentucky to parents, Myron K. Evans I and Latrina L. Evans. After graduating from Pedro Menendez High School (St. Augustine, Florida) in May of 2006, he attended Florida International University where he majored in biological sciences with a focus in developmental biology. During his time at FIU, Myron worked in the laboratory of Dr. Lidia Kos where he studied the genetics of neural crest development and the factors driving melanocyte development and melanomagenesis. In the summer of 2009, Myron attended the AMGEN Scholars Summer Research Training Program at University of California, San Francisco working in the lab of Dr. Mark von Zastrow innovating a novel assay to assess the dynamics of G-protein trafficking, work which won numerous awards at national conferences. After graduating with high honors in April of 2010, Myron relocated to North Carolina to enroll in the Developmental and Stem Cell Biology Training Program and subsequently the Department of Pathology at Duke University. After rotations, he joined the laboratory of Dr. Gayathri Devi in October of 2011 and performed his thesis work dissecting novel roles for an anti-apoptotic protein in inflammatory breast cancer disease progression and therapeutic resistance.

## EDUCATION

**Duke University, Durham, NC (June 2010 – present)**

*Doctor of Philosophy*

Department of Pathology

*Graduate Certificate in Developmental and Stem Cell Biology*

**Florida International University, Miami, FL (June 2006 – April 2010)**

*Bachelor of Science in Biological Sciences, High Honors*

Department of Biological Sciences

## HONORS, AWARDS, AND FELLOWSHIPS

1. Selection to the St. Jude National Graduate Student Symposium, 2015
2. Duke University Graduate School Travel Award, December 2014
3. Duke University Dean's Graduate Fellowship, 2010-2014
4. Duke University Development and Stem Cell Biology Training Grant, 2010-2012
5. Duke University Diversity Enhancement Fellowship, 2010-2014
6. Robert James Smiddy Honors Research Award for Undergraduate Thesis, 2010

## PUBLICATIONS AND PRESENTATIONS

### *Publications*

1. **Evans MK**, Sauer SJ, Nath S, Robinson TJ, Morse MA, Devi GR. X-linked inhibitor of apoptosis protein mediates tumor cell resistance to antibody-dependent cellular cytotoxicity. *Cell Death and Disease*, 2016 Jan;28(7):e2073.
2. Allensworth JL, **Evans MK**, Bertucci F, Aldrich AJ, Festa RA, Finetti P, Safi R, McDonnell DP, Thiele DJ, van Laere SJ, Devi GR. Disulfiram (DSF) acts as a copper ionophore to induce copper-dependent oxidative stress and mediate anti-tumor efficacy in inflammatory breast cancer. *Molecular Oncology*, 2015 Jun;9(6):1155-1168.
3. Devi GR, Allensworth JL, **Evans MK**, Sauer SJ. The role of oxidative stress in breast cancer. In *Oxidative Stress and Dietary Antioxidants*. 2014 (pp. 3-14) Waltham, MA: Academic Press.
4. **Evans MK**, Tovmasyan A, Batinic-Haberle I, Devi GR. Mn Porphyrin in combination with ascorbate acts as a pro-oxidant and mediates caspase-independent cancer cell death. *Free Radical Biology and Medicine*, 2014 Mar;68:302-14.

*Presentations*

1. **Evans MK**. A novel pro-oxidant role for manganese porphyrins in the treatment of inflammatory breast cancer. Duke Medical Center Breast Cancer Research Forum, Oral Presentation. (2012)
2. **Evans MK**, Tovmasyan A, Batinic-Haberle I, Devi GR. Manganese porphyrins in combination with ascorbate act as pro-oxidants and mediate caspase-independent cancer cell death. American Association for Cancer Research Annual Meeting, Poster Presentation. (2013)
3. Devi GR, **Evans MK**, Tovmasyan A, Batinic-Haberle I. A mechanism of cell death using a novel redox modulatory strategy to overcome therapeutic resistance in inflammatory breast cancer cells. Cold Spring Harbor Laboratory Meeting on Cell Death, Poster Presentation. (2013)
4. **Evans MK**, Allensworth JL, Devi GR. Identification and targeting of therapeutic resistance mechanisms in inflammatory breast cancer. American Cancer Society Cancer Action Network, Poster Presentation. (2014)
5. **Evans MK**, Aldrich AJ, Geradts J, Vermeulen PB, Dirix LY, van Laere SJ, Devi GR. A novel link between anti-apoptotic signaling and NF $\kappa$ B in IBC pathobiology. San Antonio Breast Cancer Symposium, Poster Presentation. (2014)

6. **Evans MK**, Robinson TJ, Geradts J, Aldrich AJ, Ramirez AG, Dirix LY, Vermeulen PB, van Laere, SJ, Devi GR. XIAP drives inflammatory breast cancer tumor growth and recurrence through activation of NF $\kappa$ B. St. Jude National Graduate Student Symposium, Oral Presentation. (2015)
7. **Evans MK**, Aldrich AJ, Geradts J, Vermeulen PB, Dirix LY, van Laere, SJ, Devi GR. XIAP drives inflammatory breast cancer tumor growth and recurrence through activation of NF $\kappa$ B. St. Jude National Graduate Student Symposium, Poster Presentation. (2015)